Report No. K-TRAN: KSU-05-1
FINAL REPORT

# FIELD VERIFICATION OF KDOT'S SUPERPAVE MIXTURE PROPERTIES TO BE USED AS INPUTS IN THE NCHRP MECHANISTIC-EMPIRICAL PAVEMENT DESIGN GUIDE

Daba Gedafa
Mustaque Hossain, Ph.D., P.E.
Stefan A. Romanoschi, Ph.D., P.E.
Kansas State University
Manhattan, Kansas

January 2009

A COOPERATIVE TRANSPORTATION RESEARCH PROGRAM
BETWEEN:

KANSAS DEPARTMENT OF TRANSPORTATION
KANSAS STATE UNIVERSITY
UNIVERSITY OF KANSAS

| | | |
|---|---|---|
| **1 Report No.**<br>K-TRAN: KSU-05-1 | **2 Government Accession No.** | **3 Recipient Catalog No.** |
| **4 Title and Subtitle**<br>Field Verification of KDOT's Superpave Mixture Properties to be Used as Inputs in the NCHRP Mechanistic-Empirical Pavement Design Guide | | **5 Report Date**<br>January 2009<br>**6 Performing Organization Code** |
| **7 Author(s)**<br>Daba Gedafa, Mustaque Hossain, Ph.D., P.E.,<br>Stefan A. Romanoschi, Ph.D., P.E. | | **8 Performing Organization Report No.** |
| **9 Performing Organization Name and Address**<br>Department of Civil Engineering<br>Kansas State University<br>2118 Fiedler Hall<br>Manhattan, Kansas 66506 | | **10 Work Unit No. (TRAIS)**<br>**11 Contract or Grant No.**<br>C1529 |
| **12 Sponsoring Agency Name and Address**<br>Kansas Department of Transportation<br>Bureau of Materials and Research<br>700 SW Harrison Street<br>Topeka, Kansas 66603-3745 | | **13 Type of Report and Period Covered**<br>Final Report<br>January 2005 - Fall 2008<br>**14 Sponsoring Agency Code**<br>RE-0364-01 |
| **15 Supplementary Notes**<br>For more information write to address in block 9. | | |

**16 Abstract**

In the Mechanistic–Empirical Pavement Design Guide (M-EPDG), prediction of flexible pavement response and performance needs an input of dynamic modulus of hot-mix asphalt (HMA) at all three levels of hierarchical inputs. This study was intended to verify that this input modulus could be achieved in the field construction.

Five newly built Superpave pavements for calibration of M-EPDG by the Kansas Department of Transportation and four Superpave pavement test sections on the Kansas perpetual pavement project on US-75 were selected as test sections in this study. Deflection data on all test sections was collected with a Dynatest 8000 Falling Weight Deflectometer. Normalized deflection data for all calibration sites and US-75 sections were used to back-calculate asphalt layer moduli using three backcalculation computer programs, EVERCALC, MODCOMP II and MODULUS. Laboratory dynamic modulus tests were conducted on asphalt concrete (AC) cores from five calibration sites and on laboratory-compacted samples from the US-75 perpetual pavement sections. Dynamic modulus was also predicted with the Witczak equation, new Witczak model and Hirsch model.

The results show that the surface deflection was highly affected by the test temperature for calibration sites whereas test temperature and pavement thickness highly affected surface deflections for perpetual pavement sections. Repeating different target loads reduces nonlinearity significantly. Laboratory dynamic modulus on US marked highways is higher than on Kansas marked highways for the calibration sites.

| | | | |
|---|---|---|---|
| **17 Key Words**<br>Mechanistic-Empirical Pavement, Superpave, hot-mix asphalt | | **18 Distribution Statement**<br>No restrictions. This document is available to the public through the National Technical Information Service, Springfield, Virginia 22161 | |
| **19 Security Classification (of this report)**<br>Unclassified | **20 Security Classification (of this page)**<br>Unclassified | **21 No. of pages**<br>247 | **22 Price** |

Form DOT F 1700.7 (8-72)

# FIELD VERIFICATION OF KDOT'S SUPERPAVE MIXTURE PROPERTIES TO BE USED AS INPUTS IN THE NCHRP MECHANISTIC-EMPIRICAL PAVEMENT DESIGN GUIDE

**Final Report**


Prepared by

Daba Gedafa
Mustaque Hossain, Ph.D., P.E.
Stefan A. Romanoschi, Ph.D., P.E.

Kansas State University
Department of Civil Engineering
2118 Fiedler Hall
Manhattan, Kansas 66506



A Report on Research Sponsored By

THE KANSAS DEPARTMENT OF TRANSPORTATION
TOPEKA, KANSAS

January 2009

## PREFACE

The Kansas Department of Transportation's (KDOT) Kansas Transportation Research and New-Developments (K-TRAN) Research Program funded this research project. It is an ongoing, cooperative and comprehensive research program addressing transportation needs of the state of Kansas utilizing academic and research resources from KDOT, Kansas State University and the University of Kansas. Transportation professionals in KDOT and the universities jointly develop the projects included in the research program.

## NOTICE

The authors and the state of Kansas do not endorse products or manufacturers. Trade and manufacturers' names appear herein solely because they are considered essential to the object of this report.

This information is available in alternative accessible formats. To obtain an alternative format, contact the Office of Transportation Information, Kansas Department of Transportation, 700 SW Harrison, Topeka, Kansas 66603-3745 or phone (785) 296-3585 (Voice) (TDD).

## DISCLAIMER

The contents of this report reflect the views of the authors who are responsible for the facts and accuracy of the data presented herein. The contents do not necessarily reflect the views or the policies of the state of Kansas. This report does not constitute a standard, specification or regulation.

# ABSTRACT

In the Mechanistic–Empirical Pavement Design Guide (M-EPDG), prediction of flexible pavement response and performance needs an input of dynamic modulus of hot-mix asphalt (HMA) at all three levels of hierarchical inputs. This study was intended to verify that this input modulus could be achieved in the field construction.

Five newly built Superpave pavements for calibration of M-EPDG by the Kansas Department of Transportation and four Superpave pavement test sections on the Kansas perpetual pavement project on US-75 were selected as test sections in this study. Deflection data on all test sections was collected with a Dynatest 8000 Falling Weight Deflectometer. Normalized deflection data for all calibration sites and US-75 sections were used to back-calculate asphalt layer moduli using three backcalculation computer programs, EVERCALC, MODCOMP II and MODULUS. Laboratory dynamic modulus tests were conducted on asphalt concrete (AC) cores from five calibration sites and on laboratory-compacted samples from the US-75 perpetual pavement sections. Dynamic modulus was also predicted with the Witczak equation, new Witczak model and Hirsch model.

The results show that the surface deflection was highly affected by the test temperature for calibration sites whereas test temperature and pavement thickness highly affected surface deflections for perpetual pavement sections. Repeating different target loads reduces nonlinearity significantly. Laboratory dynamic modulus on US marked highways is higher than on Kansas marked highways for the calibration sites. All US routes have comparable average laboratory dynamic modulus at 40$^{o}$F and Kansas routes also show the same trend. Unlike US routes, the trend remains the same

for Kansas routes at 70°F. The trend of laboratory dynamic modulus changes as the temperature changes and the degree of change depends upon the mix characteristics. In general, all backcalculation programs give comparable results for all calibration sites in general. The higher the test temperatures, the lower the backcalculated modulus irrespective of total AC thickness. This shows that the effect of temperature is greater than the AC thickness. Backcalculated modulus of perpetual pavement sections was highly affected by the test temperature and total AC thickness. Standard deviation of the backcalculated moduli varies with the temperature whereas the coefficient of variation remains about the same at all temperature levels for calibration sites. The Witczak equation and New Witczak model give the highest overall average predicted modulus at 0.1 and 25 Hz, respectively, at 40 and 70°F. Witczak equation shows the highest average predicted modulus at 25 Hz for all calibration sites. The new Witczak model and Witczak equation show comparable predicted modulus for all projects. Witczak equation and Hirsch model give the highest and lowest overall average predicted modulus at 0.1Hz, respectively, at 95°F. Dynamic moduli using the Witczak equation are the lowest at 40°F and the highest at 95°F for all US-75 sections. The results also show that the Witczak equation may underestimate the dynamic modulus at low temperature and overestimate at high temperature when compared to the laboratory-measured dynamic moduli. Percent passing No. 200 sieve and effective asphalt volume have the highest positive and negative effect, respectively, on the predicted modulus using Witczak equation. Laboratory determined and the backcalculated moduli are significantly different for all calibration sites. MODCOMP and MODULUS give statistically similar result for all calibration. In general, the results are spotty at best i.e.

some approaches tend to give similar moduli for a certain site but not for all sites. The correction factor is very small when the design modulus is taken as the dependent variable. This implies that the current modulus used in design may be conservative. Correction factors at 40 and 70$^{o}$F are the lowest and the highest, respectively. The correction factors for the laboratory modulus and the predicted modulus are consistently close to 1.00 for all calibration sites with the Hirsch model being the best closely followed by the new Witczak model at 70$^{o}$F. Correction factors at 70$^{o}$F are closer to 1.0 for test sections. Correction factors at 40 and 95$^{o}$F are the lowest and the highest, respectively. M-EPDG software, using uncalibrated models for local conditions, shows that KDOT design is very conservative for the 10-year design period. The thinner the pavement sections, the higher the AC and total permanent deformation. The existing pavement structures can serve for more than 20-years as per M-EPDG software analysis if the uncalibrated models are used. However, current experience all most all AC pavements need some type of rehabilitation after 10 years in Kansas. This may indicate the urgent need for local calibration of M-E PDG models.

According to M-EPDG, the total AC thickness for the projects under study varies from 3 to 6 in for a 10-year design period if the effect of AC surface down cracking (longitudinal cracking) is ignored. The lowest thickness is observed on K-7 which has 11 in. of AB-3. The minimum total AC thickness to serve for 10-year period considering the longitudinal cracking varies from 6 to 9 in. The lowest IRI is observed on a pavement which has the highest total AC thickness and vice versa whereas longitudinal cracking does not depend on the thickness of AC layers. Backcalculated subgrade moduli obtained from various backcalculation programs result in variable predicted

performance for different projects. Predicted modulus increases with aging and thus, results in decreased tensile strain at the bottom of the AC layer. But the fatigue life decreases with time.

# TABLE OF CONTENTS

# LIST OF FIGURES

# LIST OF TABLES

# ACKNOWLEDGEMENTS

The authors would like to thank Kansas Department of Transportation (KDOT) for sponsoring this study under the Kansas Transportation and New Developments (K-TRAN) program. The authors gratefully acknowledge the help of Mr. Cristian Dumitru, formerly with Kansas State University, in dynamic modulus testing and KDOT personnel for coring and Falling Weight Deflector (FWD) testing for this project.

# CHAPTER ONE - INTRODUCTION

## 1.1 General

The design methods adopted in the NCHRP 1-37A Guide for Mechanistic–Empirical Design of New and Rehabilitated Pavement Structures (*NCHRP, 2004*) are based on mechanistic-empirical principles. This guide is popularly known as Mechanistic–Empirical Pavement Design Guide (M-EPDG). In M-EPDG, prediction of pavement response and performance must take into account fundamental properties of layer materials. Among these, the most important property of hot-mix asphalt (HMA) is the dynamic modulus of asphalt concrete. This property represents the temperature- and time-dependent stiffness characteristics of the HMA material. Significant amount of effort has been devoted to develop a test protocol to determine the dynamic modulus of HMA (*Witczak et al., 2002*). This effort has resulted in a standard test protocol that can be used for the Simple Performance Test for Superpave® Mix Design (*NCHRP, 2002*). This test protocol calls for the use of axial compression testing for measuring the dynamic modulus. One of the issues related to the dynamic modulus is its use in forensic studies and pavement rehabilitation design.

In the hierarchical design approach proposed in M-EPDG for new HMA pavements, direct measurements of dynamic modulus are required for the highest design reliability (Level 1), which is intended for pavements with very high traffic volumes. However, dynamic modulus is used as the primary stiffness property for HMA at all three levels of hierarchical inputs in M-EPDG.

In the overlay analysis of existing HMA pavements, the modulus of the existing HMA pavements is characterized by a damaged modulus that represents the condition

at the time of overlay placement. However, according to M-EPDG, the laboratory dynamic modulus tests are not needed for measuring the in-place modulus because the test must be performed on intact but age-hardened specimens. In fact, M-EPDG contends that the resulting modulus values will likely be higher than those for new HMA mixtures. Thus, M-EPDG recommends that the modulus be determined from the deflection basin tests. However, no correlation between the laboratory dynamic modulus of asphalt concrete mixture and the backcalculated asphalt concrete layer modulus has been established to date.

Backcalculation of layer moduli from nondestructive deflection basin testing has become the state-of–the-art method in pavement structural evaluation. The use of backcalculation approaches is more promising than traditional deflection interpretation analysis because they link the measured pavement response (i.e., deflections) to the in-situ properties of the component materials in a more rational fashion. The process also provides directly the inputs needed for the application of mechanistic-empirical procedures for pavement design and rehabilitation (*Khogali and Anderson, 1996; Zhou et al., 1997; Chatti et al., 2004*).

The dynamic modulus test is relatively difficult and expensive to perform. Therefore, numerous attempts have been made to develop regression equations to estimate the dynamic modulus from mixture volumetric properties. The predictive equation developed by *Witczak et al. (2002)* is one of the most comprehensive mixture dynamic modulus models available today that can predict the dynamic modulus of dense-graded HMA mixtures over a range of temperatures, rates of loading, and aging conditions. These inputs are available from conventional binder tests and the volumetric

properties of the HMA mixture. A revised version of this model has been recommended in the design of intermediate- and low-volume roadways (design Levels 2 and 3) in M-EPDG (*NCHRP, 2007*).

## 1.2 Problem Statement

The Kansas Department of Transportation (KDOT) is currently considering adopting M-EPDG to replace the 1993 AASHTO design method that is in use now. As mentioned earlier, for new asphalt pavement design, the basic input parameter is the dynamic modulus of HMA mixture. The dynamic modulus is measured in the laboratory on the Superpave Gyratory Compactor compacted specimens during the design phase. However, verification is needed whether this input parameter can be achieved in as-constructed pavement. This can be done through in-situ deflection tests using a Falling Weight Deflectometer (FWD) and corresponding laboratory tests on the cores taken from the constructed pavements. By correlating the design values with the laboratory and field values, a correction factor can be developed that can be used in the design process to take construction variability into account.

## 1.3 Objectives of the Study

The main objectives of this study are:

- Compare backcalculated moduli of the Superpave pavements obtained from the FWD tests with the dynamic modulus values measured in the laboratory.
- Compare the predicted dynamic modulus from various prediction equations with those measured in the laboratory as well as those backcalculated from the FWD data.
- Develop a correction procedure for the design modulus based on backcalculated, laboratory-derived and predicted dynamic modulus for the Superpave mixtures in Kansas.
- Carry out sensitivity analysis of input parameters in the Witczak equation.
- Run M-EPDG software.

## 1.4 Organization of the Report

This report is divided into six chapters. The first chapter covers a brief introduction to the dynamic modulus, problem statement, study objectives and the outline of the report. Chapter 2 is a review of the literature. Chapter 3 describes the test sections and data collection procedure in the field. Chapter 4 presents the analysis of the test results. Chapter 5 presents the laboratory dynamic modulus results. Backcalcuated and predicted moduli results are presented in Chapters 6 and 7, respectively. Chapter 8 contains the statistical analysis results. Results of M-EPDG analysis for the test sections are discussed in Chapter 9. Finally, Chapter 10 presents the conclusions based on this study.

# CHAPTER TWO - LITERATURE REVIEW

## 2.1 Dynamic Modulus

The dynamic modulus is a linear viscoelastic test for asphalt materials that was originally developed at Ohio State University. It was adopted by the Asphalt Institute as the "Modulus Test of Choice" in the late 1960s. It is a fundamental property that has been measured routinely by asphalt technologists since the 1960s (*Papazian, 1962; Yeager and Wood, 1975; Tayebali et al., 1994; Francken and Partl, 1996*). It is a quotient of the stress amplitude applied to the specimen and the measured strain amplitude response for test specimens subjected to sinusoidally applied uniaxial tension or compression.

Dynamic modulus is one of the most universally used methods to characterize the HMA modulus. Research has indicated that dynamic modulus can be used as a good performance indicator for HMA design. Some of the advantages of using dynamic modulus over other stiffness parameters in HMA pavement analysis and design are: (i) allows hierarchical HMA mixture characterization; (ii) aging can be considered; (iii) time of load can be considered; (iv) can be related to SHRP Performance Graded binder specifications; (v) can be compared to FWD back-calculated modulus of HMA mixtures (*Witczak et al., 2001*); (vi) provides necessary input for structural analysis for a wide range of temperature and loading rate; (vii) gives rational way to establish mix criteria for rutting, cracking, etc. that can be linked to a predictive model (*Witczak et al., 2002*).

Measurement of dynamic modulus on asphalt mixture specimens has received considerable attention in recent years, largely because of its prominence in M-EPDG. In the hierarchical design approach proposed in M-EPDG, direct measurements of

dynamic modulus (E*) are required for the highest design reliability (Level 1), which is intended for pavements with very high traffic volumes (*Buttlar et al., 2002*). Dynamic modulus is used as the primary stiffness property for HMA at all three levels of hierarchical inputs in M-EPDG. At all analysis levels, it is determined from a master curve constructed at a reference temperature. The master curve for Level 1 analysis is developed using numerical optimization to shift the laboratory mixture E* test data into a smooth master curve of a sigmoidal form after relationship between binder viscosity and temperature is established using HMA test data. At Level 2 analysis, master curve is constructed using the current version of Witczak E* equation based on laboratory test data (*Andrei et al., 1999*). No laboratory test is required for Level 3, only mixture volumetric and gradation properties are needed.

## 2.2 Asphalt Concrete Modulus Backcalculation

The procedures used to interpret the FWD deflection data collected from the FWD tests can be divided broadly into empirical, mechanistic, and analytical methods. By far, the most encouraging method for nondestructive testing (NDT) data analysis is the analytical procedure.

The analysis of NDT data requires the estimation of material properties from measured deflections. No direct analytical solution exists for determing material properties from measured response. The lack of a direct solution method has forced the development of iterative techniques for altering the pavement response and comparing the computed and measured responses. This general process has been termed backcalculation in the technical literature (*Hossain et al., 1994*). This is usually done through static backcalculation in which layer moduli are determined by matching the

peak deflections measured under a known load with deflections generated through a theoretical model of the pavement within a specified tolerance.

Almost all pavements consist of more than two layers. As a result, backcalculation helps determine the material properties for any pavement section. The determination of pavement moduli using the static layered elastic backcalculation method is by far the most widely used procedure. The pavement materials are characterized to be elastic, homogeneous, and isotropic, with full contact between layer interfaces. The bottom boundary may be assumed to be located at some depth below the top of the subgrade or at a very large depth (half-space) (*Siddharthan et al., 1991*).

A number of backcalculation computer procedures available are: EVERCALC, MODCOMP5, MODULUS, BISDEF, CHEVDEF, ELSDEF, MICHBACK, and ELMOD. Most of these programs model the pavement structure with a layered elastic system and use an iteration scheme to find the set of layer elastic moduli that best matches the computed theoretical deflections with the measured pavement deflections. The iteration process may require a large amount of computer time. Many programs use influence zone concept to reduce the iterations (*Chou and Lytton, 1991*). The input typically required for such programs consists of measured deflections, layer thicknesses, seed moduli or moduli ranges, and the applied load or pressure (*Harichandran et al., 1993*).

It has been found that the backcalculated modulus values and their accuracy are procedure-dependent (*Chou and Lytton, 1991; Harichandran et al., 1993; Uzan, 1994*). Different layer modulus values for a given pavement structure may be obtained from different procedures. *Harichandran et al. (1993)* examined this procedure dependency

by making a comparison of several popular backcalculation algorithms based on their computed modulus values for selected problems.

### *2.2.1 Procedures for Temperature Correction*

To make a fair assessment of the structural condition of a pavement, backcalculated moduli must be corrected to a particular type of loading system (including the type of loading device, frequency of loading, and load level) and a standard set of environmental conditions. The most important environmental factor affecting surface deflections and backcalculated moduli of flexible pavement is the temperature of the asphalt layer (*Park and Kim, 1997*). The backcalculated asphalt concrete (AC) modulus has to be adjusted to a standard temperature to allow for a direct comparison between the backcalculated moduli and the laboratory moduli.

To accurately backcalculate the AC modulus, a two-step correction procedure needs to be applied. Typically, the first step consists of predicting the effective temperature of the AC layer, and the second step consists of adjusting the FWD deflection or the computed modulus to a reference temperature using a correction factor (*Park et al., 2001*). The correction of deflections is more complicated than the correction of moduli because of involvement of the parameters other than AC moduli. As a result, correction of moduli is widely used.

#### 2.2.1.1 AC Temperature

To correct the backcalculated modulus at a FWD testing temperature to a reference temperature, the effective temperature of the AC layer must be determined. Numerous procedures and relationships have been developed to estimate pavement

temperatures from the climatic data. Some are based on heat-flow theory and are calibrated by using field data, whereas others are based solely on empirical data.

*Leland et al. (1992)* developed Equation (2.1) by the quasi-Newton method process of numerical optimization SYSTAT, a statistical computer program, based on pavement depth, time of FWD testing, and pavement surface temperature. These variables are readily obtained from Michigan Department of Transportation (MDOT) database.

$$T_z = T_{surf} + (-0.345z - 0.0432z^2 + 0.00196z^3)\sin(-6.3252t + 5.0967) \quad \text{Equation 2.1}$$

where,

$T_z$= AC pavement temperature at depth z ($^oC$),

$T_{surf}$= AC pavement temperature at the surface ($^oC$),

z= depth at which temperature is to be determined (cm), and

T= time when the AC surface temperature was measured [days; 0<t<1(e.g.,

1:30pm=13.5/24=0.5625days)].

*Watson et al. (2004)* developed an equation that allows prediction of the pavement temperature at any depth based on the surface temperature with data from the Strategic Highway Research Program (SHRP) temperature database.

$$T_d = T_{surf}(1 - 0.063d + 0.007d^2 - 0.0004d^3) \quad \text{Equation 2.2}$$

where,

$T_d$ = pavement temperature ($^oF$),

$T_{surf}$ = surface temperature ($^oF$), and

$d$ = pavement depth (in).

By using the measured pavement depth temperatures from SHRP's Long Term Pavement Performance (LTPP) data base, BELLS equation was developed as a means of predicting the one-third-depth temperature (*Inge and Kim, 1995*). A third model, BELLS3 was, therefore developed for use during routine FWD testing, when the pavement surface is typically shaded for less than a minute.

#### 2.2.1.2 Modulus Correction

Several methods have been proposed for correction of backcalculated moduli of AC to a reference temperature. To determine the modulus corrected to a reference temperature, the modulus backcalculated from a deflection basin is normally multiplied by a factor. Table 2.1 shows a summary of available multiplication factors.

$$E_{T_0} = \lambda_E E_T \qquad \text{Equation 2.3}$$

where,

$E_{T_0}$ = the modulus corrected to temperature $T_0$,

$E_T$ = the backcalculated modulus of the asphalt mixture at temperature $T$, and

$\lambda_E$ = the temperature-modulus correction factor.

**Table 2.1: Summary of Multiplication Factor**

| Factor | Remark | Reference |
|---|---|---|
| $\lambda_E = 10^{-0.0002175(70^{1.886} - T^{1.886})}$ | T is in $^oF$ | Johnson and Baus,1992 |
| $\lambda_E = \frac{1}{3.177 - 1.673\log T}$ | T>1$^oC$ | Ullidtz, 1987 |
| $\lambda_E = 10^{m(T-20)}$ | m=0.018 and T in $^oC$ | Baltzer and Jansen,1994 |
| | m=0.0275 and T in $^oC$ | Kim et al., 1995 |
| $\lambda_E = 10^{slope*(T_r - T_m)}$ | $T_r$ and $T_m$ in $^oC$ | Lukanen et al., 2000 |

## 2.3 Dynamic Modulus (E*) Using Predictive Models

Laboratory dynamic modulus test is relatively difficult and expensive to perform. Therefore, numerous attempts have been made to develop regression equations to calculate the dynamic modulus from conventional volumetric mixture properties. A number of E* predictive models and related equations have been developed over the last 50 years. Historically, the E* models and equations were developed on the basis of the conventional multivariate linear regression or non-linear regression analysis of laboratory test data and the established or anticipated basic engineering behaviour and/or properties of the HMA mixture and/or its components. These models can be broadly classified into the following categories:

- Linear polynomial for logarithm (10-based) of |E*| with related nomograph for bitumen stiffness modulus such as the Shell Oil method.
- Linear polynomial for logarithm (10-based) of |E*| such as the Shook and Kallas model and all early Witczak et al. models.
- Non-linear polynomial for logarithm (10-based) of |E*| using a sigmoidal functions such as the Witczak et al. model.
- E* models primarily based on the law of mixtures, such as, Hirsch model.

The predictive equation developed by *Witczak et al. (2002)* is one of the most comprehensive mixture dynamic modulus models available today. It has the capability to predict the dynamic modulus of dense-graded HMA mixtures. It is anticipated that state agencies and other pavement designers will rely on the Witczak predictive modulus equation to obtain estimates of dynamic modulus for mixtures typical in their states. It is, therefore, of significant importance for state agencies to appreciate the

relative ranges of dynamic modulus values for mixtures made from locally available materials. Table 2.2 shows the various E* predictive models developed by the researchers since 1950s.

### *2.3.1 Aging System*

The global aging model of Mirza and Witczak “opened the door” to account for any short and long-term aging effects by using the actual viscosity as direct input into the E* model. Once a set of regression equation intercept (A) and regression slope of the viscosity-temperature relationship (VTS) is known for a particular aging condition, A and VTS for other aging conditions can be calculated using the aging models developed by *Mirza and Witczak (1995)*. They also suggested the typical values of A and VTS for different aging.

The first significant hardening of asphalt binder takes place in the pug mill or drum mixer where the heated aggregates are mixed with hot asphalt cement. During the short mixing period, the very thin films of the asphalt binder are usually exposed to air at temperatures ranging from 275 to 325$^{o}$F or more.

**Table 2.2: Review of Dynamic Modulus Predictive Models**

| Model Name | No. of Mixtures | No. of Data Points | Temperature | Frequency (Hz) | Reference |
|---|---|---|---|---|---|
| Van der Poel (Shell Oil's Early Version) Model | | | | | Van der Poel, 1954 |
| Shook and Kallas | 29 | 87 | | 4 | Shook and Kallas,1969 |
| Witczak's Early Model | 29 | 87 | | 4 | Witczak, 1972 |
| Bonnaure (Shell Oil's Later Version) Model | 9 | | | | Bonnar et al., 1977 |
| Witczak's 1981 Model | 41 | 369 | | 10 | Thickness Design, 1981 |
| Witczak, Miller and Uzan's Model | 131 | 1179 | | | Miller et al., 1983 |
| Witczak and Akhter's Models | | | | | Akhter and Witczak, 1985 |
| Witczak, Leahy, Caves and Uzan's Models | 149 | 1430 | | | Witczak et al., 1989 |
| Witczak and Fonseca's Model | 149 | 1430 | 41 to 104 | | Fonseca, 1995 |
| Andrei, Witczak and Mirza's Revised Model | 205 | 2750 | 0 to 130 | 0.1 to 25 | Andrei et al., 1999 |
| Hircsh Model | 18 | 206 | 40, 70, 100 | 0.1 and 5 | Christensen et al., 2003 |
| Witczak New Model | 346 | 7400 | 0,14,15.8,40,70,100, 130 | 0.1,0.5,1,4,5,10,16, 25 | Bari, 2005 |

Rheological changes occur through time. Some of these changes are a decrease in penetration or an increase in viscosity of the binder. These changes take place mostly from oxidation and loss of more volatile components in asphalt. This age hardening continues, although at a much slower rate, while HMA is processed through surge or storage silo, transported to the paving site, laid and compacted. This part of aging is frequently called “short term aging”.

When the pavement is opened to traffic, the age hardening process continues for its service life, though at much slower rates. This is generally called “long term aging”. The following factors have been reported to contribute to the age hardening of asphalt binders: oxidation, volatilization, polymerization, thixotropy, syneresis, and separation (*Vallerga et al., 1957; Finn, 1967*). Because asphalt cements consist of organic molecules, they react with oxygen from the environment. As a result, the structure and composition of the asphalt molecules are changed. These cause oxidative or age hardening resulting in more brittle asphalt cement.

Oxidative hardening occurs at a slow rate, but is accelerated in warmer climates. Improperly compacted asphalt pavements that usually have higher levels of air voids, will allow more oxidative hardening. Beside polymerization, thixotropy, syneresis and separation; *Traxler (1963)* suggested some additional factors, such as, effect of light and water, chemical reaction with aggregates, microbiological deterioration and adsorption of heavy asphalt components on the surface of aggregates.

# CHAPTER THREE - TEST SECTIONS AND DATA COLLECTION

## 3.1 Test Sections

Five newly built Superpave pavements, designed using the 1993 AASHTO Design Guide, and four Superpave pavement test sections on the Kansas perpetual pavement project on US-75 were selected as test sections in this study. The new projects were constructed as calibration sites for the new M-EPDG and referred to as calibration sites or in some cases, as new projects in this report. Each test section was 1,000 ft long for all new projects. Table3.1 indicates the layer type and thicknesses of these sections.

**Table 3.1: Layer Type and Thickness**

| Layer No. | Layer Type | Material Type | Thickness (in) | | | | |
|---|---|---|---|---|---|---|---|
| **a. Calibration Sites** | | | | | | | |
| | | | US-54 | US-77 | US-283 | K-7 | K-99 |
| | | | Butler | Butler | Graham | Doni. | Elk |
| 1 | Surface | SM-9.5A (PG 64-28) | 1.5[a] | 1.5 | 1.5 | 1.5 | 1.5 |
| 2 | Binder | SM-19A (PG 64-28) | 2.5 | 2.5 | 2.5 | 2.5 | 2.5 |
| 3 | Base | SM-19A (PG 64-22) | 8.5 | 8 | 7 | 5 | 7 |
| Total HMA Thickness | | | 12.5 | 12 | 11 | 9 | 11 |
| 4 | Aggregate Base | AB-3 | N.A. | N.A. | N.A. | 11 | N.A. |
| 5 | Subgrade | Modified Subgrade | 6[b] | 6[b] | 6[b] | 6[c] | 6[b] |
| **b. Perpetual Pavement Sections** | | | | | | | |
| | | | S1 | S2 | S3 | S4 | |
| 1 | Surface | SM-9.5A (PG 70-28) | 1.5 | 1.5 | 1.5 | 1.5 | |
| 2 | Binder | SM-19A (PG 70-28) | 2.5 | 2.5 | 2.5 | 2.5 | |
| 3 | Base | SM-19A (PG 64-22) | N.A. | 7.5 | 9 | 12 | |
| | | SM-19A (PG70-22) | 9 | N.A. | N.A. | N.A. | |
| | Total HMA Thickness | | 13 | 11.5 | 13 | 16 | |
| 4 | Subgrade | LTSG | 6[b] | 6[b] | 6[b] | 6[b] | |

**Note**: a-SM-9.5T PG 64-28; b-Lime Treated Subgrade (LTSG); c-fly ash modified subgrade (FASG)

All calibration sites have Superpave 9.5 mm nominal maximum aggregate size mixture (known as SM-9.5A and SM-9.5T in Kansas) with PG 64-28 binder in the surface course of 1.5 inch. thickness. Layers 2 and 3 consist of fine graded Superpave 19 mm nominal maximum aggregate size mixture, SM-19A with PG 64-28 and PG 64-22 binders, respectively. The base layer thickness varies from 5 to 8.5 inches. The K-7 site in Doniphan County has the thinnest asphalt base (5 inches) since it also has 11 inches crushed stone base, designated as AB-3 in Kansas.

On the perpetual pavement project, Section 1 (S1) and Section 2 (S2) have been designed by the Kansas Asphalt Pavement Association (KAPA). S1 has stiff binders, PG70, from top to bottom. Section 3 (S3) is a high-reliability design section and Section 4 (S4) has been designed by KDOT. S3 has stiff surface binder, less stiff base binder with higher AC content. Thus, S1 and S3 have the same thickness, but S1 is stiff and S3 is flexible. It is to be noted that perpetual pavement sections or US-75 sections have been used interchangeably.

All calibration sites have lime-treated subgrade except K-7 in Doniphan County where subgrade was modified with a Class C fly ash.

## 3.2 Data Collection

### *3.2.1 Deflection Data*

FWD testing has been established world-wide as one of the most effective tools for measuring deflections for pavement evaluation purposes. The FWD is a trailer mounted device which applies a load to the pavement surface through a circular plate with a diameter of 11.8 inches. A mass is dropped onto plate with a rubber pad generating an impulse load on the pavement which is similar, but not identical, to the

stress pulse generated by moving trucks. The magnitude of the FWD force on the pavement can be varied by altering either the mass of the drop weight or the drop height. Varying the drop mass and/or height of the FWD provides a direct opportunity to evaluate the stress sensitivity of the materials in the pavement structure. The magnitudes of the force are measured with seven geophones; one is placed at the center of the loaded area. The location of the other six sensors can be varied (*Mamlouk et al., 1988*). Deflection data for all calibration sites and perpetual pavement sections has been collected using KDOT FWD Dynatest 8000 shown in Figure 3.1.


**Figure 3.1: KDOT FWD Dynatest 8000.**

Deflection data was collected approximately 8 to 10 weeks after construction on all calibration sites. Multiple target loads were used on most test sections. The load pulse duration was between 25 and 30 milliseconds. This frequency enabled us to compare backcalculated HMA moduli with the laboratory-measured and predicted dynamic moduli at 25 Hz.

The target loads used in FWD testing were 9, 12 and/or 15 kips for all calibration sites and 9 kips for all perpetual pavement sections on US-75. Deflection measurements were made in the outside wheel path of the travel lane at 11 stations at 100 ft intervals on all calibration sites. FWD data at 7 to 9 stations were collected on the US-75 sections. The geophone spacing was 0, 8, 12, 18, 24, 36 and 48 in. for US-54, US-77 and US-283. The last sensor was located at 60 in. for the K-7 and K-99 sites and on all US-75 test sections. The pavement surface temperature was measured at the time of the test to allow for subsequent temperature corrections in the computed modulus values for the AC layers. This temperature varied from 63 $^{o}$F to 139$^{o}$F for all calibration sites and 54 $^{o}$F to 104$^{o}$F for the US-75 test sections. The variation in temperature for the US-75 sections was due to time difference even if the testing was done on the same day. Locations, test date, surface temperature and target loads for calibration sites and US-75 sections are shown in Table 3.2.

**Table 3.2: Locations, Test Date, Surface Temperature and Load**

| | County | District | Test Date | Sur. Temp Range ($^{o}$F) | Load | |
|---|---|---|---|---|---|---|
| | | | | | Target Load (kips) | Repetition |
| a. Calibration Sites | | | | | | |
| US-54 | Butler | 5 | 10/31/05 | 63-67 | 9,12,15 | Once |
| US-77 | Butler | 5 | 07/13/05 | 98-99 | 9,12,15 | Once |
| US-283 | Graham | 3 | 07/11/05 | 136-139 | 9,12,15 | Once |
| K-7 | Doniphan | 1 | 08/07/06 | 112-117 | 9,12 | Three times |
| K-99 | Elk | 4 | 07/18/07 | 114-119 | 9, 12, 15 | Three times |
| b. Perpetual Pavement Sections | | | | | | |
| S1 | Brown | 1 | 09/29/05 | 54-64 | 9 | Three times |
| S2 | Brown | 1 | 09/29/05 | 76-79 | 9 | Three times |
| S3 | Brown | 1 | 09/29/05 | 95-99 | 9 | Three times |
| S4 | Brown | 1 | 09/29/05 | 97-104 | 9 | Three times |

### *3.2.2 Samples for Laboratory Dynamic Modulus Test*

On all calibration sites, 4-in diameter, full depth cores were taken at the same locations where FWD deflections tests had been done. Cores of asphalt concrete were obtained with a small portable electric powered coring device, shown in Figure 3.2. Running water was used to cool the cutting bit of the 4-inch internal diameter core barrel.


**Figure 3.2: Coring of Asphalt Samples on K-7 in Doniphan County.**

No cores were taken from the US-75 test sections. Dynamic modulus test samples for these test sections were prepared from the mixtures mixed in the laboratory and compacted by the Superpave Gyratory compactor. The 6 inch diameter samples were then cored to get 4 inch diameter dynamic modulus test samples.

### *3.2.3 Volumetric Properties for Predicting Dynamic Modulus*

Most of the data required for predicting dynamic modulus using the Witczak equation, Hirsch model and new Witczak model have been obtained from the mix design database of KDOT. Information includes gradation of aggregates (cumulative percent retained on ¾", 3/8''and No. 4 sieves and percent passing No. 200 sieve), physical properties of the aggregates (bulk and effective specific gravities), asphalt

content and asphalt specific gravity, and theoretical maximum specific gravity of the mixture.

Bulk specific gravities of the compacted samples and the cores were determined in the laboratory based on the Kansas Standard Test Method KT-15, Procedure III. KT-15 closely follows AASHTO T 166. From these pieces of information, the air void (%), effective bitumen content (% by volume), voids in the mineral aggregates (%) and percent of VMA filled with binder (%), were calculated. The original, mix/lay-down, surface aging and aging at different viscosities have been determined at different temperature and frequency. Temperature data for different locations has been obtained from Kansas State University (KSU) weather data library.

## 3.3 Preliminary Data Analysis

It is usually wise to study the data collected and extract trends and properties to help in choosing the type of analysis. The first step is to look at the trend and repeatability of the measured deflection bowls, from the different drops (*Uzan, 1994*) and check the assumption of linear elasticity.

### *3.3.1 Deflection Data*

Irregular deflection basins are sometimes observed from FWD raw deflection data. Irregular deflections could cause problems in the evaluation of pavement layer conditions. Thus, it is important to first check whether the deflection basin is irregular before performing deflection analysis (*Xu et al., 2002*). For each pavement section, the average, standard deviation, and coefficient of variation (COV) of the normalized deflections have been calculated. Deflection has not been corrected for pavement

temperature. Figure 3.3 and Figure 3.4 show average normalized deflections for the calibration sites and the perpetual pavement sections, respectively.

US-54 and US-283 show the lowest and highest deflections at all sensors, respectively, on which deflection data was taken at the lowest and the highest temperature, respectively. This confirms the significant effect of temperature on surface deflection. Deflection on K-99 was taken at second highest temperature and the deflections are also second highest except under sensors D5 and D6, which may indicate that the subgrade for K-99 is stronger. There is a change of trend from the second lowest under center load to the second highest under the most distant sensor. In general, deflection data for all calibration sites has good trend.

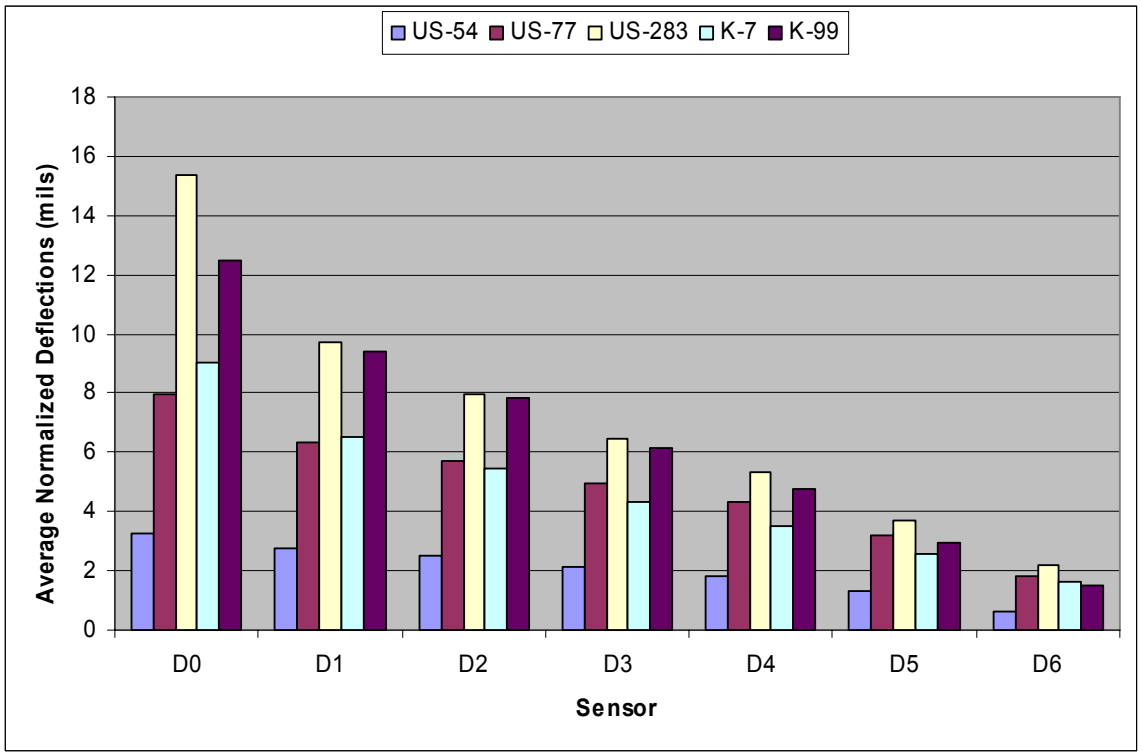


**Figure 3.3: Average Normalized Deflections for Calibration Sites.**

Perpetual pavement sections, S2 and S4, are the thinnest and the thickest, respectively. These sections show the highest and lowest deflections irrespective of test temperature. Deflection on S2 was taken at the second lowest temperature whereas deflection was measured at the highest temperature on S4. This shows that pavement thickness also highly affects the surface deflection. Test temperature on S3 was higher than that of S1, which has the same total AC thickness. Center deflection of S3 is higher, but the trend changes and this indicates the effect of test temperature decreases as distance from the center increases.

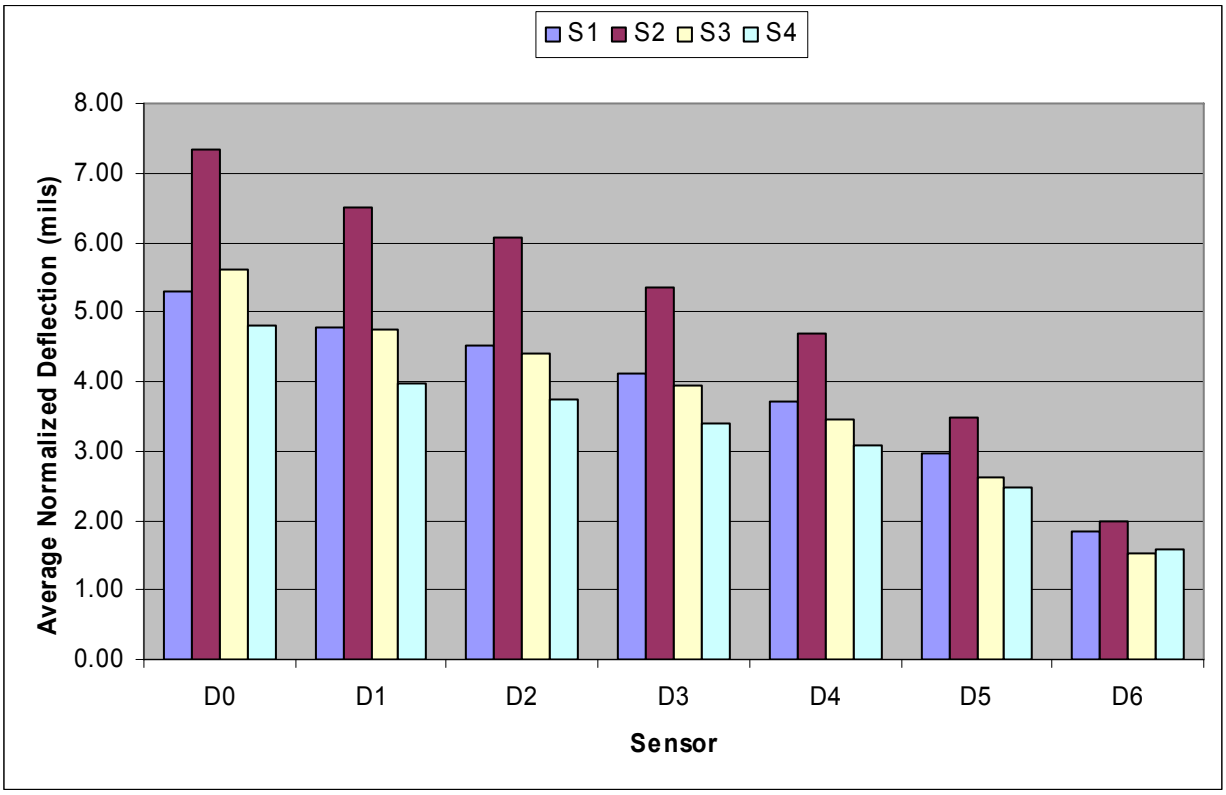


**Figure 3.4: Average Normalized Deflections for Perpetual Pavement Sections.**

Table 3.3 shows summary statistics of the FWD deflection and detailed results can be found in the Appendix A. Variation of deflection data from station to station on the same pavement section may be due to one or more of: (i) some variability in layer

thickness and material properties; (ii) variability in material properties might increase with time as a result of localized differential environmental effects; (iii) routine maintenance activities, and (iv) the inhomogeneous nature of the pavement materials (*Zaghloul et al., 2004*).

Standard deviation (STD) decreases for all new projects, whereas the coefficient of variation (COV) increases for US-54 and US-77 as distance from the center increases. There is no specific trend of COV for US-283, K-7 and K-99.

Standard deviation (STD) decreases for all test sections in general, whereas COV has no specific trend except for S1 in which COV increases as distance from the center increases. Studies have shown that in general COV increases as distance from the center increases.

**Table 3.3: Summary Statistics of FWD Deflection Data for Calibration Sites and Sections**

| | | Sensor | | | | | | |
|---|---|---|---|---|---|---|---|---|
| | | **D0** | **D1** | **D2** | **D3** | **D4** | **D5** | **D6** |
| **a. Calibration Sites** | | | | | | | | |
| **US-54** | Average (mils) | 3.28 | 2.74 | 2.49 | 2.16 | 1.85 | 1.31 | 0.63 |
| | STD (mils) | 0.34 | 0.33 | 0.31 | 0.28 | 0.24 | 0.18 | 0.12 |
| | COV(%) | 10.50 | 11.86 | 12.39 | 13.05 | 13.13 | 13.85 | 19.46 |
| **US-77** | Average (mils) | 7.97 | 6.36 | 5.73 | 4.95 | 4.32 | 3.2 | 1.8 |
| | STD (mils) | 1.54 | 1.53 | 1.47 | 1.36 | 1.26 | 1.09 | 0.81 |
| | COV(%) | 19.27 | 24.01 | 25.66 | 27.47 | 29.27 | 34.07 | 45.00 |
| **US-283** | Average (mils) | 15.35 | 9.73 | 7.95 | 6.43 | 5.31 | 3.73 | 2.21 |
| | STD (mils) | 1.49 | 1.27 | 1.05 | 0.77 | 0.54 | 0.33 | 0.22 |
| | COV(%) | 9.73 | 13.02 | 13.24 | 11.92 | 10.20 | 8.93 | 9.81 |
| **K-7** | Average (mils) | 9.01 | 6.51 | 5.43 | 4.35 | 3.52 | 2.57 | 1.62 |
| | STD (mils) | 1.20 | 0.99 | 0.81 | 0.61 | 0.46 | 0.33 | 0.22 |
| | COV(%) | 13.29 | 15.17 | 14.87 | 13.93 | 13.08 | 12.96 | 13.60 |
| **K-99** | Average (mils) | 12.46 | 9.40 | 7.81 | 6.15 | 4.77 | 2.95 | 1.49 |
| | STD (mils) | 0.30 | 0.27 | 0.23 | 0.19 | 0.15 | 0.08 | 0.02 |
| | COV(%) | 2.23 | 2.69 | 2.72 | 2.86 | 2.95 | 2.32 | 1.08 |
| **b. Perpetual Pavement Sections** | | | | | | | | |
| **S1** | Average (mils) | 5.30 | 4.78 | 4.51 | 4.10 | 3.70 | 2.96 | 1.85 |
| | STD (mils) | 0.28 | 0.29 | 0.30 | 0.30 | 0.29 | 0.27 | 0.17 |
| | COV(%) | 5.30 | 6.03 | 6.56 | 7.29 | 7.92 | 8.97 | 9.32 |
| **S2** | Average (mils) | 7.34 | 6.52 | 6.06 | 5.36 | 4.68 | 3.49 | 1.99 |
| | STD (mils) | 0.20 | 0.18 | 0.17 | 0.15 | 0.13 | 0.09 | 0.04 |
| | COV(%) | 2.67 | 2.70 | 2.84 | 2.79 | 2.71 | 2.71 | 1.86 |
| **S3** | Average (mils) | 5.62 | 4.75 | 4.42 | 3.94 | 3.46 | 2.62 | 1.53 |
| | STD (mils) | 0.12 | 0.11 | 0.10 | 0.09 | 0.08 | 0.06 | 0.04 |
| | COV(%) | 2.06 | 2.29 | 2.24 | 2.32 | 2.25 | 2.41 | 2.51 |
| **S4** | Average (mils) | 4.80 | 3.98 | 3.75 | 3.41 | 3.08 | 2.47 | 1.58 |
| | STD (mils) | 0.14 | 0.10 | 0.09 | 0.08 | 0.07 | 0.06 | 0.03 |
| | COV(%) | 3.00 | 2.43 | 2.50 | 2.49 | 2.37 | 2.28 | 1.95 |

### *3.3.2 Nonlinearity and Stress Sensitivity*

The subgrade materials have a nonlinear response to load. However, if the load is repeated several times, the effect of nonlinearity is reduced. The nonlinearity is very large when the load is applied for the first time since the strain is largely plastic. After many applications, the response is still somewhat nonlinear, but much less so.

Quantification of stress sensitivity was achieved by performing a linear regression on the FWD data. In the regression analyses, deflection was taken as the dependent variable and stress as the independent variable. Three levels of stresses have been used for all calibration sites, whereas one stress level was used in testing for all US-75 sections. Figure 3.5 shows the coefficient of determination ($R^2$) for calibration sites. Coefficient of determination ($R^2$) varies from 0.99 to 1.0 indicating that the assumption of linearity is reasonable within the stress range considered in the FWD test series.

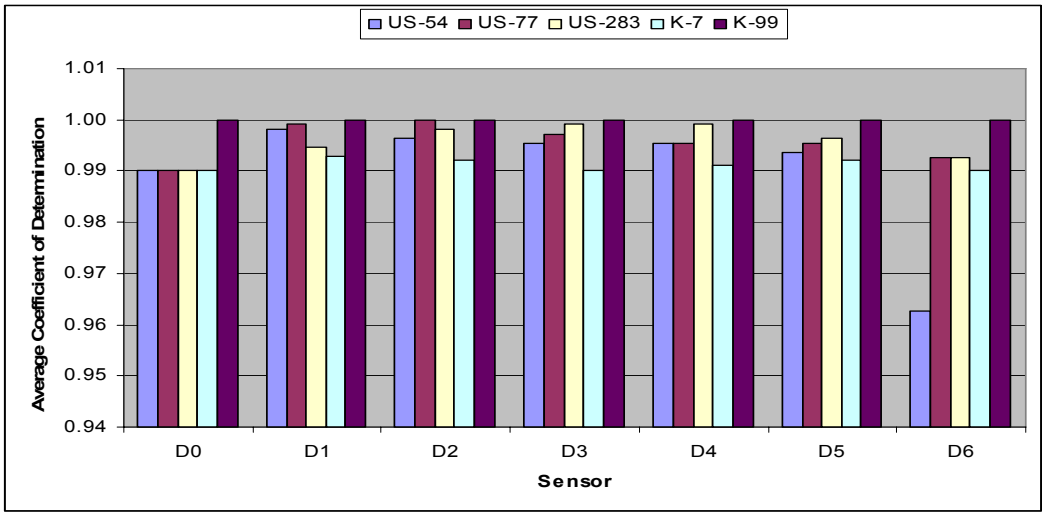


**Figure 3.4: Coefficient of Determination for Calibration Sites.**

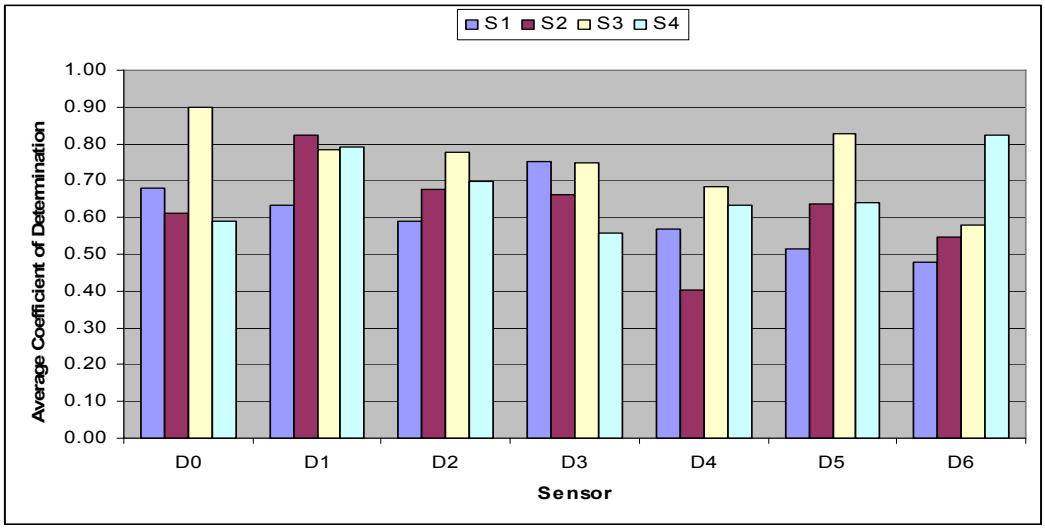


**Figure 3.5: Coefficient of Determination for Perpetual Pavement Sections.**

Figure 3.6 shows $R^2$ values for all perpetual pavement sections. Only 9 kip was used as the target load and that may be the reason why $R^2$ values are not high as compared to calibration sites. It seems that using different target loads reduces nonlinearity.

Table 3.4 shows summary statistics of stress sensitivity for all calibration sites and US-75 sections. The smallest $R^2$ for the calibration sites is 0.96 which occured under the most distant sensor for US-54. K-99 has all $R^2$ equal to 1 since three target loads were repeated three times on K-99. This clearly shows that repeating different target loads reduces nonlinearity significantly. There is no specific trend for STD and COV for all calibration sites. Coefficient of determination ($R^2$) varies from 0.48 to 0.75 for S1, 0.58 to 0.90 for S2, 0.40 to 0.82 for S3 and 0.56 to 0.83 for S4. Similarly, there is no specific trend for STD whereas the US-75 sections have very large COV. Detailed results for each of the new projects and test sections are given in the Appendix B.

**Table 3.4: Summary Statistics of Stress Sensitivity for Calibration Sites and US-75 Sections**

| | | Sensor | | | | | | |
|---|---|---|---|---|---|---|---|---|
| | | **D0** | **D1** | **D2** | **D3** | **D4** | **D5** | **D6** |
| **a. Calibration Sites** | | | | | | | | |
| **US-54** | Avg. $R^2$ | 0.99 | 1.00 | 1.00 | 1.00 | 1.00 | 0.99 | 0.96 |
| | STD | 0.005 | 0.004 | 0.005 | 0.005 | 0.005 | 0.005 | 0.094 |
| | COV (%) | 0.51 | 0.41 | 0.51 | 0.52 | 0.52 | 0.51 | 9.76 |
| **US-77** | Avg. $R^2$ | 0.99 | 1.00 | 1.00 | 1.00 | 1.00 | 1.00 | 0.99 |
| | STD | 0.005 | 0.003 | 0.000 | 0.005 | 0.005 | 0.005 | 0.005 |
| | COV (%) | 0.53 | 0.30 | 0.00 | 0.47 | 0.52 | 0.52 | 0.47 |
| **US-283** | Avg. $R^2$ | 0.99 | 0.99 | 1.00 | 1.00 | 1.00 | 1.00 | 0.99 |
| | STD | 0.004 | 0.005 | 0.004 | 0.003 | 0.003 | 0.005 | 0.005 |
| | COV (%) | 0.41 | 0.53 | 0.41 | 0.30 | 0.30 | 0.51 | 0.47 |
| **K-7** | Avg. $R^2$ | 0.99 | 0.99 | 0.99 | 0.99 | 0.99 | 0.99 | 0.99 |
| | STD | 0.000 | 0.005 | 0.004 | 0.000 | 0.003 | 0.004 | 0.000 |
| | COV (%) | 0.00 | 0.49 | 0.43 | 0.00 | 0.32 | 0.43 | 0.00 |
| **K-99** | Avg. $R^2$ | 1.00 | 1.00 | 1.00 | 1.00 | 1.00 | 1.00 | 1.00 |
| | STD | 0.00 | 0.00 | 0.00 | 0.00 | 0.00 | 0.00 | 0.00 |
| | COV (%) | 0.00 | 0.00 | 0.00 | 0.00 | 0.00 | 0.00 | 0.00 |
| **b. US-75 Sections** | | | | | | | | |
| **S1** | Avg. $R^2$ | 0.68 | 0.63 | 0.59 | 0.75 | 0.57 | 0.52 | 0.48 |
| | STD | 0.409 | 0.272 | 0.307 | 0.179 | 0.376 | 0.388 | 0.440 |
| | COV (%) | 59.87 | 43.01 | 51.90 | 23.87 | 66.27 | 75.16 | 91.96 |
| **S2** | Avg. $R^2$ | 0.90 | 0.78 | 0.78 | 0.75 | 0.68 | 0.83 | 0.58 |
| | STD | 0.144 | 0.157 | 0.354 | 0.235 | 0.316 | 0.189 | 0.390 |
| | COV (%) | 16.02 | 19.96 | 45.63 | 31.33 | 46.25 | 22.85 | 67.43 |
| **S3** | Avg. $R^2$ | 0.61 | 0.82 | 0.68 | 0.66 | 0.40 | 0.64 | 0.55 |
| | STD | 0.377 | 0.187 | 0.296 | 0.371 | 0.292 | 0.367 | 0.365 |
| | COV (%) | 61.92 | 22.73 | 43.88 | 55.96 | 72.52 | 57.66 | 66.73 |
| **S4** | Avg. $R^2$ | 0.59 | 0.79 | 0.70 | 0.56 | 0.63 | 0.64 | 0.83 |
| | STD | 0.320 | 0.320 | 0.297 | 0.359 | 0.327 | 0.264 | 0.166 |
| | COV (%) | 54.01 | 40.55 | 42.60 | 64.50 | 51.75 | 41.21 | 20.17 |

# CHAPTER FOUR - DATA ANALYSIS

## 4.1 Backcalculation of AC Modulus

For backcalulation, FWD deflection data was normalized to 9 kip. Normalized deflection data for all new projects and test sections were used to backcalculate the AC modulus layers based on the multilayered linear elastic theory. The moduli of thin surface layers or sandwiched layers are usually difficult to obtain, because surface deflections are often insensitive to changes in the moduli of these layers. Changes in the moduli of subgrade or other thick layers may mask changes in thin layers (*Chou and Lytton, 1991*). Flexible pavements are usually analyzed as three-layered systems having an asphalt concrete surface layer, a mechanically or chemically stabilized base layer, and a subgrade (*Meier et al., 1997*). In this study, all pavement sections were modeled as three layer systems by combining all asphalt concrete layers into one layer. Comparison of solutions from different programs gives an idea of the range of solutions that can be expected (*Chou and Lytton, 1991*). Thus, three backcalculation computer programs, EVERCALC, MODCOMP 5 and MODULUS, were used in this study.

In the backcalculation of pavement layer moduli, the objective is to identify a set of pavement layer moduli that would produce a deflection basin matching the measured deflection basin. Since only a finite number of sensor data points are available from the deflection measurements, the objective function in the backcalculation analysis typically involves the minimization of the root-mean- square difference ($D_{rms}$) of the measured and computed deflections. A solution that has a smaller $D_{rms}$ value is considered to be a better fit, and thus a better solution (*Fwa et al., 1997*).

$$\text{Minimize } D_{rms} = \sqrt{\frac{1}{m}\sum_{i=1}^{m}\left(\frac{d_i - D_i}{D_i}\right)} \qquad \text{Equation 4.1}$$

where,

$m$ = number of deflection-measurement points,

$d_i$ = backcalculated deflection at point i, and

$D_i$ = measured deflection at point i.

## 4.2 Temperature Correction of Backcalculauted Modulus

The most important environmental factor affecting surface deflections and backcalculated AC moduli of flexible pavements is the temperature of the asphalt concrete layer. To determine corrected AC modulus, a two-step correction procedure was followed in this study.

### *4.2.1 AC Layer Temperature*

The BELLS equation was developed using the measured temperatures at different pavement depths from the Long Term Pavement Performance (LTPP) data base for predicting temperature at the one-third depth point of the asphalt pavement (*Inge and Kim, 1995*). Mid-depth temperature was computed using BELLS3, which is used for routine testing.

$$T_d = 0.95 + 0.892T_s + (\log d - 1.25) * \left[1.83\sin\left(2\pi\frac{A}{18}\right) - 0.448T_s + 0.621T_{avg}\right] + 0.042T_s \sin\left(2\pi\frac{B}{18}\right) \qquad \text{Equation 4.2}$$

where,

$T_d$ = pavement temperature at layer mid-depth ($^oC$),

$T_s$ = infrared surface temperature ($^oC$),

$T_{avg}$ = average of high and low air temperatures on the day before testing ($^oC$),

and

d = layer mid-depth (mm).

A and B are computed as follows:

$$A = \begin{cases} t_d + 9.5 & \text{if} \quad 0 \le t_d < 5 \\ -4.5 & \text{if} \quad 5 \le t_d < 11 \\ t_d - 15.5 & \text{if} \quad 11 \le t_d < 24 \end{cases} \qquad B = \begin{cases} t_d + 9.5 & \text{if} \quad 0 \le t_d < 3 \\ -4.5 & \text{if} \quad 3 \le t_d < 9 \\ t_d - 13.5 & \text{if} \quad 9 \le t_d < 24 \end{cases}$$

where,

$t_d$ = time of day (in decimal hours).

The last two variables are used as arguments to a pair of sine functions with 18-h periods and 15.5-and 13.5-h phase lags, respectively. One cycle per day is allowed. During the other 6 hours of the day, A and B are set equal to -4.5 so that the sine functions return a value of -1.

### ***4.2.2 Temperature Correction for AC Modulus***

*Chen et al. (2000)* has developed Equation 4.3 based on deflections from intact locations. This equation was used in this study since it can be used to adjust AC modulus to any temperature. AC modulus was corrected to 40, 70, and 95 $^{o}$F temperatures in this study to compare with the laboratory and predicted moduli.

$$E_{T_w} = \frac{E_{T_c}}{\left[(1.8T_w + 32)^{2.4462} * (1.8T_c + 32)^{-2.4462}\right]} \qquad \text{Equation 4.3}$$

where,

$E_{T_w}$ = adjusted modulus of elasticity at $T_w$ (MPa),

$E_{T_c}$ = measured modulus of elasticity at $T_c$ (MPa),

$T_w$ = temperature to which the modulus of elasticity is adjusted ($^{o}$C), and

$T_c$ = mid-depth temperature at the time of FWD data collection ($^{o}$C).

## 4.3 Laboratory Test for Dynamic Modulus

Core samples were trimmed to the required height of 6 inches. Samples with a diameter of 4 inches and height of 6 inches were tested using the Universal Testing Machine (UTM-25) in the laboratory. UTM-25 is a servo-control testing machine that produces a controlled sinusoidal (haversine) compressive loading. It can apply loads over a range of frequencies from 0.01 to 30 Hz and stress levels up to 400 psi. The environmental chamber holds the temperature of the specimen constant at any set of temperature range from 14 to 140 $^{o}$F. The measurement system is fully computer-controlled. It measures and records the time history of the applied load and the axial deformations.

The load is measured with an electronic load cell that is in contact with one of the specimen caps. Hardened steel disks transfer the load from the testing machine to the specimen. Top and bottom surface friction is a very practical problem for compression type testing. In order to eliminate the possibility of having shear stresses on the specimen ends during testing, pairs of rubber membranes with vacuum grease are placed on the top and bottom of each specimen during testing.

Axial deformations are measured with linear variable differential transformers (LVDT's) placed vertically on the diametrically opposite sides of the specimen. Parallel brass studs are used to secure the LVDT's in place. Two pairs of studs are glued on the two opposite cylindrical surfaces of a specimen. The studs in a pair are 4 inches apart and are located at approximately the same distance from the top and bottom of the specimen.

AASHTO TP 62-03 (Standard Method of Test for Determining Dynamic Modulus of HMA Concrete Mixtures) (*AASHTO, 2001*) was followed except for some minor modifications in test temperature and frequencies. The underlying principle that allowed the modification of the original test protocol is the concept of time-temperature superposition (or time-temperature equivalence). That is the same modulus value of a material can be obtained either at low test temperatures and long times or at high test temperatures and short times. This theoretical justification allowed the increase in the number of frequencies and the decrease in the number of test temperatures (*NCHRP, 2002*). Some studies have suggested that one can use a three-temperature test protocol, which would require a shorter testing time, and obtain the same dynamic modulus data as the five-temperature test protocol would yield. In this study, three temperatures, 40, 70 and 95$^{o}$F, and six frequencies, 0.1, 0.5, 1, 5, 10 and 25 Hz, were used.

## 4.4 Computation of Dynamic Modulus Using Predictive Models

The effect of aging was incorporated into the determination of dynamic modulus using the global aging system (*Mirza and Witczak, 1995*). The original, mix/lay-down, surface aging and aging at different depths and corresponding viscosities were determined at different temperatures (40, 70 and 95 $^{o}$F) and frequencies (0.1, 0.5, 1, 5, 10 and 25 Hz). Temperature data for different project locations was obtained from the KSU weather data library.

For original conditions, the viscosity of the asphalt binder at the temperature of interest is determined from the ASTM viscosity temperature relationship defined by Equation (4.4). If predictions with a minimal bias are desired, the viscosity–temperature

regression coefficients (A and VTS) should be obtained from the Brookfield rotational viscometer tests, or if no binder test results are available, from the mix/lay-down conditions proposed by *Witzcak and Fonseca (1996)*. For this study, A and VTS values were taken from the M-EPDG manual corresponding to different performance grades.

$$\log\log\eta_{cri} = A + VTS\log T_R \qquad \text{Equation 4.4}$$

where,

$\eta_{ori}$ = original viscosity (cP),

$T_R$ = temperature (Rankine),

A = regression equation intercept, and

VTS = regression slope of the viscosity-temperature relationship.

Equation 4.5 presents the Global Aging System model for short-term aging. The code value is related to the hardening ratio, defined as the ratio of the log-log mix/lay-down viscosity (RTFO) to log-log original viscosity. Average hardening ratio was assumed in this study.

$$\log\log(\eta_{t=0}) = a_0 + a_1\log\log(\eta_{cri}) \qquad \text{Equation 4.5}$$

$$a_0 = 0.054405 + 0.004082 * code$$

$$a_1 = 0.972035 + 0.010886 * code$$

where,

$\eta_{t=0}$ = mix/lay-down viscosity (cP),

$\eta_{ori}$ = original viscosity (cP), and

code = hardening ratio (0 for average).

In-service viscosity aging model for surface conditions is shown in Equation 4.6. The model is a hyperbolic function and includes the effect of environment on the long

term aging. The environmental considerations enter through the use of mean annual air temperature in the parameter A.

$$\log\log(\eta_{aged}) = \frac{\log\log(\eta_{t=0}) + At}{1 + Bt} \qquad \text{Equation 4.6}$$

where,

$$A = -0.004166 + 1.41213(C) + (C)\log(Maat) + (D)\log\log(\eta_{t=0})$$

$$B = 0.197725 + 0.0683841\log(C)$$

$$C = 10^{(274.4946 - 193.831\log(T_R) + 33.9366\log(T_R)^2}$$

$$D = -14.5521 + 10.47662\log(T_R) - 1.88161\log(T_R)^2$$

$\eta_{aged}$ = aged viscosity (cP),

$\eta_{t=0}$ = viscosity at mix/lay-down (cP),

Maat = mean annual air temperature ($^oF$),

$T_R$ = temperature (Rankine), and

t = time in months.

Since bulk unit weight and air void have been determined in laboratory using core samples taken from the field, the model to adjust the aged viscosity is not required.

Finally, the depth describes the aged viscosity as a function of depth based on the aged viscosity from the surface aging model and viscosity at mix/lay-down. Equation (4.7) presents the viscosity-depth relationship.

$$\eta_{t,z} = \frac{\eta_t(4+E) - E(\eta_{t=0})(1-4z)}{4(1+Ez)} \qquad \text{Equation 4.7}$$

where,

$\eta_{t,z}$ = Aged viscosity at time $t$ and depth $z$ (Mpoise),

$\eta_t$ = Aged surface viscosity (MPoise),

$z$ = depth (in),

$E = 2383e^{(-0.0308\ maat)}$, and

Maat = mean annual air temperature ($^oF$).

In this study, dynamic modulus of the asphalt pavement layer material was estimated using the Witczak equation, new Witczak model and Hirsch model.

## 4.5 Witczak Equation

The predictive equation developed by *Witczak et al. (2002)* is one of the most comprehensive mixture dynamic modulus models available today. It is capable of predicting the dynamic modulus of dense-graded HMA mixtures over a range of temperatures, rates of loading and aging conditions from information that are usually available from the conventional binder tests and the volumetric properties of the HMA mixture. The Witczak predictive equation is shown in Equation (4.8).

$$\log E^* = 3.750063 + 0.02932\rho_{200} - 0.001767(\rho_{200})^2 - 0.002841\rho_4 - 0.058097V_a$$
$$-0.802208\left(\frac{V_{beff}}{V_{beff}+V_a}\right) + \frac{3.871977 - 0.0021\rho_4 + 0.003958\rho_{38} - 0.000017(\rho_{38})2 + 0.005471\rho_{34}}{1+e^{(-0.603313-0.313351\log(f)-0.393532\log(\eta))}} \quad \text{Equation 4.8}$$

where,

$E^*$ = dynamic modulus (psi),

$\eta$ = bitumen viscosity (MPoise),

$f$ = loading frequency (Hz),

$V_a$ = air void content (%),

$V_{beff}$ = effective bitumen content (% by volume),

$\rho_{34}$ = cumulative % retained on the ¾ in sieve,

$\rho_{38}$ = cumulative % retained on the 3/8 in sieve,

$\rho_4$ = cumulative % retained on the No.4 sieve, and

$\rho_{200}$ = % passing the No. 200 sieve.

## 4.6 Hirsch Model

During 1999 to 2001, *Pellinen (2001)* conducted dynamic modulus testing of 18 HMA mixtures. Based on this database, *Christensen et al. (2003)* developed a new dynamic modulus prediction model based on an existing version of the law of mixtures, called the Hirsch model. This model combines the series and parallel elements of phases. In applying the Hirsch model to the asphalt concrete, the relative portion of material in parallel arrangement, called contact volume, is not constant but varies with time and temperature. This model is as follows:

$$|E^*|_{mix} = Pc\left[4{,}200{,}000\left(1-\frac{VMA}{100}\right)+3|G^*|_{binder}\left(\frac{VFA * VMA}{10{,}000}\right)\right]$$
$$+(1-Pc)*\left[\frac{1-\frac{VMA}{100}}{4{,}200{,}000}+\frac{VMA}{3 * VFA * |G^*|_{binder}}\right]^{-1} \quad \text{Equation 4.9}$$

where,

$|E^*|_{mix}$ = dynamic modulus of the mixture (psi),

$|G^*|_{binder}$ = shear modulus of the binder (psi),

VMA = voids in the mineral aggregates (%),

VFA = percent of VMA filled with binder (%), and

Pc = contact volume estimated from the following equation.

$$Pc = \frac{\left(20+\frac{VFA * 3|G^*|_{binder}}{VMA}\right)^{0.58}}{650+\left(\frac{VFA * 3|G^*|_{binder}}{VMA}\right)^{0.58}} \quad \text{Equation 4.9a}$$

## 4.7 New Witczak Model

*Bari (2005)* has developed a new comprehensive Witczak equation as part of his doctoral research at Arizona State University:

$$\log_{10} E^* = -0.349 + 0.754\left(\left|G_b^*\right|^{-0.0052}\right)\left(\begin{array}{l} 6.65 - 0.032\rho_{200} + 0.0027\rho_{200}^2 + 0.011\rho_4 - 0.0001\rho_4^2 \\ +0.006\rho_{38} - 0.00014\rho_{38}^2 0.08V_a - 1.06\left(\frac{V_{beff}}{V_a + V_{beff}}\right) \end{array}\right) \quad \text{Equation 4.10}$$

$$+\frac{2.558 + 0.032V_a + 0.713\left(\frac{V_{beff}}{V_a + V_{beff}}\right) + 0.0124\rho_{38} - 0.0001\rho_{38}^2 - 0.0098\rho_{34}}{1 + e^{(-0.7814 - 0.5785\log\left|G_b^*\right| + 0.8834\log\delta_b)}}$$

where,

$E^*$ = dynamic modulus (psi),

$\rho_{200}$ = percentage of aggregates (by weight of the total aggregates) passing through No. 200 sieve (%),

$\rho_4$ = aggregates (by weight) retained on No. 4 sieve (%),

$\rho_{38}$ = aggregates (by weight) retained on the 3/8 in sieve (%),

$\rho_{34}$ = aggregates (by weight) retained on the ¾ in sieve (%),

$V_a$ = air voids (by volume of the mix) (%),

$V_{beff}$ = effective binder content (by volume of the mix) (%),

$\left|G_b^*\right|$ = dynamic shear modulus of binder (psi), and

$\delta_b$ = phase angle of binder associated with $\left|G_b^*\right|$ (deg).

*Bari (2005)* has also developed dynamic shear modulus and phase angle models, which are inputs into the dynamic modulus model, using 8,940 data points from 41 binders including nine that were modified. The final models are:

$$\left|G_b^*\right| = 0.0051 f_s \eta_{f_s,T} (\sin\delta)^{7.1542 - 0.4929 f_s + 0.0211 f_s^2} \quad \text{Equation 4.11}$$

where,

$\left|G_b^*\right|$ = dynamic shear modulus (Pa),

$f_s$ = dynamic shear loading frequency to be used with $\left|G_b^*\right|$ and $\delta_b$ (Hz),

$\eta_{f_s,T}$ = viscosity of asphalt binder as a function of loading frequency ( $f_s$ ) and temperature ( $T$ ) (cP), and

$\delta_b$ = phase angle (predicted from the $\delta_b$ model) (deg),

$$\delta_b = 90 + (b_1 + b_2 VTS') * \log(f_s * \eta_{f_s,T}) + (b_3 + b_4 VTS') * \log(f_s * \eta_{f_s,T})^2 \quad \text{Equation 4.11a}$$

$$\log\log\eta_{f_s,T} = A' + VTS' \log T_R \quad \text{Equation 4.11b}$$

$$A' = c_0 f_s^{c_1} * A \quad \text{Equation 4.11c}$$

$$VTS' = d_0 f_s^{d_1} * VTS \quad \text{Equation 4.11d}$$

where,

$\delta_b$ = phase angle (deg),

A = regression intercept from the conventional ASTM Ai-VTSi relationship,

VTS = slope from the conventional ASTM Ai-VTSi relationship,

A' = adjusted A (adjusted for loading frequency),

VTS' = adjusted VTS (adjusted for loading frequency),

$f_s$ = loading frequency in dynamic shear (Hz),

$\eta_{f_s,T}$ = viscosity of asphalt binder as a function of loading frequency ($f_s$) and temperature ($T$) (cP), and

$T_R$ = temperature in Rankine scale ($^oR$), and

$b_1, b_2, b_3, b_4, c_0, c_1, d_0$, $d_1$ = fitting parameters = -7.3146, -2.6162, 0.1124, 0.2029, 0.9699, -0.0527, 0.9668, and -0.0575, respectively.

## 4.8 KDOT Design AC Modulus

As mentioned earlier, KDOT currently follows the 1993 AASHTO Design Guide. In the Guide, Equation (4.12) can be used to compute the design modulus of AC pavements. If all asphalt layers (surface, binder and base) are considered as one layer (as assumed during backcalculation of AC modulus in this study), the composite layer coefficient is calculated by KDOT by treating the top one-third of the AC thickness as the bituminous surface and the remaining thickness as the bituminous base as shown in Equation (4.12a). These equations have been used to compute the KDOT AC design modulus in this study.

$$E = 4351 \log^{-1}\left(\frac{\text{composite } a_1 - 0.44}{0.4}\right) \qquad \text{Equation 4.12}$$

$$\text{Composite a1} = \frac{(d_1 * a_1) + (d_2 * a_2)}{(d_1 + d_2)} \qquad \text{Equation 4.12a}$$

where,

$d_1$ and $d_2$ = bituminous surface and base thickness, respectively, and

$a_1$ and $a_2$ = structural layer coefficients for the bituminous surface and base, respectively.

# CHAPTER FIVE - LABORATORY DYNAMIC MODULUS

## 5.1 Features of Dynamic Modulus (E*)

The dynamic modulus of a material is a viscoelastic test response under sinusoidal loading conditions. It is the absolute value of the peak-to-peak stress divided by the peak-to-peak strain for a material subjected to a sinusoidal loading (Yoder and Witczak, 1975). Linear viscoelasticity refers to behavior in which the dynamic modulus is independent of stress or strain. The phase angle is one of the two output variables in the dynamic modulus test. The phase angle is a direct indicator of the elastic-viscous properties of the mix or binder material. The value of zero is indicative that the material is behaving as a pure elastic material. A value of 90 indicates a pure viscous (Newtonian) material.

The complex modulus can be obtained from a standard laboratory testing. When the applied stress is normal, the complex modulus is denoted by E*. The sinusoidal stress can be represented as follows (Yoder and Witczak, 1975):

$$\sigma = \sigma_0 e^{iwt} = \sigma \cos(\omega t) + i\sigma_0 \sin(\omega t) \qquad \text{Equation 5.1}$$

where,

$\sigma$ = sinusoidal stress magnitude at time $t$,

$\sigma_0$ = maximum stress amplitude,

$\omega = 2\pi f$ = angular velocity (radians/s),

$f$ = loading frequency, and

$t$ = loading time (seconds).

As a result of the sinusoidal stress, the viscoelastic material experiences a sinusoidal strain ($\varepsilon$), which generally (but not always) lags the stress by a phase angle

($\varphi$). When stress is normal, strain is calculated based on maximum strain amplitude ($\varepsilon_0$) as:

$$\varepsilon = \varepsilon_0 e^{i(\omega t - \phi)} = \varepsilon_0 \cos(\omega t - \phi) + i\varepsilon_0 \sin(\omega t - \phi) \quad \text{Equation 5.2}$$

The ratio of sinusoidal stress to the sinusoidal strain is defined as complex modulus (E* for normal stress) and it is expressed as:

$$E^* = \frac{\sigma}{\varepsilon} = \frac{\sigma_0 e^{iwt}}{\varepsilon_0 e^{i(\omega t - \phi)}} \quad \text{Equation 5.3}$$

Complex modulus has a real and imaginary part, in which the real is called elastic/storage and the imaginary part is called viscous/loss. Finally, the ratio of stress to strain amplitude is defined as dynamic modulus ($|E^*|$). Dynamic modulus and the phase angle jointly describe the dynamic modulus.

$$|E^*| = \frac{\sigma_0}{\varepsilon_0} \quad \text{Equation 5.4}$$

## 5.2 Effect of Loading Rate on Laboratory Dynamic Modulus for Calibration Sites

Four-inch diameter and full depth cores were taken at the same locations where deflection tests were done for all calibration sites. All cores were cut to 6-inch heights using a diamond saw blade. Eleven cores were taken for each calibration sites and the number in the legend on the figures in this report shows the core number at corresponding station where deflection data was taken. Some of the cores from US-54 and US-77 were thicker than 12 inches and were cut into two test specimens, indicated as upper (U) and lower (L). The upper portion consists of surface, binder and some part of base courses whereas the lower part is totally base course. All cores were tested at 70$^o$F and only three samples were tested at all test temperatures: 40, 70, and 95$^o$F.

Results for individual projects at 70°F and six frequencies, 0.1, 0.5, 1, 10 and 25 Hz, are presented in the following sections. Detailed results at test temperatures can be found in the Appendix C.

### *5.2.1 Laboratory Dynamic Modulus for US-54*

Figure 5.1 indicates the laboratory dynamic modulus for US-54. Core 1 was missing whereas Core 3 had crack. Cores 5, 8 and 10 were cut into lower (L) and upper (U) portions, upper parts of Cores 5 and 8 were shorter than 6 inches. The core, 10U has the highest modulus at all frequencies- the magnitude is higher at a frequency of 0.5 Hz than at a frequency of 1 Hz. It confirms that the upper portion of the AC layer is stiffer than that of lower portion. The trend is similar for others except the dynamic modulus of 8L increased with frequency.

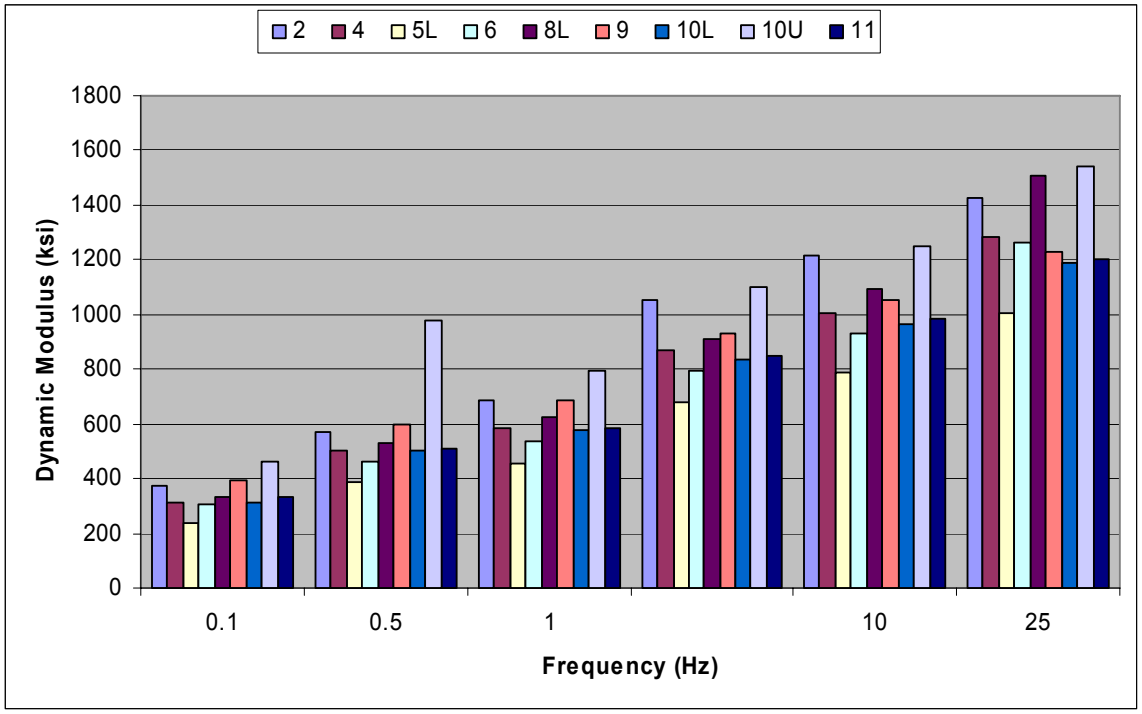


**Figure 5.1: Laboratory Dynamic Modulus for US-54 at 70°F.**

### 5.2.2 Laboratory Dynamic Modulus for US-77

Laboratory dynamic moduli for US-77 are shown in Figure 5.2. The core, 7L has the highest magnitude at all frequencies. Core 8 has the second highest modulus except at 25 Hz frequency. 6L has the lowest modulus except at 0.1 Hz whereas 10U has the lowest. 10U has the lowest modulus at 0.1 and 0.5 Hz frequencies, whereas 10L has higher modulus than 10U at all frequencies except at 25 Hz. This shows that the dynamic modulus is highly influenced by the loading frequency.

### 5.2.3 Laboratory Dynamic Modulus for US-283

All US-283 cores were less than 12 inches thick and as a result, only one sample from each core was tested as shown in Figure 5.3. Core 10 has the lowest modulus at all frequencies and Core 5 has the highest modulus at all frequencies except at the highest frequency. There is a change in trend mainly at 25 Hz.

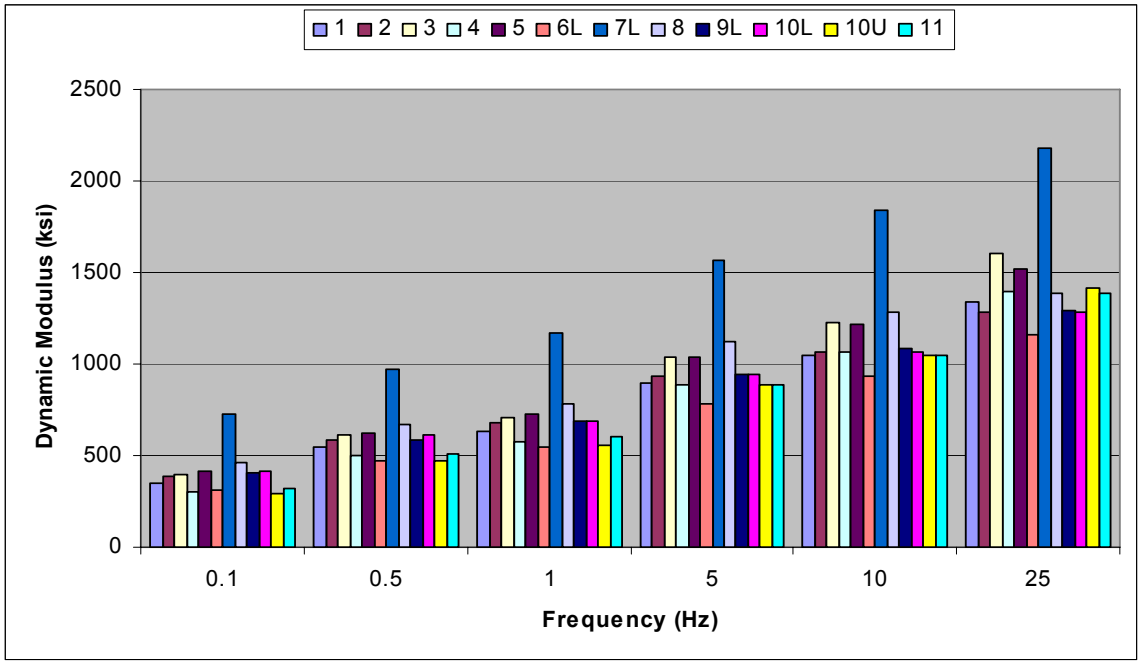


**Figure 5.2: Laboratory Dynamic Modulus for US-77 at 70°F.**

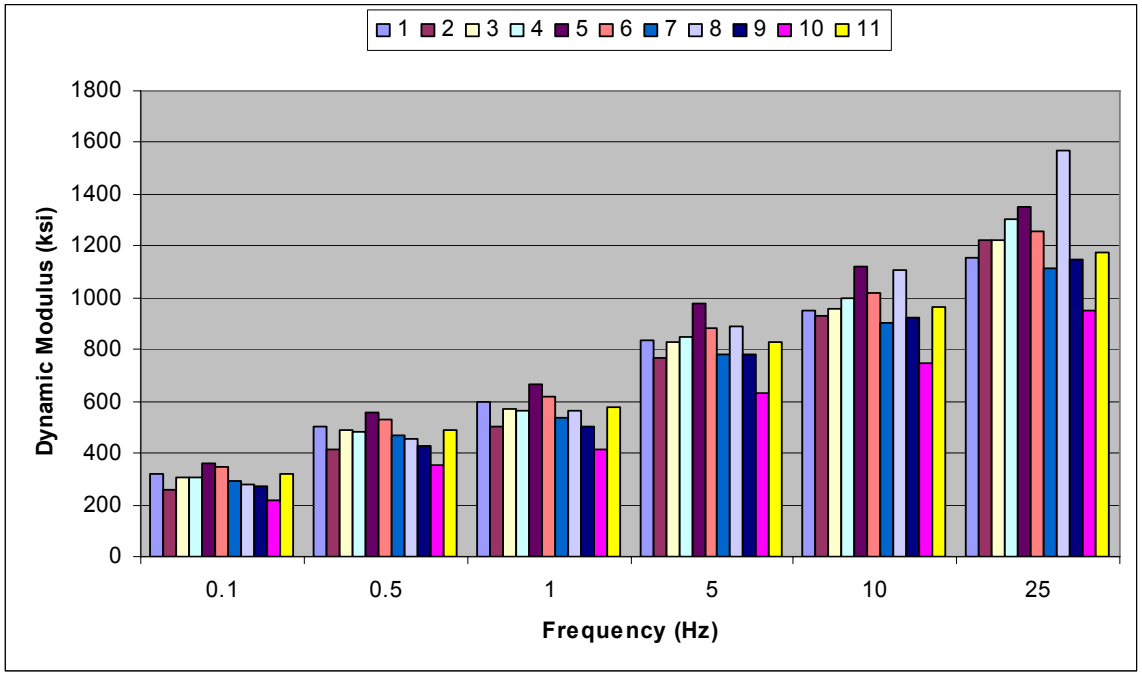


**Figure 5.3: Laboratory Dynamic Modulus for US-283 at 70°F.**

### *5.2.4 Laboratory Dynamic Modulus for K-7*

Figure 5.4 illustrates laboratory dynamic modulus for K-7. K-7 has the lowest AC thickness. The variation increases as the frequency increases. The trend also changes with the increase in frequency. Core 5 has the lowest modulus whereas Core 10 has the highest modulus except at the highest frequency.

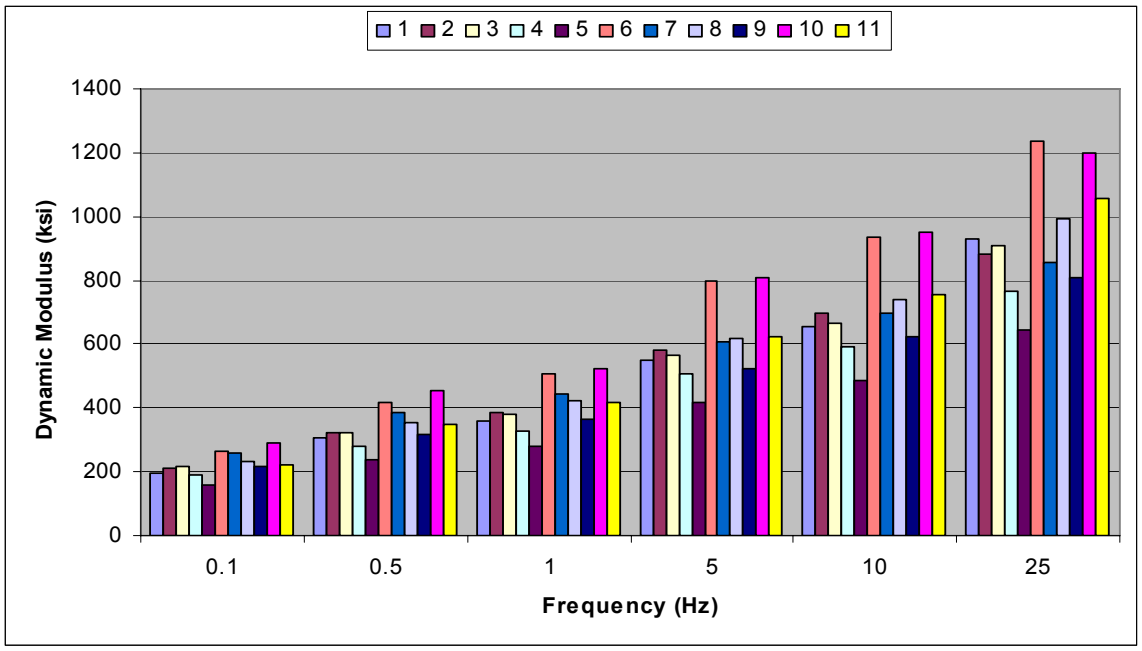


**Figure 5.4: Laboratory Dynamic Modulus for K-7 at 70°F.**

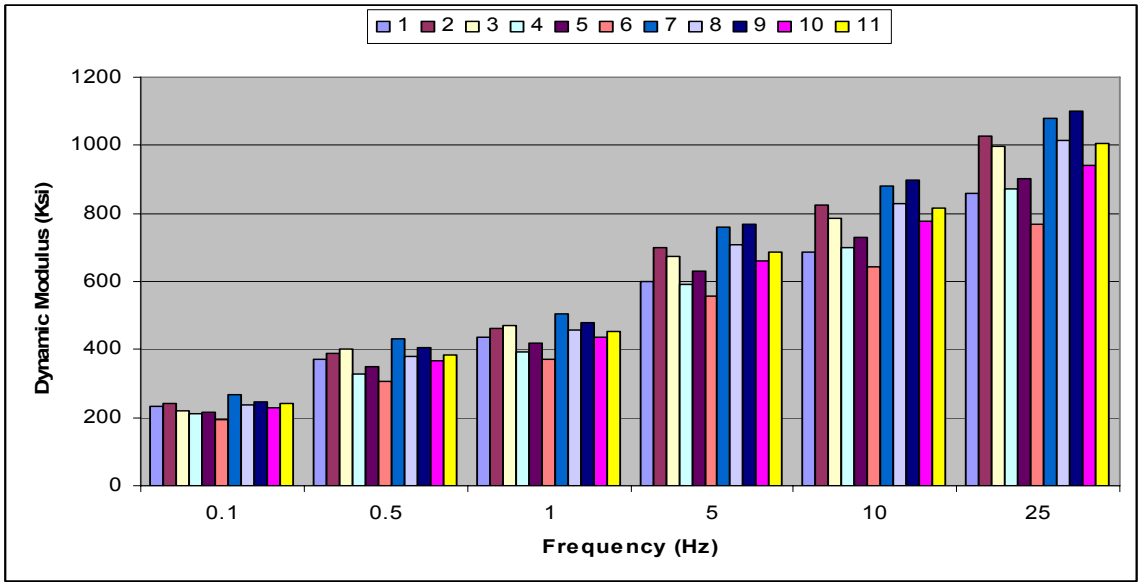


**Figure 5.5: Laboratory Dynamic Modulus for K-99 at 70°F.**

### *5.2.5 Laboratory Dynamic Modulus for K-99*

Dynamic modulus for K-99 is indicated in Figure 5.5. Core 6 has the lowest modulus. Core 7 has the highest for the first three frequencies. Core 9 has the highest

modulus for the last three frequencies. The variation increases with the frequency and the trend also changes with the frequency.

### *5.2.6 Comparison of Laboratory Dynamic Modulus for Calibration Sites*

Comparison of laboratory dynamic modulus has been done for all calibration sites at 70°F and is shown in Figure 5.6. US-77 has the highest average laboratory dynamic modulus at all frequencies, followed by US-54. K-7 has the lowest average dynamic modulus, followed by K-99.

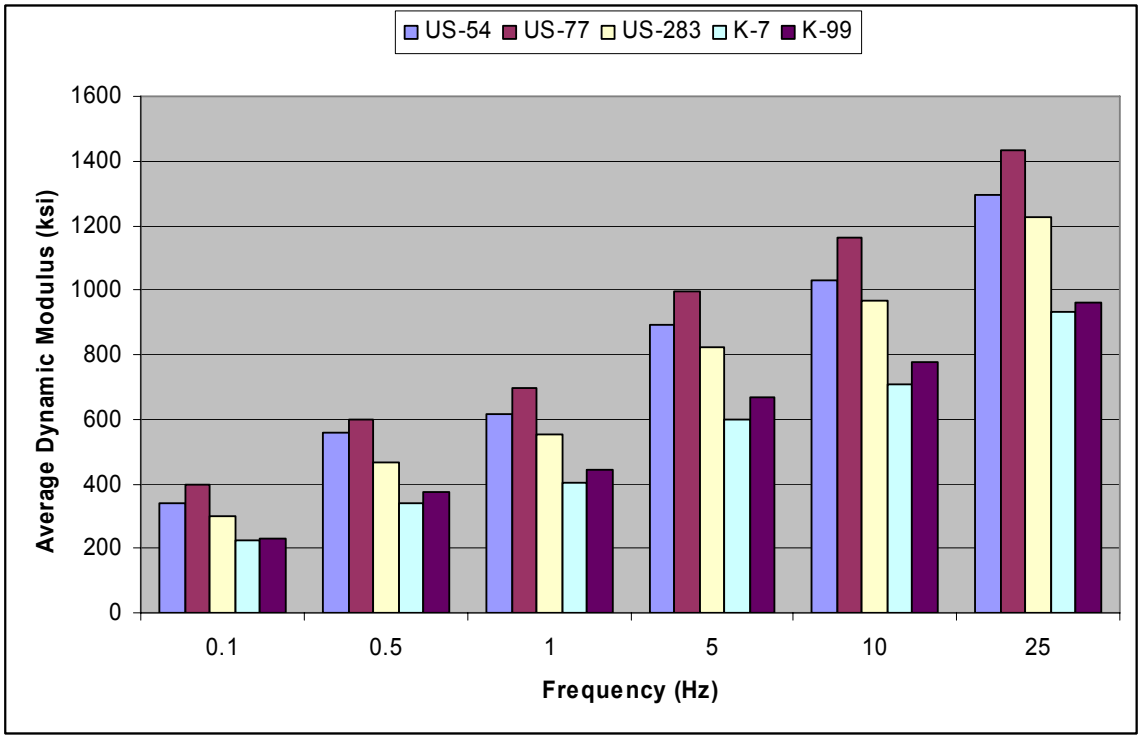


**Figure 5.6: Comparison of Laboratory Dynamic Modulus for Calibration Sites.**

Table 5.1 shows summary statistics of laboratory dynamic modulus for all calibration sites. The standard deviation (STD) increases with the increase in frequency for calibration sites. US-77 has the highest and K-7 has the lowest STD at all frequencies. The coefficients of variation (COV) for K-7 and K-99 slightly increase with the increase in frequency whereas there is no specific trend for the US-highways.

**Table 5.1: Comparison of Laboratory Dynamic Modulus for Calibration Sites at 70◦F**

| | | Frequency (Hz) | | | | | |
|---|---|---|---|---|---|---|---|
| | | 0.1 | 0.5 | 1 | 5 | 10 | 25 |
| **US-54** | **Av. Mod. (ksi)** | 341 | 561 | 615 | 891 | 1032 | 1295 |
| | **STD (ksi)** | 63 | 169 | 98 | 130 | 143 | 170 |
| | **COV(%)** | 18.3 | 30.1 | 15.9 | 14.6 | 13.8 | 13.1 |
| **US-77** | **Av. Mod. (ksi)** | 398 | 597 | 697 | 994 | 1160 | 1435 |
| | **STD (ksi)** | 116.0 | 133.0 | 165.0 | 201.0 | 235.0 | 260.0 |
| | **COV(%)** | 29.2 | 22.2 | 23.7 | 20.2 | 20.2 | 18.1 |
| **US-283** | **Av. Mod. (ksi)** | 298 | 469 | 555 | 823 | 966 | 1226 |
| | **STD (ksi)** | 40.0 | 56.0 | 66.0 | 88.0 | 102.0 | 155.0 |
| | **COV(%)** | 13.3 | 12.0 | 12.0 | 10.7 | 10.6 | 12.7 |
| **K-7** | **Av. Mod. (ksi)** | 222 | 341 | 402 | 599 | 708 | 935 |
| | **STD (ksi)** | 37.0 | 61.0 | 72.0 | 117.0 | 136.0 | 178.0 |
| | **COV(%)** | 16.7 | 17.9 | 18.0 | 19.5 | 19.3 | 19.1 |
| **K-99** | **Av. Mod. (ksi)** | 231 | 374 | 444 | 667 | 779 | 960 |
| | **STD (ksi)** | 20.0 | 35.0 | 39.0 | 67.0 | 82.0 | 101.0 |
| | **COV(%)** | 8.4 | 9.4 | 8.9 | 10.1 | 10.5 | 10.6 |

## 5.3 Effect of Temperature on Laboratory Dynamic Modulus

Comparison of laboratory dynamic modulus for calibration sites and perpetual pavement sections has been done at: 40, 70 and 95$^{o}$F and at a frequency of 25 Hz.

### *5.3.1 Effect of Temperature on Laboratory Dynamic Modulus for Calibration Sites*

Figure 5.6 shows the comparison of average laboratory dynamic modulus at three temperatures: 40, 70, and 95$^{o}$F and at a frequency of 25 Hz. K-7 cores were not tested at 95$^{o}$F since the sample started to soften at this temperature and consequently LVDT's could not be glued to the specimens.

All US routes have comparable average laboratory dynamic modulus at 40$^{o}$F and Kansas routes also show the same trend. The trend remains the same for Kansas routes at 70$^{o}$F unlike US routes. US-77 has the highest modulus at 70$^{o}$F whereas US-54 has the highest moudlus at 40$^{o}$F.

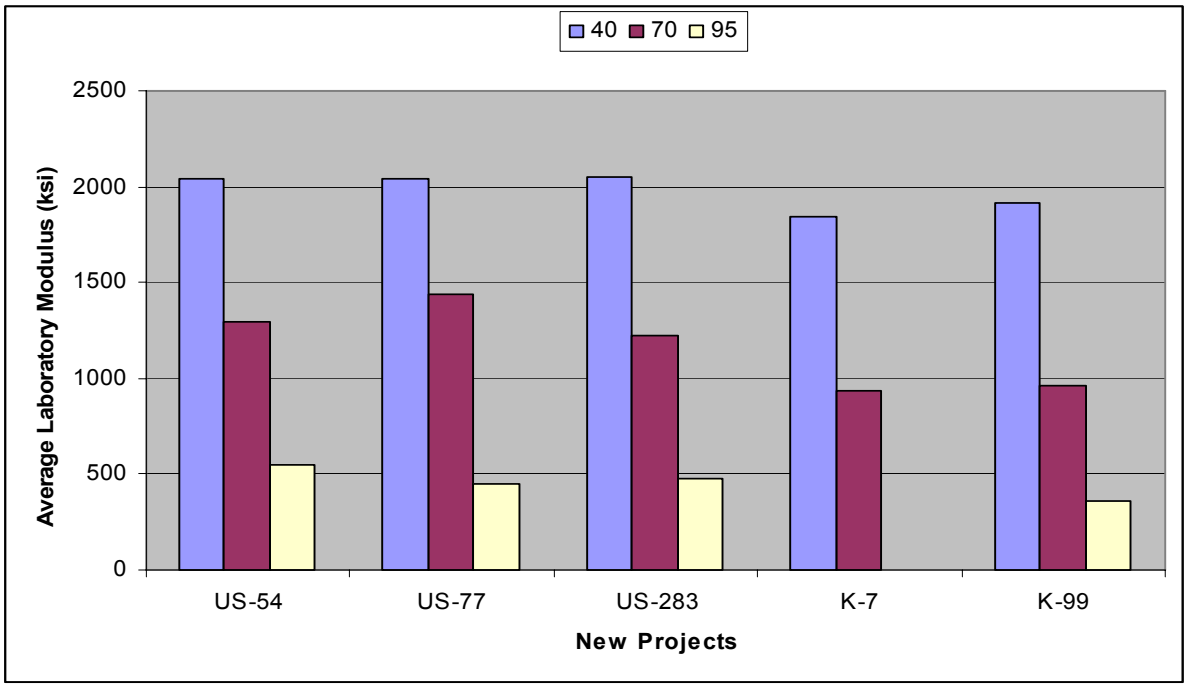


**Figure 5.7: Laboratory Dynamic Modulus for Calibration Sites.**

### *5.3.2 Effect of Temperature on Laboratory Dynamic Modulus for US-75 Sections*

For the test sections on US-75, samples of six different mixes in different layers of the sections were tested. The dynamic modulus was then calculated using Equation (5.5) based on the respective thickness of each mix in each section. As a result, only one modulus was calculated for each section as shown in Figure 5.8.

$$E_{eq} = \frac{\sum E_1 d_1}{\sum d_1} \qquad \text{Equation 5.5}$$

where,

$E_{eq}$ = equivalent dynamic modulus (ksi),

$E_i$ = dynamic modulus of mix in layer (ksi); and

$d_i$ = thickness of mix in layer i (in).

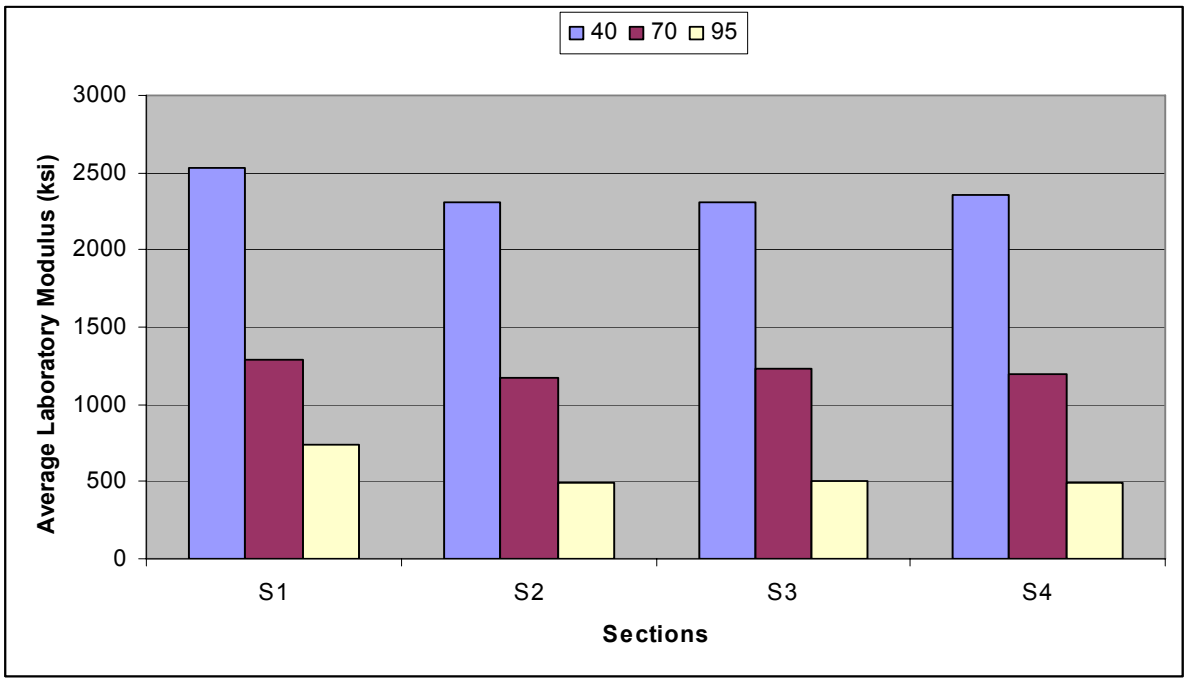


**Figure 5.8: Laboratory Dynamic Modulus for US-75 Sections at Various Temperatures (°F)**

Sections 2, 3 and 4 have comparable modulus at all temperatures. Section 1 has the highest dynamic modulus at all temperatures. This section has a modified, siffer binder in the base layer. Table 5.2 indicates the summary statistics of the laboratory dynamic modulus test results. All core samples were tested at 70°F, and three samples were tested at 40 °F and 95°F for all calibration sites except K-7. K-7 has the highest and K-99 has the lowest STD and COV at 40°F. US-77 has the highest average laboratory dynamic modulus and STD, whereas K-7 has the highest COV at 70°F. US-54 has the highest average modulus, lowest standard deviation and coefficient of variation at 95°F. This confirms that the dynamic modulus changes as the temperature changes and the degree of change depends upon the mix characteristics.

Dynamic modulus for Sections S1, S2, S3 and S4 are 2,536, 2,312, 2,307 and 2,357 ksi, respectively. The test was done only at 70°F and Equation 4.3 was used to convert to other temperatures. As a result, the trend is the same at all temperatures

except the change in magnitude. The mixture for Section S3 has the highest asphalt content, and it also shows the lowest dynamic modulus.

**Table 5.2: Comparison of Dynamic Modulus at Various Temperatures (◦F)**

| | 40°F | | | 70°F | | | 95°F | | |
|---|---|---|---|---|---|---|---|---|---|
| | **Avg. Mod (ksi)** | **S.D. (ksi)** | **COV (%)** | **Avg. Mod (ksi)** | **S.D. (ksi)** | **COV (%)** | **Avg. Mod (ksi)** | **S.D. (ksi)** | **COV (%)** |
| **a. Calibration Sites** | | | | | | | | | |
| **US-54** | 2037 | 304.3 | 14.9 | 1295 | 170.0 | 13.1 | 547 | 7.1 | 1.3 |
| **US-77** | 2039 | 112.7 | 5.5 | 1435 | 260.3 | 18.1 | 451 | 19.8 | 4.4 |
| **US-283** | 2046 | 145.5 | 7.1 | 1226 | 155.1 | 12.7 | 478 | 8.6 | 1.8 |
| **K-7** | 1845 | 338.2 | 18.3 | 935 | 178.1 | 19.1 | - | - | - |
| **K-99** | 1915 | 45.0 | 2.3 | 960 | 101.0 | 10.6 | 359 | 30.5 | 8.5 |
| **b. US-75 Test Sections** | | | | | | | | | |
| S-1 | 2536 | | | 1294 | | | 741 | | |
| S-2 | 2312 | | | 1170 | | | 498 | | |
| S-3 | 2307 | | | 1233 | | | 507 | | |
| S-4 | 2357 | | | 1191 | | | 489 | | |

# CHAPTER SIX - BACKCALCULATED MODULUS

## 6.1 Comparative Study of Backculation

Different backcalculation programs often give different results for the following reasons:

- The numerical routine used to calculate pavement surface deflections may be different,
- The method of searching for new values of the layer moduli may be different,
- Some methods try to correct for the stress dependency of the moduli,
- Criteria for determing convergence may be different, and
- Moduli ranges set by individual analysts may be different.

Three backcalculation computer programs have been used in this study: EVERCALC, MODCOMP 5 and MODULUS. The first two use iterative methods and the last one uses optimization method. Four methods have been used to determine seed modulus: (i) engineering judgment based on past experience; (ii) regression equations developed from past records; (iii) recommended seed values from backcalculation software, and (iv) forward calculation of deflection data.

## 6.2 EVERCALC

EVERCALC is a linear-elastic analysis backcalculation program that has been developed by the Washington State Department of Transportation. It uses WESLEA as the response analysis program, a complex integration algorithm based on Wendle's rule and nonlinear least-squares optimization technique with CHEVRONX (extended precision version of CHEVERON) as the forward-calculation program (*Chen et al., 1999*). It is capable of evaluating a flexible pavement structure containing up to five

layers. The program uses an iterative approach to find a set of moduli that would provide a calculated deflection basin closest to the measured deflection basin as characterized by the root-mean-square (RMS) technique. The program also has the capability of reading raw deflection data files for batch processing, which minimizes the amount of time required for entering the deflection data and the possibility of making transcription errors (*Zhou et al., 1997*).

It requires a set of seed modulus values to start, and adopts Newton's method to search for the set of deflections that best match the measured deflections. It uses regression equations to determine seed moduli for flexible pavements with up to three layers. The seed moduli must be user defined when the number of layers exceeds three.

### 6.3 MODCOMP

MODCOMP has been developed and upgraded by *Irwin (1994)*. Linear and non-linear pavement models can be considered using Modcomp. It is intended to be a researcher's tool. It can compute depth-to-stiff layers by comparing the rate of change of the outer measured deflections to how they would be expected to change if the subgrade was semi-infinite with a constant modulus. This method gives an approximate depth to rigid bottom, and it has the best accuracy if the rigid bottom is shallow. It can have up to 12 layers in the pavement system, but it is wise not to have too many unknown layers. The program generally works best if there are four or five unknown layers. Deflections are assigned to unknown layers in three ways: assigned by the computer, assigned by the user, or interpolated by the computer. Tolerances are

specified as a way of indicating when the solution is close enough. There are two tolerances: a deflection fit and the modulus rate of convergence.

MODSHELL, a user interface for MODCPMP5, is a menu-driven program that will enable the creation of new data files, editing of existing data files, processing of files, viewing of the output files on the screen, printing of output files and deleting files in MODCOMP5. Data can be entered in either SI metric system or the U.S. customary system of units. Some of the inputs to solve linear problems using MODCOMP5 are: layer type (known or unknown), load, deflection data, seed moduli, and poisson's ratio. $K_0$, density, $k_1$ and $k_2$ are required if the problem has one or more nonlinear layers.

## 6.4 MODULUS

MODULUS matches the measured deflection basin with a data base of deflection basins computed in advance for a variety of layer moduli (*Harichandran et al., 1994*). It has the capability to determine the depth to stiff layer, or subgrade thickness. It is calculated using "line of influence". This concept is related to the stress softening in the subgrade so that the depth to bedrock is a function of the ratio between the subgrade modulus and the modulus of the material underneath (*Rohde and Scullion, 1990*).

MODULUS can backcalculate up to four unknown layer moduli (including subgrade modulus). Backcalculating more than four unknown moduli is not recommended because of possible non-uniqueness. The calculated surface deflections and matching errors reported by the MODULUS program are obtained by interpolation of the pre-generated data base. Thus, the values are not exact (*Chou and Lytton, 1991*).

*Lytton (1989)* indicates that MODULUS has the advantages of speed, availability, and consistency of results compared with similar backcalculation programs. It uses a unique method to reduce the size of the data base so that the time to generate it and the time to find the solution from it are greatly reduced. The generated deflection data base is based on the ratio of layer moduli to the subgrade moduli. Thus the size of the data base is reduced by an order. The pattern search algorithm and the Lagrange interpolation techniques are used to find the layer moduli that minimize the error between the measured and the computed basins.

## 6.5 Point-by-Point Comparison of Backcalculated Modulus

Comparison of backcalculated modulus using three backcalculation programs, EVERCALC, MODCOMP 5 and MODULUS, have been done for the calibration sites and the perpetual pavement sections separately at 70$^{o}$F.

### *6.5.1 Comparison of Backcalculated Modulus for Calibration Sites*

Figure 6.1 shows the backcalculated moduli using three software programs for all calibration sites. AC modulus was corrected to 70$^{o}$F using mid-depth temperature. All programs yield comparable results for all calibration sites except EVERCALC gives unusual results for US-77. US-54 has the highest backcalculated modulus, which was tested at the lowest temperature. US-283 was tested at the highest temperature and it resulted in the lowest backcalculated modulus. The higher the test temperatures, the lower the backcalculated modulus irrespective of AC total thickness. This shows that the effect of temperature is greater than the AC thickness.

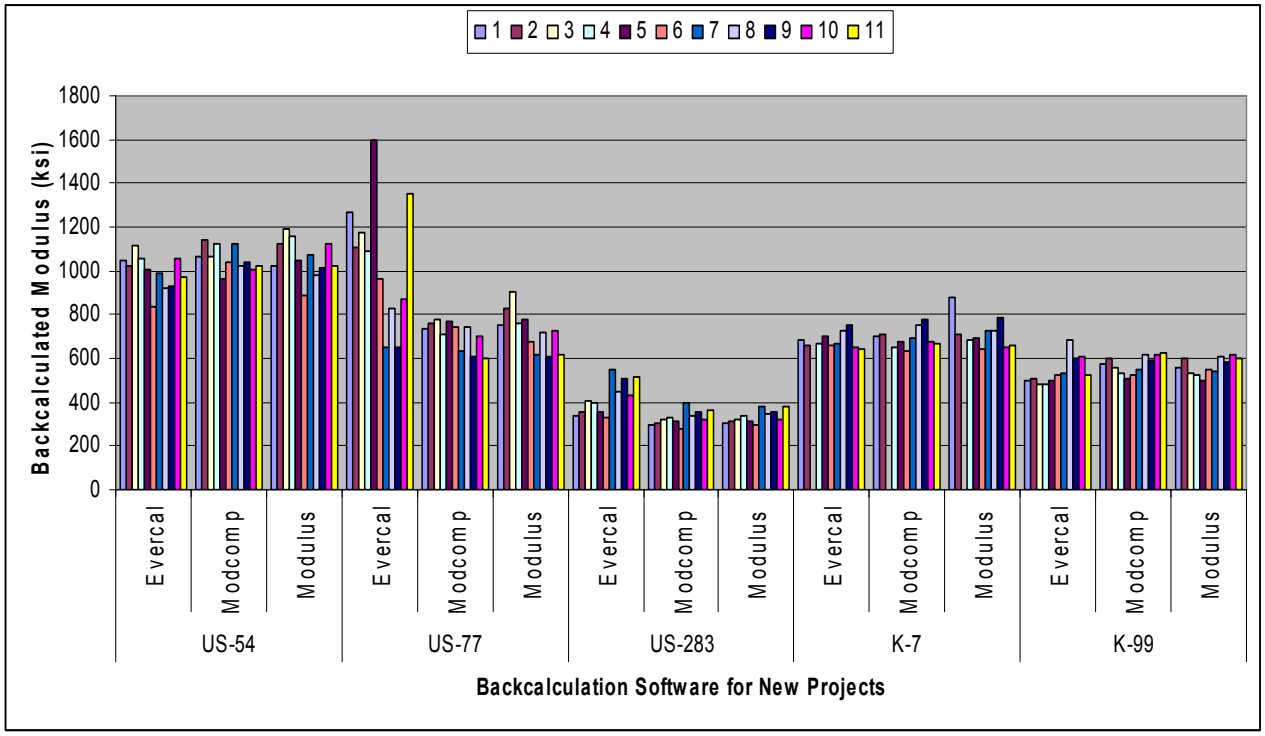


**Figure 6.1: AC Backcalculated Modulus for Calibration Sites at 70°F.**

Table 6.1 tabulates the backculated moduli corrected to 70°F using the three programs for all calibration sites. US-54 shows consistent results at all stations. Station 3 has the highest backcalculated modulus whereas Station 6 has the lowest backcaculated modulus using EVERCALC and MODULUS. Station 2 has the highest modulus whereas Station 5 has the lowest backculalted modulus using MODCOMP. In general, the backculated modulus using all three programs is comparable.

**Table 6.1: Comparison of Backcalculated Modulus for Calibration Sites at 70°F**

| | | Station No. | | | | | | | | | | |
|---|---|---|---|---|---|---|---|---|---|---|---|---|
| | | **1** | **2** | **3** | **4** | **5** | **6** | **7** | **8** | **9** | **10** | **11** |
| **US-54** | **Ever. (ksi)** | 1046 | 1023 | 1119 | 1055 | 1009 | 836 | 985 | 917 | 927 | 1054 | 976 |
| | **Modc.(ksi)** | 1067 | 1143 | 1068 | 1127 | 963 | 1036 | 1125 | 1020 | 1036 | 1004 | 1020 |
| | **Modu.(ksi)** | 1019 | 1126 | 1191 | 1156 | 1045 | 888 | 1070 | 982 | 1013 | 1121 | 1023 |
| **US-77** | **Ever. (ksi)** | 1271 | 1103 | 1171 | 1088 | 1595 | 965 | 647 | 832 | 654 | 872 | 1356 |
| | **Modc.(ksi)** | 739 | 758 | 780 | 707 | 769 | 741 | 635 | 740 | 606 | 700 | 600 |
| | **Modu.(ksi)** | 755 | 824 | 905 | 759 | 774 | 679 | 615 | 717 | 612 | 728 | 613 |
| **US-283** | **Ever. (ksi)** | 335 | 357 | 404 | 399 | 353 | 331 | 548 | 446 | 506 | 429 | 517 |
| | **Modc.(ksi)** | 299 | 303 | 317 | 328 | 315 | 278 | 395 | 336 | 357 | 317 | 364 |
| | **Modu.(ksi)** | 304 | 316 | 320 | 341 | 314 | 293 | 383 | 343 | 359 | 321 | 377 |
| **K-7** | **Ever. (ksi)** | 681 | 660 | | 666 | 703 | 661 | 670 | 723 | 749 | 652 | 639 |
| | **Modc.(ksi)** | 700 | 711 | | 652 | 675 | 632 | 697 | 755 | 778 | 675 | 668 |
| | **Modu.(ksi)** | 876 | 714 | | 682 | 696 | 643 | 729 | 725 | 783 | 649 | 658 |
| **K-99** | **Ever. (ksi)** | 497 | 511 | 482 | 482 | 495 | 520 | 533 | 688 | 602 | 607 | 527 |
| | **Modc.(ksi)** | 573 | 601 | 557 | 534 | 510 | 522 | 549 | 615 | 592 | 615 | 624 |
| | **Modu.(ksi)** | 557 | 598 | 536 | 522 | 500 | 547 | 540 | 609 | 587 | 620 | 596 |

US-77 has the highest variation in backculated modulus using EVERCALC. Stations 1 to 5 and Station 11 have very high backcalculated modulus. Station 3 has the highest modulus using MODCOMP and MODULUS whereas Station 1 has the highest modulus using EVERCALC. Station 9 has the lowest modulus using EVERCAL and MODULUS whereas Station 11 has the lowest using MODCOMP.

US-283 has the lowest backcalculated modulus since deflections were measured at the highest temperature. Station 7 and 6 has the highest and the lowest backcalculated modulus using all the three programss, respectively.

There is no backcalculated modulus at Station 3 on K-7 due to unusual deflection data. The backcalculated moduli for K-7 are very consistent using three programs. Station 6 has the lowest backcalcuted modulus using Modulus and Modcomp whereas Station 2 has the lowest using EVERCALC even if the difference in magnitude with

Station 6 is only 1000 psi. K-7 has the highest modulus at Station 9 using EVERCAL and MODCOMP whereas Station 1 using MODULUS.

MODCOMP and MODULUS give the lowest modulus at Station 5 whereas EVERCALC shows the lowest moduli at Stations 3 and 4. The three programss give the highest modulus at different stations unlike all other calibration sites: EVERCALC at Station 8, MODCOMP at Station 11 and MODULUS at Station 10 even if the variation in magnitude is not significant from a practical point of view.

### *6.5.2 Comparison of Backcalculated Modulus for Perpetual Pavement Sections*

Figure 6.2 shows the backcalculated moduli for all perpetual pavement sections on US-75. The order of sections in terms of thickness from the thinnest to the thickest: S2, S1, S3 and S4. It is to be noted that S1 and S3 have the same thickness, but the S1 has stiff binder in all layers (considered as stiff) and S3 has stiff surface binder only but with higher AC content (considered as flexible). The order of test temperature from the lowest to the highest: S1, S2, S3 and S4. Order of backcalculated modulus from lowest to highest: S1, S4, S3 and S2. This result clearly shows the effect of temperature, total AC thickness and binder stiffness on the backcalculated moduli.

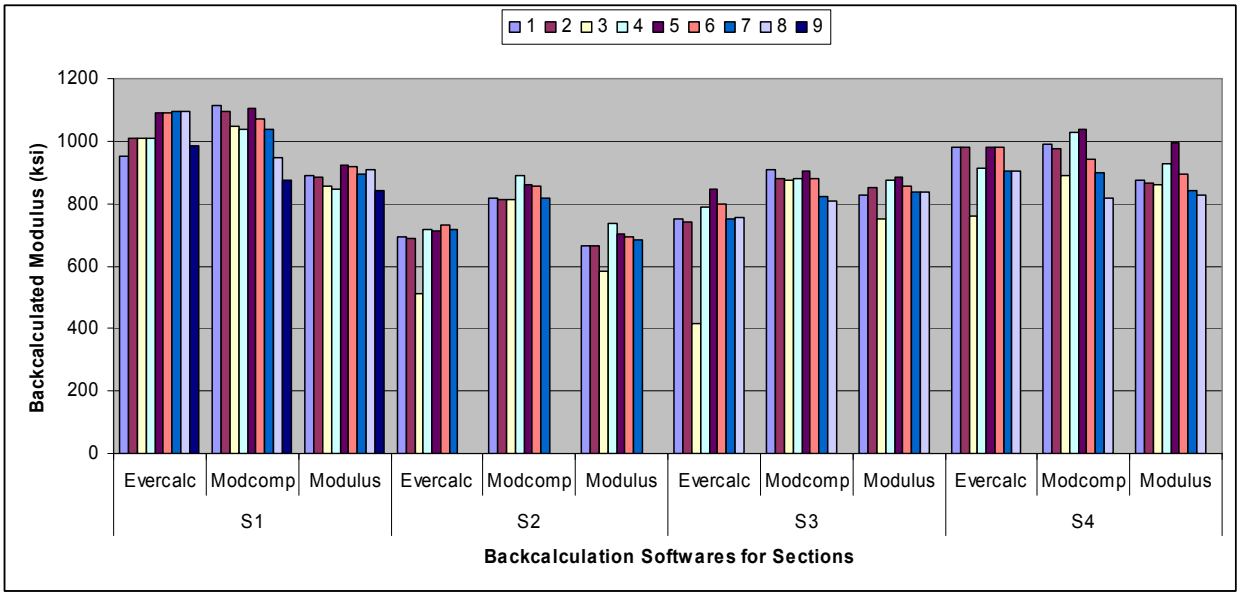


**Figure 6.2: Comparison of Backcalculated Modulus for US-75 Sections at 70°F.**

The numerical values of the backcalculated moduli for sections can be seen from Table 6.2. Deflection data has been taken at 9, 7, 8 and 8 stations for S1, S2, S3 and S4, respectively.

EVERCALC and MODCOMP give the lowest and the highest backcalculated moduli, respectively at Station 1 for S1. Station 9 has the lowest backcalculated modulus using MODCOMP and MODULUS. Stations 7 and 8 have equal backcalculated modulus using EVERCALC. Station 5 has the highest backcalculated modulus with MODULUS software.

All the three programs give the lowest backculated modulus at Station 5 for S2. Station 4 has the highest backcalculated modulus using MODCOMP and MODULUS whereas Station 6 has the highest backcalculated modulus using EVERCALC.

Station 3 has the lowest backcalculated modulus using all three programs for S3 like that of S2. Station 5 has the highest backcalculated modulus using EVERCALC and MODULUS whereas Station 1 has the highest modulus using MODCOMP.

**Table 6.2: Comparison of Backcalculated Modulus for Sections at 70◦F**

| | | Station No. | | | | | | | | |
|---|---|---|---|---|---|---|---|---|---|---|
| | | **1** | **2** | **3** | **4** | **5** | **6** | **7** | **8** | **9** |
| **S1** | **Ever. (ksi)** | 951 | 1007 | 1007 | 1007 | 1088 | 1092 | 1093 | 1093 | 983 |
| | **Modc.(ksi)** | 1114 | 1097 | 1048 | 1039 | 1105 | 1072 | 1039 | 949 | 874 |
| | **Modu.(ksi)** | 890 | 886 | 858 | 847 | 922 | 920 | 892 | 908 | 843 |
| **S2** | **Ever. (ksi)** | 695 | 688 | 513 | 717 | 710 | 731 | 717 | | |
| | **Modc.(ksi)** | 819 | 813 | 812 | 889 | 860 | 858 | 817 | | |
| | **Modu.(ksi)** | 666 | 664 | 585 | 736 | 703 | 691 | 684 | | |
| **S3** | **Ever. (ksi)** | 749 | 742 | 415 | 790 | 847 | 800 | 751 | 754 | |
| | **Modc.(ksi)** | 907 | 880 | 876 | 880 | 903 | 882 | 823 | 809 | |
| | **Modu.(ksi)** | 826 | 853 | 751 | 874 | 885 | 858 | 836 | 838 | |
| **S4** | **Ever. (ksi)** | 982 | 982 | 762 | 912 | 978 | 978 | 904 | 904 | |
| | **Modc.(ksi)** | 990 | 977 | 891 | 1029 | 1038 | 942 | 898 | 818 | |
| | **Modu.(ksi)** | 875 | 863 | 860 | 926 | 994 | 894 | 842 | 828 | |

Stations 1 and 2 have equal backcalculated modulus using EVERCALC for S4. Station 5 has the highest backcalculated modulus using MODCOMP and MODULUS. Station 3 has the lowest modulus using EVERCALC whereas Station 8 has the lowest using MODULUS and MODCOMP.

All programs yield the lowest baclculated modulus at the same station for S2 and S3 whereas MODCOMP and MODULUS give the lowest moduli for S1 and S4. MODCOMP and MODULUS give the highest backcalculated value at the same station for S2 and S4. It can be concluded that both MODCOMP and MODULUS yield similar results at the same stations even if MODCOMP gives higher backcalculated modulus at different stations for various sections. MODCOMP gives the highest backcalculated

modulus at all stations for S2 and generally, the highest for S1, S3 and S4 at all stations.

## 6.6 Effect of Temperature on Backcalculated Modulus

The backcalculated moduli were corrected to 40, 70 and 95$^{o}$F and a comparison of average corrected backcalculated modulus has been made for all calibration sites and perpetual pavement sections on US-75.

### *6.6.1 Effect of Temperature on Backcalculated Modulus for Calibration Sites*

Figure 6.3 shows the comparison of backcalculed AC moduli obtained from different backcalculation programs at various temperatures. These moduli are comparable for all calibration sites except on US-77, where the EVERCALC backcalculated AC modulus is very high. US-54, which was tested at the lowest temperature, has the highest average AC modulus and US-283, which was tested at the highest temperature, has the lowest AC modulus. US-77 and K-7 were tested at comparable temperature and their AC moduli are also comparable. This implies that the test temperature affects the backcalculated AC moduli significantly.

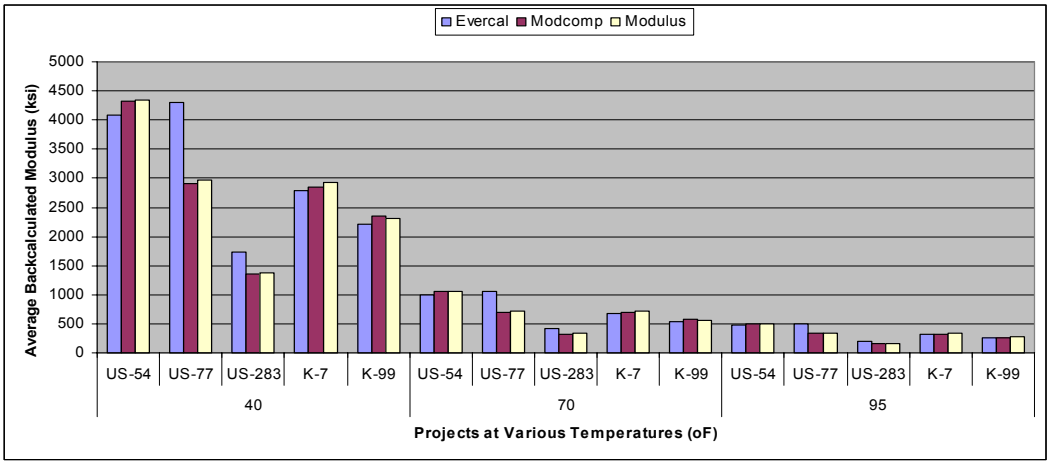


**Figure 6.3: Average Backcalculated Moduli for Calibration Sites at Various Temperatures.**

Table 6.3 lists the average backcalculed modulus, standard deviation (STD) and coefficient of variation (COV) for all calibration sites. The STD varies with the temperature where as COV remains about the same at all temperature levels. US-77 has the highest average modulus, STD and COV using EVERCAL. US-54 has the highest average AC modulus using MODCOMP and MODULUS. US-77 has the highest STD using the MODCOMP and the highest STD and COV using MODULUS. US-283 has lowest average modulus using all softwares at all temperatures. K-7 has the lowest STD using EVERCALC and the lowest COV using EVERCALC and MODCOMP. K-99 has the least COV using MODULUS. Overall there is no definite trend in the point statistics of the backcalculations results.

**Table 6.3: Summary Statistics of Backcalculated Modulus for Calibration Sites**

| | | EVERCAL | | | MODCOMP | | | MODULUS | | |
|---|---|---|---|---|---|---|---|---|---|---|
| **Temp. ($^oF$)** | | **Avg. Mod. (ksi)** | **STD (ksi)** | **COV (%)** | **Avg. Mod. (ksi)** | **STD (ksi)** | **COV (%)** | **Avg. Mod. (ksi)** | **STD (ksi)** | **COV (%)** |
| **40** | **US-54** | 4081 | 324.6 | 8.0 | 4328 | 233.4 | 5.4 | 4338 | 357.1 | 8.2 |
| | **US-77** | 4308 | 1205.1 | 28.0 | 2899 | 266.0 | 9.2 | 2975 | 381.1 | 12.8 |
| | **US-283** | 1724 | 313.1 | 18.2 | 1346 | 136.7 | 10.2 | 1369 | 121.0 | 8.8 |
| | **K-7** | 2791 | 141.0 | 5.1 | 2847 | 184.4 | 6.5 | 2934 | 290.1 | 9.9 |
| | **K-99** | 2216 | 266.6 | 12.0 | 2346 | 164.8 | 7.0 | 2315 | 160.8 | 6.9 |
| **70** | **US-54** | 995 | 79.1 | 8.0 | 1055 | 56.9 | 5.4 | 1058 | 87.1 | 8.2 |
| | **US-77** | 1050 | 293.8 | 28.0 | 707 | 64.9 | 9.2 | 725 | 92.9 | 12.8 |
| | **US-283** | 420 | 76.3 | 18.2 | 328 | 33.3 | 10.2 | 334 | 29.5 | 8.8 |
| | **K-7** | 680 | 34.4 | 5.1 | 694 | 45.0 | 6.5 | 715 | 70.7 | 9.9 |
| | **K-99** | 540 | 65.0 | 12.0 | 572 | 40.2 | 7.0 | 565 | 39.2 | 6.9 |
| **95** | **US-54** | 468 | 37.2 | 8.0 | 496 | 26.8 | 5.4 | 498 | 41.0 | 8.2 |
| | **US-77** | 494 | 138.2 | 28.0 | 333 | 30.5 | 9.2 | 341 | 43.7 | 12.8 |
| | **US-283** | 198 | 35.9 | 18.2 | 154 | 15.7 | 10.2 | 157 | 13.9 | 8.8 |
| | **K-7** | 320 | 16.2 | 5.1 | 327 | 21.1 | 6.5 | 337 | 33.3 | 9.9 |
| | **K-99** | 254 | 30.6 | 12.0 | 266 | 18.4 | 6.9 | 269 | 18.9 | 7.0 |

### *6.6.2 Effect of Temperature on Backcalculated Modulus for US-75 Sections*

Figure 6.4 shows the average backcalculed AC moduli obtained from different backcalculation programs for the US-75 test sections. S1, S4, S3 and S2 have moduli values in a descending order. S1 was tested at the lowest temperature and also has the stiffest mix. S3 and S4 were tested at comparable temperatures. S4 has a very high backcalculated AC modulus, most probably due to the influence of thickness since it is a very thick section. S3 was tested at a temperature cooler than S2 and is thicker than S2. The effects of pavement thickness, mixture stiffness and test temperature are clearly seen from these results.

Table 6.4 shows the summary statistics of the backcalculated moduli for the perpetual pavement test sections. S1 has the highest average backcalculated modulus at all temperatures for all programs. STD and COV are in a descending order using EVERCALC: S3, S2, S4 and S1. The order changes when MODCOMP is used: S1, S4, S3 and S2 for STD whereas S4 and S1 interchange for COV. The orders using STD: S4, S2, S3 and S1 and COV: S2, S4, S3 and S1, respectively. The order of COV changes depending upon the magnitude of the average backcalculated modulus.

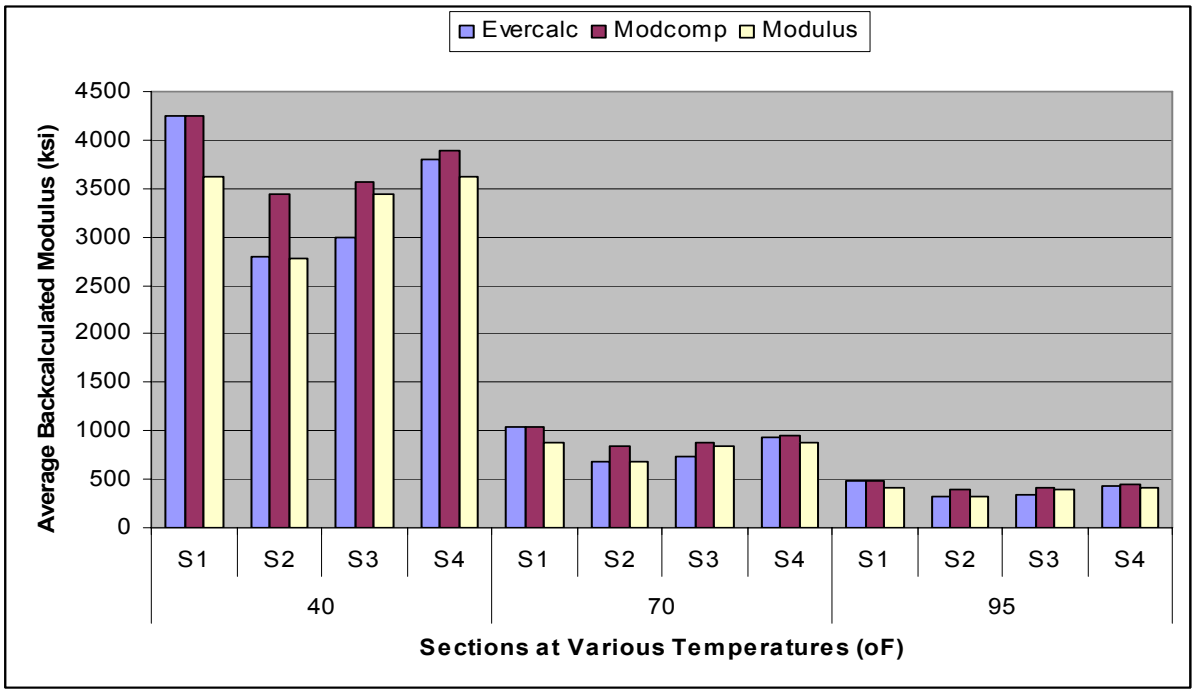


**Figure 6.4: Average Backcalculated Moduli for US-75 Sections at Various Temperatures.**

**Table 6.4: Summary Statistics of Backcalculated Modulus for Perpetual Pavement Sections**

| Temp (°F) | Sec. | EVERCALC | | | MODCOMP | | | MODULUS | | |
|---|---|---|---|---|---|---|---|---|---|---|
| | | Avg. Mod (ksi) | STD (ksi) | COV (%) | Avg. Mod (ksi) | STD (ksi) | COV (%) | Avg. Mod (ksi) | STD (ksi) | COV (%) |
| **40** | S1 | 4247 | 228.6 | 5.4 | 4256 | 323.6 | 7.6 | 3630 | 121.8 | 3.4 |
| | S2 | 2795 | 311.1 | 11.1 | 3439 | 124.8 | 3.6 | 2772 | 191.8 | 6.9 |
| | S3 | 2998 | 543.2 | 18.1 | 3568 | 145.7 | 4.1 | 3446 | 168.9 | 4.9 |
| | S4 | 3795 | 308.5 | 8.1 | 3888 | 309.7 | 8.0 | 3630 | 219.8 | 6.1 |
| **70** | S1 | 1035 | 55.7 | 5.4 | 1038 | 78.9 | 7.6 | 885 | 29.7 | 3.4 |
| | S2 | 682 | 75.9 | 11.1 | 839 | 30.4 | 3.6 | 676 | 46.8 | 6.9 |
| | S3 | 731 | 132.4 | 18.1 | 870 | 35.5 | 4.1 | 840 | 41.2 | 4.9 |
| | S4 | 925 | 75.2 | 8.1 | 948 | 75.5 | 8.0 | 885 | 53.6 | 6.1 |
| **95** | S1 | 487 | 26.2 | 5.4 | 488 | 37.1 | 7.6 | 416 | 14.0 | 3.4 |
| | S2 | 321 | 35.7 | 11.1 | 394 | 14.3 | 3.6 | 318 | 22.0 | 6.9 |
| | S3 | 344 | 62.3 | 18.1 | 409 | 16.7 | 4.1 | 395 | 19.4 | 4.9 |
| | S4 | 435 | 35.4 | 8.1 | 446 | 35.5 | 8.0 | 416 | 25.2 | 6.1 |

# CHAPTER SEVEN - PREDICTED DYNAMIC MODULUS OF HMA

Dynamic modulus was predicted for each HMA mix in each layer using Hirsch model, new Witczak model and Witczak equation. The overall AC modulus was computed using Equation (5.5) based on individual layer thickness of the mixture.

## 7.1 Predicted Dynamic Modulus for Calibration Sites

### *7.1.1 Predicted Dynamic Modulus for US-54*

Figure 7.1 shows the average predicted modulus at various temperatures and frequencies for US-54. Hirsch model yields the highest average predicted modulus at the highest frequency and lowest temperature. The Witczak equation shows the highest average predicted modulus at the lowest frequency and all temperatures.

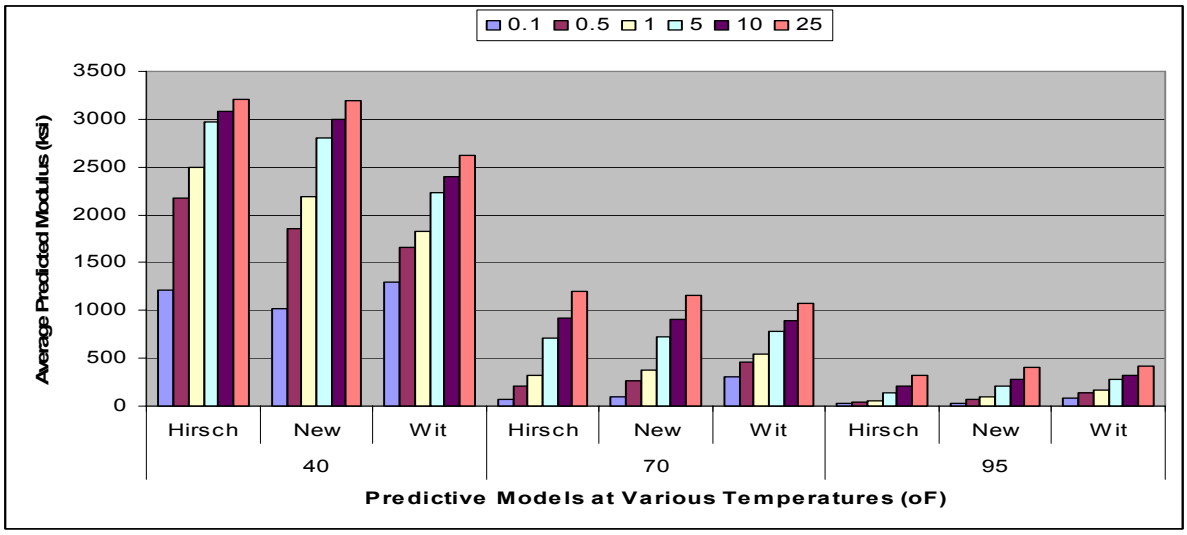


**Figure 7.1: Average Predicted Modulus for US-54.**

Table 7.1 tabulates the summary statistics of predicted modulus for US-54. At the lowest temperature and frequency, Witczak equation and New Witczak model give the highest and lowest average predicted modulus, respectively. At the lowest temperature

and highest frequency, Hirsch model shows the highest modulus and Witczak equation indicates the lowest modulus. The STD increases with an increase in frequency at 40oF using New Witczak model and Witczak equation. The COV decreases with an increase in frequency at 40oF using Hirsch and Witczak New models whereas it remains constant at all temperatures and frequencies using Witczak equation. Hirsch model gives the smallest COV at all frequencies.

Hirsch model and Witczak equation give the lowest and the highest average predicted modulus, respectively at 0.1 Hz and 70$^{o}$F. The STD increases with an increase in frequency using all predictive models at 70$^{o}$F. The COV decreases with an increase in frequency using Hirsch and Witczak New models at 70$^{o}$F.

Hirsch model and Witczak equation show the lowest and the highest average predicted modulus, respectively at all frequencies at 95$^{o}$F. COV increases with an increase in frequency using Hirsch model and decreases/constant using New Witczak model and Witczak equation. The STD shows trends that are similar to at 70$^{o}$F.

**Table 7.1: Summary Statistics of Predicted Modulus for US-54**

| Temp.(°F) | Method | | Moduli (ksi) | | | | | |
|---|---|---|---|---|---|---|---|---|
| | | Frequency (Hz) | 0.1 | 0.5 | 1 | 5 | 10 | 25 |
| 40 | Hirsch | Av.Mod. | 1209 | 2173 | 2489 | 2966 | 3089 | 3201 |
| | | STD | 23.1 | 28.6 | 28.0 | 25.2 | 24.0 | 22.6 |
| | | COV (%) | 1.9 | 1.3 | 1.1 | 0.8 | 0.8 | 0.7 |
| | New | Av.Mod. | 1015 | 1848 | 2183 | 2799 | 2992 | 3190 |
| | | STD | 19.3 | 34.3 | 40.3 | 51.0 | 54.3 | 57.7 |
| | | COV (%) | 1.9 | 1.9 | 1.8 | 1.8 | 1.8 | 1.8 |
| | Wit | Av.Mod. | 1301 | 1664 | 1830 | 2225 | 2397 | 2622 |
| | | STD | 26.3 | 33.6 | 37.0 | 44.9 | 48.4 | 53.0 |
| | | COV (%) | 2.0 | 2.0 | 2.0 | 2.0 | 2.0 | 2.0 |
| 70 | Hirsch | Av.Mod. | 72 | 213 | 325 | 713 | 918 | 1195 |
| | | STD | 1.5 | 5.3 | 8.0 | 15.8 | 19.1 | 22.8 |
| | | COV (%) | 2.1 | 2.5 | 2.4 | 2.2 | 2.1 | 1.9 |
| | New | Av.Mod. | 104 | 261 | 371 | 728 | 912 | 1164 |
| | | STD | 2.1 | 5.2 | 7.4 | 14.1 | 17.5 | 22.2 |
| | | COV (%) | 2.1 | 2.0 | 2.0 | 1.9 | 1.9 | 1.9 |
| | Wit | Av.Mod. | 308 | 465 | 548 | 781 | 899 | 1070 |
| | | STD | 6.2 | 9.4 | 11.1 | 15.8 | 18.1 | 21.6 |
| | | COV (%) | 2.0 | 2.0 | 2.0 | 2.0 | 2.0 | 2.0 |
| 95 | Hirsch | Av.Mod. | 32 | 45 | 60 | 144 | 207 | 319 |
| | | STD | 0.2 | 0.7 | 1.2 | 3.5 | 5.1 | 7.8 |
| | | COV (%) | 0.6 | 1.5 | 1.9 | 2.4 | 2.5 | 2.4 |
| | New | Av.Mod. | 34 | 67 | 94 | 203 | 276 | 399 |
| | | STD | 0.7 | 1.4 | 1.9 | 4.1 | 5.5 | 7.9 |
| | | COV (%) | 2.1 | 2.1 | 2.1 | 2.0 | 2.0 | 2.0 |
| | Wit | Av.Mod. | 88 | 142 | 173 | 272 | 328 | 414 |
| | | STD | 1.8 | 2.9 | 3.5 | 5.5 | 6.6 | 8.4 |
| | | COV (%) | 2.0 | 2.0 | 2.0 | 2.0 | 2.0 | 2.0 |

### *7.1.2 Predicted Dynamic Modulus for US-77*

The average predicted modulus is shown in Figure 7.2. New Witczak model gives the lowest and the highest average predicted modulus at 0.1 Hz and 25 Hz, respectively at 40°F. The trend is the same at the highest temperature.

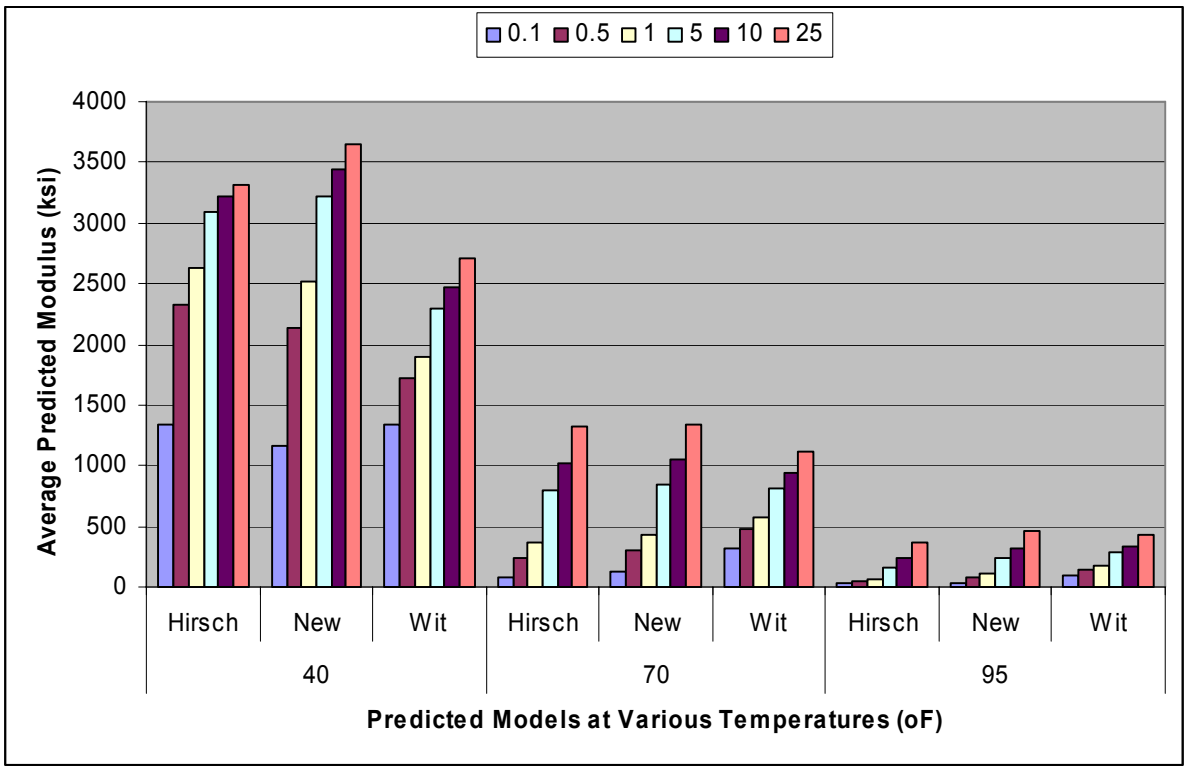


**Figure 7.2: Average Predicted Modulus for US-77.**

Summary statistics of predicted modulus for US-77 is shown in Table 7.2. At 0.1 Hz and 40°F, the average predicted modulus in descending order is shown by: Witczak equation, Hirsch model and New Witczak model. At 25 Hz and 40°F, the average predicted modulus in descending order is shown by: New Witczak model, Witczak equation and Hirsch model. STD decreases with frequency using all predictive models at all temperatures except at 0.1 Hz. COV decreases with increase in frequency using

Hirsch model whereas it remains more/less constant using New Witczak model and constant using Witczak equation at all temperatures.

At 0.1 Hz and 70°F and 95°F, average predicted modulus in descending order is given by: Witczak equation, New Witzcak model and Hirsch model unlike at 40°F. New Witczak model gives the highest and Witczak equation gives the lowest average predicted modulus at 25 Hz and 70°F similar trend to 40°F. At 25 Hz and 95°F, average predicted modulus in descending order is shown by: New Witzcak model, Witczak equation and Hirsch model unlike at 70°F.

**Table 7.2: Summary Statistics of Predicted Modulus for US-77**

| Temp. (°F) | Model | | Moduli(ksi) | | | | | |
|---|---|---|---|---|---|---|---|---|
| | | **Frequency (Hz)** | **0.1** | **0.5** | **1** | **5** | **10** | **25** |
| **40** | Hirsch | Av.Mod. | 1336 | 2324 | 2636 | 3096 | 3212 | 3316 |
| | | STD | 50.4 | 58.3 | 56.1 | 48.6 | 45.7 | 42.7 |
| | | COV (%) | 3.8 | 2.5 | 2.1 | 1.6 | 1.4 | 1.3 |
| | New | Av.Mod. | 1171 | 2129 | 2514 | 3220 | 3441 | 3648 |
| | | STD | 37.3 | 68.0 | 80.4 | 103.0 | 110.0 | 117.2 |
| | | COV (%) | 3.2 | 3.2 | 3.2 | 3.2 | 3.2 | 3.2 |
| | Wit | Av.Mod. | 1343 | 1718 | 1889 | 2295 | 2472 | 2704 |
| | | STD | 36.9 | 47.2 | 51.9 | 63.0 | 67.9 | 74.3 |
| | | COV (%) | 2.7 | 2.7 | 2.7 | 2.7 | 2.7 | 2.7 |
| **70** | Hirsch | Av.Mod. | 81 | 243 | 370 | 800 | 1021 | 1316 |
| | | STD | 3.7 | 12.4 | 18.5 | 35.7 | 42.6 | 49.7 |
| | | COV (%) | 4.5 | 5.1 | 5.0 | 4.5 | 4.2 | 3.8 |
| | New | Av.Mod. | 121 | 302 | 430 | 842 | 1054 | 1337 |
| | | STD | 3.8 | 9.5 | 13.6 | 26.8 | 33.6 | 42.9 |
| | | COV (%) | 3.1 | 3.2 | 3.2 | 3.2 | 3.2 | 3.2 |
| | Wit | Av.Mod. | 322 | 484 | 571 | 813 | 935 | 1111 |
| | | STD | 8.8 | 13.3 | 15.7 | 22.3 | 25.7 | 30.5 |
| | | COV (%) | 2.7 | 2.7 | 2.7 | 2.7 | 2.7 | 2.7 |
| **95** | Hirsch | Av.Mod. | 33 | 48 | 67 | 164 | 235 | 362 |
| | | STD | 0.4 | 1.6 | 2.8 | 8.3 | 12.1 | 18.2 |
| | | COV (%) | 1.1 | 3.2 | 4.2 | 5.1 | 5.1 | 5.0 |
| | New | Av.Mod. | 39 | 78 | 109 | 235 | 320 | 459 |
| | | STD | 1.2 | 2.4 | 3.4 | 7.4 | 10.1 | 14.6 |
| | | COV (%) | 3.1 | 3.1 | 3.1 | 3.2 | 3.2 | 3.2 |
| | Wit | Av.Mod. | 91 | 147 | 180 | 282 | 339 | 429 |
| | | STD | 2.5 | 4.0 | 4.9 | 7.7 | 9.3 | 11.8 |
| | | COV (%) | 2.7 | 2.7 | 2.7 | 2.7 | 2.7 | 2.7 |

### *7.1.3 Predicted Dynamic Modulus for US-283*

Figure 7.3 indicates the average predicted modulus for US-283. At 25 Hz, Witczak equation gives the lowest and highest average predicted modulus at 40°F and 95°F, respectively. The magnitude of average predicted modulus changes with frequency and temperature using different predictive models.

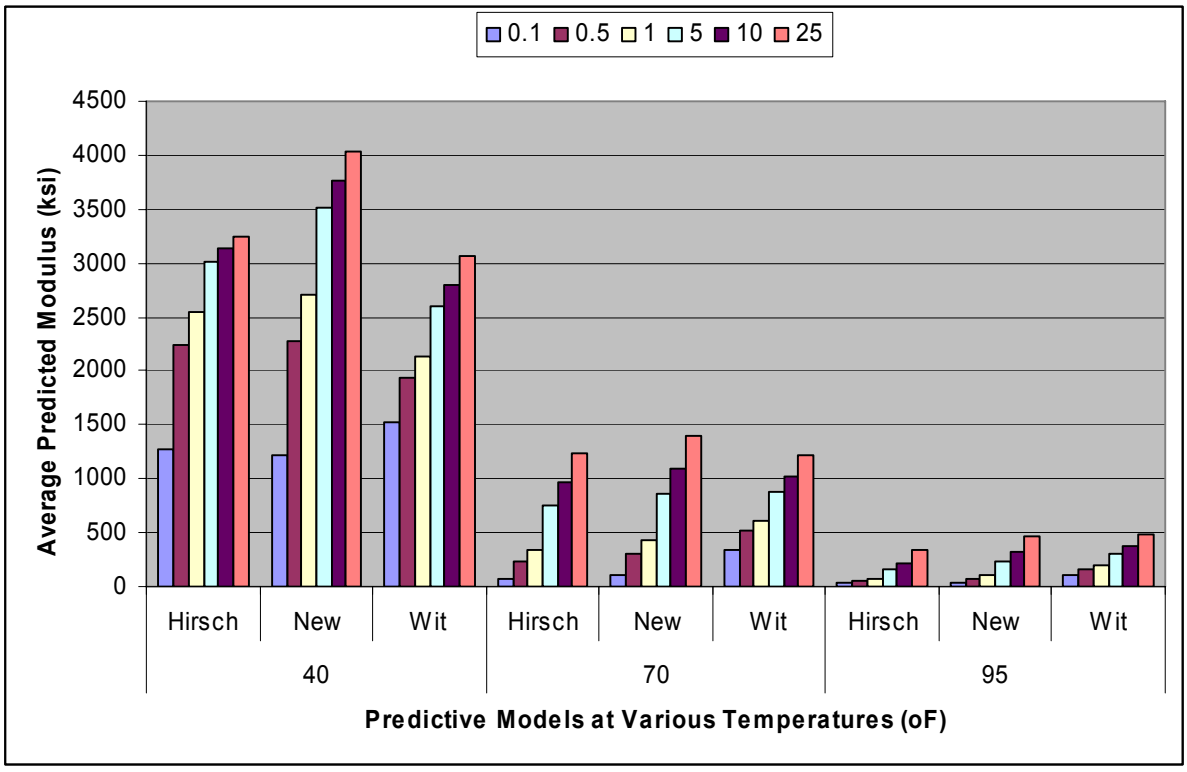


**Figure 7.3: Average Predicted Modulus for US-283.**

Summary statistics of the predicted modulus for US-283 are shown in Table 7.3. At 0.1 Hz and 40°F, the average predicted modulus in descending order is shown by: Witczak equation, Hirsch model and New Witczak model like US-77. At 25 Hz and 40°F, the average predicted modulus in descending order is shown by: New Witczak model, Hirsch model and Witczak equation unlike US-77. STD decreases with frequency using all predictive models at all temperatures except at 0.1 Hz like US-77. COV decreases

with increase in frequency using Hirsch model and New Witczak model whereas it remains constant using Witczak equation at all temperatures.

At 0.1 Hz and 70°F and 95°F, average predicted modulus in descending order is given by: Witczak equation, New Witzcak model and Hirsch model like US-77. New Witczak model gives the highest and Witczak equation gives the lowest average predicted modulus at 25 Hz and 70°F like US-77. At 25 Hz and 95°F, average predicted modulus in descending order is shown by: Witczak equation, New Witzcak model, and Hirsch model.

**Table 7.3: Summary Statistics of Predicted Modulus for US-283**

| Temp. (°F) | Models | | Moduli (ksi) | | | | | |
|---|---|---|---|---|---|---|---|---|
| | | Frequency (Hz) | 0.1 | 0.5 | 1 | 5 | 10 | 25 |
| 40 | Hirsch | Av.Mod. | 1267 | 2235 | 2548 | 3014 | 3133 | 3241 |
| | | STD | 42.9 | 50.9 | 49.4 | 43.6 | 41.3 | 38.8 |
| | | COV (%) | 3.4 | 2.3 | 1.9 | 1.4 | 1.3 | 1.2 |
| | New | Av.Mod. | 1225 | 2281 | 2712 | 3515 | 3768 | 4029 |
| | | STD | 37.8 | 69.7 | 82.7 | 106.6 | 114.1 | 121.9 |
| | | COV (%) | 3.1 | 3.1 | 3.0 | 3.0 | 3.0 | 3.0 |
| | Wit | Av.Mod. | 1515 | 1940 | 2133 | 2596 | 2796 | 3060 |
| | | STD | 43.2 | 55.3 | 60.8 | 74.0 | 79.7 | 87.2 |
| | | COV (%) | 2.9 | 2.9 | 2.9 | 2.9 | 2.9 | 2.9 |
| 70 | Hirsch | Av.Mod. | 76 | 227 | 345 | 749 | 959 | 1242 |
| | | STD | 3.0 | 10.3 | 15.3 | 29.8 | 35.8 | 42.1 |
| | | COV (%) | 4.0 | 4.5 | 4.4 | 4.0 | 3.7 | 3.4 |
| | New | Av.Mod. | 116 | 298 | 430 | 863 | 1090 | 1405 |
| | | STD | 3.6 | 9.3 | 13.4 | 26.7 | 33.7 | 43.3 |
| | | COV (%) | 3.2 | 3.1 | 3.1 | 3.1 | 3.1 | 3.1 |
| | Wit | Av.Mod. | 346 | 523 | 618 | 885 | 1020 | 1217 |
| | | STD | 9.8 | 14.9 | 17.6 | 25.2 | 29.0 | 34.6 |
| | | COV (%) | 2.8 | 2.8 | 2.8 | 2.8 | 2.8 | 2.8 |
| 95 | Hirsch | Av.Mod. | 33 | 46 | 63 | 153 | 219 | 337 |
| | | STD | 0.3 | 1.3 | 2.3 | 6.8 | 9.9 | 15.0 |
| | | COV (%) | 1.0 | 2.8 | 3.6 | 4.5 | 4.5 | 4.5 |
| | New | Av.Mod. | 36 | 73 | 103 | 229 | 315 | 461 |
| | | STD | 1.2 | 2.3 | 3.3 | 7.2 | 9.9 | 14.4 |
| | | COV (%) | 3.2 | 3.2 | 3.2 | 3.1 | 3.1 | 3.1 |
| | Wit | Av.Mod. | 100 | 162 | 198 | 312 | 375 | 475 |
| | | STD | 2.8 | 4.6 | 5.6 | 8.9 | 10.7 | 13.5 |
| | | COV (%) | 2.8 | 2.8 | 2.8 | 2.8 | 2.8 | 2.8 |

### *7.1.4 Predicted Dynamic Modulus for K-7*

Figure 7.4 illustrates the average predicted modulus for K-7. At 25 Hz, Witczak equation gives the lowest and New Witczak model gives the highest average predicted modulus at all temperatures unlike most of the new projects, respectively. At 0.1 Hz, Witczak equation gives the lowest average predicted modulus at all temperatures.

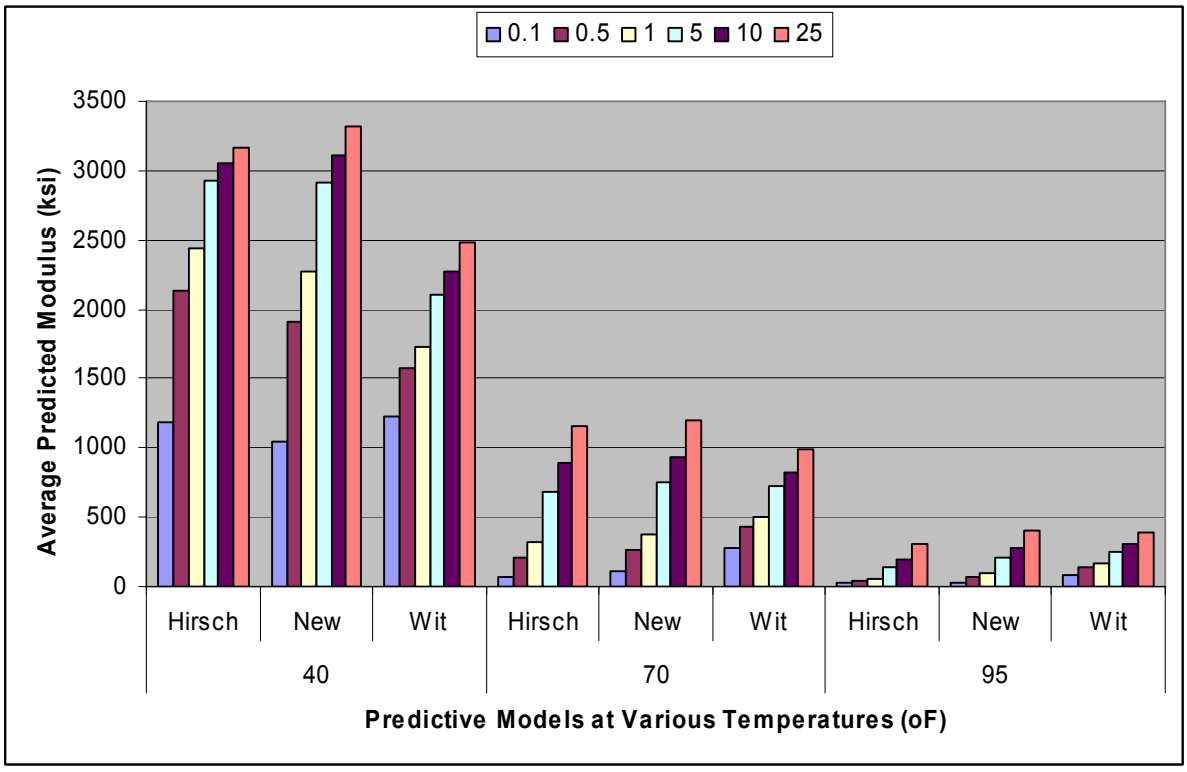


**Figure 7.4: Average Predicted Modulus for K-7.**

Table 7.4 shows summary statistics of predicted modulus for K-7. At 0.1 Hz and 40$^{o}$F, the average predicted modulus in descending order is shown by: Witczak equation, Hirsch model and New Witczak model like US-77 and US-283. At 25 Hz and 40$^{o}$F, the average predicted modulus in descending order is shown by: New Witczak model, Hirsch model and Witczak equation like US-283. STD increases with frequency using all predictive models at all temperatures except Hirsch model at 40$^{o}$F. COV

decreases with increase in frequency using Hirsch model and New Witczak model whereas it remains constant using Witczak equation at all temperatures except Hirsch model at 95$^{o}$F.

At 0.1 Hz and 70$^{o}$F and 95$^{o}$F, average predicted modulus in descending order is given by: Witczak equation, New Witzcak model and Hirsch model like US-77 and US-283. New Witczak model gives the highest and Witczak equation gives the lowest average predicted modulus at 25 Hz and 70$^{o}$F like US-77 and US-283. At 25 Hz and 95$^{o}$F, average predicted modulus in descending order is shown by: New Witzcak model, Witczak equation, and Hirsch model.

**Table 7.4: Summary Statistics of Predicted Modulus for K-7**

| Temp. ($^{o}$F) | Models | | Moduli (ksi) | | | | | |
|---|---|---|---|---|---|---|---|---|
| | | Frequency (Hz) | 0.1 | 0.5 | 1 | 5 | 10 | 25 |
| 40 | Hirsch | Av.Mod. | 1181 | 2131 | 2447 | 2926 | 3049 | 3163 |
| | | STD | 22.3 | 27.8 | 27.4 | 24.7 | 23.6 | 22.3 |
| | | COV (%) | 1.9 | 1.3 | 1.1 | 0.8 | 0.8 | 0.7 |
| | New | Av.Mod. | 1050 | 1917 | 2267 | 2914 | 3117 | 3325 |
| | | STD | 19.9 | 35.4 | 41.5 | 52.6 | 56.0 | 59.5 |
| | | COV (%) | 1.9 | 1.8 | 1.8 | 1.8 | 1.8 | 1.8 |
| | Wit | Av.Mod. | 1233 | 1576 | 1733 | 2106 | 2268 | 2481 |
| | | STD | 25.1 | 32.0 | 35.2 | 42.8 | 46.1 | 50.4 |
| | | COV (%) | 2.0 | 2.0 | 2.0 | 2.0 | 2.0 | 2.0 |
| 70 | Hirsch | Av.Mod. | 70 | 206 | 315 | 689 | 887 | 1157 |
| | | STD | 1.5 | 5.0 | 7.6 | 15.1 | 18.3 | 21.9 |
| | | COV (%) | 2.1 | 2.4 | 2.4 | 2.2 | 2.1 | 1.9 |
| | New | Av.Mod. | 106 | 266 | 380 | 748 | 938 | 1199 |
| | | STD | 2.2 | 5.3 | 7.5 | 14.4 | 17.9 | 22.7 |
| | | COV (%) | 2.1 | 2.0 | 2.0 | 1.9 | 1.9 | 1.9 |
| | Wit | Av.Mod. | 283 | 427 | 504 | 720 | 830 | 989 |
| | | STD | 5.7 | 8.7 | 10.2 | 14.7 | 16.9 | 20.1 |
| | | COV (%) | 2.0 | 2.0 | 2.0 | 2.0 | 2.0 | 2.0 |
| 95 | Hirsch | Av.Mod. | 32 | 44 | 59 | 139 | 200 | 307 |
| | | STD | 0.2 | 0.6 | 1.1 | 3.3 | 4.9 | 7.4 |
| | | COV (%) | 0.5 | 1.4 | 1.9 | 2.4 | 2.4 | 2.4 |
| | New | Av.Mod. | 34 | 68 | 95 | 206 | 281 | 407 |
| | | STD | 0.7 | 1.4 | 2.0 | 4.2 | 5.6 | 8.0 |
| | | COV (%) | 2.2 | 2.1 | 2.1 | 2.0 | 2.0 | 2.0 |
| | Wit | Av.Mod. | 82 | 133 | 162 | 255 | 306 | 388 |
| | | STD | 1.7 | 2.7 | 3.3 | 5.2 | 6.2 | 7.9 |
| | | COV (%) | 2.0 | 2.0 | 2.0 | 2.0 | 2.0 | 2.0 |

### *7.1.5 Predicted Dynamic Modulus for K-99*

The average predicted modulus for K-99 is shown in Figure 7.5. At 25 Hz and 40°F, highest to lowest average predicted modulus is given by: New Witczak model, Hirsch model and Witczak equation and vice versa at 0.1 Hz and 40°F. There is a change in trend as temperature increases.

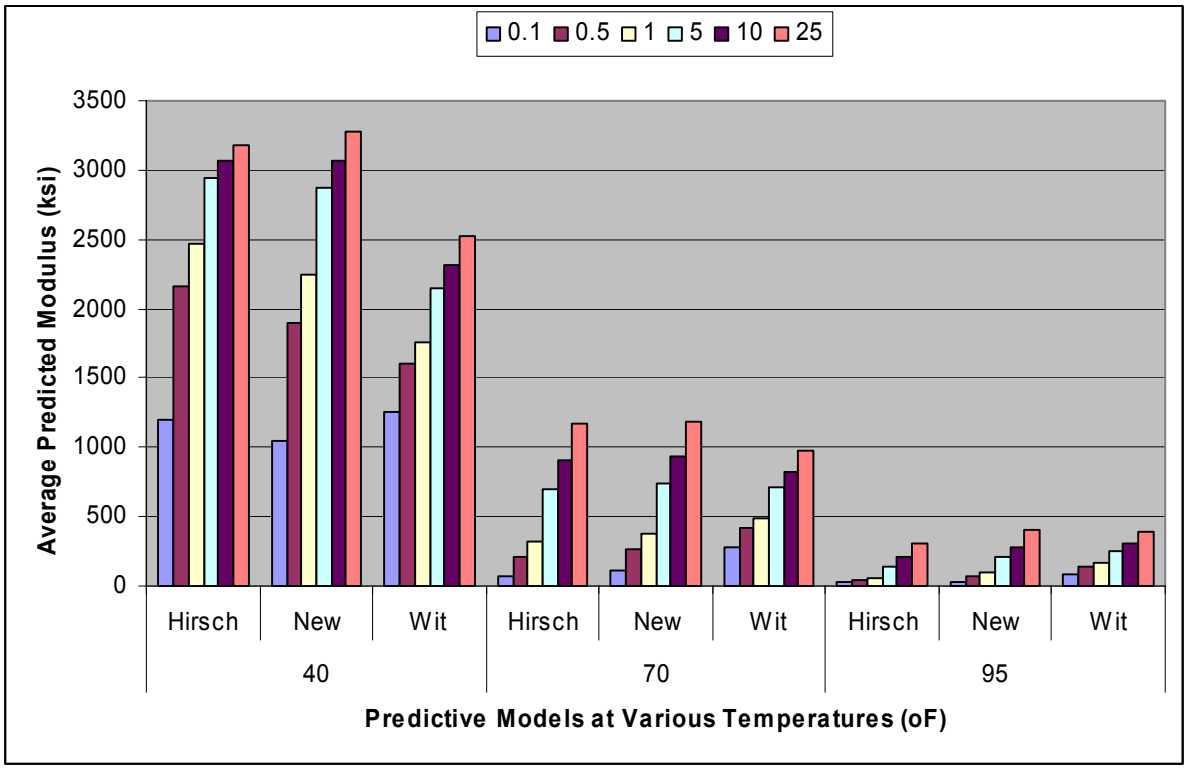


**Figure 7.5: Average Predicted Modulus for K-99.**

Table 7.5 shows summary statistics of the predicted modulus for K-99. At 0.1 Hz and 40°F, the average predicted modulus in descending order is shown by: Witczak equation, Hirsch model and New Witczak model. At 25 Hz and 40°F, the average predicted modulus in descending order is shown by: New Witczak model, Hirsch model and Witczak equation. STD increases with frequency using all predictive models at all temperatures except Hirsch model at 40°F. COV decreases with increase in frequency

using Hirsch and New Witczak models whereas it remains constant using Witczak equation at all temperatures except Hirsch model at 95°F.

At 0.1 Hz and 70°F and 95°F, average predicted modulus in descending order is given by: Witczak equation, New Witzcak model and Hirsch model. New Witczak model gives the highest and Witczak equation gives the lowest average predicted modulus at 25 Hz and 70°F. At 25 Hz and 95°F, average predicted modulus in descending order is shown by: New Witzcak model, Witczak equation, and Hirsch model.

**Table 7.5: Summary Statistics of Predicted Modulus for K-99**

| | | | Frequency (Hz) | | | | | |
|---|---|---|---|---|---|---|---|---|
| | | | **0.1** | **0.5** | **1** | **5** | **10** | **25** |
| **40** | **Hirsch** | **Av.Mod. (ksi)** | 1201 | 2157 | 2472 | 2949 | 3072 | 3184 |
| | | **STD (ksi)** | 37.0 | 45.6 | 44.8 | 40.2 | 38.3 | 36.2 |
| | | **COV (%)** | 3.1 | 2.1 | 1.8 | 1.4 | 1.2 | 1.1 |
| | **New** | **Av.Mod. (ksi)** | 1046 | 1898 | 2240 | 2873 | 3071 | 3276 |
| | | **STD (ksi)** | 31.7 | 56.1 | 65.8 | 83.4 | 88.8 | 94.4 |
| | | **COV (%)** | 3.0 | 3.0 | 2.9 | 2.9 | 2.9 | 2.9 |
| | **Wit** | **Av.Mod. (ksi)** | 1254 | 1604 | 1763 | 2144 | 2309 | 2527 |
| | | **STD (ksi)** | 39.6 | 50.6 | 55.6 | 67.7 | 72.9 | 79.7 |
| | | **COV (%)** | 3.2 | 3.2 | 3.2 | 3.2 | 3.2 | 3.2 |
| **70** | **Hirsch** | **Av.Mod. (ksi)** | 72 | 211 | 321 | 702 | 903 | 1176 |
| | | **STD (ksi)** | 2.5 | 8.5 | 12.7 | 25.2 | 30.4 | 36.3 |
| | | **COV (%)** | 3.4 | 4.0 | 4.0 | 3.6 | 3.4 | 3.1 |
| | **New** | **Av.Mod. (ksi)** | 107 | 267 | 380 | 743 | 930 | 1186 |
| | | **STD (ksi)** | 3.5 | 8.5 | 11.9 | 22.8 | 28.3 | 35.8 |
| | | **COV (%)** | 3.3 | 3.2 | 3.1 | 3.1 | 3.0 | 3.0 |
| | **Wit** | **Av.Mod. (ksi)** | 276 | 418 | 495 | 711 | 820 | 979 |
| | | **STD (ksi)** | 8.7 | 13.2 | 15.6 | 22.5 | 25.9 | 30.9 |
| | | **COV (%)** | 3.2 | 3.2 | 3.2 | 3.2 | 3.2 | 3.2 |
| **95** | **Hirsch** | **Av.Mod. (ksi)** | 32 | 45 | 60 | 142 | 204 | 314 |
| | | **STD (ksi)** | 0.3 | 1.0 | 1.9 | 5.6 | 8.2 | 12.4 |
| | | **COV (%)** | 0.9 | 2.4 | 3.1 | 3.9 | 4.0 | 4.0 |
| | **New** | **Av.Mod. (ksi)** | 35 | 69 | 96 | 207 | 281 | 406 |
| | | **STD (ksi)** | 1.2 | 2.3 | 3.1 | 6.6 | 8.9 | 12.7 |
| | | **COV (%)** | 3.4 | 3.3 | 3.3 | 3.2 | 3.2 | 3.1 |
| | **Wit** | **Av.Mod. (ksi)** | 83 | 134 | 163 | 257 | 309 | 392 |
| | | **STD (ksi)** | 2.6 | 4.2 | 5.2 | 8.1 | 9.8 | 12.4 |
| | | **COV (%)** | 3.2 | 3.2 | 3.2 | 3.2 | 3.2 | 3.2 |

## 7.2 Comparison of Predicted Dynamic Modulus for New Project

### *7.2.1 Comparison of Predicted Dynamic Modulus for Calibration Sites at 40°F*

Figure 7.6 indicates the average predicted modulus for calibration sites at 40°F. US-283 has the highest predicted modulus using New Witczak model at 25 Hz. Witczak equation shows the lowest and highest average predicted modulus at 25 Hz and 0.1 Hz, respectively. Hirsch and New Witczak models show comparable predicted modulus for US-54, K-7 and K-99. The largest discrepancy between Hirsch and New Witczak models is seen for US-283.

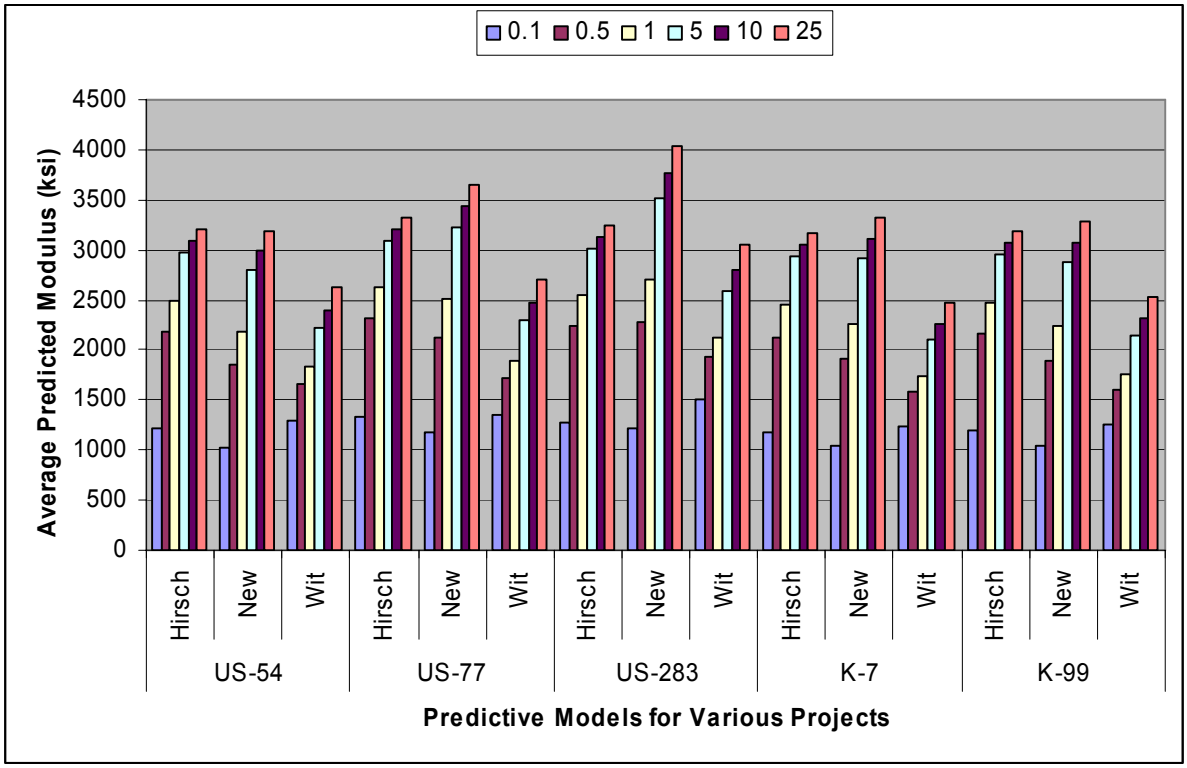


**Figure 7.6: Comparison of Average Predicted Modulus for Calibration Sites at 40°F.**

Table 7.6 indicates summary statistics of predicted modulus for calibration sites at 40°F. Average predicted modulus using Hirsch model at all frequencies in

descending order: US-77, US-283, US-54, K-99 and K-7. The order changes when New Witczak model is used: US-283, US-77, K-7, K-99 and US-54. The order also changes when Witczak equation is used: US-283, US-77, US-54, K-99 and K-7. This shows different predictive models show different result for the same SuperPave mixture. Witczak equation and New Witczak model give the highest overall average predicted modulus at 0.1 and 25 Hz, respectively.

STD in descending order at 0.1 and 25 Hz using Hirsch model: US-77, US-283, K-99, US-54 and K-7 unlike average predicted modulus. The order using New Witczak model: US-283, US-77, K-99, K-7 and US-54 unlike the average predicted modulus. The order using Witczak equation: US-283, K-99, US-77, US-54, and K-7 unlike average predicted modulus.

**Table 7.6: Summary Statistics of Predicted Modulus for Calibration Sites at 40°F**

| Sites | Models | Frequency (Hz) | | | | | | | | | | | | | | | | | |
|---|---|---|---|---|---|---|---|---|---|---|---|---|---|---|---|---|---|---|---|
| | | 0.1 | | | 0.5 | | | 1 | | | 5 | | | 10 | | | 25 | | |
| | | Av. Mod. (ksi) | STD (ksi) | COV (%) | Av. Mod. (ksi) | STD (ksi) | COV (%) | Av. Mod. (ksi) | STD (ksi) | COV (%) | Av. Mod. (ksi) | STD (ksi) | COV (%) | Av. Mod. (ksi) | STD (ksi) | COV (%) | Av. Mod. (ksi) | STD (ksi) | COV (%) |
| **US-54** | **Hirsch** | 1209 | 23.1 | 1.9 | 2173 | 28.6 | 1.3 | 2489 | 28 | 1.1 | 2966 | 25 | 0.8 | 3089 | 24 | 0.8 | 3201 | 22.6 | 0.7 |
| | **New** | 1015 | 19.3 | 1.9 | 1848 | 34.3 | 1.9 | 2183 | 40.3 | 1.8 | 2799 | 51 | 1.8 | 2992 | 54 | 1.8 | 3190 | 57.7 | 1.8 |
| | **Wit** | 1301 | 26.3 | 3.8 | 1664 | 33.6 | 2.5 | 1830 | 37 | 2.1 | 2225 | 45 | 1.6 | 2397 | 48 | 1.4 | 2622 | 53 | 1.3 |
| **US-77** | **Hirsch** | 1336 | 50.4 | 3.2 | 2324 | 58.3 | 3.2 | 2636 | 56.1 | 3.2 | 3096 | 49 | 3.2 | 3212 | 46 | 3.2 | 3316 | 42.7 | 3.2 |
| | **New** | 1171 | 37.3 | 3.4 | 2129 | 68 | 2.3 | 2514 | 80.4 | 1.9 | 3220 | 103 | 1.4 | 3441 | 110 | 1.3 | 3648 | 117.2 | 1.2 |
| | **Wit** | 1343 | 36.9 | 3.1 | 1718 | 47.2 | 3.1 | 1889 | 51.9 | 3 | 2295 | 63 | 3 | 2472 | 68 | 3 | 2704 | 74.3 | 3 |
| **US-283** | **Hirsch** | 1267 | 42.9 | 1.9 | 2235 | 50.9 | 1.3 | 2548 | 49.4 | 1.1 | 3014 | 44 | 0.8 | 3133 | 41 | 0.8 | 3241 | 38.8 | 0.7 |
| | **New** | 1225 | 37.8 | 1.9 | 2281 | 69.7 | 1.8 | 2712 | 82.7 | 1.8 | 3515 | 107 | 1.8 | 3768 | 114 | 1.8 | 4029 | 121.9 | 1.8 |
| | **Wit** | 1515 | 43.2 | 3.1 | 1940 | 55.3 | 2.1 | 2133 | 60.8 | 1.8 | 2596 | 74 | 1.4 | 2796 | 80 | 1.2 | 3060 | 87.2 | 1.1 |
| **K-7** | **Hirsch** | 1181 | 22.3 | 3 | 2131 | 27.8 | 3 | 2447 | 27.4 | 2.9 | 2926 | 25 | 2.9 | 3049 | 24 | 2.9 | 3163 | 22.3 | 2.9 |
| | **New** | 1050 | 19.9 | 2 | 1917 | 35.4 | 2 | 2267 | 41.5 | 2 | 2914 | 53 | 2 | 3117 | 56 | 2 | 3325 | 59.5 | 2 |
| | **Wit** | 1233 | 25.1 | 2.7 | 1576 | 32 | 2.7 | 1733 | 35.2 | 2.7 | 2106 | 43 | 2.7 | 2268 | 46 | 2.7 | 2481 | 50.4 | 2.7 |
| **K-99** | **Hirsch** | 1201 | 37 | 2.9 | 2157 | 45.6 | 2.9 | 2472 | 44.8 | 2.9 | 2949 | 40 | 2.9 | 3072 | 38 | 2.9 | 3184 | 36.2 | 2.9 |
| | **New** | 1046 | 31.7 | 2 | 1898 | 56.1 | 2 | 2240 | 65.8 | 2 | 2873 | 83 | 2 | 3071 | 89 | 2 | 3276 | 94.4 | 2 |
| | **Wit** | 1254 | 39.6 | 3.2 | 1604 | 50.6 | 3.2 | 1763 | 55.6 | 3.2 | 2144 | 68 | 3.2 | 2309 | 73 | 3.2 | 2527 | 79.7 | 3.2 |

COV in descending order at 0.1 and 25 Hz using Hirsch and New Witczak models: US-77, K-7, K-99, US-54 and US-283. Using Witczak equation, the order changes to: US-54, K-99, US-77, US-283 and K-7. This shows different projects have different COV using various predictive models. Based on COV, New Witczak model is the best results overall at 40°F.

### *7.2.2 Comparison of Predicted Dynamic Modulus for Calibration Sites at 70°F*

Average predicted modulus for calibration sites at 70°F is indicated in Figure 7.7. US-283 has the highest predicted modulus using New Witczak model at 25 Hz. Witczak equation shows the lowest and highest average predicted modulus at 25 Hz and 0.1 Hz, respectively. Hirsch and New Witczak models show comparable predicted modulus for US-54, US-77, K-7 and K-99. The largest discrepancy between Hirsch and New Witczak models is seen for US-283.

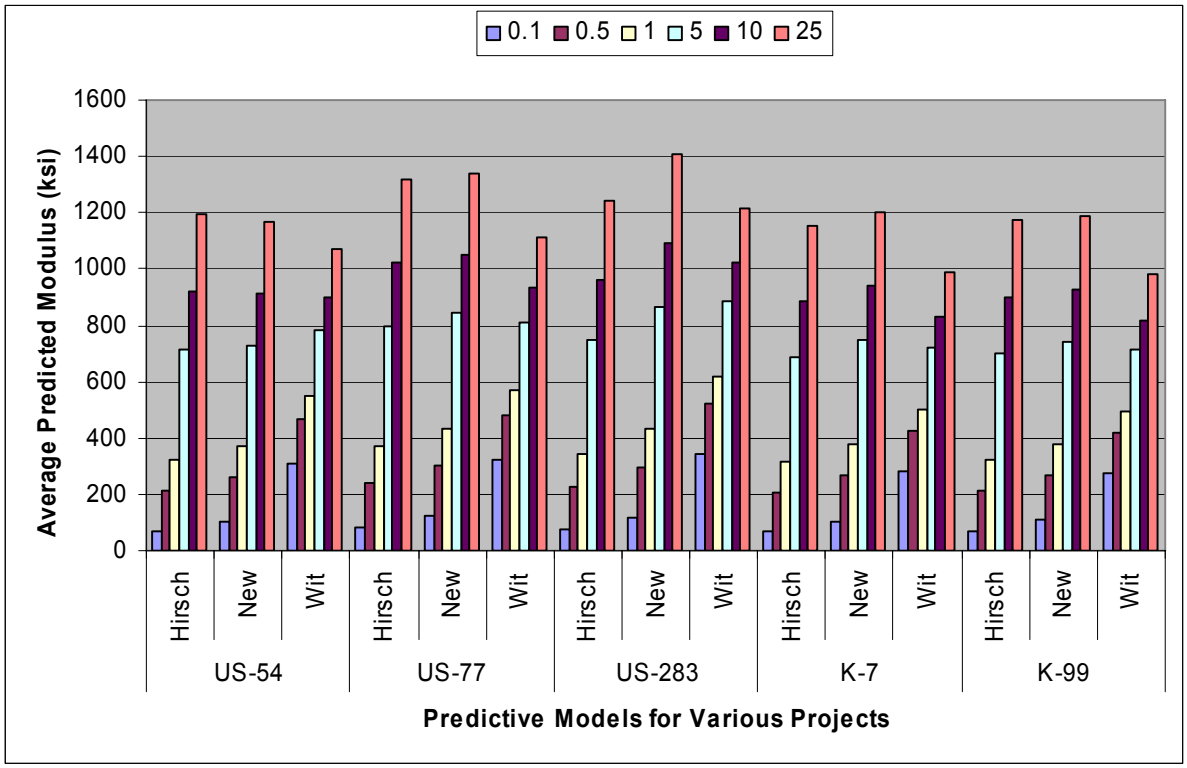


**Figure 7.7: Comparison of Average Predicted Modulus for Calibration Sites at 70°F.**

Table 7.7 indicates summary statistics of predicted modulus for calibration sites at 70°F. Average predicted modulus using Hirsch model at all frequencies in descending order: US-77, US-283, US-54, K-99 and K-7 like at 40°F. The order

changes when New Witczak model is used: US-77, US-283, K-99, K-7 and US-54 unlike at 40$^{o}$F. The order also changes when Witczak equation is used: US-283, US-77, US-54, K-99 and K-7 unlike at 40$^{o}$F. Witczak equation and New Witczak model give the highest overall average predicted modulus at 0.1 and 25 Hz, respectively like at 40$^{o}$F.

**Table 7.7: Summary Statistics of Predicted Modulus for Calibration Sites at 70°F**

| Sites/ Projects | Model | Frequency (Hz) | | | | | | | | | | | | | | | | | |
|---|---|---|---|---|---|---|---|---|---|---|---|---|---|---|---|---|---|---|---|
| | | 0.1 | | | 0.5 | | | 1 | | | 5 | | | 10 | | | 25 | | |
| | | Av. Mod. (ksi) | STD (ksi) | COV (%) | Av. Mod. (ksi) | STD (ksi) | COV (%) | Av. Mod. (ksi) | STD (ksi) | COV (%) | Av. Mod. (ksi) | STD (ksi) | COV (%) | Av. Mod. (ksi) | STD (ksi) | COV (%) | Av. Mod. (ksi) | STD (ksi) | COV (%) |
| **US-54** | **Hirsch** | 72 | 1.5 | 2.1 | 213 | 5.3 | 2.5 | 325 | 8 | 2.4 | 713 | 16 | 2.2 | 918 | 19 | 2.1 | 1195 | 22.8 | 1.9 |
| | **New** | 104 | 2.1 | 2.1 | 261 | 5.2 | 2 | 371 | 7.4 | 2 | 728 | 14 | 1.9 | 912 | 18 | 1.9 | 1164 | 22.2 | 1.9 |
| | **Wit** | 308 | 6.2 | 4.5 | 465 | 9.4 | 5.1 | 548 | 11.1 | 5 | 781 | 16 | 4.5 | 899 | 18 | 4.2 | 1070 | 21.6 | 3.8 |
| **US-77** | **Hirsch** | 81 | 3.7 | 3.1 | 243 | 12.4 | 3.2 | 370 | 18.5 | 3.2 | 800 | 36 | 3.2 | 1021 | 43 | 3.2 | 1316 | 49.7 | 3.2 |
| | **New** | 121 | 3.8 | 4 | 302 | 9.5 | 4.5 | 430 | 13.6 | 4.4 | 842 | 27 | 4 | 1054 | 34 | 3.7 | 1337 | 42.9 | 3.4 |
| | **Wit** | 322 | 8.8 | 3.2 | 484 | 13.3 | 3.1 | 571 | 15.7 | 3.1 | 813 | 22 | 3.1 | 935 | 26 | 3.1 | 1111 | 30.5 | 3.1 |
| **US-283** | **Hirsch** | 76 | 3 | 2.1 | 227 | 10.3 | 2.4 | 345 | 15.3 | 2.4 | 749 | 30 | 2.2 | 959 | 36 | 2.1 | 1242 | 42.1 | 1.9 |
| | **New** | 116 | 3.6 | 2.1 | 298 | 9.3 | 2 | 430 | 13.4 | 2 | 863 | 27 | 1.9 | 1090 | 34 | 1.9 | 1405 | 43.3 | 1.9 |
| | **Wit** | 346 | 9.8 | 3.4 | 523 | 14.9 | 4 | 618 | 17.6 | 4 | 885 | 25 | 3.6 | 1020 | 29 | 3.4 | 1217 | 34.6 | 3.1 |
| **K-7** | **Hirsch** | 70 | 1.5 | 3.3 | 206 | 5 | 3.2 | 315 | 7.6 | 3.1 | 689 | 15 | 3.1 | 887 | 18 | 3 | 1157 | 21.9 | 3 |
| | **New** | 106 | 2.2 | 2 | 266 | 5.3 | 2 | 380 | 7.5 | 2 | 748 | 14 | 2 | 938 | 18 | 2 | 1199 | 22.7 | 2 |
| | **Wit** | 283 | 5.7 | 2.7 | 427 | 8.7 | 2.7 | 504 | 10.2 | 2.7 | 720 | 15 | 2.7 | 830 | 17 | 2.7 | 989 | 20.1 | 2.7 |
| **K-99** | **Hirsch** | 72 | 2.5 | 2.8 | 211 | 8.5 | 2.8 | 321 | 12.7 | 2.8 | 702 | 25 | 2.8 | 903 | 30 | 2.8 | 1176 | 36.3 | 2.8 |
| | **New** | 107 | 3.5 | 2 | 267 | 8.5 | 2 | 380 | 11.9 | 2 | 743 | 23 | 2 | 930 | 28 | 2 | 1186 | 35.8 | 2 |
| | **Wit** | 276 | 8.7 | 3.2 | 418 | 13.2 | 3.2 | 495 | 15.6 | 3.2 | 711 | 23 | 3.2 | 820 | 26 | 3.2 | 979 | 30.9 | 3.2 |

STD in descending order at 0.1 and 25 Hz using Hirsch and New Witczak models: US-77, US-283, K-99, K-7 and US-54. The order using Witczak equation: US-283, US-77, K-99, US-54, and K-7. COV in descending order using Hirsch model: K-7, US-77, K-99, US-54 and US-283; New Witczak model: US-77, US-54, US-283, K-7 and K-99; Witczak equation: US-54, US-283, US-77, K-7 and K-99. New Witczak model is the best based on COV at 70oF.

### *7.2.3 Comparison of Predicted Dynamic Modulus for Calibration Sites at 95°F*

Average predicted modulus for calibration sites at 95°F is indicated in Figure 7.8. US-77 has the highest predicted modulus using Witczak equation at 25 Hz unlike at 70°F. Witczak equation shows the highest average predicted modulus at 25 Hz for all new projects. New Witczak model and Witczak equation show comparable predicted modulus.

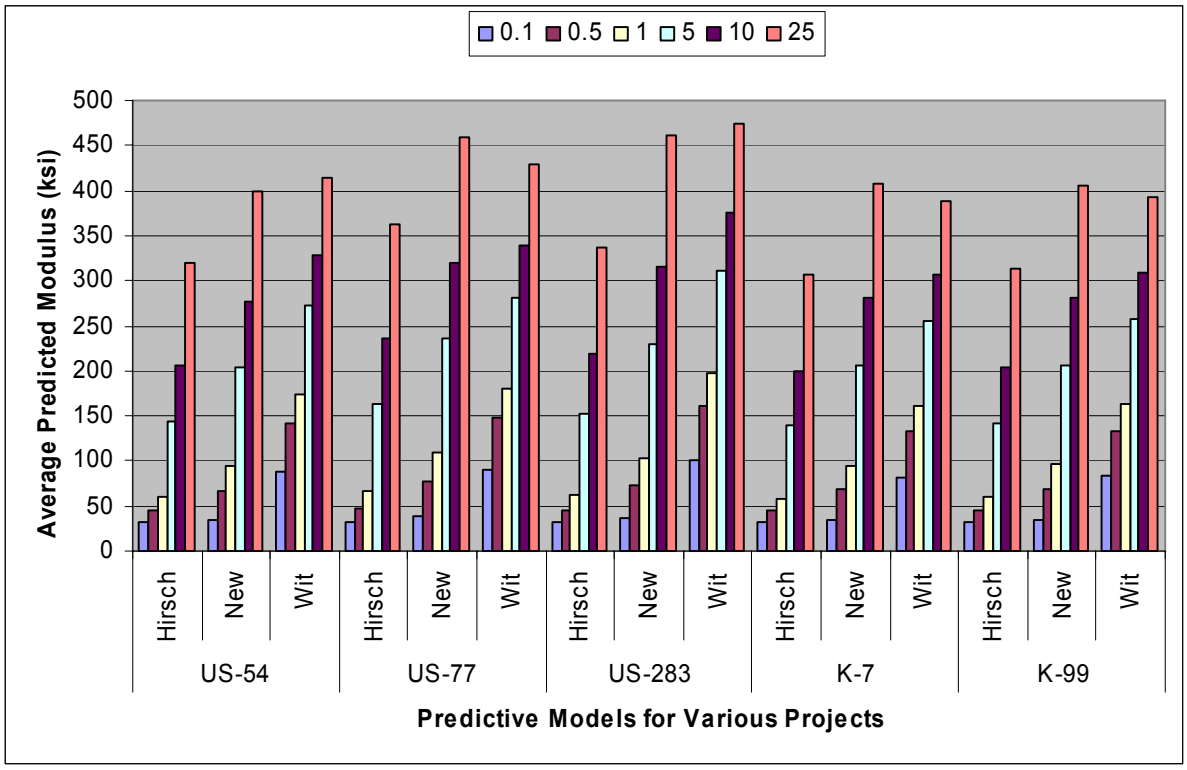


**Figure 7.8: Comparison of Average Predicted Modulus for Calibration Sites at 95°F.**

Table 7.8 indicates summary statistics of predicted modulus for calibration sites at 95°F. Average predicted modulus using Hirsch and New Witczak models at all frequencies in descending order: US-77, US-283, K-99, US-54 and K-7 unlike at 40 and 70°F. The order changes when Witczak equation is used: US-283, US-77, US-54, K-99

and K-7 like at 70$^{o}$F. Witczak equation and Hirsch model give the highest and lowest overall average predicted modulus at 0.1Hz, respectively.

STD in descending order using Hirsch and New Witczak models: US-77, US-283, K-99, US-54 and K-7; Witczak equation: K-99, US-283, US-77, US-54 and K-7., respectively.

**Table 7.8: Summary Statistics of Predicted Modulus for Calibration Sites at 95°F**

| Sites | Model | Frequency (Hz) | | | | | | | | | | | | | | | | | |
|---|---|---|---|---|---|---|---|---|---|---|---|---|---|---|---|---|---|---|---|
| | | 0.1 | | | 0.5 | | | 1 | | | 5 | | | 10 | | | 25 | | |
| | | Av. Mod. (ksi) | STD (ksi) | COV (%) | Av. Mod. (ksi) | STD (ksi) | COV (%) | Av. Mod. (ksi) | STD (ksi) | COV (%) | Av. Mod. (ksi) | STD (ksi) | COV (%) | Av. Mod. (ksi) | STD (ksi) | COV (%) | Av. Mod. (ksi) | STD (ksi) | COV (%) |
| **US-54** | **Hirsch** | 32 | 0.2 | 0.6 | 45 | 0.7 | 1.5 | 60 | 1.2 | 1.9 | 144 | 3.5 | 2.4 | 207 | 5.1 | 2.5 | 319 | 7.8 | 2.4 |
| | **New** | 34 | 0.7 | 2.1 | 67 | 1.4 | 2.1 | 94 | 1.9 | 2.1 | 203 | 4.1 | 2 | 276 | 5.5 | 2 | 399 | 7.9 | 2 |
| | **Wit** | 88 | 1.8 | 1.1 | 142 | 2.9 | 3.2 | 173 | 3.5 | 4.2 | 272 | 5.5 | 5.1 | 328 | 6.6 | 5.1 | 414 | 8.4 | 5 |
| **US-77** | **Hirsch** | 33 | 0.4 | 3.1 | 48 | 1.6 | 3.1 | 67 | 2.8 | 3.1 | 164 | 8.3 | 3.2 | 235 | 12 | 3.2 | 362 | 18.2 | 3.2 |
| | **New** | 39 | 1.2 | 1 | 78 | 2.4 | 2.8 | 109 | 3.4 | 3.6 | 235 | 7.4 | 4.5 | 320 | 10 | 4.5 | 459 | 14.6 | 4.5 |
| | **Wit** | 91 | 2.5 | 3.2 | 147 | 4 | 3.2 | 180 | 4.9 | 3.2 | 282 | 7.7 | 3.1 | 339 | 9.3 | 3.1 | 429 | 11.8 | 3.1 |
| **US-283** | **Hirsch** | 33 | 0.3 | 0.5 | 46 | 1.3 | 1.4 | 63 | 2.3 | 1.9 | 153 | 6.8 | 2.4 | 219 | 9.9 | 2.4 | 337 | 15 | 2.4 |
| | **New** | 36 | 1.2 | 2.2 | 73 | 2.3 | 2.1 | 103 | 3.3 | 2.1 | 229 | 7.2 | 2 | 315 | 9.9 | 2 | 461 | 14.4 | 2 |
| | **Wit** | 100 | 2.8 | 0.9 | 162 | 4.6 | 2.4 | 198 | 5.6 | 3.1 | 312 | 8.9 | 3.9 | 375 | 11 | 4 | 475 | 13.5 | 4 |
| **K-7** | **Hirsch** | 32 | 0.2 | 3.4 | 44 | 0.6 | 3.3 | 59 | 1.1 | 3.3 | 139 | 3.3 | 3.2 | 200 | 4.9 | 3.2 | 307 | 7.4 | 3.1 |
| | **New** | 34 | 0.7 | 2 | 68 | 1.4 | 2 | 95 | 2 | 2 | 206 | 4.2 | 2 | 281 | 5.6 | 2 | 407 | 8 | 2 |
| | **Wit** | 82 | 1.7 | 2.7 | 133 | 2.7 | 2.7 | 162 | 3.3 | 2.7 | 255 | 5.2 | 2.7 | 306 | 6.2 | 2.7 | 388 | 7.9 | 2.7 |
| **K-99** | **Hirsch** | 32 | 0.3 | 2.8 | 45 | 1 | 2.8 | 60 | 1.9 | 2.8 | 142 | 5.6 | 2.8 | 204 | 8.2 | 2.8 | 314 | 12.4 | 2.8 |
| | **New** | 35 | 1.2 | 2 | 69 | 2.3 | 2 | 96 | 3.1 | 2 | 207 | 6.6 | 2 | 281 | 8.9 | 2 | 406 | 12.7 | 2 |
| | **Wit** | 83 | 2.6 | 3.2 | 134 | 4.2 | 3.2 | 163 | 5.2 | 3.2 | 257 | 8.1 | 3.2 | 309 | 9.8 | 3.2 | 392 | 12.4 | 3.2 |

COV in descending order using Hirsch model: K-7, US-77, K-99, US-54 and US-283; New Witczak model: US-283, K-7, K-99, US-54 and US-77; Witczak equation:US-77, K-7, K-99, US-54 and US-283, respectively. New Witczak model shows the least COV in general, similar trend at 40 and 70oF.

## 7.3 Predicted Dynamic Modulus at 25 Hz and Various Temperatures

Comparison has been made for calibration sites and US-75 sections at temperatures of 40, 70 and 95°F and frequency of 25 Hz.

Figure 7.9 illustrates the computed AC dynamic moduli. The new Witczak model shows the highest average predicted modulus for all calibration sites except on US-54. AC dynamic modulus from the new Witczak model is comparable with that from the Hirsch model at 40 and 70°F whereas it gives comparable results with the Witczak equation at 95°F. The Witczak equation gives the lowest average modulus at 40°F, but the trend changes with temperature.

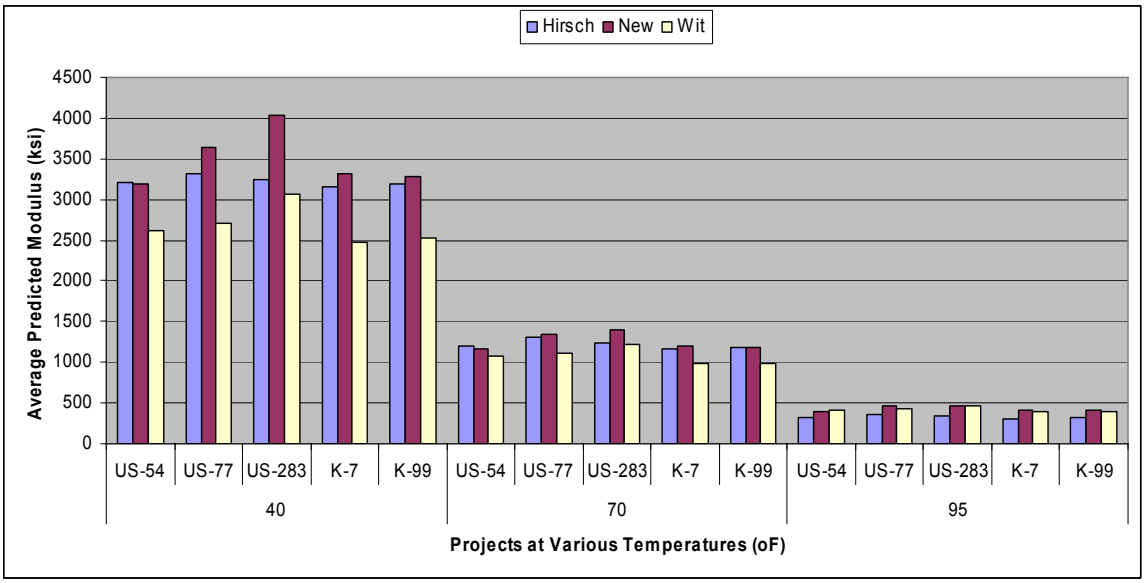


**Figure 7.9: Modulus Using Prediction Models for Calibration Sites at 25Hz.**

Figure 7.10 the average predicted modulus for perpetual pavement sections at 25Hz. At 40°F, the average predicted modulus in descending order: New Witczak model, Hirsch model, and Witczak equation. At 70°F, the order changes to: New Witczak model, Witczak equation, and Hirsch model. At 95°F, Witczak equation shows

the highest followed by New Witczak model. Dynamic moduli using the Witczak equation are the lowest at 40°F and the highest at 95°F for all calibration sites.

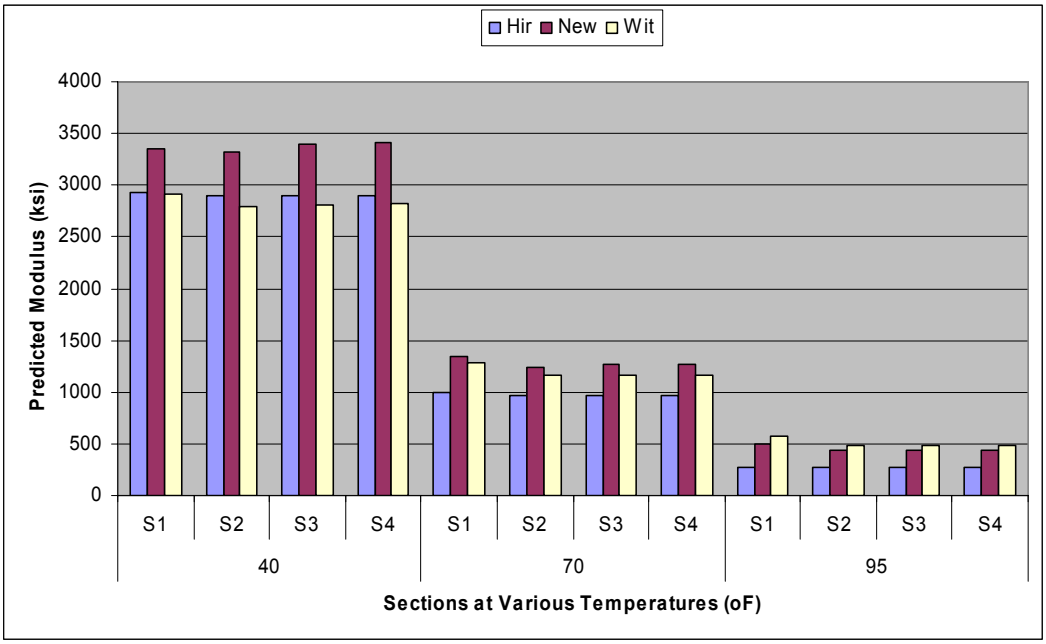


**Figure 7.10: Modulus Using Prediction Models for US-75 Sections at 25Hz.**

Table 7.9 shows the summary statistics of the predicted dynamic moduli for all calibration sites and US-75 sections. The new Witczak model, Hirsch model and Witczak equation show the highest to the lowest average modulus for calibration sites at all temperatures except on US-54. Hirsch model gave the highest modulus for US-54. The coefficient of variation increases as the temperature increases for all projects at all temperatures. US-54 and K-7 have least COV and not much difference from model to model. Thus US-54 and K-7 are best characterized by all models. The standard deviation of AC moduli for calibration sites predicted from the Witczak equation decreases as the temperature increases but no specific trend is evident for the Hirsch model. The result shows that the Witczak equation may underestimate the dynamic

modulus at low temperature and overestimate at high temperature when compared to the laboratory-measured dynamic moduli.

**Table 7.9: Summary Statistics of Predicted Modulus at 25 Hz**

| | | Hirsch | | | New | | | Wit | | |
|---|---|---|---|---|---|---|---|---|---|---|
| | | Avg. Mod. (ksi) | Std. dev. (ksi) | COV (%) | Avg. Mod. (ksi) | Std. dev. (ksi) | COV (%) | Avg. Mod. (ksi) | Std. dev. (ksi) | COV (%) |
| **a. Calibration Sites** | | | | | | | | | | |
| **40** | **US-54** | 3201 | 22.6 | 0.7 | 3190 | 57.7 | 1.8 | 2622 | 53 | 2 |
| | **US-77** | 3316 | 42.7 | 1.3 | 3648 | 117.2 | 3.2 | 2704 | 74.3 | 2.7 |
| | **US-283** | 3241 | 38.8 | 1.2 | 4029 | 121.9 | 3 | 3060 | 87.2 | 2.9 |
| | **K-7** | 3163 | 22.3 | 0.7 | 3325 | 59.5 | 1.8 | 2481 | 50.4 | 2 |
| | **K-99** | 3184 | 36.2 | 1.1 | 3276 | 94.4 | 2.9 | 2527 | 79.7 | 3.2 |
| **70** | **US-54** | 1195 | 22.8 | 1.9 | 1164 | 22.2 | 1.9 | 1070 | 21.6 | 2 |
| | **US-77** | 1316 | 49.7 | 3.8 | 1337 | 42.9 | 3.2 | 1111 | 30.5 | 2.7 |
| | **US-283** | 1242 | 42.1 | 3.4 | 1405 | 43.3 | 3.1 | 1217 | 34.6 | 2.8 |
| | **K-7** | 1157 | 21.9 | 1.9 | 1199 | 22.7 | 1.9 | 989 | 20.1 | 2 |
| | **K-99** | 1176 | 36.3 | 3.1 | 1186 | 35.8 | 3 | 979 | 30.9 | 3.2 |
| **95** | **US-54** | 319 | 7.8 | 2.4 | 399 | 7.9 | 2 | 414 | 8.4 | 2 |
| | **US-77** | 362 | 18.2 | 5 | 459 | 14.6 | 3.2 | 429 | 11.8 | 2.7 |
| | **US-283** | 337 | 15 | 4.5 | 461 | 14.4 | 3.1 | 475 | 13.5 | 2.8 |
| | **K-7** | 307 | 7.4 | 2.4 | 407 | 8 | 2 | 388 | 7.9 | 2 |
| | **K-99** | 314 | 12.4 | 4 | 406 | 12.7 | 3.1 | 392 | 12.4 | 3.2 |
| **b. US-75 Sections** | | | | | | | | | | |
| **40** | **S1** | 2923 | | | 3355 | | | 2911 | | |
| | **S2** | 2897 | | | 3328 | | | 2794 | | |
| | **S3** | 2901 | | | 3390 | | | 2814 | | |
| | **S4** | 2892 | | | 3410 | | | 2825 | | |
| **70** | **S1** | 990 | | | 1337 | | | 1288 | | |
| | **S2** | 970 | | | 1243 | | | 1164 | | |
| | **S3** | 973 | | | 1264 | | | 1168 | | |
| | **S4** | 966 | | | 1271 | | | 1167 | | |
| **95** | **S1** | 278 | | | 498 | | | 570 | | |
| | **S2** | 271 | | | 436 | | | 490 | | |
| | **S3** | 273 | | | 441 | | | 489 | | |
| | **S4** | 270 | | | 441 | | | 486 | | |

## 7.4 Effect of Aging on Predicted Modulus Using Witczak Equation

Effect of aging on predicted modulus using Witczak equation has been considered at three temperatures: 40, 70 and 95$^{o}$F and six frequencies: 0.1, 0.5, 1.0, 5.0, 10.0 and 25.0 Hz. Viscosity at 40$^{o}$F was more than the threshold value specified in M-EPDG and as a result, there was no difference in predicted modulus due to aging. Modulus has been predicted using the Witczak equation based on initial, 5-year and 10-year viscosities.

Figure 7.11 shows effect of aging on predicted modulus for US-54 at 70$^{o}$F. There is an increase in predicted modulus with an increase in age, but the rate of increase reduces with time. The difference between predicted modulus initially and after 5 years is greater than the difference between the predicted moduli at 5 and 10 years though the rate of increase in predicted modulus due to the increase in frequency remains similar initially, after 5 and 10 years. This may indicate that the aging process slows down with time.

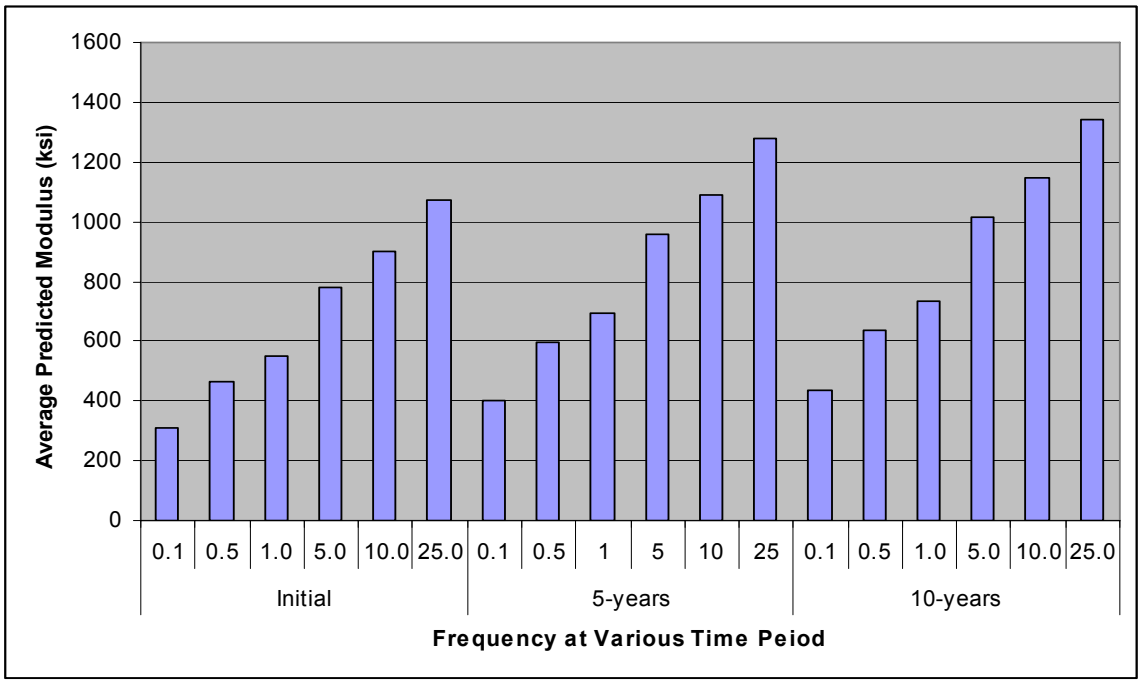


**Figure 7.11: Effect of Aging on Predicted Modulus for US-54 at 70°F.**

The effect of aging on predicted modulus for US-77 at 70°F is indicated in Figure 7.12. The rate of increase in predicted modulus decreases with time. The rate of increase in predicted modulus due to the increase in frequency remains similar initially, after 5 and 10 years.

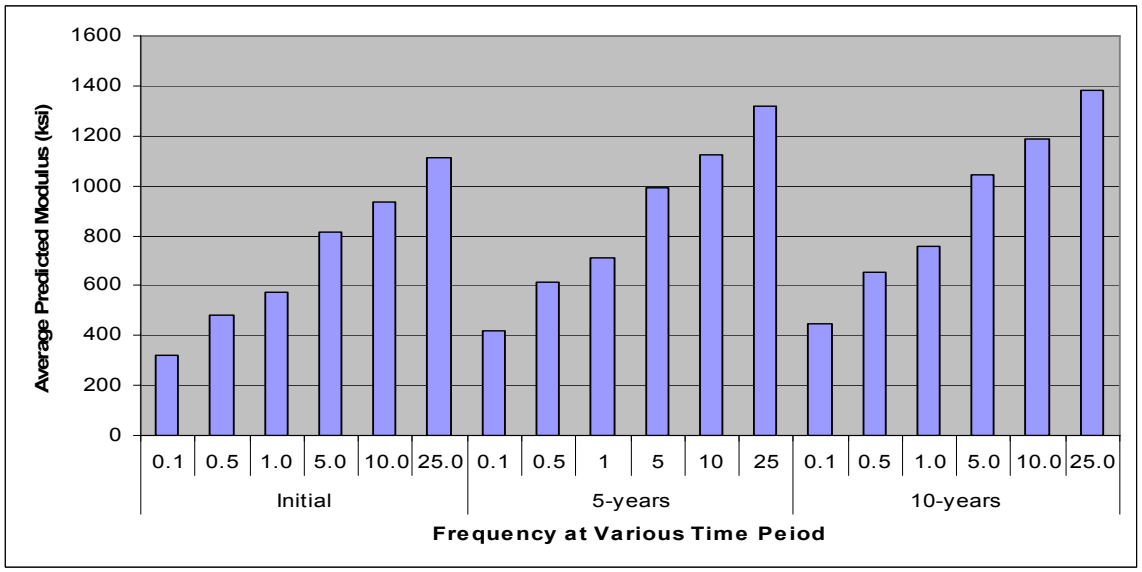


**Figure 7.12: Effect of Aging on Predicted Modulus for US-77 at 70°F.**

For US-283, difference between the initial and the predicted modulus after 5 years is significant, but there is a small difference between the predicted modulus after 5 and 10 years as shown in 7.12. The rate of increase in predicted modulus due to the increase in frequency remains similar initially and after 5 and 10 years.

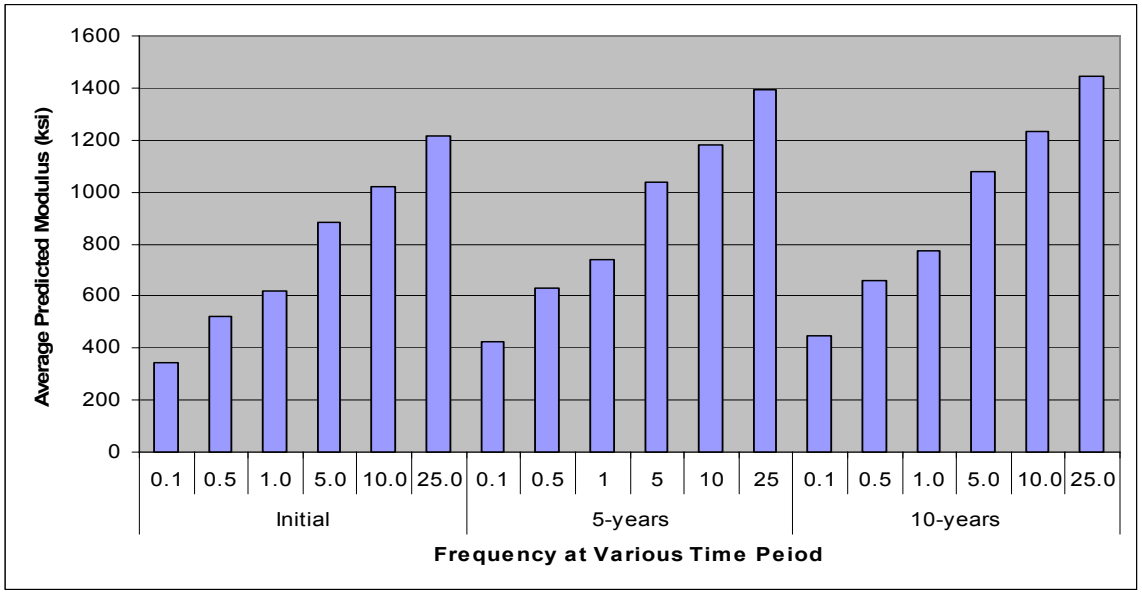


**Figure 7.13: Effect of Aging on Predicted Modulus for US-283 at 70$^{o}$F.**

The trend is similar for K-7 as indicated in Figure 7.14. The difference between the initial predicted modulus and modulus after 5 years increases with increase in frequency whereas the difference between the predicted moduli after 5 and 10 years remains more or less the same. The rate of increase in predicted modulus due to the increase in frequency remains similar initially and after 5 and 10 years.

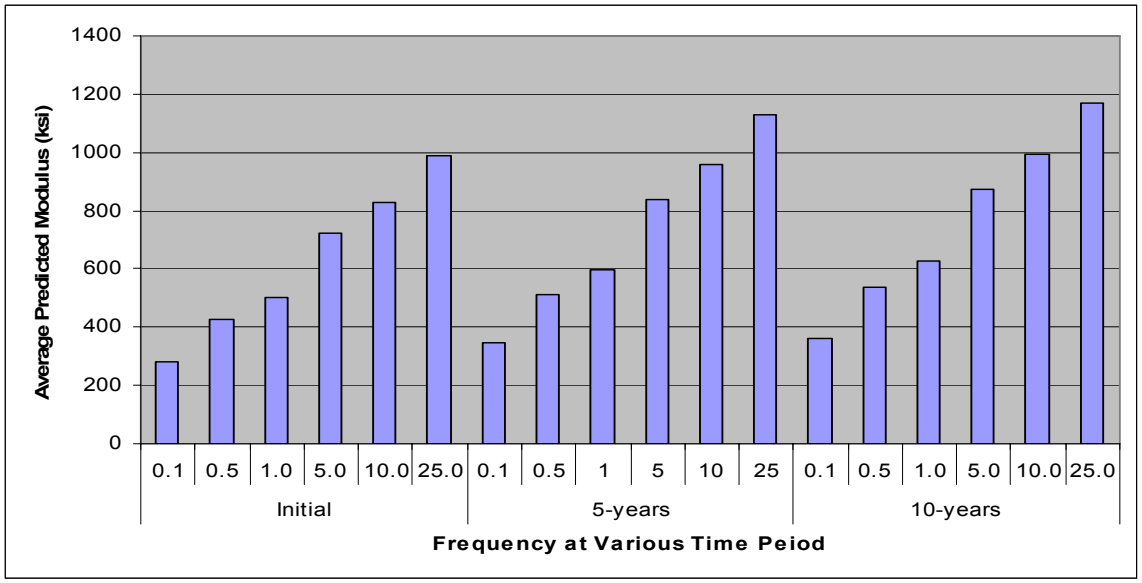


**Figure 7.14: Effect of Aging on Predicted Modulus for K-7 at 70°F.**

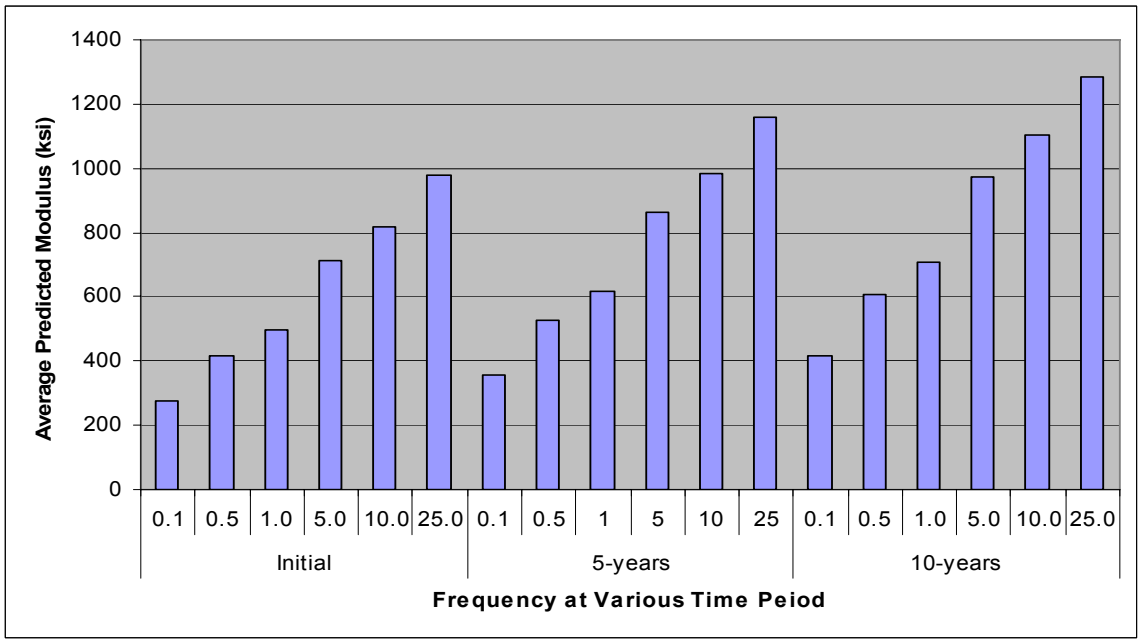


**Figure 7.15: Effect of Aging on Predicted Modulus for K-99 at 70°F.**

The rate of increase in predicted modulus increases with age for K-99 unlike other projects as shown in Figure 7.14. The effect of aging on predicted modulus at 95°F is not significant and the detailed results are given in the Appendix E.

### *7.4.1 Significant Difference Test for the Effect of Aging on Predicted Modulus*

Significant difference test using the Contrast option in Proc GLM has been done at 5% significance level. Siginifant difference test results at 70$^{o}$F have been tabulated in Table 7.10 There is a significant difference between initial, 5-year and 10-year predicted moduli. It shows that aging has significant effect on the predicted modulus at 70$^{o}$F.

Significant difference test results at 95$^{o}$F are shown in Table 7.11. Initial predicted modulus is significantly different than the predicted modulus after 5 and 10 years, respectively for all calibration sites. There is no significant difference between the predicted modulus after 5 and 10 years for US-77, US-283 and K-7. This indicates that the rate of increase in predicted modulus decreases with time.

**Table 7.10: Significant Difference Test for the Effect of Aging on Predicted Modulus at 70°F**

| | | Frequency (Hz) | | | | | | | | | | | |
|---|---|---|---|---|---|---|---|---|---|---|---|---|---|
| | | 0.1 | | 0.5 | | 1 | | 5 | | 10 | | 25 | |
| | | P-value | Similar | P-value | Similar | P-value | Similar | P-value | Similar | P-value | Similar | P-value | Similar |
| US-54 | Initial vs 5yrs | <.0001 | No | <.0001 | No | <.0001 | No | <.0001 | No | <.0001 | No | <.0001 | No |
| | Initial vs 10yrs | <.0001 | No | <.0001 | No | <.0001 | No | <.0001 | No | <.0001 | No | <.0001 | No |
| | 5yrs vs 10yrs | <.0001 | No | <.0001 | No | <.0001 | No | <.0001 | No | <.0001 | No | <.0001 | No |
| US-77 | Initial vs 5yrs | <.0001 | No | <.0001 | No | <.0001 | No | <.0001 | No | <.0001 | No | <.0001 | No |
| | Initial vs 10yrs | <.0001 | No | <.0001 | No | <.0001 | No | <.0001 | No | <.0001 | No | <.0001 | No |
| | 5yrs vs 10yrs | <.0001 | No | <.0001 | No | <.0001 | No | <.0001 | No | <.0001 | No | <.0001 | No |
| US-283 | Initial vs 5yrs | <.0001 | No | <.0001 | No | <.0001 | No | <.0001 | No | <.0001 | No | <.0001 | No |
| | Initial vs 10yrs | <.0001 | No | <.0001 | No | <.0001 | No | <.0001 | No | <.0001 | No | <.0001 | No |
| | 5yrs vs 10yrs | <.0001 | No | 0.0001 | No | 0.0003 | No | 0.001 | No | 0.0018 | No | 0.0038 | No |
| K-7 | Initial vs 5yrs | <.0001 | No | <.0001 | No | <.0001 | No | <.0001 | No | <.0001 | No | <.0001 | No |
| | Initial vs 10yrs | <.0001 | No | <.0001 | No | <.0001 | No | <.0001 | No | <.0001 | No | <.0001 | No |
| | 5yrs vs 10yrs | <.0001 | No | <.0001 | No | <.0001 | No | <.0001 | No | <.0001 | No | 0.0002 | No |
| K-99 | Initial vs 5yrs | <.0001 | No | <.0001 | No | <.0001 | No | <.0001 | No | <.0001 | No | <.0001 | No |
| | Initial vs 10yrs | <.0001 | No | <.0001 | No | <.0001 | No | <.0001 | No | <.0001 | No | <.0001 | No |
| | 5yrs vs 10yrs | <.0001 | No | <.0001 | No | <.0001 | No | <.0001 | No | <.0001 | No | 0.0002 | No |

**Table 7.11: Significant Difference Test for the Effect of Aging on Predicted Modulus at 95°F**

| | | Frequency (Hz) | | | | | | | | | | | |
|---|---|---|---|---|---|---|---|---|---|---|---|---|---|
| | | 0.1 | | 0.5 | | 1 | | 5 | | 10 | | 25 | |
| | | P-value | Similar | P-value | Similar | P-value | Similar | P-value | Similar | P-value | Similar | P-value | Similar |
| US-54 | Initial vs 5yrs | <.0001 | No | <.0001 | No | <.0001 | No | <.0001 | No | <.0001 | No | <.0001 | No |
| | Initial vs 10yrs | <.0001 | No | <.0001 | No | <.0001 | No | <.0001 | No | <.0001 | No | <.0001 | No |
| | 5yrs vs 10yrs | 0.0088 | No | 0.0465 | No | <.0001 | No | Yes | No | Yes | No | 0.1013 | Yes |
| US-77 | Initial vs 5yrs | <.0001 | No | <.0001 | No | <.0001 | No | <.0001 | No | <.0001 | No | <.0001 | No |
| | Initial vs 10yrs | <.0001 | No | <.0001 | No | <.0001 | No | <.0001 | No | <.0001 | No | <.0001 | No |
| | 5yrs vs 10yrs | 0.0603 | Yes | 0.0514 | Yes | 0.0564 | Yes | 0.0681 | Yes | 0.0894 | Yes | 0.1005 | Yes |
| US-283 | Initial vs 5yrs | <.0001 | No | <.0001 | No | <.0001 | No | <.0001 | No | <.0001 | No | <.0001 | No |
| | Initial vs 10yrs | <.0001 | No | <.0001 | No | <.0001 | No | <.0001 | No | <.0001 | No | <.0001 | No |
| | 5yrs vs 10yrs | 0.3405 | Yes | 0.2929 | Yes | 0.3336 | Yes | 0.3485 | Yes | 0.3694 | Yes | 0.3818 | Yes |
| K-7 | Initial vs 5yrs | <.0001 | No | <.0001 | No | <.0001 | No | <.0001 | No | <.0001 | No | <.0001 | No |
| | Initial vs 10yrs | <.0001 | No | <.0001 | No | <.0001 | No | <.0001 | No | <.0001 | No | <.0001 | No |
| | 5yrs vs 10yrs | 0.1751 | Yes | 0.157 | Yes | 0.3336 | Yes | 0.2009 | Yes | 0.2557 | Yes | 0.2482 | Yes |
| K-99 | Initial vs 5yrs | <.0001 | No | <.0001 | No | <.0001 | No | <.0001 | No | <.0001 | No | <.0001 | No |
| | Initial vs 10yrs | <.0001 | No | <.0001 | No | <.0001 | No | <.0001 | No | <.0001 | No | <.0001 | No |
| | 5yrs vs 10yrs | 0.0002 | Yes | 0.0004 | No | 0.0004 | No | 0.0011 | No | 0.001 | No | 0.0023 | No |

## 7.5 Sensitivity Analysis for the Witczak Equation

Sensitivity analysis at 10 percent interval (-25% to +25% i.e. -25% shows 75% of the original value and +25% indicates 125% of the original value) has been done for calibration sites using Witczak equation based on the following parameters: percent retained on ¾ in sieve (rho34), 3/8 in sieve (rho38) and 3/16 in sieve (rho4), percent passing sieve # 200 (rho200), percent air voids (VA) and percent effective asphalt content ($V_{eff}$). Average predicted modulus at 25 Hz and 70$^{o}$F has been discussed for new projects and results at 40 and 95$^{o}$F are given in the Appendix F.

### *7.5.1 Sensitivity Analysis for US-54*

Sensitivity analysis for US-54 is shown in Figure 7.16. Predicted modulus is fairly insensitive to rho34 since percent retained on rho34 is small. Rho34, rho38, and rho200 have positive effects on the predicted modulus whereas Rho4, VA and $V_{eff}$ have negative effects on the predicted modulus. The highest average modulus is observed when the sensitivity to $V_{eff}$ is -25%.

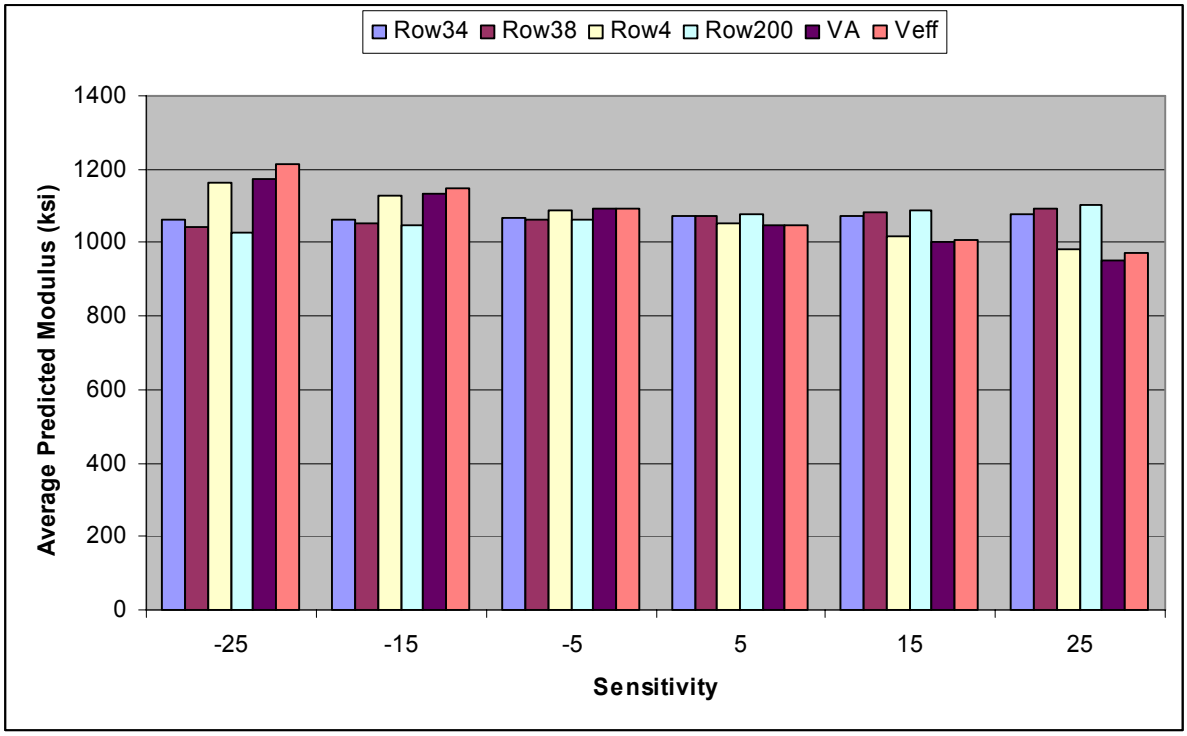


**Figure 7.16: Sensitivity Analysis for US-54 at 70°F and 25 Hz.**

### *7.5.2 Sensitivity Analysis for US-77*

Sensitivity analysis results for US-77 are shown in Figure 7.17. Rho34 and rho200 have positive effects on the predicted modulus whereas the effect of rho38 does not show any clear trend. Rho4, VA and $V_{eff}$ have negative effects on the predicted modulus.

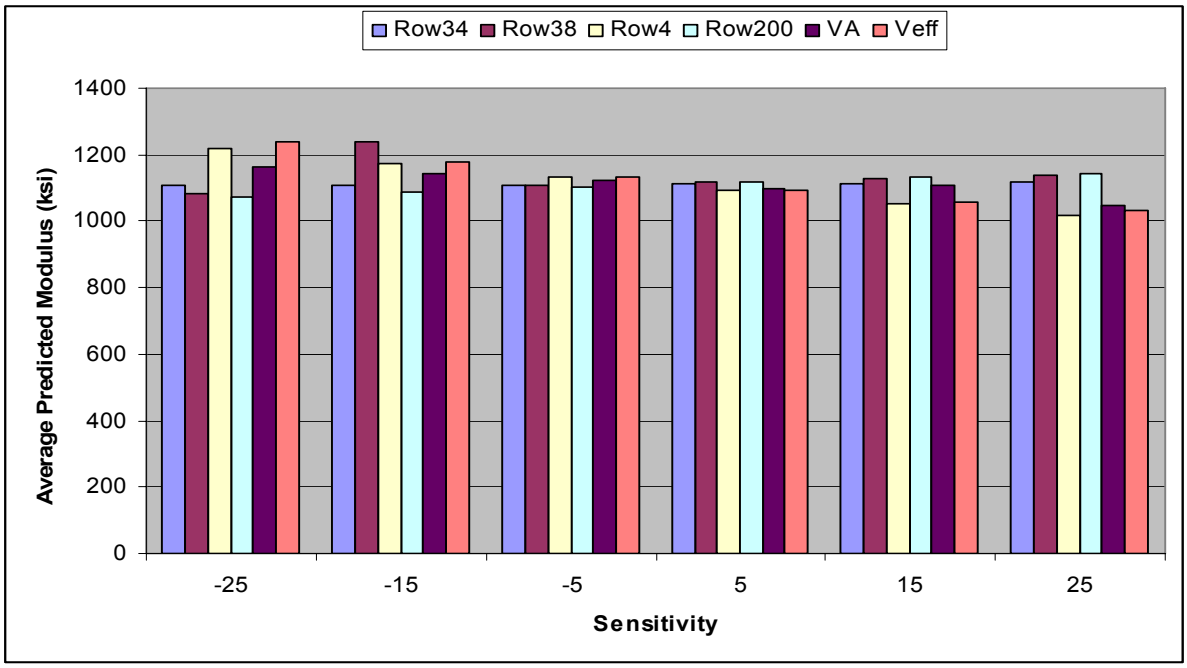


**Figure 7.17: Sensitivity Analysis for US-77 at 70°F and 25 Hz.**

### *7.5.3 Sensitivity Analysis for US-283*

Sensitivity analysis for US-283 is shown in Figure . Rho34, rho38 and rho200 have positive effects on the predicted modulus. Rho4, VA and $V_{eff}$ have negative effects on the predicted modulus.

### *7.5.4 Sensitivity Analysis for K-7*

Sensitivity analysis for K-7 is shown in Figure 7.19. Rho34 does not have any effect and as a result, is not included in sensitivity analysis for K-7. Rho38 and rho200 have positive effects on the predicted modulus. Rho4, VA and $V_{eff}$ have negative effects on the predicted modulus.

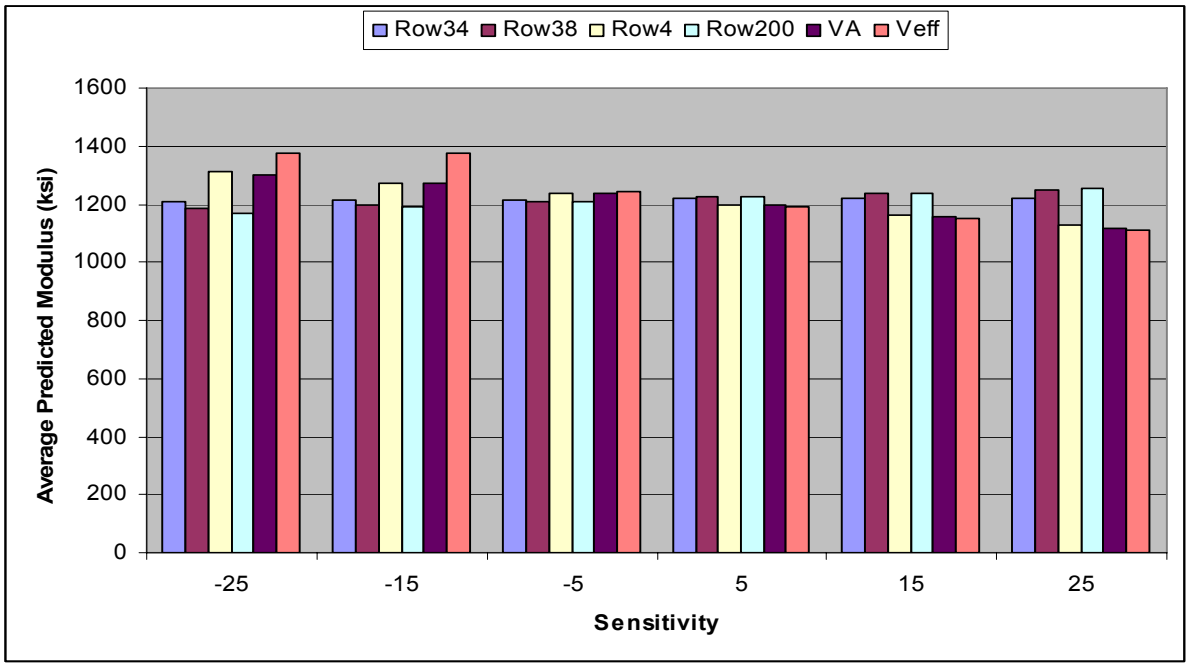


**Figure 7.18: Sensitivity Analysis for US-283 at 70°F and 25 Hz.**

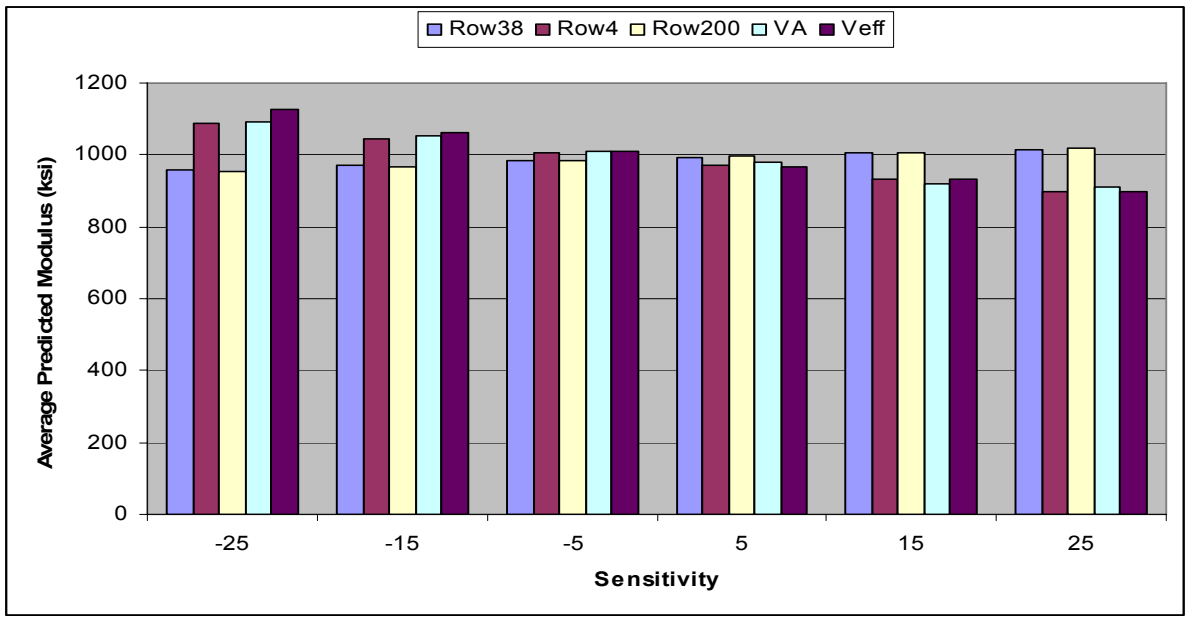


**Figure 7.19: Sensitivity Analysis for K-7 at 70°F and 25 Hz.**

### *7.5.5 Sensitivity Analysis for K-99*

Figure 7.20 shows sensitivity analysis for K-99. Rho34, rho38 and rho200 have positive effects on the predicted modulus whereas rho4, VA and $V_{eff}$ have negative effects on the predicted modulus. The highest average modulus is observed when the sensitivity to $V_{eff}$ is -25%.

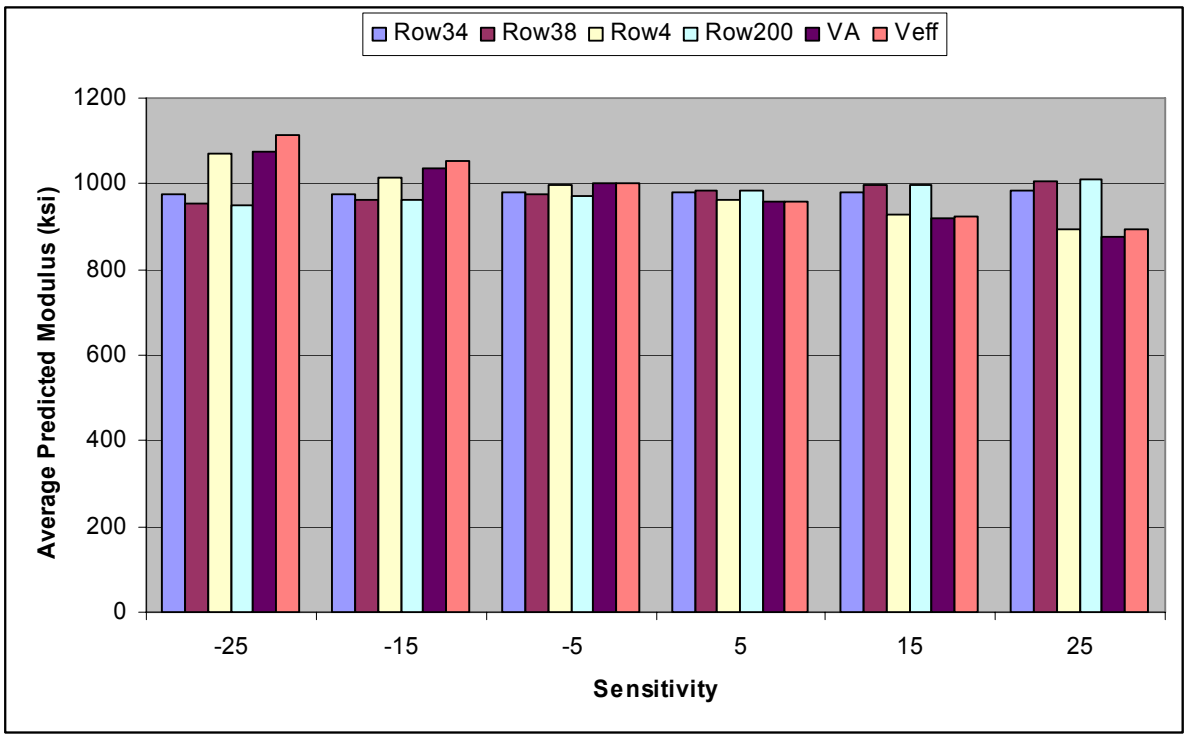


**Figure 7.20: Sensitivity Analysis for K-99 at 70°F and 25 Hz.**

# CHAPTER EIGHT - STATISTICAL ANALYSIS

Comparison of average dynamic modulus has been made at various temperatures for the calibration sites and perpetual pavement sections. Backcalculated, laboratory and predicted dynamic moduli have been compared at a frequency of 25 Hz. Significant difference tests have been done and correction factors have also been developed.

## 8.1 Comparison of Average Dynamic Modulus

### *8.1.1 Comparison of Average Dynamic Modulus for Calibration Sites*

At 40$^{o}$F, backcalculated moduli are the highest for US-54 since it was measured at the lowest temperature. The models tend to over predict at this temperature as compared to laboratory modulus. Predicted moduli are the highest for US-283, K-7 and K-99 except predicted modulus using Witczak equation for K-7 as illustrated in Figure 8.1. Backcalculated modulus using EVERCALC is the highest for US-77, followed by predicted moduli using the Hirsch and New Witczak models. Laboratory dynamic moduli are the lowest for calibration sites except US-283.

The trend changes with the increase in temperature. At 70$^{o}$F, laboratory dynamic moduli are the highest for US-54 and US-77 whereas predicted moduli are the highest for US-283, K-7 and K-99. Backcalculated moduli are the lowest for all new projects. At this temperature, predicted and laboratory moduli are close.

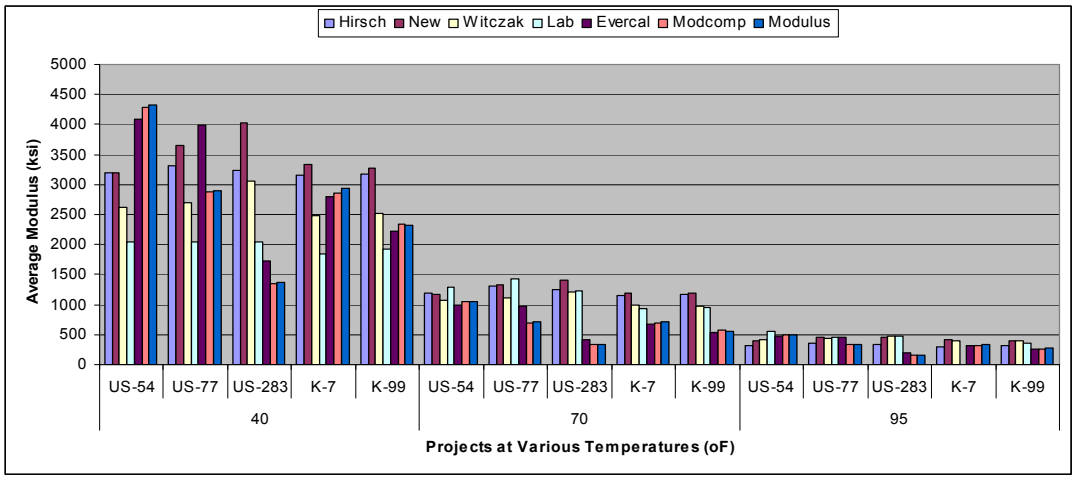


**Figure 8.1: Comparison of Dynamic Modulus for Calibration Sites.**

At 95$^{o}$F, laboratory dynamic modulus is the highest for US-54 whereas predicted moduli are the highest for US-283, K-7 and K-99. New Witczak model shows the highest modulus for US-77. Backcalculated moduli are the lowest for all projects except US-54. Predicted moduli are the lowest for US-54. Predicted and laboratory moduli are very close in general.

### *8.1.2 Comparison of Average Dynamic Modulus for US-75 Sections*

Comparison has been done for the perpetual pavement sections on US-75. The results are illustrated in Figure 8.2. Backcalculated moduli are the highest for S1, S2 and S4 at 40$^{o}$ F. Predicted modulus using new Witczak model is higher than the backcalculated moduli using EVERCALC. Predicted moduli are the highest for S3 except that the backcalculated modulus from MODCOMP. Laboratory dynamic moduli are the lowest for all sections. Models and backcalculation programs tend to over predict at this temperature.

At 70°F, new Witczak model shows the highest moduli for all projects, but the result is comparable to the laboratory dynamic modulus and other predicted moduli. Predicted and laboratory are similar in general. Backcalculated moduli are the lowest.

Laboratory dynamic moduli are the highest at 95°F for all US-75 sections except S4 in which Witczak equation gives the highest. Hirsch model shows the lowest moduli followed by backcalcuated moduli.

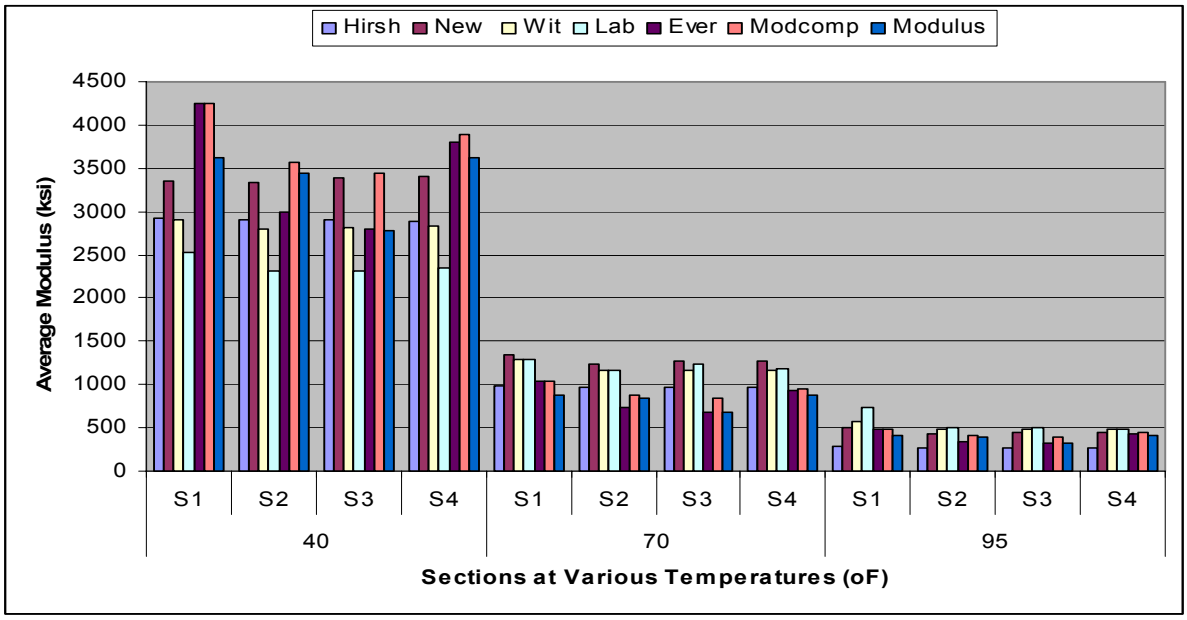


**Figure 8.2: Comparison of Dynamic Modulus for Perpetual Pavement Sections.**

## 8.2 Summary Statistics of Dynamic Modulus

### *8.2.1 Summary Statistics of Dynamic Modulus at 40°F*

Table 8.1 tabulates summary statistics of dynamic modulus at 40°F and 25Hz. MODULUS and EVERCALC shows the highest moduli for US-54 and US-77, respectively whereas new Witczak model shows the highest moduli for US-283, K-7 and K-99. Hirsch model shows the lowest STD and most consistent COV for all calibration sites. EVERCALC shows the highest STD for calibration sites except K-7. EVERCALC

shows the highest COV for US-77, US-283, and K-99. Laboratory test shows the highest COV for US-54 and K-7.

Only one value has been computed for all US-75 test sections and as a result, STD and COV have not been computed. MODCOMP and laboratory test shows the highest and lowest average moduli, respectively.

**Table 8.1: Summary Statistics of Dynamic Modulus at 40°F and 25 Hz**

| | | Predictive Models | | | Lab | Backcalculation Programs | | |
|---|---|---|---|---|---|---|---|---|
| | | Hirsch | New | Witczak | | Everca | Modcomp | Modulus |
| **a. Calibration Sites** | | | | | | | | |
| **US-54** | **Avg.Mod. (ksi)** | 3201 | 3190 | 2622 | 2037 | 4080 | 4276 | 4331 |
| | **STD (ksi)** | 22.6 | 57.7 | 53.0 | 304.3 | 306.2 | 234.5 | 332.9 |
| | **COV (%)** | 0.7 | 1.8 | 2.0 | 14.9 | 7.5 | 5.5 | 7.7 |
| **US-77** | **Avg.Mod. (ksi)** | 3316 | 3648 | 2704 | 2039 | 3980 | 2870 | 2904 |
| | **STD (ksi)** | 42.7 | 117.2 | 74.3 | 112.7 | 1144.1 | 257.2 | 349.5 |
| | **COV (%)** | 1.3 | 3.2 | 2.7 | 5.5 | 28.7 | 9.0 | 12.0 |
| **US-283** | **Avg.Mod. (ksi)** | 3241 | 4029 | 3060 | 2046 | 1724 | 1346 | 1369 |
| | **STD (ksi)** | 38.8 | 121.9 | 87.2 | 145.5 | 313.1 | 136.7 | 121.0 |
| | **COV (%)** | 1.2 | 3.0 | 2.9 | 7.1 | 18.2 | 10.2 | 8.8 |
| **K-7** | **Avg.Mod. (ksi)** | 3163 | 3325 | 2481 | 1845 | 2791 | 2847 | 2934 |
| | **STD (ksi)** | 22.3 | 59.5 | 50.4 | 338.2 | 141.0 | 184.4 | 290.1 |
| | **COV (%)** | 0.7 | 1.8 | 2.0 | 18.3 | 5.1 | 6.5 | 9.9 |
| **K-99** | **Avg.Mod. (ksi)** | 3184 | 3276 | 2527 | 1915 | 2216 | 2346 | 2315 |
| | **STD (ksi)** | 36.2 | 94.4 | 79.7 | 44.9 | 266.6 | 164.8 | 160.8 |
| | **COV (%)** | 1.1 | 2.9 | 3.2 | 2.3 | 12.0 | 7.0 | 6.9 |
| **b. US-75 Sections** | | | | | | | | |
| **S1** | **Avg.Mod. (ksi)** | 2923 | 3355 | 2911 | 2536 | 4247 | 4256 | 3630 |
| **S2** | **Avg.Mod. (ksi)** | 2897 | 3328 | 2794 | 2312 | 2998 | 3568 | 3446 |
| **S3** | **Avg.Mod. (ksi)** | 2901 | 3390 | 2814 | 2307 | 2795 | 3439 | 2772 |
| **S4** | **Avg.Mod. (ksi)** | 2892 | 3410 | 2825 | 2357 | 3795 | 3888 | 3630 |

### *8.2.2 Summary Statistics of Dynamic Modulus at 70°F*

Table 8.2 shows that Laboratory dynamic modulus is the highest for US-54 and US-77, whereas new Witczak model shows the highest modulus for US-283, K-7 and K-99. KDOT design modulus, described in Chapter 2 earlier and calculated only at 70°F using Equation (4.12) in this report, is the lowest for all projects. Laboratory result

shows the highest STD for all calibration sites except US-77 in which EVERCALC shows the highest STD. EVERCALC shows the highest COV for US-77, US-283 and K-99 whereas laboratory result shows the highest for US-54 and K-7. Predictive models show more consistent COV in general.

New Witczak model shows the highest moduli whereas KDOT design modulus is the lowest for all US-75 sections.

**Table 8.2: Summary Statistics of Dynamic Modulus at 70°F and 25 Hz**

| | | Predictive Models | | | Lab | Backcalculation Programs | | | KDOTDesign |
|---|---|---|---|---|---|---|---|---|---|
| | | Hirsch | New | Wit | | Ever | Modc. | Modu. | |
| **a. Calibration Sites** | | | | | | | | | |
| **US-54** | **Avg.Mod. (ksi)** | 1195 | 1164 | 1070 | 1295 | 995 | 1043 | 1056 | 283 |
| | **STD (ksi)** | 22.8 | 22.2 | 21.6 | 170.0 | 74.7 | 57.2 | 81.2 | 0 |
| | **COV (%)** | 1.9 | 1.9 | 2.0 | 13.1 | 7.5 | 5.5 | 7.7 | 0 |
| **US-77** | **Avg.Mod. (ksi)** | 1316 | 1337 | 1111 | 1435 | 970 | 700 | 708 | 286 |
| | **STD (ksi)** | 49.7 | 42.9 | 30.5 | 260.3 | 278.9 | 62.7 | 85.2 | 0 |
| | **COV (%)** | 3.8 | 3.2 | 2.7 | 18.1 | 28.7 | 9.0 | 12.0 | 0 |
| **US-283** | **Avg.Mod. (ksi)** | 1242 | 1405 | 1217 | 1226 | 420 | 328 | 334 | 289 |
| | **STD (ksi)** | 42.1 | 43.3 | 34.6 | 155.1 | 76.3 | 33.3 | 29.5 | 0 |
| | **COV (%)** | 3.4 | 3.1 | 2.8 | 12.7 | 18.2 | 10.2 | 8.8 | 0 |
| **K-7** | **Avg.Mod. (ksi)** | 1157 | 1199 | 989 | 935 | 680 | 694 | 715 | 301 |
| | **STD (ksi)** | 21.9 | 22.7 | 20.1 | 178.1 | 34.4 | 45.0 | 70.7 | 0 |
| | **COV (%)** | 1.9 | 1.9 | 2.0 | 19.1 | 5.1 | 6.5 | 9.9 | 0 |
| **K-99** | **Avg.Mod. (ksi)** | 1176 | 1186 | 979 | 960 | 540 | 572 | 565 | 291 |
| | **STD (ksi)** | 36.3 | 35.8 | 30.9 | 101.4 | 65.0 | 40.2 | 39.2 | 0 |
| | **COV (%)** | 3.1 | 3.0 | 3.2 | 10.6 | 12.0 | 7.0 | 6.9 | 0 |
| **b. US-75 Sections** | | | | | | | | | |
| **S1** | **Avg.Mod. (ksi)** | 990 | 1337 | 1288 | 1294 | 1035 | 1038 | 885 | 291 |
| **S2** | **Avg.Mod. (ksi)** | 970 | 1243 | 1164 | 1170 | 731 | 870 | 840 | 291 |
| **S3** | **Avg.Mod. (ksi)** | 973 | 1264 | 1168 | 1233 | 682 | 839 | 676 | 291 |
| **S4** | **Avg.Mod. (ksi)** | 966 | 1271 | 1167 | 1191 | 925 | 948 | 885 | 291 |

### *8.2.3 Summary Statistics of Dynamic Modulus at 95°F*

The new Witczak model shows the highest moduli for US-77, K-7 and K-99 whereas laboratory moduli are the highest for US-54 and US-283 as can be seen from Table 8.3. Hirsch model shows the lowest moduli for US-54; MODCOMP shows the lowest moduli for US-77 and US-283 and EVERCALC shows the lowest for K-7 and K-

99. Modulus shows the highest STD and COV for US-54 and K-7 whereas EVERCALC indicates the highest STD and COV for US-77, US-283 and K-99. Laboratory result shows the lowest STD and COV for US-54 and US-283; Witczak equation shows the lowest STD and COV for US-77 and Hirsch model shows the lowest for K-7 and K-99. Predictive models give more consistent COV.

Hirsch model and Witczak equation shows the lowest and highest average dynamic moduli, respectively, for all US-75 sections.

**Table 8.3: Summary Statistics of Dynamic Modulus at 95$^{o}$F and 25 Hz**

| | | Predictive Models | | | Lab | Backcalculation Programs | | |
|---|---|---|---|---|---|---|---|---|
| | | Hirsch | New | Witczak | | Ever. | Modc. | Modu. |
| **a. Calibration Sites** | | | | | | | | |
| **US-54** | **Avg.Mod. (ksi)** | 319 | 399 | 414 | 547 | 468 | 490 | 497 |
| | **STD (ksi)** | 7.8 | 7.9 | 8.4 | 7.1 | 35.1 | 26.9 | 38.2 |
| | **COV (%)** | 2.4 | 2.0 | 2.0 | 1.3 | 7.5 | 5.5 | 7.7 |
| **US-77** | **Avg.Mod. (ksi)** | 362 | 459 | 429 | 451 | 457 | 329 | 333 |
| | **STD (ksi)** | 18.2 | 14.6 | 11.8 | 19.8 | 131.2 | 29.5 | 40.1 |
| | **COV (%)** | 5.0 | 3.2 | 2.7 | 4.4 | 28.7 | 9.0 | 12.0 |
| **US-283** | **Avg.Mod. (ksi)** | 337 | 461 | 475 | 478 | 198 | 154 | 157 |
| | **STD (ksi)** | 15.0 | 14.4 | 13.5 | 8.6 | 35.9 | 15.7 | 13.9 |
| | **COV (%)** | 4.5 | 3.1 | 2.8 | 1.8 | 18.2 | 10.2 | 8.8 |
| **K-7** | **Avg.Mod. (ksi)** | 307 | 407 | 388 | N.A. | 320 | 327 | 337 |
| | **STD (ksi)** | 7.4 | 8.0 | 7.9 | N.A. | 16.2 | 21.1 | 33.3 |
| | **COV (%)** | 2.4 | 2.0 | 2.0 | N.A. | 5.1 | 6.5 | 9.9 |
| **K-99** | **Avg.Mod. (ksi)** | 314 | 406 | 392 | 359 | 254 | 266 | 269 |
| | **STD (ksi)** | 12.4 | 12.7 | 12.4 | 30.5 | 30.6 | 18.4 | 18.9 |
| | **COV (%)** | 4.0 | 3.1 | 3.2 | 8.5 | 12.0 | 6.9 | 7.0 |
| **b. US-75 Sections** | | | | | | | | |
| **S1** | **Avg.Mod. (ksi)** | 278 | 498 | 570 | 741 | 487 | 488 | 416 |
| **S2** | **Avg.Mod. (ksi)** | 271 | 436 | 490 | 498 | 344 | 409 | 395 |
| **S3** | **Avg.Mod. (ksi)** | 273 | 441 | 489 | 507 | 321 | 394 | 318 |
| **S4** | **Avg.Mod. (ksi)** | 270 | 441 | 486 | 489 | 435 | 446 | 416 |

## 8.3 Significant Difference Test for Calibration Sites

Statistical analysis for comparing dynamic moduli obtained from various approaches was done by the Statistical Analysis System (SAS) software. Contrast option in Proc GLM has been used to test the significant difference. Comparison was made at 5% level of significance. Dynamic moduli, obtained at a temperature of 40, 70 and 95$^{o}$F and frequency of 25 Hz, were used for comparison. It is to be noted significant difference test has been done for the laboratory and predicted moduli at 25 Hz and backcalculated moduli.

Significant differences among the average AC moduli from various approaches were only investigated for the calibration sites because of absence of replicate values for the US-75 sections. The KDOT AC design modulus was not included in the significant difference test since it was found to be quite different from all other moduli. The p-value was used to test the significance of the difference among the average dynamic moduli at all temperatures.

The analysis results at 40$^{o}$F have been tabulated in Table 8.4. The new Witczak model-predicted moduli are statistically similar to only Hirsch model-predicted moduli except for K-7. Laboratory determined and the backcaculated moduli are significantly different for calibration sites. MODCOMP and MODULUS give statistically similar result for calibration sites. In general, the results are spotty at best i.e. some approaches tend to give similar moduli for a certain site but not for all sites.

Significant difference test at 70$^{o}$F is shown in Table 8.5. The new Witczak model-predicted moduli are statistically similar to Hirsch model-predicted moduli only. Laboratory determined and the backcaculated moduli are significantly different for all

calibration sites and overall. MODCOMP and MODULUS give statistically similar result for all calibration sites. In general, the results are similar to the once at 70$^{o}$F.

Dynamic moduli using Hirsch model are significantly different from those of new Witczak model at 95$^{o}$F as shown in Table 8.6. There is significant difference between the dynamic moduli predicted using new Witczak model and Witczak equation and backcalculated using MODCOMP and MODULUS for all calibration sites. Backcalculated and laboratory moduli are significantly different for all except US-54. MODCOMP and MODULUS give statistically similar results at all temperatures.

**Table 8.4: Significant Difference Test for Calibration Sites at 40°F and 25 Hz**

| Depend.variable | Indep. variable | US-54 | | US-77 | | US-283 | | K-7 | | K-99 | | Overall | |
|---|---|---|---|---|---|---|---|---|---|---|---|---|---|
| | | p-value | Sim. | p-value | Sim. | p-value | Sim. | p-value | Sim. | p-value | Sim. | p-value | Sim. |
| **Hirsch** | New | 0.9311 | Yes | 0.3304 | Yes | 0.0004 | No | 0.4574 | Yes | 0.4114 | Yes | 0.3406 | Yes |
| | Wit | 0.0335 | No | 0.0539 | Yes | 0.2664 | Yes | 0.0043 | No | <0.0001 | No | 0.0509 | Yes |
| | Lab | 0.0002 | No | 0.0008 | No | <.0001 | No | <.0001 | No | <0.0001 | No | <.0001 | No |
| | Modcomp | 0.0002 | No | 0.1483 | Yes | <.0001 | No | 0.0546 | Yes | <0.0001 | No | 0.0733 | Yes |
| | Modulus | 0.0013 | No | 0.1149 | Yes | <.0001 | No | 0.3832 | Yes | <0.0001 | No | 0.0724 | Yes |
| | Evercalc | 0.0132 | No | <.0001 | No | <.0001 | No | 0.0430 | No | <0.0001 | No | 0.5361 | Yes |
| **New** | Wit | 0.0283 | No | 0.0076 | No | <.0001 | No | 0.0010 | No | <0.0001 | No | 0.0042 | No |
| | Lab | 0.0001 | No | 0.0001 | No | <.0001 | No | <.0001 | No | <0.0001 | No | <.0001 | No |
| | Modcomp | 0.0002 | No | 0.0237 | No | <.0001 | No | 0.0125 | No | <0.0001 | No | 0.0067 | No |
| | Modulus | 0.0015 | No | 0.0176 | No | <.0001 | No | 0.1182 | Yes | <0.0001 | No | 0.0066 | No |
| | Evercalc | 0.0157 | No | 0.0006 | No | <.0001 | No | 0.0098 | No | <0.0001 | No | 0.1177 | Yes |
| **Witczak** | Lab | 0.0170 | No | 0.0505 | Yes | <.0001 | No | 0.0079 | No | <0.0001 | No | 0.0131 | No |
| | Modcomp | <.0001 | No | 0.5745 | Yes | <.0001 | No | 0.2141 | Yes | 0.1117 | Yes | 0.8679 | Yes |
| | Modulus | <.0001 | No | 0.6783 | Yes | <.0001 | No | 0.0255 | No | 0.0670 | Yes | 0.8725 | Yes |
| | Evercalc | 0.0001 | No | <.0001 | No | <.0001 | No | 0.2600 | Yes | 0.0008 | No | 0.1782 | Yes |
| **Lab** | Modcomp | <.0001 | No | 0.0168 | No | 0.0005 | No | 0.0006 | No | 0.0004 | No | 0.0083 | No |
| | Modulus | <.0001 | No | 0.0225 | No | 0.0008 | No | <.0001 | No | 0.0007 | No | 0.0084 | No |
| | Evercalc | <.0001 | No | <.0001 | No | 0.0224 | No | 0.0008 | No | 0.0552 | Yes | 0.0002 | No |
| **Modcom.** | Modulus | 0.3556 | Yes | 0.8818 | Yes | 0.7940 | Yes | 0.2510 | Yes | 0.7776 | Yes | 0.9954 | Yes |
| | Evercalc | 0.0507 | Yes | <.0001 | No | 0.0671 | Yes | 0.9004 | Yes | 0.0229 | No | 0.2372 | Yes |
| **Modulus** | Evercalc | 0.2567 | Yes | <.0001 | No | 0.1077 | Yes | 0.2064 | Yes | 0.0398 | No | 0.2350 | Yes |

**Table 8.5: Significant Difference Test for Calibration Sites at 70°F and 25 Hz**

| Depend. variable | Indep. variable | US-54 | | US-77 | | US-283 | | K-7 | | K-99 | | Overall | |
|---|---|---|---|---|---|---|---|---|---|---|---|---|---|
| | | p-value | Sim. | p-value | Sim. | p-value | Sim. | p-value | Sim. | p-value | Sim. | p-value | Sim. |
| **Hirsch** | New | 0.4078 | Yes | 0.7515 | Yes | <.0001 | No | 0.2366 | Yes | 0.6378 | Yes | 0.2714 | Yes |
| | Wit | 0.0017 | No | 0.0015 | No | 0.4157 | Yes | <.0001 | No | <0.0001 | No | 0.0002 | No |
| | Lab | 0.0203 | No | 0.0784 | Yes | 0.6065 | Yes | <.0001 | No | <0.0001 | No | 0.2268 | Yes |
| | Modcomp | 0.0002 | No | <.0001 | No | <.0001 | No | <.0001 | No | <0.0001 | No | <.0001 | No |
| | Modulus | 0.0001 | No | <.0001 | No | <.0001 | No | <.0001 | No | <0.0001 | No | <.0001 | No |
| | Evercalc | <.0001 | No | <.0001 | No | <.0001 | No | <.0001 | No | <0.0001 | No | <.0001 | No |
| **New** | Wit | 0.0171 | No | 0.0005 | No | <.0001 | No | <.0001 | No | <0.0001 | No | <.0001 | No |
| | Lab | 0.0021 | No | 0.1468 | Yes | <.0001 | No | <.0001 | No | <0.0001 | No | 0.0213 | No |
| | Modcomp | 0.0029 | No | <.0001 | No | <.0001 | No | <.0001 | No | <0.0001 | No | <.0001 | No |
| | Modulus | 0.0019 | No | <.0001 | No | <.0001 | No | <.0001 | No | <0.0001 | No | <.0001 | No |
| | Evercalc | <.0001 | No | <.0001 | No | <.0001 | No | <.0001 | No | <0.0001 | No | <.0001 | No |
| **Witczak** | Lab | <.0001 | No | <.0001 | Yes | 0.7640 | Yes | 0.1889 | Yes | 0.4239 | Yes | 0.0127 | No |
| | Modcomp | 0.5118 | Yes | <.0001 | No | <.0001 | No | <.0001 | No | <0.0001 | No | <.0001 | No |
| | Modulus | 0.4253 | Yes | <.0001 | No | <.0001 | No | <.0001 | No | <0.0001 | No | <.0001 | No |
| | Evercalc | 0.0098 | No | 0.2101 | Yes | <.0001 | No | <.0001 | No | <0.0001 | No | <.0001 | No |
| **Lab** | Modcomp | <.0001 | No | <.0001 | No | <.0001 | No | <.0001 | No | <0.0001 | No | <.0001 | No |
| | Modulus | <.0001 | No | <.0001 | No | <.0001 | No | <.0001 | No | <0.0001 | No | <.0001 | No |
| | Evercalc | <.0001 | No | <.0001 | No | <.0001 | No | <.0001 | No | <0.0001 | No | <.0001 | No |
| **Modcom.** | Modulus | 0.8868 | Yes | 0.7576 | Yes | 0.8552 | Yes | 0.5518 | Yes | 0.7586 | Yes | 0.8560 | Yes |
| | Evercalc | 0.0486 | No | <.0001 | No | 0.0039 | No | 0.7006 | Yes | 0.1827 | Yes | 0.0696 | Yes |
| **Modulus** | Evercalc | 0.0663 | Yes | <.0001 | No | 0.0065 | No | 0.3286 | Yes | 0.3032 | Yes | 0.1023 | Yes |

**Table 8.6: Significant Difference Test for Calibration Sites at 95°F and 25 Hz**

| Depend.variable | Indep. variable | US-54 | | US-77 | | US-283 | | K-7 | | K-99 | | Overall | |
|---|---|---|---|---|---|---|---|---|---|---|---|---|---|
| | | p-value | Sim. | p-value | Sim. | p-value | Sim. | p-value | Sim. | p-value | Sim. | p-value | Sim. |
| **Hirsch** | New | 0.0053 | No | 0.0121 | No | <.0001 | No | <.0001 | No | <.0001 | No | 0.0167 | No |
| | Wit | 0.0014 | No | 0.0607 | Yes | <.0001 | No | <.0001 | No | 0.0002 | No | 0.0204 | No |
| | Lab | <.0001 | No | 0.0132 | No | <.0001 | No | <.0001 | No | 0.0093 | No | 0.0023 | No |
| | Modcomp | <.0001 | No | 0.4383 | Yes | <.0001 | No | 0.0064 | No | 0.0116 | No | 0.6253 | Yes |
| | Modulus | <.0001 | No | 0.3585 | Yes | <.0001 | No | <.0001 | No | 0.0177 | No | 0.5320 | Yes |
| | Evercalc | 0.0002 | No | <.0001 | No | <.0001 | No | 0.0565 | Yes | 0.0005 | No | 0.4866 | Yes |
| **New** | Wit | 0.5084 | Yes | 0.4151 | Yes | 0.4620 | Yes | 0.0104 | No | 0.3613 | Yes | 0.9378 | Yes |
| | Lab | <.0001 | No | 0.9648 | Yes | 0.2985 | Yes | <.0001 | No | 0.0121 | No | 0.4772 | Yes |
| | Modcomp | 0.0015 | No | 0.0025 | No | <.0001 | No | <.0001 | No | <0.0001 | No | 0.0044 | No |
| | Modulus | 0.0117 | No | 0.0018 | No | <.0001 | No | <.0001 | No | <0.0001 | No | 0.0029 | No |
| | Evercalc | 0.1286 | Yes | 0.0062 | No | <.0001 | No | <.0001 | No | <0.0001 | No | 0.0847 | Yes |
| **Witczak** | Lab | 0.0002 | No | 0.4399 | Yes | 0.7512 | Yes | <.0001 | Yes | 0.0732 | Yes | 0.4306 | Yes |
| | Modcomp | 0.0057 | No | 0.0132 | No | <.0001 | No | <.0001 | No | <0.0001 | No | 0.0055 | No |
| | Modulus | 0.0434 | No | 0.0098 | No | <.0001 | No | <.0001 | No | <0.0001 | No | 0.0037 | No |
| | Evercalc | 0.3650 | Yes | 0.0012 | No | <.0001 | No | <.0001 | No | <0.0001 | No | 0.0993 | Yes |
| **Lab** | Modcomp | 0.0872 | Yes | 0.0027 | No | <.0001 | No | N.A. | No | <0.0001 | No | 0.0005 | No |
| | Modulus | 0.0122 | No | 0.0020 | No | <.0001 | No | N.A. | No | <0.0001 | No | 0.0003 | No |
| | Evercalc | 0.0010 | No | 0.0057 | No | <.0001 | No | N.A. | No | <0.0001 | No | 0.0161 | No |
| **Modcom.** | Modulus | 0.3174 | Yes | 0.8816 | Yes | 0.7931 | Yes | 0.1827 | Yes | 0.8340 | Yes | 0.8910 | Yes |
| | Evercalc | 0.0359 | No | <.0001 | No | 0.0651 | Yes | 0.3827 | Yes | 0.1412 | Yes | 0.2379 | Yes |
| **Modulus** | Evercalc | 0.2198 | Yes | <.0001 | No | 0.1048 | Yes | 0.0297 | No | 0.0980 | Yes | 0.1885 | Yes |

## 8.4 Correction Factors

Correction factor (parameter estimate) has been estimated using SAS for all calibration sites and US-75 sections at 40 $^{o}$F, 70 $^{o}$F and 95$^{o}$F. The correction factor for KDOT design modulus was done only at 70$^{o}$F. The correction factor may help in getting the right dynamic modulus input into M-EPDG. In this part of analysis, the design modulus, laboratory dynamic modulus, and backcalculated modulus were taken as dependent variables and the rest as independent variables. The correction factor is very small when the KDOT design modulus is taken as the dependent variable. This implies that the current modulus used in design using the 1993 AASHTO Design guide may be conservative. The moduli obtained in the laboratory tests and in the field are, by far, higher than that used for design.

### *8.4.1 Correction Factors for Calibration Sites*

Table 8.7 tabulates the numerical values of the correction factors for all calibration sites. When the KDOT design modulus is used as a dependent variable, the correction factor varies from 0.21 to 0.29 for US-54, 0.19 to 0.40 for US-77, 0.21 to 0.87 for US-283, 0.26 to 0.44 for K-7, 0.25 to 0.53 for K-99. The highest correction factor is observed for US-283. Overall, the correction factor varies from 0.23 to 0.39.

When the laboratory dynamic modulus is used as the dependent variable at 40$^{o}$F, the correction factor varies from 0.47 to 0.76 for US-54, 0.4 to 0.76 for US-77, 0.51 to 1.58 for US-283, 0.56 to 0.75 for K-7, 0.59 to 0.91 for K-99 and 0.56 to 0.74 overall. At 70$^{o}$F, the correction factor varies from 1.08 to 1.32 for US-54, 1.07 to 2.01 for US-77, 0.87 to 3.7 for US-283, 0.79 to 1.37 for K-7, 0.81 to 1.76 for K-99 and 0.93 to 1.61 overall; at 95$^{o}$F, the correction factor varies from 0.78 to 1.40 for US-54, 0.78 to

1.40 for US-77, 1.01 to 3.19 for US-283, 0.89 to 1.48 for K-99 and 1.06 to 1.39 overall. Correction factors at 40 $^{o}$F and 70$^{o}$F are the lowest and the highest, respectively. The largest discrepancy was observed for US-283 for backcalculated moduli where FWD testing was done at a very high temperature. The correction factors for the laboratory modulus and the predicted modulus are consistently close to 1.00 for all with the Hirsch model being the best closely followed by the new Witczak model at 70$^{o}$F.

**Table 8.7: Correction Factors for Calibration Sites**

| | | US54 | | | US77 | | | US-283 | | | K-7 | | | K99 | | | Overall | | |
|---|---|---|---|---|---|---|---|---|---|---|---|---|---|---|---|---|---|---|---|
| **Dependent** | **Independent** | **40** | **70** | **95** | **40** | **70** | **95** | **40** | **70** | **95** | **40** | **70** | **95** | **40** | **70** | **95** | **40** | **70** | **95** |
| **Design** | Hir | | 0.23 | | | 0.22 | | | 0.23 | | | 0.26 | | | 0.25 | | | 0.24 | |
| | New | | 0.24 | | | 0.21 | | | 0.21 | | | 0.25 | | | 0.25 | | | 0.23 | |
| | Wit | | 0.26 | | | 0.26 | | | 0.24 | | | 0.31 | | | 0.30 | | | 0.27 | |
| | Lab | | 0.21 | | | 0.19 | | | 0.23 | | | 0.31 | | | 0.30 | | | 0.23 | |
| | Modcomp | | 0.27 | | | 0.40 | | | 0.87 | | | 0.43 | | | 0.51 | | | 0.39 | |
| | Modulus | | 0.27 | | | 0.39 | | | 0.86 | | | 0.42 | | | 0.51 | | | 0.39 | |
| | Evercalc | | 0.29 | | | 0.26 | | | 0.67 | | | 0.44 | | | 0.53 | | | 0.35 | |
| **Lab** | Hir | 0.63 | 1.08 | 1.28 | 0.62 | 1.09 | 1.28 | 0.63 | 0.99 | 1.43 | 0.58 | 0.81 | | 0.60 | 0.82 | 1.15 | 0.61 | 0.97 | 1.39 |
| | New | 0.63 | 1.10 | 1.00 | 0.57 | 1.07 | 1.00 | 0.51 | 0.87 | 1.04 | 0.56 | 0.79 | | 0.59 | 0.81 | 0.89 | 0.57 | 0.93 | 1.06 |
| | Wit | 0.76 | 1.20 | 1.06 | 0.76 | 1.29 | 1.06 | 0.67 | 1.01 | 1.01 | 0.75 | 0.95 | | 0.76 | 0.98 | 0.92 | 0.74 | 1.09 | 1.08 |
| | Modcomp | 0.47 | 1.23 | 1.38 | 0.71 | 2.01 | 1.38 | 1.58 | 3.70 | 3.19 | 0.67 | 1.34 | | 0.81 | 1.68 | 1.34 | 0.64 | 1.61 | 1.30 |
| | Modulus | 0.49 | 1.23 | 1.40 | 0.72 | 1.95 | 1.40 | 1.53 | 3.64 | 3.09 | 0.61 | 1.29 | | 0.82 | 1.70 | 1.32 | 0.65 | 1.59 | 1.34 |
| | Evercalc | 0.53 | 1.32 | 0.78 | 0.40 | 1.29 | 0.78 | 1.22 | 2.82 | 2.45 | 0.68 | 1.37 | | 0.91 | 1.76 | 1.48 | 0.56 | 1.45 | 1.09 |
| **Modcomp** | Hir | 1.33 | 0.87 | 0.91 | 0.87 | 0.53 | 0.91 | 0.42 | 0.26 | 0.46 | 0.90 | 0.60 | 1.07 | 0.70 | 0.49 | 0.84 | 0.86 | 0.53 | 0.95 |
| | New | 1.33 | 0.89 | 0.72 | 0.79 | 0.52 | 0.72 | 0.33 | 0.23 | 0.33 | 0.86 | 0.58 | 0.81 | 0.68 | 0.48 | 0.65 | 0.77 | 0.51 | 0.73 |
| | Wit | 1.62 | 0.97 | 0.77 | 1.06 | 0.63 | 0.77 | 0.44 | 0.27 | 0.32 | 1.15 | 0.71 | 0.85 | 0.87 | 0.58 | 0.68 | 1.01 | 0.60 | 0.74 |
| **Modulus** | Hir | 1.34 | 0.88 | 0.92 | 0.88 | 0.54 | 0.92 | 0.42 | 0.27 | 0.47 | 0.93 | 0.62 | 1.10 | 0.67 | 0.48 | 0.86 | 0.87 | 0.54 | 0.96 |
| | New | 1.35 | 0.90 | 0.72 | 0.79 | 0.53 | 0.72 | 0.34 | 0.24 | 0.34 | 0.89 | 0.60 | 0.83 | 0.65 | 0.48 | 0.66 | 0.78 | 0.51 | 0.74 |
| | Wit | 1.64 | 0.98 | 0.78 | 1.07 | 0.64 | 0.78 | 0.45 | 0.27 | 0.33 | 1.19 | 0.73 | 0.87 | 0.84 | 0.58 | 0.69 | 1.02 | 0.60 | 0.75 |
| **Evercalc** | Hir | 1.26 | 0.82 | 1.25 | 1.20 | 0.73 | 1.25 | 0.53 | 0.34 | 0.59 | 0.88 | 0.59 | 1.05 | 0.69 | 0.46 | 0.81 | 0.95 | 0.60 | 1.06 |
| | New | 1.26 | 0.84 | 0.99 | 1.09 | 0.72 | 0.99 | 0.43 | 0.30 | 0.43 | 0.84 | 0.57 | 0.79 | 0.67 | 0.45 | 0.63 | 0.86 | 0.57 | 0.81 |
| | Wit | 1.53 | 0.92 | 1.06 | 1.47 | 0.87 | 1.06 | 0.56 | 0.35 | 0.42 | 1.13 | 0.69 | 0.83 | 0.87 | 0.55 | 0.65 | 1.12 | 0.67 | 0.82 |

### *8.4.2 Correction Factors for US-75 Sections*

Table 8.8 tabulates the numerical values of the correction factors for all US-75 sections. When the design modulus is used as a dependent variable at 70$^{o}$F, the correction factor varies from 0.23 to 0.33 for S1, 0.23 to 0.37 for S2, 0.23 to 0.43 for S3, 0.23 to 0.33 for S4 and 0.23 to 0.35 overall. In general, these correction factors are similar to those of calibration sites.

When the laboratory dynamic modulus is used as the dependent variable at 40$^{o}$F, the correction factor varies from 0.59 to 0.87 for S1, 0.65 to 0.83 for S2, 0.67 to 0.83 for S3, 0.60 to 0.83 for K-7 and 0.62 to 0.84 overall; at 70$^{o}$F, the correction factor varies from 0.97 to 1.46 for S1, 0.94 to 1.50 for S2, 0.98 to 1.82 for S3, 0.94 to 1.34 for S4 and 0.96 to 1.46 overall. At 95$^{o}$F, the correction factor varies from 1.30 to 2.66 for S1, 1.02 to 1.84 for S2, 1.04 to 1.86 for S3, 1.01 to 1.81for S4 and 1.02 to 1.83 overall. Correction factors at 70$^{o}$F are closer to 1.0 for the test sections. Correction factors at 40 and 95$^{o}$F are the lowest and the highest, respectively.

When the backcalculated modulus is used as the dependent variable at 40$^{o}$F, the correction factor varies from 1.08 to 1.46 for S1, 0.96 to 1.28 for S2, 0.82 to 1.22 for S3, 1.06 to 1.38 for S4 and 1.01 to 1.35 overall. At 70$^{o}$F, the correction factor varies from 0.66 to 1.05 for S1, 0.62 to 0.90 for S2, 0.53 to 0.86 for S3, 0.70 to 0.98 for S4 and 0.65 to 0.96 overall. At 95$^{o}$F, the correction factor varies from 0.75 to 1.76 for S1, 0.74 to 1.51 for S2, 0.65 to 1.45 for S3, 0.86 to 1.65 for S4 and 0.77 to 1.54 overall.

**Table 8.8: Correction Factors for US-75 Sections**

| | | S1 | | | S2 | | | S3 | | | S4 | | | Overall | | |
|---|---|---|---|---|---|---|---|---|---|---|---|---|---|---|---|---|
| **Dependent** | **Independent** | **40** | **70** | **95** | **40** | **70** | **95** | **40** | **70** | **95** | **40** | **70** | **95** | **40** | **70** | **95** |
| **Design** | Hir | | 0.29 | | | 0.30 | | | 0.30 | | | 0.30 | | | 0.30 | |
| | New | | 0.22 | | | 0.23 | | | 0.23 | | | 0.23 | | | 0.23 | |
| | Wit | | 0.23 | | | 0.25 | | | 0.25 | | | 0.25 | | | 0.24 | |
| | Lab | | 0.22 | | | 0.25 | | | 0.24 | | | 0.24 | | | 0.24 | |
| | Modcomp | | 0.28 | | | 0.33 | | | 0.35 | | | 0.31 | | | 0.31 | |
| | Modulus | | 0.33 | | | 0.34 | | | 0.43 | | | 0.33 | | | 0.35 | |
| | Evercalc | | 0.28 | | | 0.37 | | | 0.42 | | | 0.32 | | | 0.33 | |
| **Lab** | Hir | 0.87 | 1.31 | 2.66 | 0.80 | 1.21 | 1.84 | 0.80 | 1.27 | 1.86 | 0.82 | 1.23 | 1.81 | 0.82 | 1.26 | 1.83 |
| | New | 0.76 | 0.97 | 1.49 | 0.69 | 0.94 | 1.14 | 0.68 | 0.98 | 1.15 | 0.69 | 0.94 | 1.11 | 0.71 | 0.96 | 1.13 |
| | Wit | 0.87 | 1.00 | 1.30 | 0.83 | 1.01 | 1.02 | 0.82 | 1.06 | 1.04 | 0.83 | 1.02 | 1.01 | 0.84 | 1.02 | 1.02 |
| | Modcomp | 0.59 | 1.24 | 1.52 | 0.65 | 1.34 | 1.22 | 0.67 | 1.47 | 1.28 | 0.60 | 1.25 | 1.09 | 0.62 | 1.30 | 1.18 |
| | Modulus | 0.70 | 1.46 | 1.51 | 0.66 | 1.37 | 1.24 | 0.83 | 1.82 | 1.59 | 0.65 | 1.34 | 1.17 | 0.69 | 1.46 | 1.29 |
| | Evercalc | 0.60 | 1.25 | 1.78 | 0.72 | 1.50 | 1.36 | 0.82 | 1.79 | 1.57 | 0.62 | 1.29 | 1.12 | 0.65 | 1.38 | 1.29 |
| **Modcomp** | Hir | 1.46 | 1.05 | 1.75 | 1.23 | 0.90 | 1.51 | 1.19 | 0.86 | 1.45 | 1.34 | 0.98 | 1.65 | 1.32 | 0.96 | 1.54 |
| | New | 1.27 | 0.78 | 0.98 | 1.07 | 0.70 | 0.94 | 1.01 | 0.66 | 0.89 | 1.14 | 0.75 | 1.01 | 1.13 | 0.73 | 0.95 |
| | Wit | 1.46 | 0.81 | 0.85 | 1.28 | 0.75 | 0.83 | 1.22 | 0.72 | 0.81 | 1.38 | 0.81 | 0.92 | 1.35 | 0.78 | 0.86 |
| **Modulus** | Hir | 1.24 | 0.89 | 1.76 | 1.21 | 0.88 | 1.48 | 0.96 | 0.69 | 1.16 | 1.26 | 0.92 | 1.54 | 1.17 | 0.85 | 1.40 |
| | New | 1.08 | 0.66 | 0.98 | 1.05 | 0.69 | 0.92 | 0.82 | 0.53 | 0.72 | 1.06 | 0.70 | 0.94 | 1.01 | 0.65 | 0.86 |
| | Wit | 1.25 | 0.69 | 0.86 | 1.25 | 0.73 | 0.82 | 0.98 | 0.58 | 0.65 | 1.29 | 0.76 | 0.86 | 1.20 | 0.69 | 0.78 |
| **Evercalc** | Hir | 1.45 | 1.05 | 1.50 | 1.10 | 0.80 | 1.35 | 0.96 | 0.70 | 1.17 | 1.31 | 0.95 | 1.61 | 1.23 | 0.89 | 1.39 |
| | New | 1.27 | 0.77 | 0.84 | 0.96 | 0.62 | 0.84 | 0.82 | 0.54 | 0.73 | 1.11 | 0.72 | 0.99 | 1.06 | 0.68 | 0.86 |
| | Wit | 1.46 | 0.80 | 0.73 | 1.14 | 0.67 | 0.74 | 0.99 | 0.58 | 0.66 | 1.34 | 0.78 | 0.90 | 1.26 | 0.72 | 0.77 |

# CHAPTER NINE - ANALYSIS USING M-EPDG SOFTWARE

## 9.1 Introduction

The most widely used procedure for design of flexible pavements is specified in the *Guide for Design of Pavement Structures*, published in 1986 and 1993, by the American Association of State Highway and Transportation Officials (*AASHTO, 1986; AASHTO 1993*). A few states use the 1972 AASHTO Interim Guide procedure, their own empirical or mechanistic-empirical procedures, or a design catalog (*Hall, 2003*). The design methodologies in all those versions of the AASHTO Guide are based on the empirical performance equations developed using the AASHO Road Test data from the late 1950's.

Due to the limitations of earlier guides, a design guide, based as fully as possible on mechanistic principles, was developed under the National Cooperative Highway Research Program (NCHRP) (*NCHRP, 2004*). The procedure is capable of developing mechanistic-empirical design while accounting for local environmental conditions, local materials, and actual highway traffic distribution by means of axle load spectra. Since the resulting procedure is very sound and flexible and it considerably surpasses the capabilities of any currently available pavement design and analysis tools, it is highly anticipated that it will be adopted by AASHTO as the new AASHTO design method for pavements structures.

## 9.2 Background of M-EPDG Procedure

Mechanistic-empirical (M-E) design combines the elements of mechanical modeling and performance observations in determining required pavement thickness for a given set of design inputs. The mechanical model is based on elementary physics and

determines pavement response to wheel loads or environmental condition in terms of stress, strain, and displacement. The empirical part of the design uses the pavement response to predict the life of the pavement on the basis of actual field performance (*Timm et al., 1998*). *Yoder and Witczak (1975)* pointed out that for any pavement design procedure to be completely rational in nature, three elements must be fully considered: (i) the theory used to predict the assumed failure or distress parameter; (ii) the evaluation of the materials properties applicable to the selected theory; and (iii) the determination of the relationship between the magnitude of the parameter in question to the performance level desired. The newly developed M-E design guide considered all three elements. One of the advantages of M-E design over traditional empirical procedure is better utilization and characterization of available materials (*Timm et al., 1998*).

## 9.3 Design Approach in M-EPDG

In the M-EPDG analysis, the designer first considers site conditions (traffic, climate, material and existing pavement condition, if applicable in case of rehabilitation) and construction conditions in proposing a trial design for a new pavement or rehabilitation. The trial design is then evaluated for adequacy against some predetermined failure criteria. Key distresses and smoothness are predicted from the computed structural responses of stress, strain and deflection due to given traffic and environmental loads. If the design does not meet desired performance criteria at a preselected level of reliability, it is revised and the evaluation process is repeated as necessary (*NCHRP, 2004*). This approach makes it possible to optimize the design and

to more fully ensure that specific distress types will not develop. The detail approach is shown in Figure 9.1.

## 9.4 M-EPDG Design Features

Due to climatic variation and repeated traffic loads over the design life of a pavement, very high amount of uncertainty and variability exists in the pavement design and construction processes (*NCHRP, 2004*). In M-EPDG, the key outputs are the individual distress quantities. Therefore, the reliability term has been incorporated in M-EPDG to come up with an analytical solution, which allows the designer to design a pavement with an acceptable level of distress at the end of design life. Design reliability is defined as the probability that each of the key distress types and smoothness will be less than a critical level over the design period. Therefore, failure criteria are associated with this design reliability. The failure criteria and design reliability are also the required inputs for M-EPDG analysis although the designer and the agency have the control over these values. The design can fail if the predicted distress is greater than the allowable amount or if the predicted distresses are unacceptable.

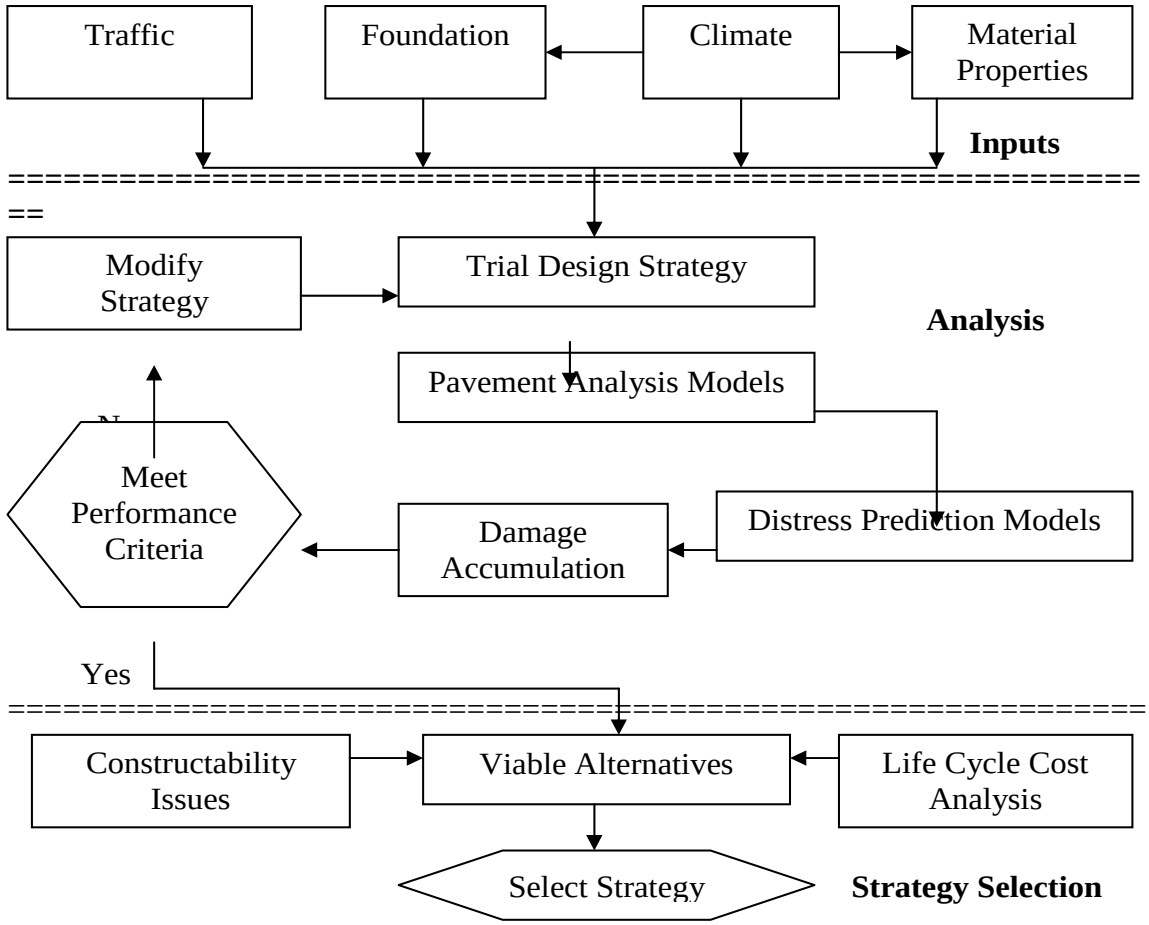


**Figure 9.1: Overall design process for flexible pavements (*NCHRP, 2004*).**

## 9.5 M-EPDG Design Inputs

Hierarchical approach is used for the design inputs in M-EPDG. This approach provides the designer with several levels of "design efficacy" that can be related to the class of highway under consideration or to the level of reliability of design desired. The hierarchical approach is primarily employed for traffic, materials, and environmental inputs (*NCHRP, 2004*). In general, three levels of inputs are provided.

Level 1 is an advanced design procedure and provides the highest practically achievable level of reliability and recommended for design in the heaviest traffic

corridors or wherever there are dire safety or economic consequences of early failure. The design inputs are also of the highest practically achievable level and generally require site-specific data collection and/or testing.

Level 2 is the input level expected to be used in routine design. Level 2 inputs are typically user selected, possibly from an agency database. The data can be derived from a less than optimum testing program or can be estimated empirically.

Level 3 is typically the lowest class of design and should be used where there are minimal consequences of early failure. Inputs typically are user-selected default values or typical averages for the region.

Input data used for the M-EPDG analysis of flexible pavements are categorized as: General Information, Site/Projection Identification, Analysis parameters, Traffic, Climate, Pavement structures and Miscellaneous. Each of them is discussed below.

### *9.5.1 General Information*

The general information inputs include design life, construction month, traffic opening month, and pavement type. All pavement sections in this study were flexible pavements and analyzed for different design period.

### *9.5.2 Site/Project Identification*

Project location, project identification, and functional class of the pavements are included under this input category. Project location defines the climatic conditions for the pavement design. The functional class influences the default design criteria, helps determine the default vehicle classification, and aids in the selection of the vehicle operating speed input.

### *9.5.3 Analysis Parameters*

The flexible design is based on surface-down and bottom-up fatigue cracking of the asphalt surface, hot-mix asphalt (HMA) thermal cracking, fatigue cracking in chemically stabilized layers, permanent deformation for both asphalt layers and the whole pavement, and smoothness. Since there are no stabilized layers in this study, fatigue cracking in chemically stabilized layers is not applicable. Default performance criteria for these parameters are given in Table 9.1.

**Table 9.1: Default Performance Criteria for the Study**

| No. | Distress Type | Distress Target | Reliability Level (%) |
|---|---|---|---|
| **1** | Terminal IRI (in/mi) | 164 | 90 |
| **2** | AC Surface Down Cracking (Long. cracking) (ft/mi) | 1000 | 90 |
| **3** | AC Bottom Up Cracking (Alligator cracking) (%) | 25 | 90 |
| **4** | AC Thermal Fracture (Transverse cracking) (ft/mi) | 1000 | 90 |
| **5** | Chemically Stabilized Layer (Fatigue Fracture) | 25 | 90 |
| **6** | Permanent Deformation (AC only) (in) | 0.25 | 90 |
| **7** | Permanent Deformation (Total pavement) (in) | 0.75 | 90 |

### *9.5.4 Traffic*

Traffic data is one of the key elements required for the design and analysis of pavement structures. The basic required information are annual average daily truck traffic (AADTT) for the base year, percent trucks in the design direction, percent trucks in the design lane, and operational speed of the vehicles. Three functions are available to estimate future truck traffic volumes: no growth, linear growth, and compound growth. Linear growth rate was used in this study.

Project-specific linear traffic growth rates varied from 0.9 to 1.7%. Directional and lane distribution factors for trucks were taken as 60% and 100%, respectively. Percent of trucks in the AADT varied from 13 to 26% as indicated in Table 9.2. For this study,

some other required traffic inputs were derived from the M-EPDG level 3 or default values.

**Table 9.2: Summary of Traffic Data for Calibration Sites**

| | US-54 | US-77 | US-283 | K-7 | K-99 |
|---|---|---|---|---|---|
| **Initial two-way AADT** | 3959 | 1217 | 1046 | 1251 | 1862 |
| **Percent of Trucks** | 13 | 26 | 20 | 14 | 16 |
| **Linear growth rate (%)** | 1.5 | 1.4 | 0.9 | 1.4 | 1.7 |
| **Operational speed (mph)** | 70 | 60 | 65 | 55 | 55 |
| **No. of lanes in each direction** | 1 | 1 | 1 | 1 | 1 |
| **Directional distribution (%)** | 60 | 60 | 60 | 60 | 60 |
| **Lane distribution (%)** | 100 | 100 | 100 | 100 | 100 |

### *9.5.5 Climate*

Environmental conditions have significant effects on the performance of flexible pavements. The seasonal damage and distress accumulation algorithms in the M-EPDG design methodology require hourly data for six weather parameters such as air temperature, precipitation, wind speed, percentage sunshine, relative humidity and seasonal or constant water table depth at the project site (*NCHRP, 2004*). The design guide recommends that the weather inputs be obtained from weather stations located near the project site. At least 24 months of actual weather station data are required for the computations.

The design guide software includes a database of appropriate weather histories from nearly 900 weather stations throughout the United States. This database is accessed by specifying the latitude, longitude, and elevation of the project site. The Design Guide software locates the six closest weather stations to the site. Specification of the weather inputs is identical at all three hierarchical input levels in M-EPDG. In this study, project specific virtual weather stations were created by interpolation of climatic data from the selected physical weather stations.

### *9.5.6 Pavement Structures*

Input values for pavement structure properties are organized into drainage and surface characteristics, layer properties, and distress potential. Flexible pavement design procedure allows a wide variety of asphalt, base, and layer thicknesses. The original pavement structure defined by the user usually has 4 to 6 layers. However, M-EPDG may subdivide the pavement structure into 12 to 15 sublayers for modeling of temperature and moisture variations. Sublayering depends on material type, layer thickness, and the location of the layer within the pavement structure. A maximum of 19 layers can be analyzed.

The inputs required for the AC layer were thickness, PG binder grade, gradation, Superpave mixture volumetric properties, Poisson's ratio, reference temperature, etc. The software computed dynamic modulus (E*) using the default Witczak's predictive equation that takes into account gradation, volumetric properties, asphalt binder grade, and reference temperature (*NCHRP, 2004*).

### *9.5.7 Miscellaneous*

The thermo-hydraulic properties required as inputs into M-EPDG are groundwater depth, infiltration and drainage properties, physical/index properties, hydraulic conductivity, thermal conductivity, heat capacity, etc. (*Barry and Schwartz, 2005*). The recommended calibrated values of 1.25 BTU/hr-ft-°F and 0.28 BTU/lb-°F were used for thermal conductivity and heat capacity, respectively. Physical and index properties were derived based on the gradation of the unbound materials. Surface shortwave absorptivity and drainage path length were chosen based on the default inputs, and were 0.85 and 12 ft, respectively.

## 9.6 Results and Discussions

M-EPDG software version 1.0 was used to analyze only calibration sites. Level 1 analysis requires laboratory dynamic modulus at 10, 40, 70, 100 and 130$^{o}$F. However, laboratory test has been done only at 40 $^{o}$F, 70 $^{o}$F and 95$^{o}$F. Both level 1 and 2 require dynamic shear modulus and shear angle at an angular frequency of 10 rad/sec at the same temperatures. As a result, level 1 and 2 analyses were not done in this study.

Four cases have been considered at level 3 using default distress target. The existing pavement structure was analyzed for a 10-year analysis period as Case 1. Case 2 considers the maximum number of years the existing pavement structure will be in a serviceable condition. Minimum thickness of different layers to serve for ten years has been found by ignoring and considering longitudinal cracking as Cases 3 and 4, respectively. Each case has been discussed separately.

Analysis results using the existing pavement structure for all calibration sites are tabulated in Table 9.3. Distresses predicted are by far less than the target distress limit. The initial IRI is 64 in/mi for projects. The lowest and highest IRI is 86.1 and 89.3 in/mi, respectively. Longitudinal and transverse crack is zero and one, respectively. The thinner the pavement sections, the higher the AC and total permanent deformation.

**Table 9.3: Distress Predicted Using 10-year Analysis Period**

| | Distress Predicted | | | | | Distress Target |
|---|---|---|---|---|---|---|
| | US-54 | US-77 | US-283 | K-7 | K-99 | |
| **IRI (in/mi)** | 86.7 | 86.1 | 87.5 | 89.3 | 89 | 164 |
| **Long. Cracking (ft/mi)** | 0 | 0 | 0 | 0 | 0 | 1000 |
| **Alligator Cracking (%)** | 0 | 0 | 0 | 0.1 | 0.1 | 25 |
| **Transverse Cracking (ft/mi)** | 1 | 1 | 1 | 1 | 1 | 1000 |
| **AC permanent deformation (in)** | 0.08 | 0.05 | 0.07 | 0.09 | 0.09 | 0.25 |
| **Total permanent deformation (in)** | 0.29 | 0.28 | 0.31 | 0.33 | 0.34 | 0.75 |

Table 9.4 tabulates the maximum number of years the existing pavement structure will be in a serviceable condition. K-7 has the thinnest total AC thickness and as a result, it has the least service period. US-77 has the highest service period since it has the highest total thickness. The lowest and highest IRI is observed on US-283 and US-77, respectively. Insignificant longitudinal cracking are observed on only K-99. The lowest and highest AC and total permanent deformation are observed on US-77 and K-99, respectively.

**Table 9.4: Analysis Period for Existing Pavement Structure**

| | Distress Predicted | | | | | Distress Target |
|---|---|---|---|---|---|---|
| | **US-54** | **US-77** | **US-283** | **K-7** | **K-99** | |
| **Years** | 24 | 25 | 23 | 22 | 23 | |
| **IRI (in/mi)** | 120.1 | 121.7 | 118.3 | 119.9 | 120.3 | 164 |
| **Long. Cracking (ft/mi)** | 0 | 0 | 0 | 0 | 0.1 | 1000 |
| **Alligator Cracking (%)** | 0.1 | 0 | 0.1 | 0.1 | 0.4 | 25 |
| **Transverse Cracking (ft/mi)** | 1 | 1 | 1 | 0 | 1 | 1000 |
| **AC permanent deformation (in)** | 0.12 | 0.08 | 0.1 | 0.13 | 0.14 | 0.25 |
| **Total permanent deformation (in)** | 0.37 | 0.35 | 0.38 | 0.41 | 0.44 | 0.75 |

The causes and effects of AC surface down cracking (longitudinal cracking) are not well understood yet and it was ignored in this case to determine the minimum thicknesses of different layers to serve for 10 years as shown in Table 9.5. The lowest to highest total AC thickness to serve for 10 years are: 3, 4.5, 4.5, 5.5 and 6 in for K-7, US-283, US-77, US-54 and K-99, respectively. K-7 has the thinnest total AC thickness since it has 11 inches of AB-3. K-7 and US-54 have the lowest and highest alligator cracking, respectively. US-283 and US-54 have the lowest and highest AC permanent deformation whereas K-99 and US-54 have the lowest and highest total permanent deformation.

**Table 9.5: Minimum Layer Thicknesses Ignoring Longitudinal Cracking**

| | | Distress Predicted | | | | |
|---|---|---|---|---|---|---|
| | | **US-54** | **US-77** | **US-283** | **K-7** | **K-99** |
| **Layer Thickness** | **Surface (in)** | 1.5 | 1.5 | 1.5 | 1 | 1.5 |
| | **Binder (in)** | 2 | 2 | 2 | 1 | 2.5 |
| | **Base (in)** | 2 | 1 | 1 | 1 | 2 |
| | **Total HAM Thickness** | 5.5 | 4.5 | 4.5 | 3.0 | 6.0 |
| | **AB3 (in)** | N.A. | N.A. | N.A. | 11 | N.A. |
| **Distresses** | **IRI (in/mi)** | 100.4 | 102.3 | 100.9 | 101.7 | 99.1 |
| | **Long. Cracking (ft/mi)** | 839 | 1010 | 959 | 63.1 | 4260 |
| | **Alligator Cracking (%)** | 6.1 | 4.7 | 3.8 | 1.4 | 5.7 |
| | **Transverse Cracking (ft/mi)** | 1 | 1 | 1 | 1 | 1 |
| | **AC permanent deformation (in)** | 0.15 | 0.14 | 0.11 | 0.13 | 0.13 |
| | **Total permanent deformation (in)** | 0.54 | 0.6 | 0.58 | 0.59 | 0.52 |

The minimum total AC thickness to serve for a 10-year period considering the longitudinal cracking and the results are shown in Table 9.6. The lowest to highest total AC thickness to serve for 10 years considering longitudinal cracking: 6, 6.5, 7.5, 7.5 and 9 in for K-7, US-77, US-54, US-283 and K-99, respectively. The lowest total AC thickness is observed for K-7 which has 11 inches of AB-3. The lowest IRI is observed on a pavement which has the highest total AC thickness and vice versa. The highest longitudinal cracking is observed on US-77 and K-99. This shows that longitudinal cracking does not depend on the thickness of AC layers. Transverse cracking is constant for all calibration sites. US-283 has the lowest AC and total permanent deformation.

**Table 9.6: Minimum Layer Thicknesses Considering Longitudinal Cracking**

| | | Distress Predicted | | | | |
|---|---|---|---|---|---|---|
| | | **US-54** | **US-77** | **US-283** | **K-7** | **K-99** |
| **Layer Thickness** | **Surface (in)** | 1.5 | 1.5 | 1.5 | 1.5 | 1.5 |
| | **Binder (in)** | 2 | 2 | 2.5 | 2.5 | 2.5 |
| | **Base (in)** | 4 | 3 | 3.5 | 2 | 5 |
| | **Total HMA Thickness** | 7.5 | 6.5 | 7.5 | 6 | 9 |
| | **AB3 (in)** | N.A. | N.A. | N.A. | 11 | N.A. |
| **Distresses** | **IRI (in/mi)** | 92.3 | 92 | 91.4 | 93.1 | 91.4 |
| | **Long. Cracking (ft/mi)** | 2.9 | 8.8 | 2.6 | 4.1 | 8.8 |
| | **Alligator Cracking (%)** | 0.7 | 0.4 | 0.2 | 0.4 | 0.5 |
| | **Transverse Cracking (ft/mi)** | 1 | 1 | 1 | 1 | 1 |
| | **AC permanent deformation (in)** | 0.12 | 0.08 | 0.08 | 0.1 | 0.11 |
| | **Total permanent deformation (in)** | 0.42 | 0.42 | 0.4 | 0.42 | 0.4 |

### *9.6.1 Effect of Subgrade Modulus on Predicted Distress*

Backcalculation programs, Evercalc, Modcomp 5 and Modulus, have been used to backcalculate subgrade modulus. One-third of the backcalculated subgrade modulus was used as the subgrade design modulus to run the M-EPDG software for a 10-year analysis period.

The design subgrade modulus varies from 2,121 to 27,345 psi for US-54 as indicated in Table 9.7. Transverse and longitudinal cracking remain the same at all subgrade moduli. IRI and alligator cracking and total permanent deformation decrease with an increase in subgrade modulus whereas the AC permanent deformation increases/remains constant with an increase in subgrade modulus. No failure has been observed.

**Table 9.7: Effect of Subgrade Modulus on Predicted Modulus for US-54**

| | Backcalculated Subgrade Modulus (psi) | | | | | | | | | |
|---|---|---|---|---|---|---|---|---|---|---|
| | 2121 | | 3704 | | 4107 | | 5158 | | 27345 | |
| **Distress** | Predicted Distress | Relibility | Predicted Distress | Reliability | Predicted Distress | Reliability | Predicted Distress | Reliability | Predicted Distress | Reliability |
| **IRI (in/mi)** | 98.7 | 99.09 | 92.3 | 99.69 | 91.4 | 99.75 | 89.5 | 99.83 | 82.30 | 99.97 |
| **Long. Cracking (ft/mi)** | 0 | 99.99 | 0 | 99.99 | 0 | 99.99 | 0 | 99.99 | 0 | 99.99 |
| **Alligator Cracking (%)** | 0.2 | 99.99 | 0.1 | 99.99 | 0.1 | 99.99 | 0.1 | 99.99 | 0 | 99.99 |
| **Transverse Cracking (ft/mi)** | 1 | 99.99 | 1 | 99.99 | 1 | 99.99 | 1 | 99.99 | 1 | 99.99 |
| **AC permanent deformation (in)** | 0.07 | 99.99 | 0.08 | 99.99 | 0.08 | 99.99 | 0.08 | 99.99 | 0.08 | 99.99 |
| **Total permanent deformation (in)** | 0.59 | 95.72 | 0.43 | 99.99 | 0.41 | 99.99 | 0.36 | 99.99 | 0.18 | 99.99 |

**Table 9.8: Effect of Subgrade Modulus on Predicted Modulus for US-77**

| | Backcalculated Subgrade Modulus (psi) | | | | | | | |
|---|---|---|---|---|---|---|---|---|
| | 1145 | | 2056 | | 3070 | | s9694 | |
| **Distress** | Predicted Distress | Reliability | Predicted Distress | Reliability | Predicted Distress | Reliability | Predicted Distress | Reliability |
| **IRI (in/mi)** | 108.90 | 96.7 | 98.60 | 99.09 | 93.5 | 99.61 | 84.5 | 99.95 |
| **Long. Cracking (ft/mi)** | 0 | 99.99 | 0 | 99.99 | 0 | 99.99 | 0 | 99.99 |
| **Alligator Cracking (%)** | 0.1 | 99.99 | 0.1 | 99.99 | 0 | 99.99 | 0 | 99.99 |
| **Transverse Cracking (ft/mi)** | 1 | 99.99 | 1 | 99.99 | 1 | 99.99 | 1 | 99.99 |
| **AC permanent deformation (in)** | 0.04 | 99.99 | 0.05 | 99.99 | 0.05 | 99.99 | 0.05 | 99.99 |
| **Total permanent deformation (in)** | 0.84 | 20.18 | 0.59 | 99.99 | 0.46 | 99.99 | 0.24 | 99.99 |

The design subgrade modulus varies from 1,145 to 9,694 psi for US-77 as indicated in Table 9.8. Transverse and longitudinal cracking remain the same at all subgrade moduli. IRI, alligator cracking and total permanent deformation decrease with an increase in subgrade modulus whereas AC permanent deformation increases/remains constant with an increase in subgrade modulus. There is a failure in total pavement deformation when subgrade modulus is 1,145 psi. The result shows that the stronger the subgrade, the higher AC permanent deformation.

The design subgrade modulus varies from 1,124 to 8,667 psi for US-283 as indicated in Table 9.9. Transverse and longitudinal cracking remain the same at all subgrade modulus. IRI, alligator cracking and total permanent deformation decrease with an increase in subgrade modulus whereas AC permanent deformation increases/remains constant with an increase in subgrade modulus. There is a failure due to total pavement deformation when the subgrade modulus is 1,124 psi.

The design subgrade modulus varies from 6,340 to 10,053 psi for K-7 as indicated in Table9.10. Transverse cracking, longitudinal cracking and AC performanent deformation remain the same at all subgrade modulus. IRI, alligator cracking and total permanent deformation decrease with an increase in subgrade modulus. There is no failure at any subgrade modulus.

For K-99, the design subgrade modulus varies from 6,564 to 10,133 psi as indicated in Table 9.11. Transverse cracking remains constant at all subgrade modulus. IRI, alligator cracking and AC permanent deformation decrease with an increase in subgrade modulus whereas longitudinal cracking and total performanent deformation

decrease with an increase in the subgrade modulus. There is no failure at any subgrade modulus.

**Table 9.9: Effect of Subgrade Modulus on Predicted Modulus for US-283**

| | Backcalculated Subgrade Modulus (psi) | | | | | | | | | |
|---|---|---|---|---|---|---|---|---|---|---|
| | 1124 | | 2714 | | 6572 | | 7788 | | 8667 | |
| Distress | Predicted Distress | Reli-ability | Predicted Distress | Reli-ability | Predicted Distress | Reli-ability | Predicted Distress | Reli-ability | Predicted Distress | Reli-ability |
| IRI (in/mi) | 113.3 | 94.97 | 97.3 | 99.26 | 88.3 | 99.87 | 87.3 | 99.9 | 88.9 | 99.85 |
| Long. Cracking (ft/mi) | 0 | 99.999 | 0 | 99.999 | 0 | 99.999 | 0 | 99.999 | 0 | 99.999 |
| Alligator Cracking (%) | 0.1 | 99.999 | 0.1 | 99.999 | 0 | 99.999 | 0 | 99.999 | 0 | 99.999 |
| Transverse Cracking (ft/mi) | 1 | 99.999 | 1 | 99.999 | 1 | 99.999 | 1 | 99.999 | 1 | 99.999 |
| AC permanent deformation (in) | 0.06 | 99.999 | 0.06 | 99.999 | 0.07 | 99.999 | 0.07 | 99.999 | 0.09 | 99.999 |
| Total permanent deformation (in) | 0.95 | 4.88 | 0.55 | 98.57 | 0.33 | 99.999 | 0.3 | 99.999 | 0.32 | 99.999 |

**Table 9.10: Effect of Subgrade Modulus on Predicted Modulus for K-7**

| | Backcalculated Subgrade Modulus (psi) | | | | | | | |
|---|---|---|---|---|---|---|---|---|
| | 6340 | | 7583 | | 9348 | | 10053 | |
| Distress | Predicted Distress | Relia-bility | Predicted Distress | Relia-bility | Predicted Distress | Reli-ability | Predicted Distress | Reli-ability |
| IRI (in/mi) | 90.8 | 99.77 | 89.7 | 99.82 | 88.5 | 99.86 | 88.1 | 99.87 |
| Long. Cracking (ft/mi) | 0 | 99.99 | 0 | 99.99 | 0 | 99.99 | 0 | 99.99 |
| Alligator Cracking (%) | 0.1 | 99.99 | 0.1 | 99.99 | 0 | 99.99 | 0 | 99.99 |
| Transverse Cracking (ft/mi) | 1 | 99.99 | 1 | 99.99 | 1 | 99.99 | 1 | 99.99 |
| AC permanent deformation (in) | 0.09 | 99.99 | 0.09 | 99.99 | 0.09 | 99.99 | 0.09 | 99.99 |
| Total permanent deformation (in) | 0.37 | 99.99 | 0.34 | 99.99 | 0.31 | 99.99 | 0.3 | 99.99 |

**Table 9.11: Effect of Subgrade Modulus on Predicted Modulus for K-99**

| | Backcalculated Subgrade Modulus (psi) | | | | | |
|---|---|---|---|---|---|---|
| | 6564 | | 6709 | | 10133 | |
| **Distress** | Predicted Distress | Reli-ability | Predicted Distress | Reli-ability | Predicted Distress | Reli-ability |
| **IRI (in/mi)** | 90 | 99.81 | 89.8 | 99.82 | 87.3 | 99.99 |
| **Long. Cracking (ft/mi)** | 0 | 99.99 | 0 | 99.99 | 0.1 | 99.99 |
| **Alligator Cracking (%)** | 0.2 | 99.99 | 0.2 | 99.99 | 0.1 | 99.99 |
| **Transverse Cracking (ft/mi)** | 1 | 99.99 | 1 | 99.99 | 1 | 99.99 |
| **AC permanent deformation (in)** | 0.09 | 99.99 | 0.09 | 99.99 | 0.1 | 99.99 |
| **Total permanent deformation (in)** | 0.37 | 99.99 | 0.37 | 99.99 | 0.3 | 99.99 |

It should be noted that all performance models used in this study are the nationally calibrated default ones. The projects in this report are in their early stage of life and no distress is expected or has been observed. It may take about 10 years to verify the predicted results. As a result, the conclusion drawn regarding thickness only reflects what the uncalibrated model predicts.

## 9.7 Effect of Aging on Fatigue Life

Initial, 5 and 10-year dynamic moduli have been predicted using the Witczak equation to determine the effect of aging on fatigue life. The predicted dynamic modulus increases with aging. These dynamic moduli have been used to predict tensile strain at the bottom of the AC layer for all calibration sites using KENLAYER (Huang, 2003). KENLAYER has also been used to calculate the fatigue life using the Asphalt Institute model. KENLAYER calculates allowable repetitions, damage index, and fatigue life. The AASHTO method was used to predict number of load repetitions for all calibration sites based on data in Table 9.2.

$$n_i = (ADT)_0(T)(T_f)(G)(Y)(D)(L)(365) \qquad \text{Equation 9.1}$$

where,

$n_i$ = predicted load repetions at time $i$,

$ADT_0$ = daily traffic at the start of design period,

T = the percentage of trucks in the ADT,

$T_f$ = the number of 18-kip single axle load applications,

$(G)(Y) = \frac{(1+r)^Y - 1}{r}$ = total growth factor where $r$ = is growth factor

D = directional distribution, and

L = lane distribution.

M-EPDG method has also been used to calculate allowable number of load repetitions. Alligator cracking is one of load-related cracking that is predicted by M-EPDG. M-EPDG assumes that alligator cracks initiate at the bottom of the AC or HMA layers and propagate to the surface with continued traffic. The allowable number of load

axle load applications needed for the incremental damage index approach to predict load related alligator cracks is shown in Equation (9.2). Site specific predicted dynamic modulus, calculated tensile strain at the bottom of HMA layer, total HMA thickness, air voids and effective asphalt content have been used to calculate allowable number of load repetitions. Default values for other parameters were used.

$$N_{f-HMA} = k_{f1}(C)(C_H)\beta_{f1}\left(\varepsilon_t\right)^{k_{f2}\beta_{f2}}\left(E_{HMA}\right)^{k_{f3}\beta_{f3}} \quad \text{Equation 9.2}$$

where:

$N_{f-HMA}$ = allowable number of axle load applications for a flexible pavement and HMA overlays;

$\varepsilon_t$ = tensile strain at critical locations and calculated by the structural response model (in/in);

$E_{HMA}$ = dynamic modulus of the HMA measured in compression (psi);

$k_{f1}, k_{f2}, k_{f3}$ = global field calibration parameters (from the NCHRP 1-40D re-calibration;

$k_{f1} = 0.007566, k_{f2} = -3.9492,$ and $k_{f3} = -1.281$).

$\beta_{f1}, \beta_{f2}, \beta_{f3}$ = local or mixture specific field calibration constants; for the global calibration effort, these constants were set to 1.0.

$$C = 10^M$$

$$M = 4.84\left(\frac{V_{be}}{V_a + V_{be}} - 0.69\right)$$

$V_{be}$ = effective asphalt content by volume (%);

$V_a$ = percent air voids in the HMA mixture;

$C_H$ = thickness correction term, dependent on type of cracking:

$$C_H = \frac{1}{0.000398 + \frac{0.003602}{1 + e^{(11.02 - 3.49H_{HMA})}}}$$

$H_{HMA}$ = total HMA thickness (in).

Table 9.12 shows the effect of aging on fatigue life. There is an increase in predicted dynamic modulus due to aging. As the modulus increases, tensile strain at the bottom of the AC/HMA layer decreases. There is an increase in both predicted ($n$) and allowable ($N$) number of load repetitions as well. Fatigue life has been calculated as the ratio of allowable to predicted load repetitions. Fatigue life is very high using both KENLAYER and M-EPDG methods although it reduces with time. The M-EPDG method gives higher fatigue life. In summary, the increase in dynamic modulus with aging results in a decrease in tensile strain. The rate of increase in predicted number of load repetitions is greater than that of the allowable number of load repetitions and as a result, fatigue life decreases with time.

**Table 9.12: Effect of Aging on Fatigue Life**

| | Route | Predicted Modulus (ksi) | Tensile Strain | n | KENLAYER | | M-EPDG | |
|---|---|---|---|---|---|---|---|---|
| | | | | | N | Life (yrs) | N | Life (yrs) |
| **Initial** | US-54 | 1070 | -4.81E-05 | 1.13E+05 | 9.19E+07 | 816 | 1.92E+09 | 17053 |
| | US-77 | 1111 | -4.98E-05 | 6.93E+04 | 7.94E+07 | 1146 | 2.05E+09 | 29626 |
| | US-283 | 1217 | -5.30E-05 | 4.58E+04 | 5.96E+07 | 1301 | 1.55E+09 | 33727 |
| | K-7 | 989 | -7.41E-05 | 3.84E+04 | 2.36E+07 | 616 | 3.01E+08 | 7847 |
| | K-99 | 979 | -6.32E-05 | 6.52E+04 | 4.02E+07 | 616 | 6.88E+08 | 10551 |
| **5 yrs** | US-54 | 1280 | -4.15E-05 | 5.81E+05 | 1.28E+08 | 220 | 2.73E+09 | 4702 |
| | US-77 | 1319 | -4.32E-05 | 3.56E+05 | 1.09E+08 | 306 | 2.87E+09 | 8053 |
| | US-283 | 1395 | -4.74E-05 | 2.33E+05 | 7.65E+07 | 328 | 2.01E+09 | 8633 |
| | K-7 | 1130 | -6.74E-05 | 1.97E+05 | 2.88E+07 | 146 | 3.68E+08 | 1867 |
| | K-99 | 1161 | -5.51E-05 | 3.38E+05 | 5.47E+07 | 162 | 9.54E+08 | 2826 |
| **10 yrs** | US-54 | 1342 | -3.99E-05 | 1.21E+06 | 1.40E+08 | 116 | 3.00E+09 | 2486 |
| | US-77 | 1382 | -4.16E-05 | 7.38E+05 | 1.19E+08 | 161 | 3.15E+09 | 4262 |
| | US-283 | 1447 | -4.60E-05 | 4.77E+05 | 8.19E+07 | 172 | 2.16E+09 | 4535 |
| | K-7 | 1170 | -6.58E-05 | 4.09E+05 | 3.03E+07 | 74 | 3.88E+08 | 951 |
| | K-99 | 1286 | -5.07E-05 | 7.05E+05 | 6.59E+07 | 94 | 1.16E+09 | 1648 |

# CHAPTER TEN - CONCLUSIONS

Based on this study, the following conclusions can be made:

- Surface deflection was highly affected by the test temperature for new projects whereas test temperature and pavement thickness highly affected surface deflections for the perpetual pavement sections.
- Repeating different target loads reduces nonlinearity significantly.
- Laboratory dynamic modulus on the US highways is higher than the Kansas highways for new projects.
- All US highways have comparable average laboratory dynamic modulus at 40$^{o}$F and Kansas routes also show the same trend. Unlike US highways, the trend remains the same for Kansas routes at 70$^{o}$F.
- The trend of laboratory dynamic modulus changes as the temperature changes and the degree of change depends upon the mix characteristics, surface or binder.
- In general, all backcalculation programs give comparable results for all new projects. The higher the test temperatures, the lower backcalculated modulus irrespective of total AC thickness. This shows that the effect of temperature is greater than the AC thickness.
- Backculated modulus of the perpetual pavement sections was highly affected by the test temperature and total AC thickness.
- Standard deviation of the backcalculated moduli varies with test temperature whereas the coefficient of variation remains about the same at all temperature levels for new projects.

- The Witczak equation and New Witczak model give the highest overall average predicted modulus at 0.1 and 25 Hz, respectively, at 40 and 70$^{o}$F.
- Witczak equation shows the highest average predicted modulus at 25 Hz for all new projects. The new Witczak model and Witczak equation show comparable predicted modulus for all projects. Witczak equation and Hirsch model give the highest and lowest overall average predicted modulus at 0.1Hz, respectively, at 95$^{o}$F.
- Dynamic moduli using the Witczak equation are the lowest at 40$^{o}$F and the highest at 95$^{o}$F for all test sections.The result shows that the Witczak equation may underestimate the dynamic modulus at low temperature and overestimate at high temperature when compared to the laboratory-measured dynamic moduli.
- Percent passing No. 200 sieve and effective asphalt volume have the highest positive and negative effect, respectively, on the predicted modulus using the Witczak equation.
- Laboratory measured and backcaculated moduli are significantly different for all projects. MODCOMP and MODULUS give statistically similar results for all projects. In general, the results are spotty at best i.e. some approaches tend to give similar moduli for a certain project but not for all projects.
- The correction factor is very small when the KDOT design modulus is taken as the dependent variable. This implies that the current modulus used in design may be conservative.

  Correction factors at 40 and 70$^{o}$F are the lowest and the highest, respectively. The correction factors for the laboratory and predicted moduli are consistently

close to 1.00 for all new projects with the Hirsch model being the best closely followed by the new Witczak model at 70$^{o}$F.

- Correction factors at 70$^{o}$F are closer to 1.0 for perpetual pavement sections. Correction factors at 40 and 95$^{o}$F are the lowest and the highest, respectively.
- M-EPDG software shows that KDOT design is very conservative for the 10-year design period when using the uncalibarted models. The thinner the pavement sections, the higher the AC and total permanent deformation.
- The existing pavement structures can serve for more than 20-years as per M-EPDG software analysis using nationally calibrated default performance models. However, this does not reflect the actual pavement performance observed in Kansas.
- Total AC thickness varies from 3 to 6 inches for a 10-year design period if the effect of AC surface down cracking (longitudinal cracking) is ignored. The lowest thickness is observed on K-7 which has 11 inches of AB-3.
- The minimum total AC thickness to serve for 10-year period considering the longitudinal cracking varies from 6 to 9 in. Longitudinal cracking does not depend on the thickness of AC layers. The lowest IRI is observed on a pavement which has the highest total AC thickness. Backcalculated subgrade moduli obtained from various backcalculation programs result in variable predicted performance for different projects.
- The dynamic modulus increases with aging. However, the fatigue life decreases with time since the rate of increase in predicted number of load repetitions becomes greater than that of the allowable number of load repetitions.

# REFERENCES


AASHTO. *Guide for Design of Pavement Structures*. AASHTO, Washington, D.C., 1986.

AASHTO. *Guide for Design of Pavement Structures*. AASHTO, Washington, D.C., 1993.

AASHTO. Standard Method of Test for Determining Dynamic Modulus of Hot-Mix Asphalt Concrete Mixtures. *AASHTO Designation: TP 62-03*, Washington, D.C., 2001.

Akhter, G. F., and M. W. Witczak. Sensitivity of Flexible Pavement Performance to Bituminous Mix Properties. In *Transportation Research Record 1034*, TRB, National Research Council, Washington, D.C., 1985.

Andrei, D., M.W.Witczak, and M.W. Mirza, Development of a Revised Predictive Model for the Dynamic (Complex) Modulus of Asphalt Mixtures. *Inter Team Technical Report Prepared for the NCHRP 1-37A Project*. Department of Civil Engineering, University of Maryland, College Park, MD, March 1999.

Baltzer, S., and J. M. Jansen. Temperature Correction of Asphalt-Moduli for FWD-Measurements. In *Proceedings of 4$^{th}$ International Conference on the Bearing Capacity of Roads and Airfields*, Vol. 1, Minneapolis, Minn., 1994, 753-760.

Bari, J. *Development of a New Revised Version of the Witczak E* Predictive Models for Hot Mix Asphalt Mixtures.* Ph.D. Dissertation, Arizona State University, Dec. 2005.

Barry, C. R. and C. Schwartz. Geotechnical Aspects of Pavements. *Report No. FHWA NHI-05-037*. National Highway Institute, Federal Highway Administration, Washington, D.C., January 2005.

Bonnaure, F.G., G. Guest, A. Gravois, and P. Uge. A New Method of Predicting the Stiffness of Asphalt Paving Mixtures.In *Journal of the Association of Asphalt Paving Technologies*. Vol. 46, 1977.

Buttlar, W.G., J.M. Bauer, and D.S. Sherman. Dynamic Modulus of Asphalt Concrete with a Hollow Cylinder Tensile Tester. In *Transportation Research Record 1789*, TRB, National Research Council, Washington, D.C., 2002, pp. 183–190.

Chang, D.-W., Y. V. Kang, J. M. Roesset, and K. H. Stokoe II. Effect of Depth to Bedrock on Deflection Basins Obtained with Dynaflect and Falling Weight Deflectometer Tests. In Transportation Research Record 1355, TRB, National Research Council, Washington, D.C., 1992, pp. 8–16.

Chatti, K., Y. Ji, and R. Harichandran. Dynamic Time Domain Backcalculation of Layer Moduli, Damping, and Thicknesses in Flexible Pavements. In *Transportation Research Record 1869*, TRB, National Research Council, Washington, D.C., 2004, pp. 106–116.

Chen, J., M. Hossain, and T. M. Latorella. Use of Falling Weight Deflectometer and Dynamic Cone Penetrometer in Pavement Evaluation. In *Transportation Research Record 1655*, TRB, National Research Council, Washington, D.C., 1999, pp.145-151.

Chen, D.H., J. Bilyeu, H.H. Lin, and M. Murphy. Temperature Correction on Falling Weight Deflectometer Measurements. In *Transportation Research Record 1716*, TRB, National Research Council, Washington, D.C., 2000, pp.30-39.

Chou, Y. J., and R. L. Lytton. Accuracy and Consistency of Backcalculated Pavement Layer Moduli. In *Transportation Research Record 1022*, TRB, National Research Council, Washington, D.C., 1991, pp. 1–7.

Christensen, D. W., T. K. Pellinen, and R. F. Bonaquist. Hirsch Model for Estimating the Modulus of Asphalt Concrete. In *Journal of the Association of Asphalt Paving Technologists, Vol. 72*, 2003, pp. 97–121.

Finn, F.N. Factors Involved in the Design of Asphalt Pavement Surfaces. HRB*, National Cooperative Highway Research Program (NCHRP) Report 39*, 1967.

Fonesca, O.A. *Development of a Time-Dependent Model for the Dynamic Modulus of Asphalt Mixes*. Ph.D. Dissertation, University of Maryland, College Park, 1995.

Francken, L., and M. Partl. Complex Modulus Testing of Asphaltic Concrete: RILEM Interlaboratory Test Program. In *Transportation Research Record 1545*, TRB, National Research Council, Washington, D.C., 1996, pp. 133–142.

Fwa, T.F., C.Y.Tan, and W.T. Chan. Backcalculation Analysis of Pavement-Layer Moduli Using Genetic Algorithms. In *Transportation Research Record 1570*, TRB, National Research Council, Washington, D.C., 1997, pp.134-142.

Hall, K.T. *State of the Art and Practice in Rigid Pavement Design. Transportation in the New Millennium.* TRB, National Research Council, Washington, D.C., 2000.

Harichandran, R. S., T. Mahmood, A. R. Raab, and G. Y. Baladi. Modified Newton Algorithm for Backcalculation of Pavement Layer Properties. In *Transportation Research Record 1384*, TRB, National Research Council, Washington, D.C., 1993, pp. 15-22.

Harichandran, R. S., T. Mahmood, A. R. Raab, and G. Y. Baladi. Backcalculation of Pavement Moduli, Thicknesses and Stiff Layer Depth using a Modified Newton Method. *STP 1198, ASTM*, Philadelphia, Pa., 1994, pp. 68–82.

Hossain, M., J. Zaniewski, and S. Rajan. Estimation of Pavement-Layer Moduli Using Nonlinear Optimization Optimization Technique, In *Journal of Transportation Engineering*, Vol. 120, No. 3, 1994, pp.376-393.

Huang, Y. Pavement Analaysis and Design. 2nd Edition. Prentice Hall, New Jersey, 2003.

Inge, E. H., Jr., and Y. R. Kim. Prediction of Effective Asphalt Layer Temperature. In *Transportation Research Record 1473*, TRB, National Research Council, Washington, D.C., 1995, pp. 93–100.

Irwin, L.H. Instructional Guide for Back-calculation and the Use of MODCOMP3 Version 3.6., *CLRP Publication No. 94-10*, Cornell University, Local Roads Program, March 1994.

Johnson, A. M., and R. L. Baus. Alternative Method for Temperature Correction of Backcalculated Equivalent Pavement Moduli. In *Transportation Research Record 1355*, TRB, National Research Council, Washington, D.C., 1992.

Khogali, W.E.I. and K. O. Anderson. Evaluation of Seasonal Variability in Cohesive Subgrades Using Backcalculation. In *Transportation Research Record 1546*, TRB, National Research Council, Washington, D.C., 1996, pp.140-150.

Kim, Y.R. B. O. Hibbs and Y. C. Lee. Temperature Correction of Deflections and Backcalculated Asphalt Concrete Moduli, *Transportation Research Record 1473*, TRB, National Research Council, Washington, D.C., 1995, pp.55-62.

Leland, W., M. Hill, J. P. Welna, and G. K. Birkenbeuel. *SYSTAT for Windows: Statistics, Version 5*. SYSTAT, Inc., Evanston, Ill.,1992.

Lukanen, E. O., R. Stubstad, and R. C. Briggs. Temperature Predictions and Adjustment Factors for Asphalt Pavements. *Report FHWA-RD-98- 085*. FHWA, U.S. Department of Transportation, 2000.

Lytton, R. L. Backcalculation of Pavement Layer Properties. In Nondestructive Testing of Pavements and Backcalculation of Moduli (A. J. Bush III and Y. G. Baladi, eds.), *ASTM STP 1026*, ASTM, Philadelphia, Pa., 1989, pp. 7–38.

Mamlouk, M.S., W. N. Houston, S. L. Houston, and J. P. Zaniewski, Rational Characterization of Pavement Structures Using Deflection Analysis, *FHWA-AZ88-254*, I, Arizona Department of Transportation, Phoenix, AZ, FHWA, 1988.

Meier, R.W., D.R. Alexander, and R.B. Freeman. Using Artificial Neural Networks as a Forward Approach to Backcalculation. In *Transportation Research Record 1570*, TRB, National Research Council, Washington, D.C., 1997, pp. 126-133.

Miller, J. S., J. Uzan, and M. W. Witczak. Modification of Asphalt Institute's Bituminous Mix Modulus Predictive Equation. In *Transportation Research Record 911*, TRB, National Research Council, Washington, D.C., 1983.

Mirza, M. W. and M. W. Witczak. Development of a Global Aging System for Short and Long Term Aging of Asphalt Cements.In *Journal of the Association of Asphalt Paving Technologists*, Vol. 64, 1995, pp. 393–430.

NCHRP. Simple Performance Test for Superpave Mix Design. *NCHRP Report 465*, Transportation Research Board, Washington, D.C., 2002.

NCHRP. Guide for Mechanistic-Empirical Design of New and Rehabilitated Pavement Structures. *Final Report for Project 1-37A*. Part 1, Chapter 1. Transportation Research Board, National Research Council, Washington, D.C., 2004.

NCHRP. *Interim User Manual for the M-E Pavement Design Guide*. TRB, Washington, D.C., 2007.

Papazian, H. S. The Response of Linear Viscoelastic Materials in the Frequency Domain with Emphasis on Asphalt Concrete. In *Proceeding of International Conference on the Structural Design of Asphalt Pavements*, Ann Arbor, Mich., 1962, pp. 454–463.

Park, S. W., and Y.R.Kim. Temperature Correction of Backcalculated Moduli and Deflections Using Linear Viscoelasticity and Time-Temperature Superposition. In *Transportation Research Record 1570*, TRB, National Research Council, Washington, D.C., 1997, pp. 108-117.

Park, D.Y, N. Buch, and K. Chatti. Effective Layer Temperature Prediction Model and Temperature Correction via Falling Weight Deflectometer Deflections. In *Transportation Research Record 1764*, TRB, National Research Council, Washington, D.C., 2001, pp.97-111

Pellinen, T.K. *Investigation of the Use of Dynamic Modulus as an Indicator of HMA Performance*. Ph.D. Dissertation. Arizona State University, Tempe, 2001.

Rohde, G. T., and T. Scullion. *Modulus 4.0: Expansion and Validation of the MODULUS Backcalculation System.* Research Report 1123-3. Texas Transportation Institute, Texas A&M University System, College Station, Nov. 1990.

Shook, J. F., and B. F. Kallas. Factors Influencing the Dynamic Modulus of Asphalt Concrete. In *Proceedings of Association of Asphalt Paving Technologists*, Los Angeles, Calif., 1969.

Siddharthan, R., G. M. Norris, and J. A. Epps. Use of FWD data for Pavement Material Characterization and Performance, In *Journal of Transportation Engineering*, Vol. 117, No. 6, 1991, pp.660-678.

Tayebali, A. A., B. Tsai, and C. L. Monismith. *Stiffness of Asphalt- Aggregate Mixes. SHRP Report A-388*, TRB, National Research Council, Washington, D.C., 1994.

*Thickness Design-Asphalt Pavements for Air Carrier Airports. Manual Series No. 1 (MS-11)*, 3rd Edition. Asphalt Institute, College Park, MD, September 1981.

Timm, D., Birgisson, B., and D. Newcomb. 1998. Development of Mechanistic-Empirical Pavement Design in Minnesota. In *Transportation Research Record No. 1626*, TRB, National Research Council, Washington, D.C., pp. 181-188.

Traxler, R.N. Durability of Asphalt Cements. In *Proceeding of the Association of Asphalt Paving Technologists*, AAPT, Vol. 32, 1963.

Ullidtz, P. *Pavement Analysis*. Elsevier, New York, 1987.

Uzan, J. Dynamic Linear Back Calculation of Pavement Material Parameters, In Journal of Transportation Engineering, Vol. 120, No.1, 1994, pp.109-126.

Vallergra, B.A., C.L. Monismith, and K. Granthem. A Study of Some Factors Infuencing the Weathering of Paving Asphalts. In *Proceeding of Association of Asphalt Paving Technologies*, Vol. 26, 1957.

Van Gurp, C. Effect of Temperature Gradients and Season on Deflection Data. In the *Proceedings of 4th International Conference on the Bearing Capacity of Roads and Airfields*, Trondheim, Norway, 1994, pp. 199–214.

Watson, D.E., J. Zhang, and R.B. Powell. Analysis of Temperature Data for the National Center for Asphalt Technology Test Track. In *Transportation Research Record 1891*, TRB, National Research Council, Washington, D.C., 2004, pp. 68–75.

Witczak, M. W. Design of Full-Depth Asphalt Airfield Pavements. In *Proceedings of 3rd International Conference on Structural Design of Asphalt Pavements*, Vol. 1, London, 1972.

Witczak, M. W. *The Universal Airport Pavement Design System, Report II: Asphaltic Mixture Material Characterization*. University of Maryland, College Park, May 1989.

Witczak M.W. *Simple Performance Test: Test Results and Recommendations. Interim Task C Report, Superpave Support and Performace Models Management (NCHRP 9-19) Project.* Arizona State University, Tempe, AZ, 2001.

Witczak, M. W., T. K. Pellinen, and M. M. El-Basyouny. Pursuit of the Simple Performance Test for Asphalt Concrete Fracture/Cracking. In *Journal of the Association of Asphalt Paving Technologists*, Vol. 71, 2002, pp. 767–778.

Xu, B., S. R. Ranjithan, and Y. R. Kim. New Condition Assessment Procedure for Asphalt Pavement Layers Using Falling Weight Deflectometer Deflections. In *Transportation Research Record 1806*, TRB, National Research Council, Washington, D.C., 2002, pp.57-69.

Yeager, L. L., and L. E. Wood. Recommended Procedure for Determining the Dynamic Modulus of Asphalt Mixtures. In *Transportation Research Record 549*, TRB, National Research Council, Washington, D.C., 1975, pp. 26–38.

Yoder, E. J., and M.W. Witczak. *Principles of Pavement Design*. New York: John Wiley and Sons, 1975.

Zaghloul, S., T. Hoover, D. J. Swan, N. Vitillo, R. Sauber, and A. A. Jumikis. Enhancing Backcalculation Procedures through Consideration of Thickness Variability. In *Transportation Research Record 1869*, TRB, National Research Council, Washington, D.C., 2004, pp. 80–87.

Zhou, H., G. R. Rada, and G. E. Elkins. Investigation of Backcalculated Moduli Using Deflections Obtained at Various Locations in a Pavement Structure. In *Transportation Research Record 1570*, 1997, pp.96-107.

# APPENDIX A - AVERAGE NORMALIZED DEFLECTION

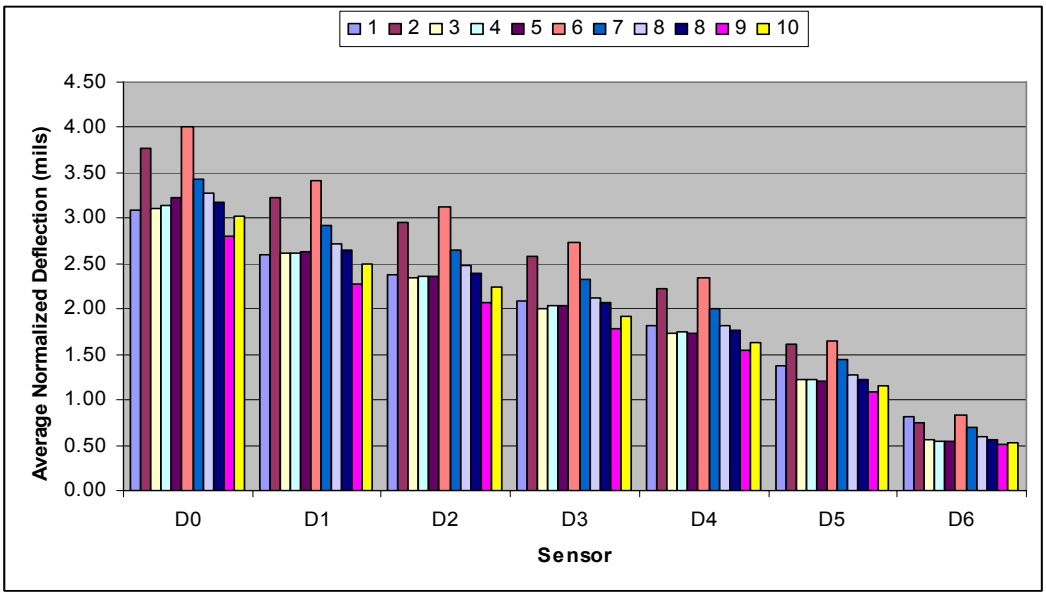


**Figure A.1: Variation of Average Normalized Deflection for US-54.**

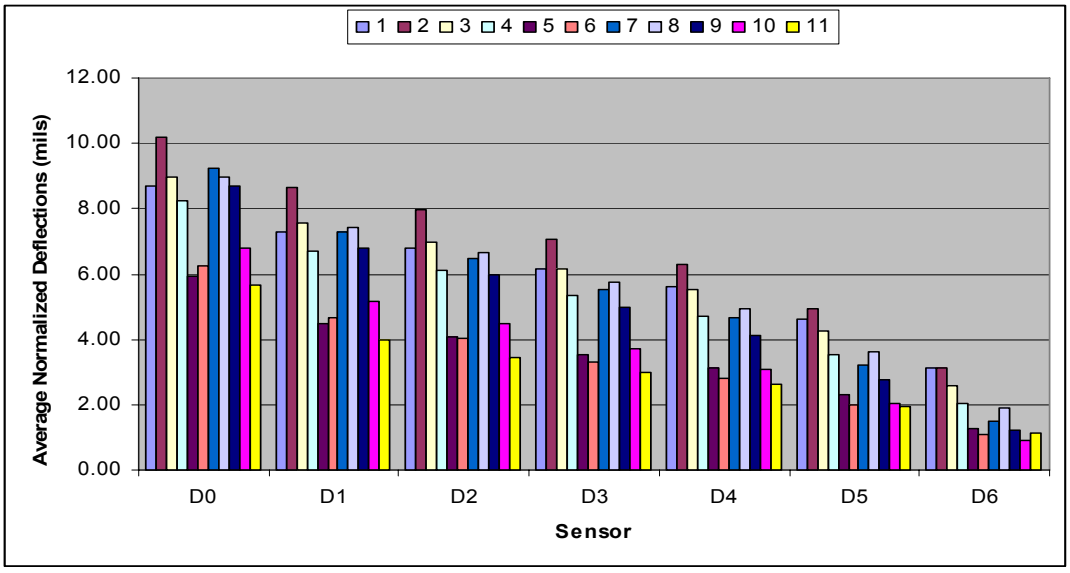


**Figure A.2: Variation of Average Normalized Deflection for US-77.**

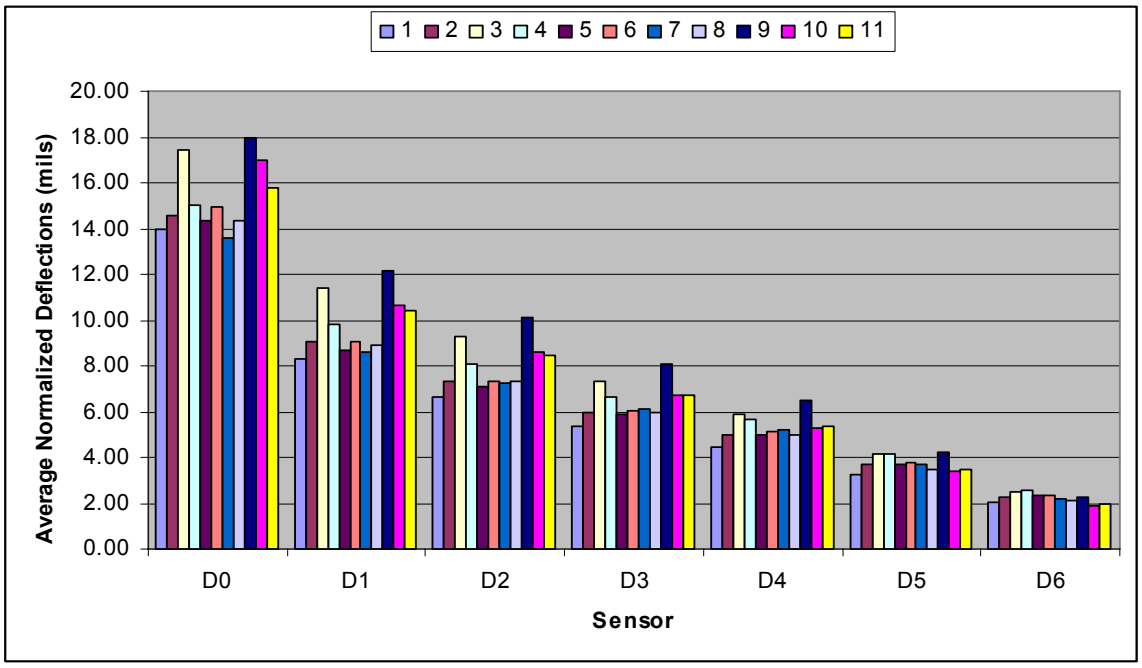


**Figure A.3: Variation of Average Normalized Deflection for US-283.**

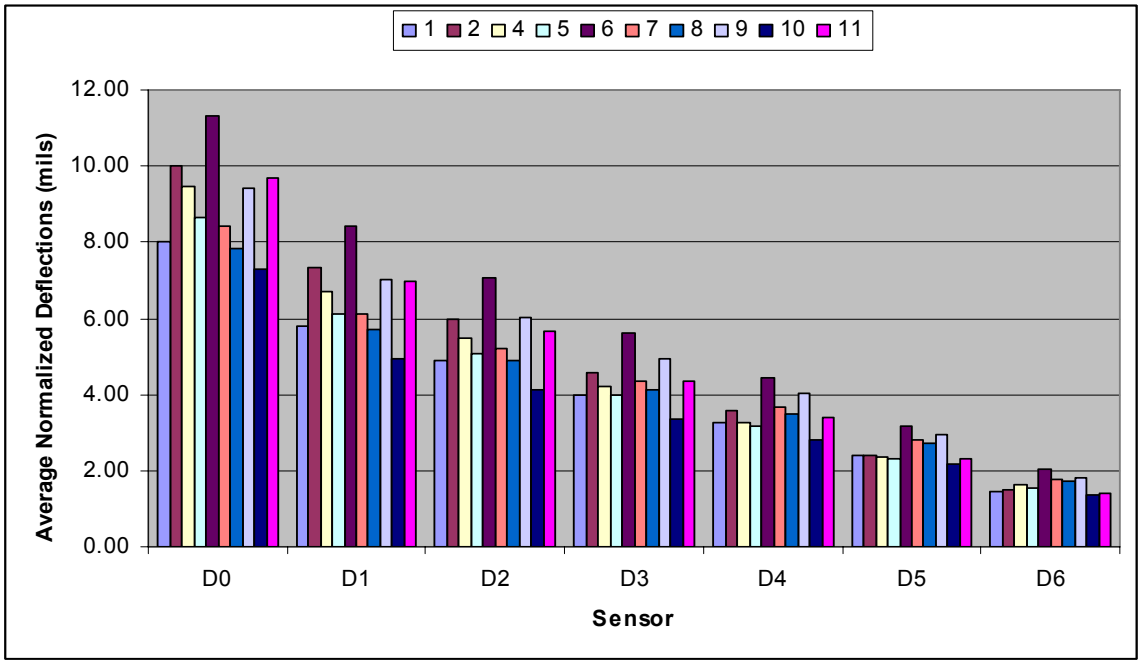


**Figure A.4: Variation of Average Normalized Deflection for K-7.**

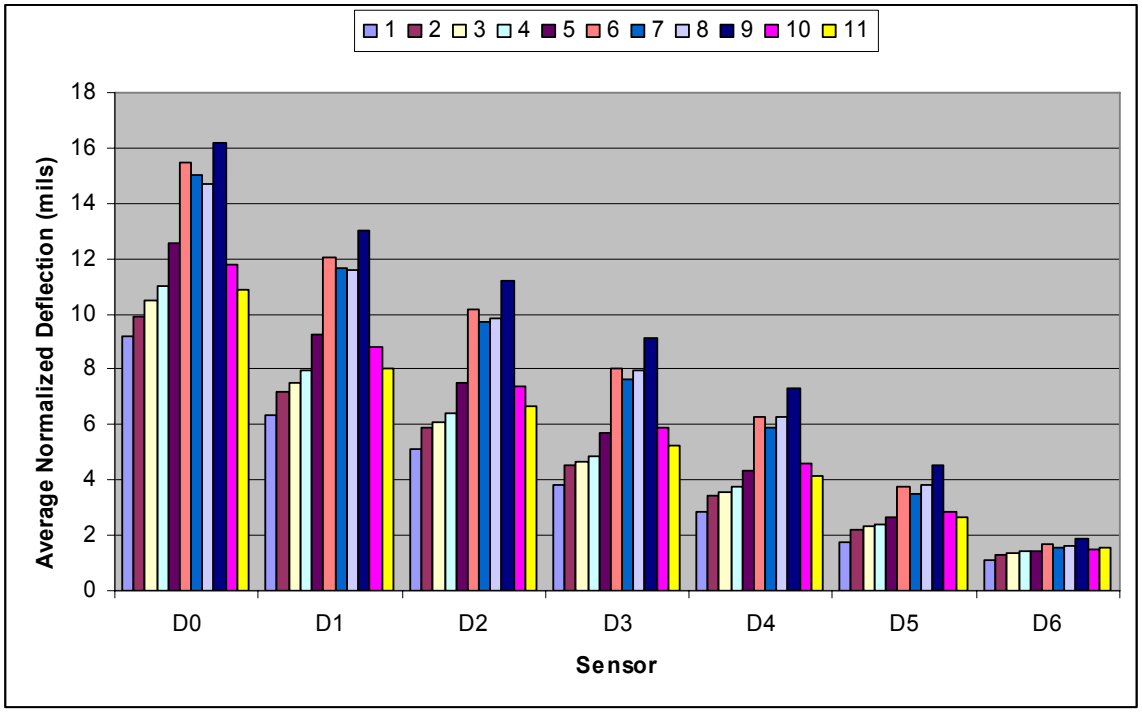


**Figure A.5: Variation of Average Normalized Deflection for K-99.**

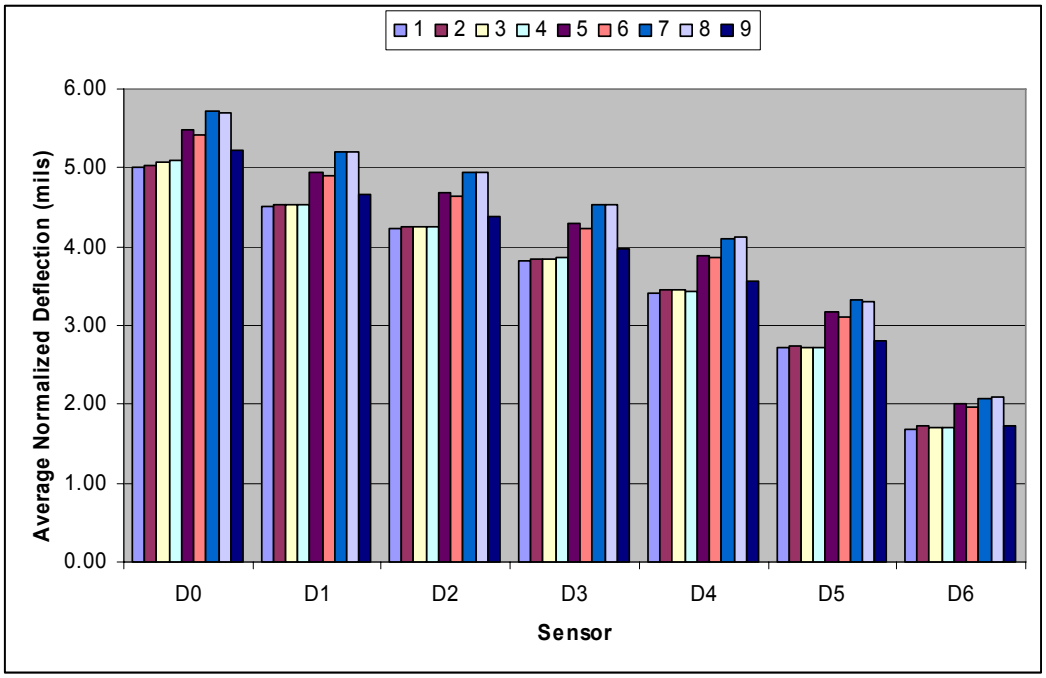


**Figure A.6: Variation of Average Normalized Deflection for S1**

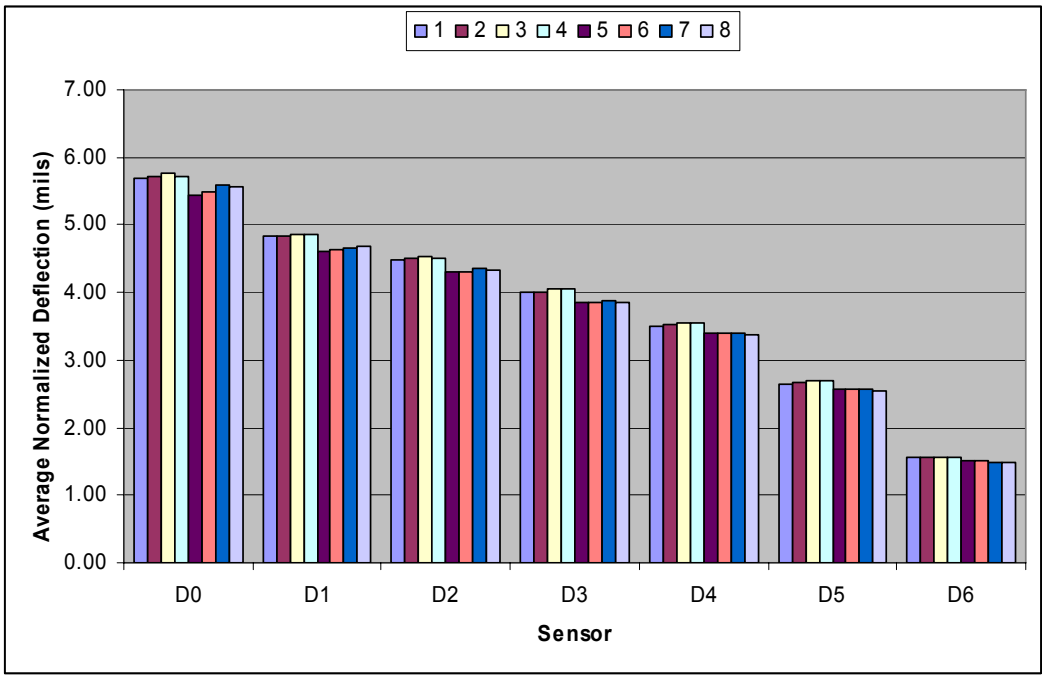


**Figure A.7: Variation of Average Normalized Deflection for S2**

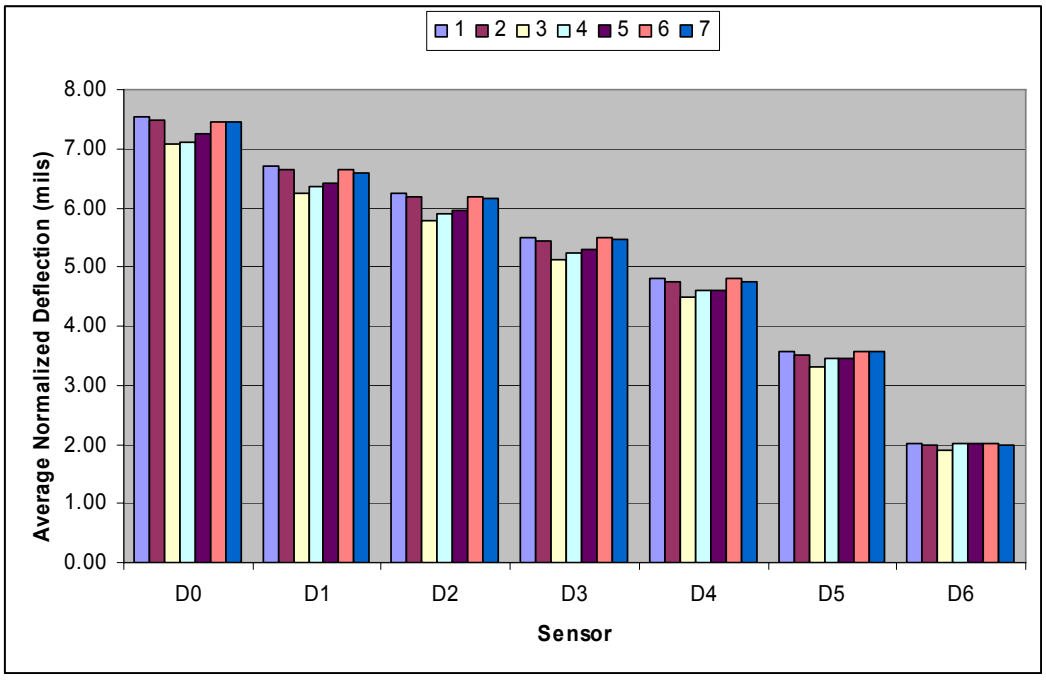


**Figure A.8: Variation of Average Normalized Deflection for S3**

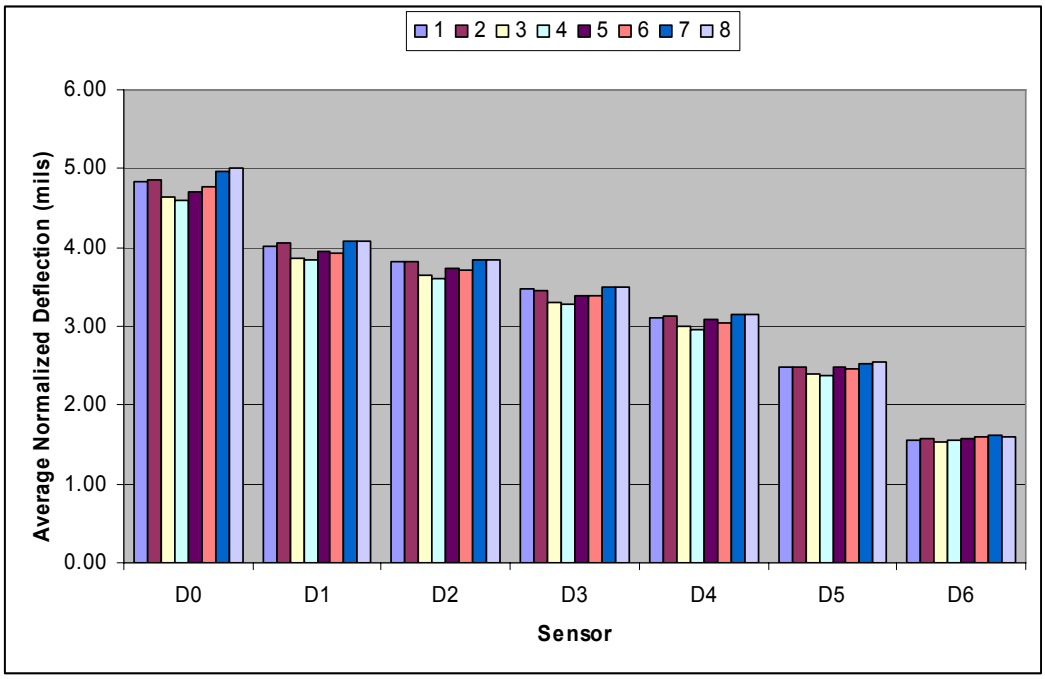


**Figure A.9: Variation of Average Normalized Deflection for S4**

# APPENDIX B - NONLINEARITY AND STRESS SENSITIVITY

**Table B.1: Summary of $R^2$ for US-54**

| Station No. | Sensor No. | | | | | | |
|---|---|---|---|---|---|---|---|
| | D0 | D1 | D2 | D3 | D4 | D5 | D6 |
| 1 | 0.99 | 1 | 1 | 1 | 1 | 1 | 0.99 |
| 2 | 0.99 | 1 | 1 | 0.99 | 1 | 0.99 | 0.99 |
| 3 | 0.99 | 0.99 | 0.99 | 1 | 1 | 0.99 | 1 |
| 4 | 0.99 | 1 | 0.99 | 0.99 | 1 | 0.99 | 0.99 |
| 5 | 1 | 1 | 1 | 0.99 | 1 | 0.99 | 0.99 |
| 6 | 1 | 1 | 0.99 | 0.99 | 0.99 | 1 | 0.99 |
| 7 | 0.99 | 1 | 1 | 0.99 | 0.99 | 0.99 | 0.99 |
| 8 | 1 | 1 | 1 | 1 | 0.99 | 0.99 | 0.68 |
| **9** | **0.99** | **0.99** | **1** | **1** | **0.99** | **1** | **1** |
| **10** | **1** | **1** | **0.99** | **1** | **0.99** | **1** | **0.98** |
| **11** | **0.99** | **1** | **1** | **1** | **1** | **0.99** | **0.99** |

**Table B.2: Summary of $R^2$ for US-77**

| Station No. | Sensor No. | | | | | | |
|---|---|---|---|---|---|---|---|
| | 1 | 2 | 3 | 4 | 5 | 6 | 7 |
| 1 | 0.99 | 1 | 1 | 1 | 1 | 1 | 1 |
| 2 | 1 | 1 | 1 | 0.99 | 0.99 | 0.99 | 0.99 |
| 3 | 0.99 | 0.99 | 1 | 1 | 1 | 1 | 1 |
| 4 | 1 | 1 | 1 | 1 | 1 | 0.99 | 0.99 |
| 5 | 1 | 1 | 1 | 0.99 | 1 | 1 | 0.99 |
| 6 | 0.99 | 1 | 1 | 1 | 1 | 1 | 0.99 |
| 7 | 1 | 1 | 1 | 0.99 | 1 | 0.99 | 1 |
| 8 | 0.99 | 1 | 1 | 1 | 0.99 | 1 | 0.99 |
| **9** | **0.99** | **1** | **1** | **1** | **0.99** | **0.99** | **0.99** |
| **10** | **0.99** | **1** | **1** | **1** | **0.99** | **0.99** | **0.99** |
| **11** | **1** | **1** | **1** | **1** | **0.99** | **1** | **0.99** |

**Table B.3: Summary of $R^2$ for US-283**

| Station No. | Sensor No. | | | | | | |
|---|---|---|---|---|---|---|---|
| | 1 | 2 | 3 | 4 | 5 | 6 | 7 |
| 1 | 1 | 1 | 1 | 1 | 0.99 | 0.99 | 0.99 |
| 2 | 0.99 | 1 | 1 | 1 | 1 | 0.99 | 0.99 |
| 4 | 0.99 | 0.99 | 1 | 1 | 1 | 0.99 | 1 |
| 5 | 0.99 | 1 | 1 | 1 | 1 | 1 | 0.99 |
| 6 | 1 | 1 | 1 | 1 | 1 | 1 | 1 |
| 7 | 0.99 | 0.99 | 1 | 1 | 1 | 1 | 0.99 |
| 8 | 0.99 | 0.99 | 0.99 | 1 | 1 | 1 | 0.99 |
| **9** | **0.99** | **1** | **1** | **1** | **1** | **0.99** | **1** |
| **10** | **0.99** | **0.99** | **1** | **1** | **1** | **1** | **0.99** |
| **11** | **0.99** | **0.99** | **1** | **1** | **1** | **1** | **0.99** |

**Table B.4: Summary of $R^2$ for K-7**

| Station No. | Sensor No. | | | | | | |
|---|---|---|---|---|---|---|---|
| | 1 | 2 | 3 | 4 | 5 | 6 | 7 |
| 1 | 0.99 | 1 | 0.99 | 0.99 | 0.99 | 0.99 | 0.99 |
| 2 | 0.99 | 0.99 | 1 | 0.99 | 0.99 | 0.99 | 0.99 |
| 4 | 0.99 | 0.99 | 0.99 | 0.99 | 1 | 0.99 | 0.99 |
| 5 | 0.99 | 1 | 1 | 0.99 | 0.99 | 0.99 | 0.99 |
| 6 | 0.99 | 0.99 | 0.99 | 0.99 | 0.99 | 0.99 | 0.99 |
| 7 | 0.99 | 1 | 0.99 | 0.99 | 0.99 | 0.99 | 0.99 |
| 8 | 0.99 | 0.99 | 0.99 | 0.99 | 0.99 | 1 | 0.99 |
| 9 | 0.99 | 0.99 | 0.99 | 0.99 | 0.99 | 1 | 0.99 |
| **10** | **0.99** | **0.99** | **0.99** | **0.99** | **0.99** | **0.99** | **0.99** |
| **11** | **0.99** | **0.99** | **0.99** | **0.99** | **0.99** | **0.99** | **0.99** |

**Table B.5: Summary of $R^2$ for K-99**

| Station No. | Sensor No. | | | | | | |
|---|---|---|---|---|---|---|---|
| | 1 | 2 | 3 | 4 | 5 | 6 | 7 |
| 1 | 1.00 | 1.00 | 1.00 | 1.00 | 1.00 | 1.00 | 1.00 |
| 2 | 1.00 | 1.00 | 1.00 | 1.00 | 1.00 | 1.00 | 1.00 |
| 3 | 1.00 | 1.00 | 1.00 | 1.00 | 1.00 | 1.00 | 1.00 |
| 4 | 1.00 | 1.00 | 1.00 | 1.00 | 1.00 | 1.00 | 1.00 |
| 5 | 1.00 | 1.00 | 1.00 | 1.00 | 1.00 | 1.00 | 1.00 |
| 6 | 1.00 | 1.00 | 1.00 | 1.00 | 1.00 | 1.00 | 1.00 |
| 7 | 1.00 | 1.00 | 1.00 | 1.00 | 1.00 | 1.00 | 1.00 |
| 8 | 1.00 | 1.00 | 1.00 | 1.00 | 1.00 | 1.00 | 1.00 |
| 9 | 1.00 | 1.00 | 1.00 | 1.00 | 1.00 | 1.00 | 1.00 |
| **10** | **1.00** | **1.00** | **1.00** | **1.00** | **1.00** | **1.00** | **1.00** |
| **11** | **1.00** | **1.00** | **1.00** | **1.00** | **1.00** | **1.00** | **1.00** |

**Table B.6: Summary of $R^2$ for S1**

| Station No | Sensor No. | | | | | | |
|---|---|---|---|---|---|---|---|
| | 1 | 2 | 3 | 4 | 5 | 6 | 7 |
| 1 | 0.994 | 0.310 | 0.310 | 0.998 | 0.996 | 0.004 | 0.069 |
| 2 | 0.992 | 0.925 | 0.846 | 0.888 | 0.144 | 1.000 | 0.719 |
| 3 | 0.384 | 0.515 | 0.515 | 0.700 | 0.485 | 0.925 | 0.003 |
| 4 | 0.676 | 0.818 | 0.750 | 0.693 | 0.250 | 0.250 | 0.429 |
| 5 | 0.987 | 0.525 | 0.000 | 0.525 | 0.709 | 0.211 | 0.998 |
| 6 | 0.127 | 0.303 | 0.512 | 0.512 | 0.007 | 0.512 | 0.061 |
| 7 | 0.002 | 0.920 | 0.988 | 0.927 | 0.945 | 0.979 | 0.080 |
| 8 | 0.984 | 0.958 | 0.556 | 0.633 | 0.996 | 0.633 | 0.984 |
| 9 | 0.996 | 0.419 | 0.843 | 0.887 | 0.574 | 0.131 | 0.968 |

**Table B.7: Summary of $R^2$ for S2**

| Station No | Sensor No. | | | | | | |
|---|---|---|---|---|---|---|---|
| | 1 | 2 | 3 | 4 | 5 | 6 | 7 |
| 1 | 0.92 | 0.98 | 0.96 | 0.88 | 1.00 | 0.93 | 0.68 |
| 2 | 0.30 | 1.00 | 0.80 | 0.89 | 0.07 | 0.00 | 0.70 |
| 3 | 0.01 | 0.84 | 0.65 | 0.86 | 0.35 | 0.84 | 0.99 |
| 4 | 0.94 | 0.98 | 0.77 | 0.51 | 0.27 | 0.93 | 0.20 |
| 5 | 0.97 | 0.73 | 0.41 | 0.12 | 0.41 | 0.41 | 0.12 |
| 6 | 0.43 | 0.43 | 0.10 | 0.10 | 0.14 | 1.00 | 0.10 |
| 7 | 0.36 | 0.84 | 1.00 | 0.99 | 0.60 | 0.27 | 0.60 |
| 8 | 0.94 | 0.79 | 0.71 | 0.95 | 0.38 | 0.71 | 0.98 |

**Table B.8: Summary of $R^2$ for S3**

| Station No | Sensor No. | | | | | | |
|---|---|---|---|---|---|---|---|
| | 1 | 2 | 3 | 4 | 5 | 6 | 7 |
| 1 | 0.59 | 0.62 | 0.14 | 0.50 | 0.86 | 0.89 | 0.14 |
| 2 | 0.98 | 0.99 | 1.00 | 0.62 | 0.60 | 1.00 | 0.98 |
| 3 | 0.95 | 0.94 | 0.97 | 0.96 | 0.98 | 0.84 | 0.84 |
| 4 | 0.90 | 0.86 | 1.00 | 0.99 | 0.50 | 0.91 | 1.00 |
| 5 | 1.00 | 0.76 | 0.96 | 0.44 | 0.10 | 0.44 | 0.62 |
| 6 | 0.89 | 0.57 | 0.96 | 0.75 | 0.99 | 0.96 | 0.43 |
| 7 | 1.00 | 0.75 | 0.40 | 0.98 | 0.75 | 0.75 | 0.04 |

**Table B.9: Summary of $R^2$ for S4**

| Station No | Sensor No. | | | | | | |
|---|---|---|---|---|---|---|---|
| | **1** | **2** | **3** | **4** | **5** | **6** | **7** |
| **1** | 0.41 | 0.94 | 0.84 | 0.31 | 0.90 | 0.59 | 0.77 |
| **2** | 0.76 | 0.98 | 0.77 | 0.94 | 0.33 | 0.94 | 0.66 |
| **3** | 0.40 | 0.92 | 0.17 | 0.34 | 0.98 | 0.47 | 1.00 |
| **4** | 0.88 | 0.93 | 0.97 | 1.00 | 0.42 | 0.87 | 0.89 |
| **5** | 0.46 | 0.84 | 0.54 | 0.09 | 0.91 | 0.46 | 0.99 |
| **6** | 0.98 | 0.90 | 0.90 | 0.38 | 0.51 | 0.73 | 0.70 |
| **7** | 0.03 | 0.80 | 0.99 | 0.98 | 0.89 | 0.89 | 1.00 |
| **8** | 0.82 | 0.01 | 0.40 | 0.41 | 0.12 | 0.18 | 0.59 |

# APPENDIX C - LABORATORY DYNAMIC MODULUS FOR NEW PROJECTS

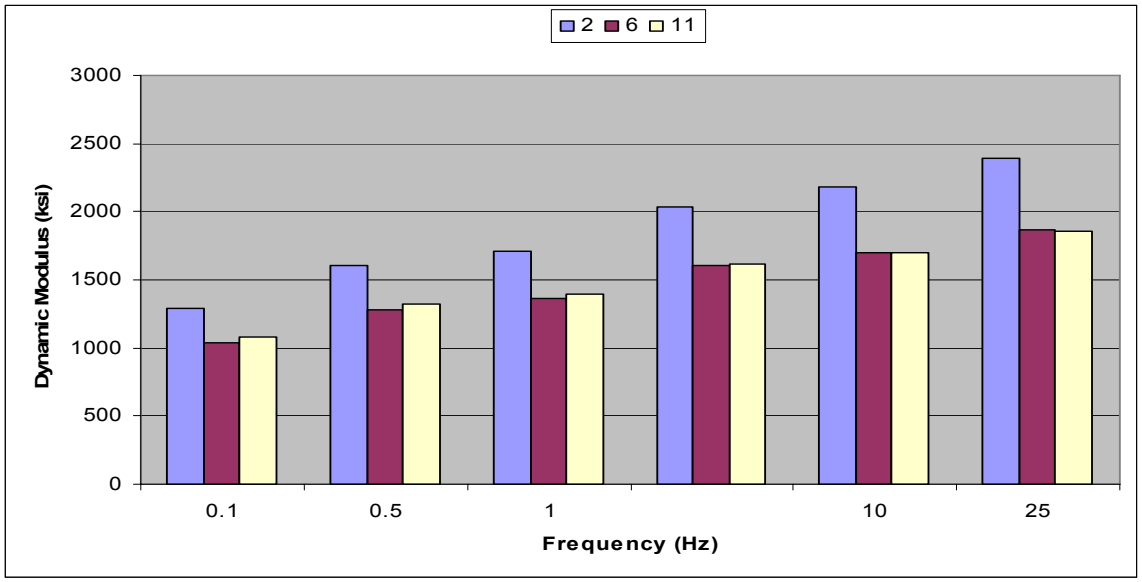


**Figure C.1: Dynamic Modulus for US-54 at 40°F.**

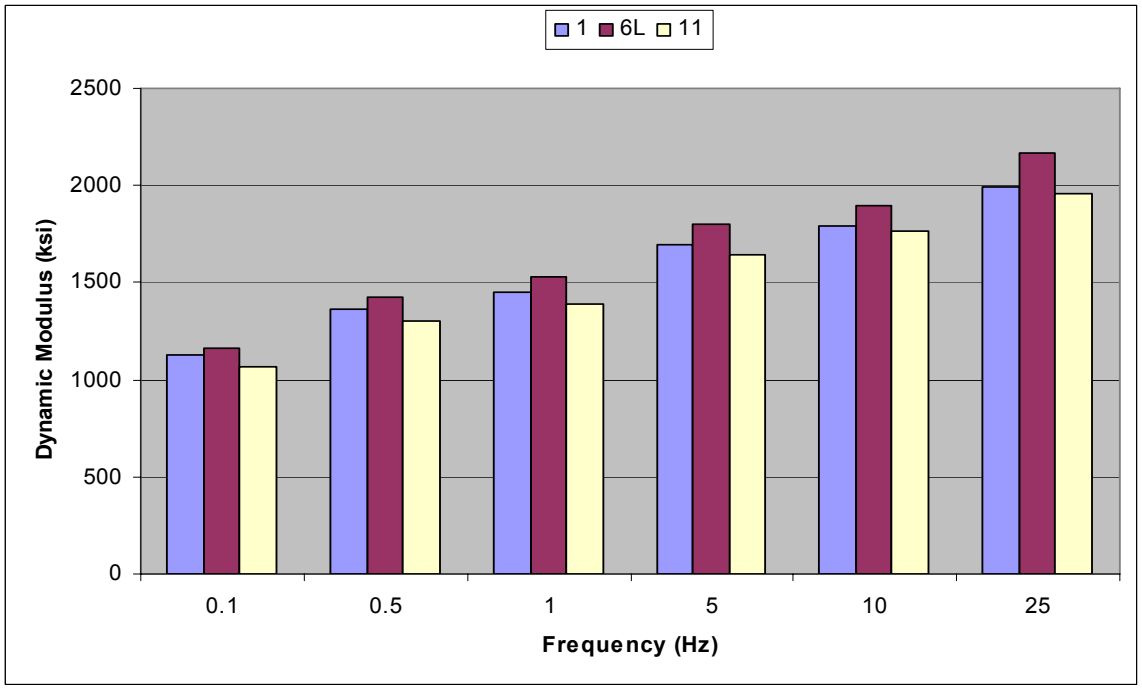


**Figure C.2: Dynamic Modulus for US-77 at 40°F.**

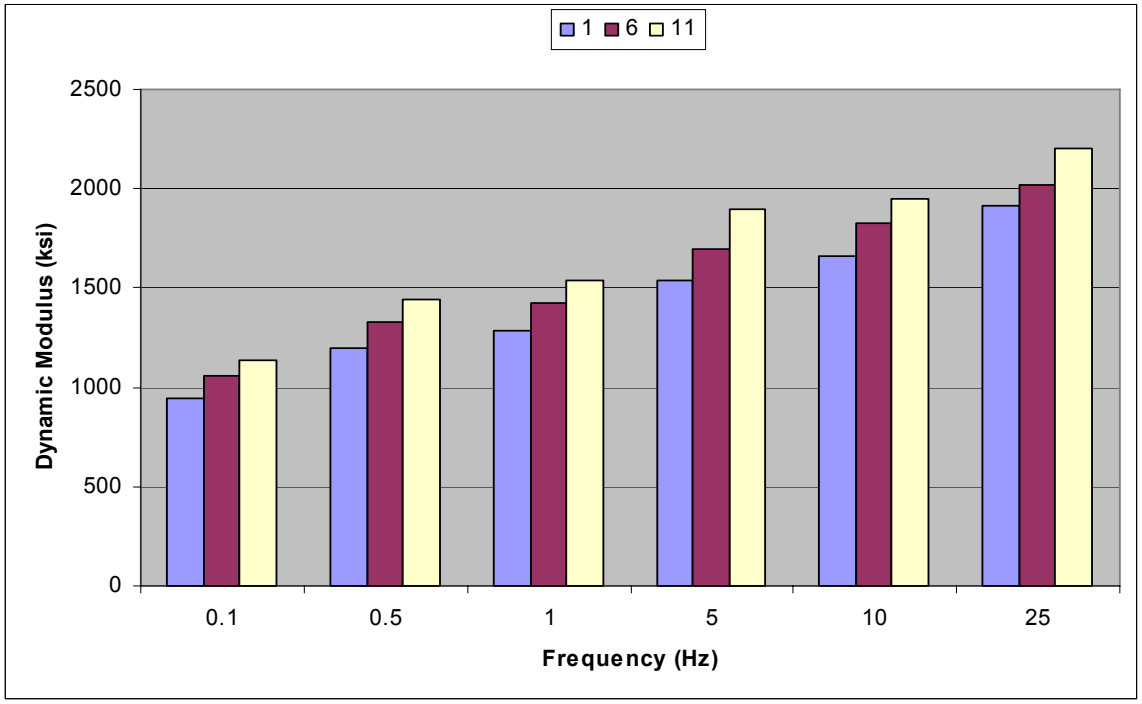


**Figure C.3: Dynamic Modulus for US-283 at 40°F.**

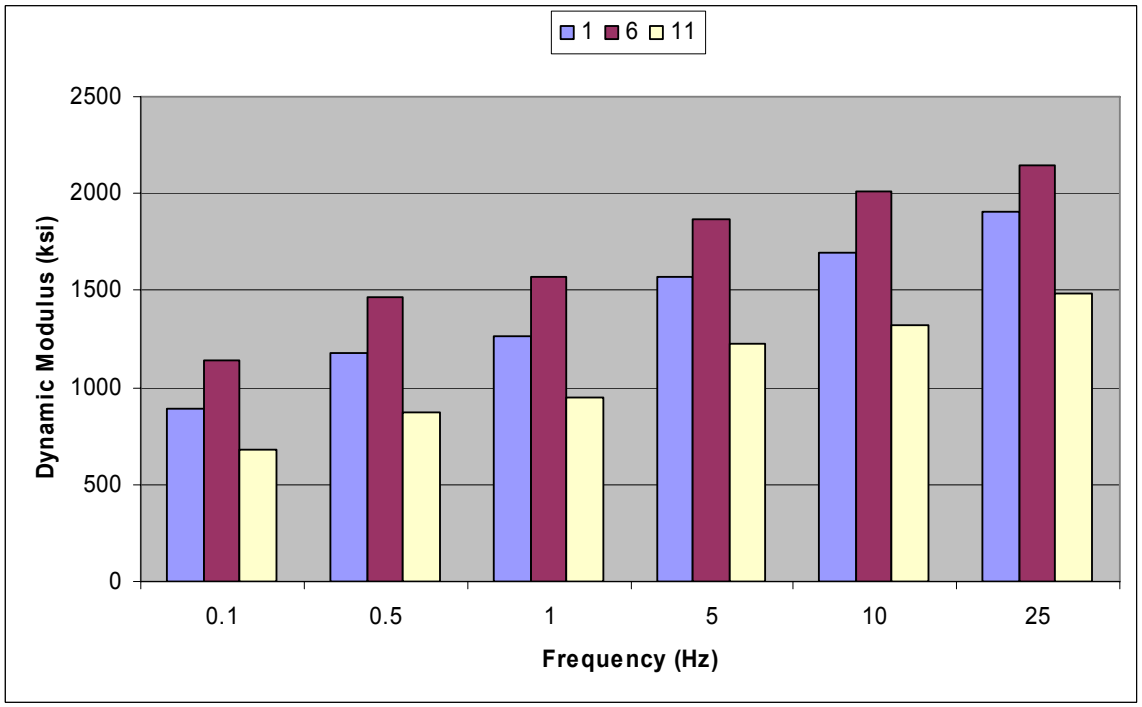


**Figure C.4: Dynamic Modulus for K-7 at 40°F.**

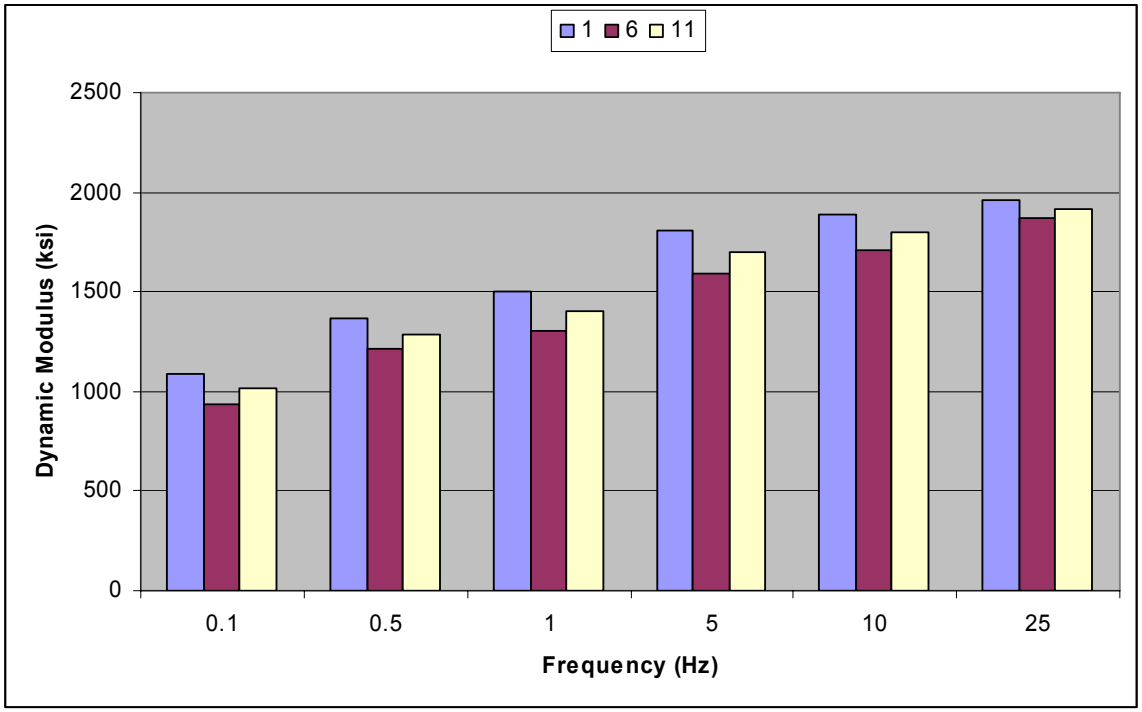


**Figure C.5: Dynamic Modulus for K-99 at 40°F.**

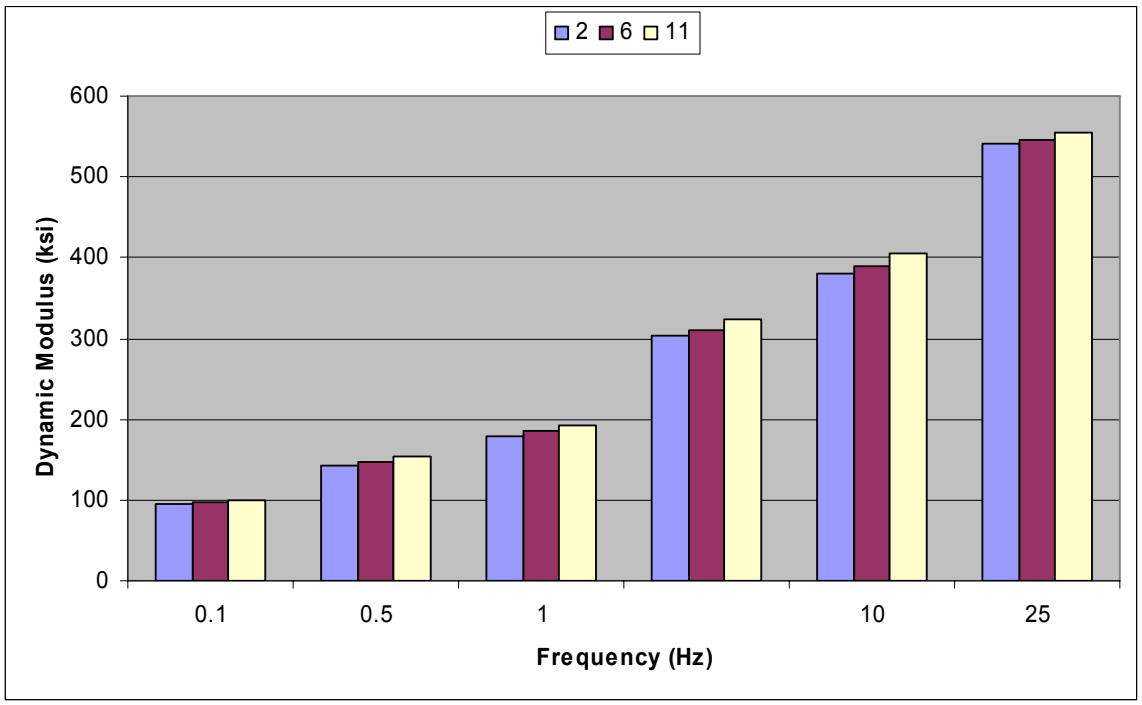


**Figure C.6: Dynamic Modulus for US-54 at 95°F.**

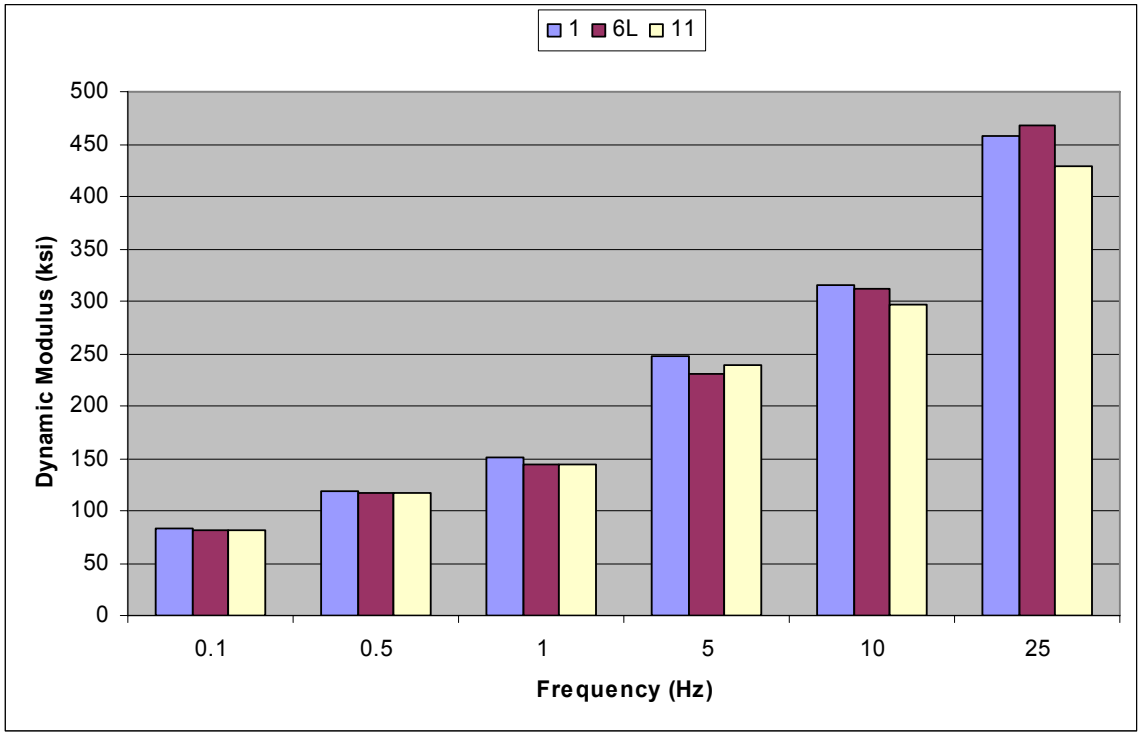


**Figure C.7: Dynamic Modulus for US-77 at 95°F.**

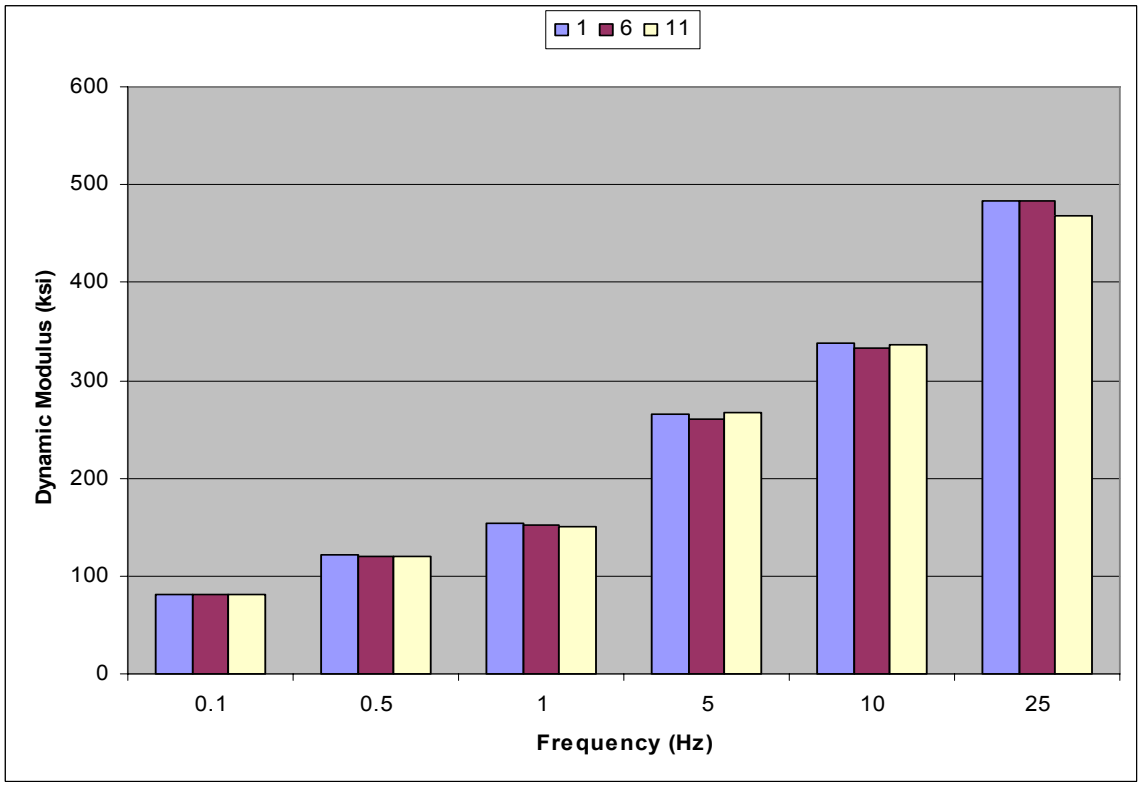


**Figure C.8: Dynamic Modulus for US-283 at 95°F.**

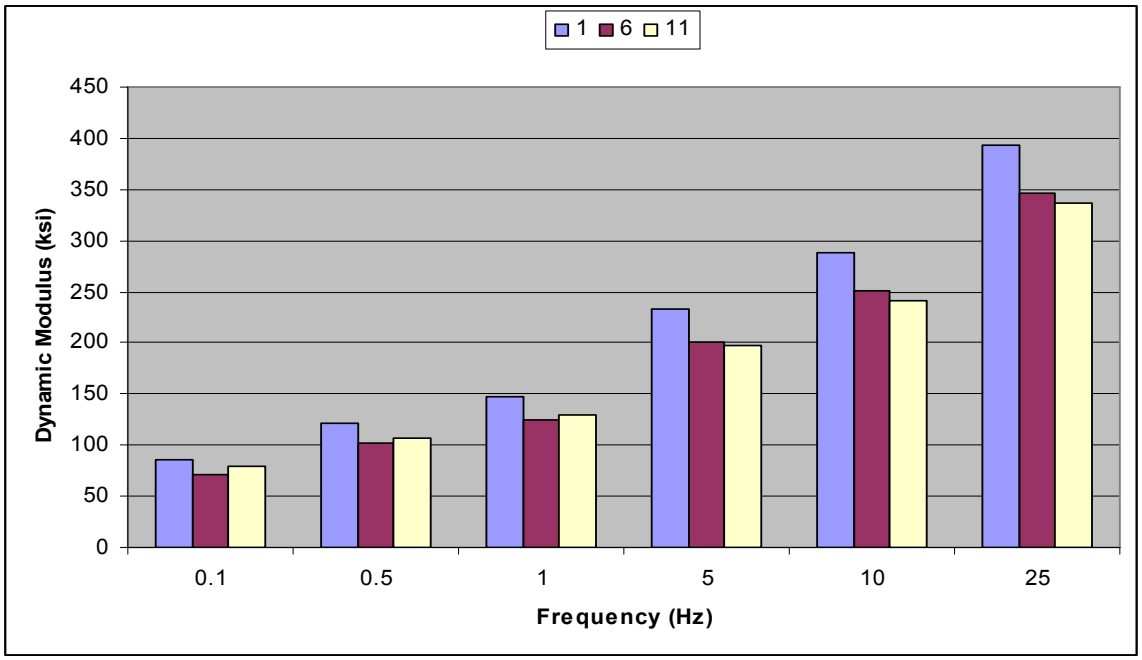


**Figure C.9: Dynamic Modulus for K-99 at 95°F.**

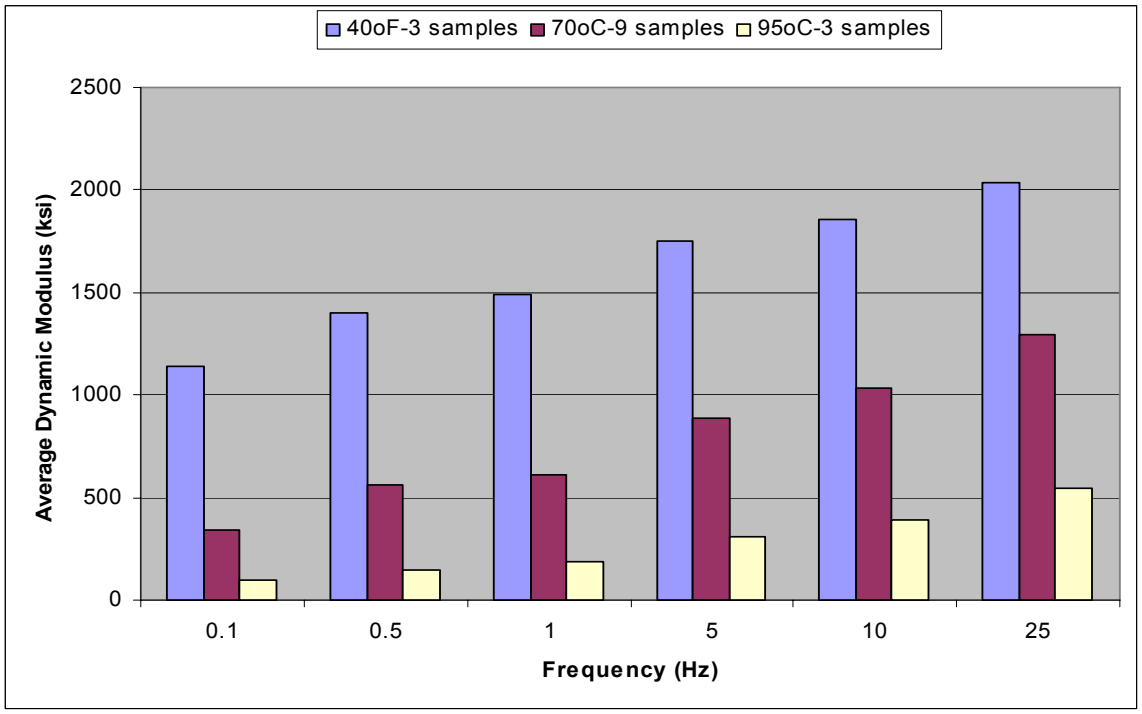


**Figure C.10: Effect of Temperature for US-54.**

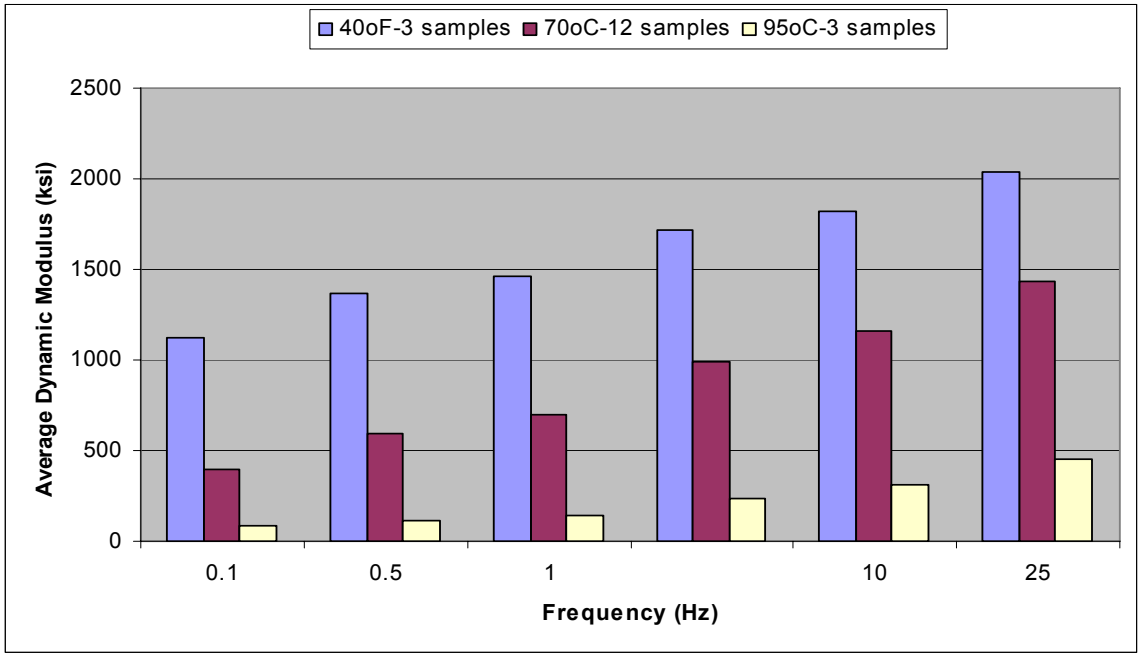


**Figure C.11: Effect of Temperature for US-77.**

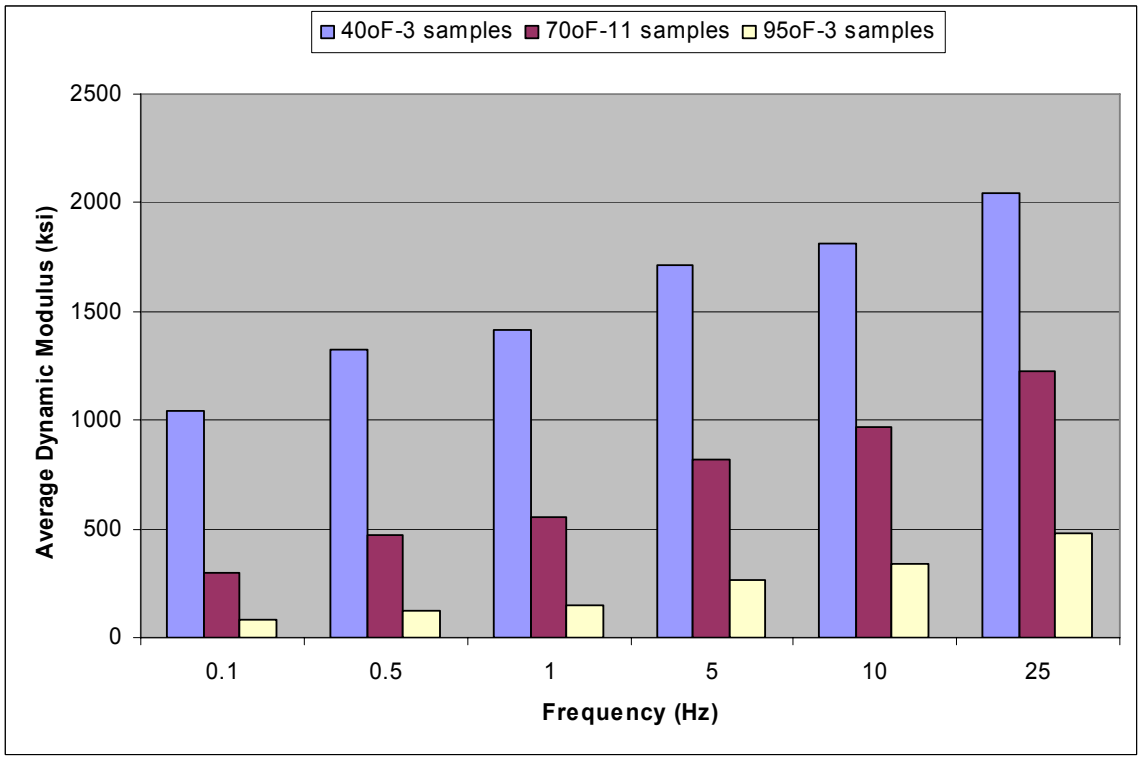


**Figure C.12: Effect of Temperature for US-283.**

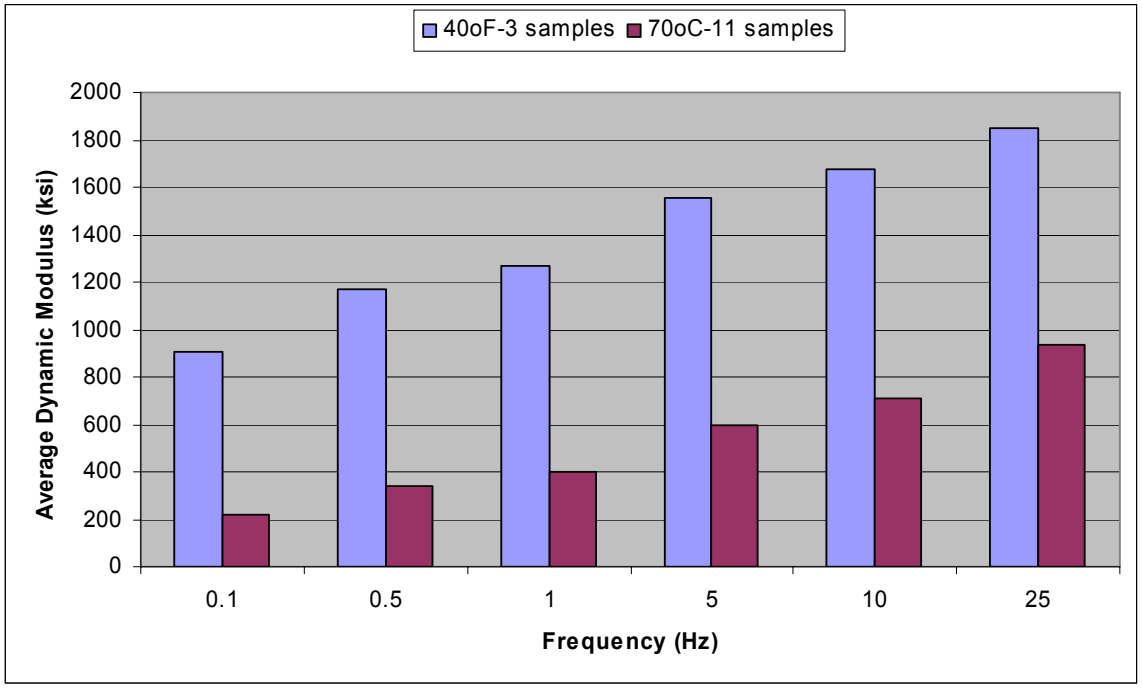


**Figure C.13: Effect of Temperature for K-7.**

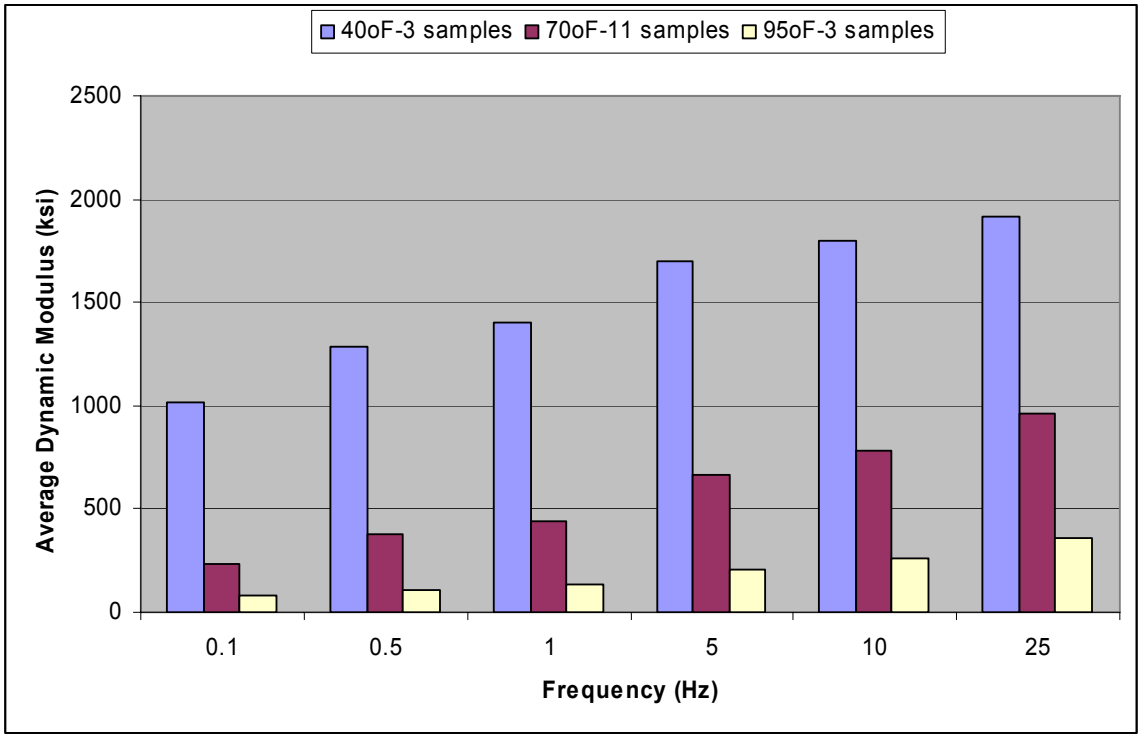


**Figure C.14: Effect of Temperature for K-99**

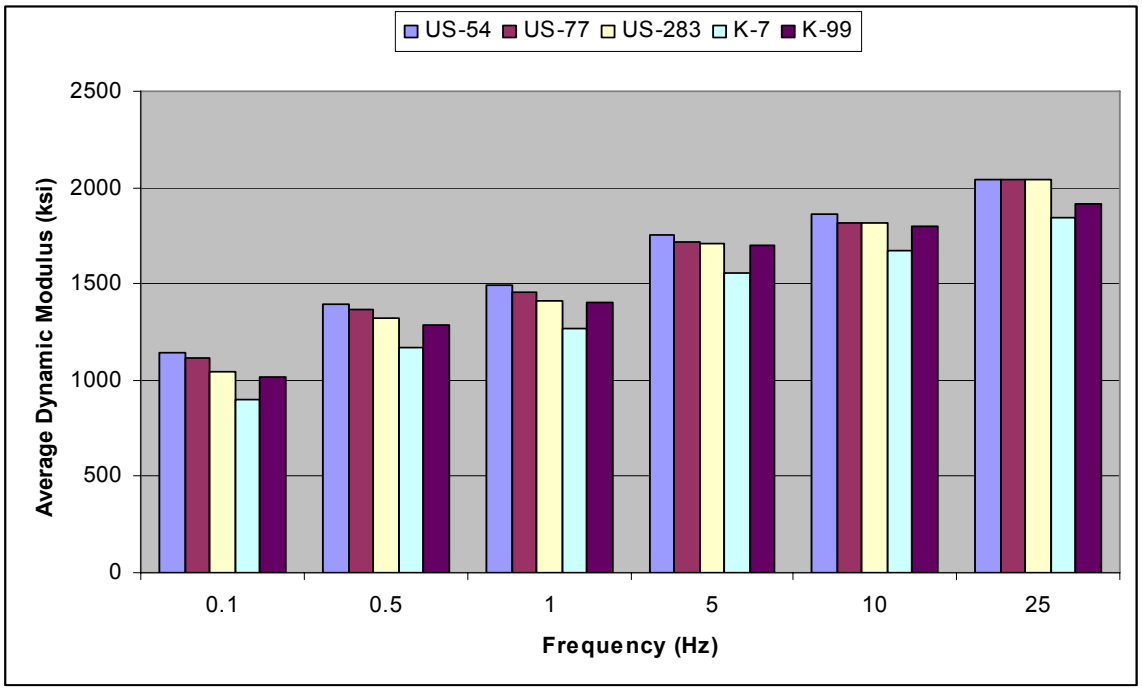


**Figure C.15: Comparison of Dynamic Modulus at 40°F.**

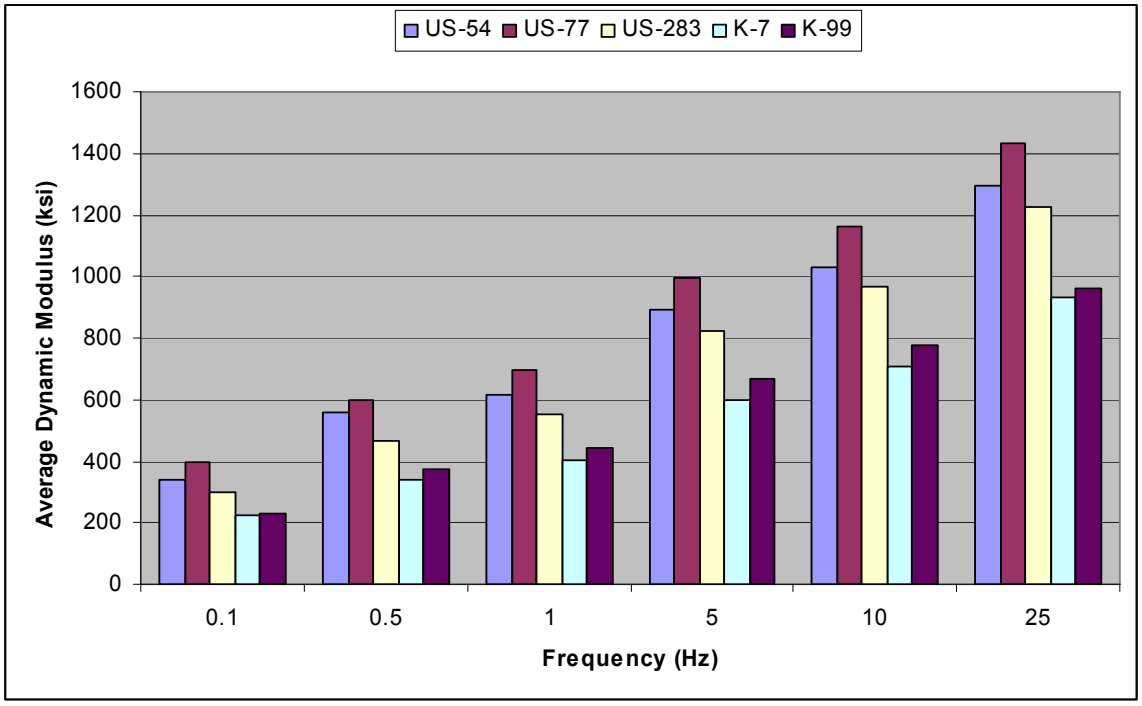


**Figure C.16: Comparison of Dynamic Modulus at 70°C.**

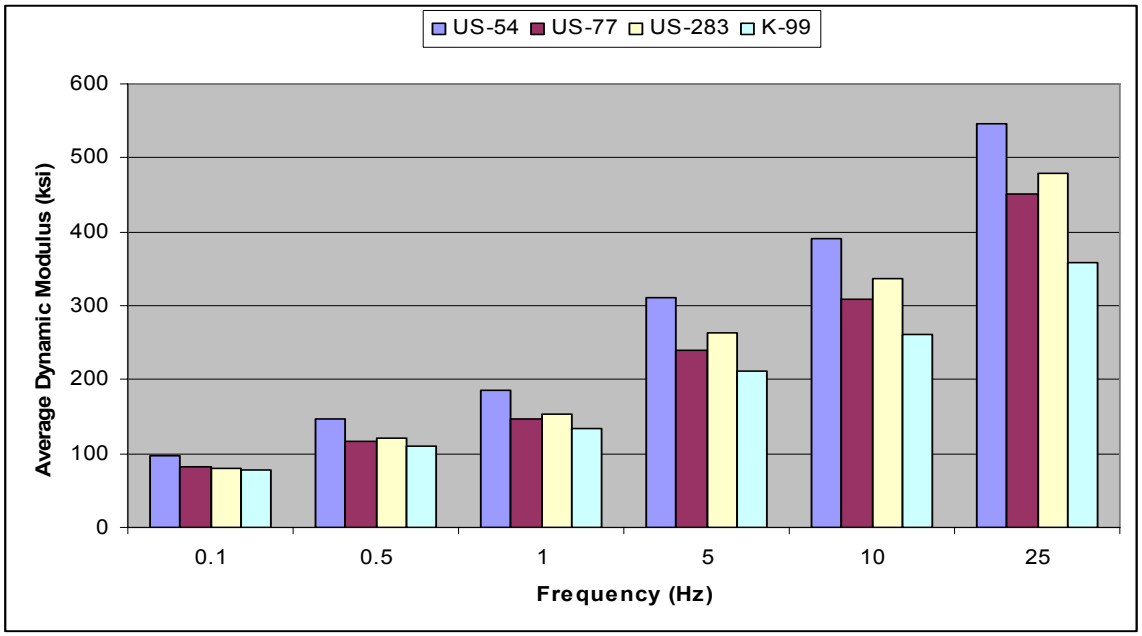


**Figure C.17: Comparison of Dynamic Modulus at 95°F.**

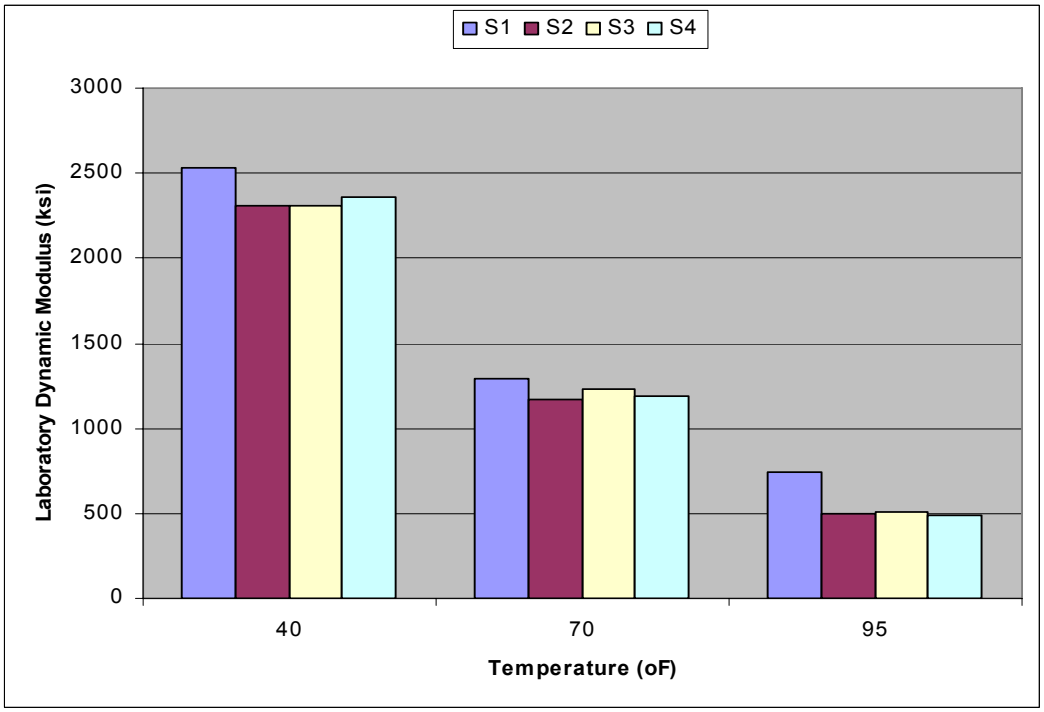


**Figure C.18: Comparison of Dynamic Modulus of Sections at 25Hz.**

**Table C.1: Summary Statistics of Dynamic Modulus at 40°F**

| | | Frequency (Hz) | | | | | |
|---|---|---|---|---|---|---|---|
| | | 0.1 | 0.5 | 1 | 5 | 10 | 25 |
| **a. New Projects** | | | | | | | |
| **US-54** | **Av.Mod. (ksi)** | 1138 | 1398 | 1490 | 1752 | 1860 | 2037 |
| | **STD (ksi)** | 136 | 176 | 191 | 244 | 276 | 304 |
| | **COV(%)** | 12.0 | 12.6 | 12.8 | 14.0 | 14.8 | 14.9 |
| **US-77** | **Av.Mod. (ksi)** | 1119 | 1363 | 1458 | 1715 | 1820 | 2039 |
| | **STD (ksi)** | 52 | 64 | 69 | 78 | 71 | 113 |
| | **COV(%)** | 4.6 | 4.7 | 4.8 | 4.6 | 3.9 | 5.5 |
| **US-283** | **Av.Mod. (ksi)** | 1047 | 1324 | 1416 | 1710 | 1814 | 2046 |
| | **STD (ksi)** | 97 | 121 | 127 | 177 | 143 | 145 |
| | **COV(%)** | 9.3 | 9.2 | 9.0 | 10.3 | 7.9 | 7.1 |
| **K-7** | **Av.Mod. (ksi)** | 903 | 1172 | 1265 | 1552 | 1675 | 1845 |
| | **STD (ksi)** | 234 | 298 | 312 | 324 | 346 | 338 |
| | **COV(%)** | 25.9 | 25.4 | 24.6 | 20.9 | 20.7 | 18.3 |
| **K-99** | **Av.Mod. (ksi)** | 1013 | 1289 | 1400 | 1699 | 1796 | 1915 |
| | **STD (ksi)** | 79 | 78 | 99 | 111 | 89 | 45 |
| | **COV(%)** | 7.8 | 6.1 | 7.1 | 6.6 | 5.0 | 2.3 |
| **b. Perpetual Pavement Sections** | | | | | | | |
| **S1** | **Av.Mod. (ksi)** | | | | | | 2536 |
| **S2** | **Av.Mod. (ksi)** | | | | | | 2312 |
| **S3** | **Av.Mod. (ksi)** | | | | | | 2307 |
| **S4** | **Av.Mod. (ksi)** | | | | | | 2357 |

**Table C.2: Summary Statistics of Dynamic Modulus at 95°F**

| | | Frequency (Hz) | | | | | |
|---|---|---|---|---|---|---|---|
| | | 0.1 | 0.5 | 1 | 5 | 10 | 25 |
| **a. New Projects** | | | | | | | |
| **US-54** | **Av.Mod. (ksi)** | 97.71 | 147.22 | 185.36 | 311.84 | 391.27 | 546.95 |
| | **STD (ksi)** | 2.5 | 5.8 | 6.2 | 10.1 | 12.3 | 7.1 |
| | **COV(%)** | 2.60 | 3.91 | 3.37 | 3.23 | 3.13 | 1.29 |
| **US-77** | **Av.Mod. (ksi)** | 81.75 | 117.00 | 146.20 | 238.98 | 307.92 | 451.22 |
| | **STD (ksi)** | 0.7 | 1.3 | 3.4 | 8.9 | 9.3 | 19.8 |
| | **COV(%)** | 0.80 | 1.11 | 2.33 | 3.73 | 3.03 | 4.39 |
| **US-283** | **Av.Mod. (ksi)** | 80.84 | 120.33 | 152.49 | 264.17 | 335.91 | 478.10 |
| | **STD (ksi)** | 0.5 | 1.1 | 1.9 | 2.8 | 2.5 | 8.6 |
| | **COV(%)** | 0.58 | 0.87 | 1.27 | 1.07 | 0.75 | 1.80 |
| **K-99** | **Av.Mod. (ksi)** | 78.56 | 110.23 | 134.07 | 210.60 | 260.73 | 358.68 |
| | **STD (ksi)** | 6.9 | 9.4 | 11.9 | 20.2 | 24.9 | 30.5 |
| | **COV(%)** | 8.77 | 8.54 | 8.87 | 9.58 | 9.53 | 8.50 |
| **b. Perpetual Pavement Sections** | | | | | | | |
| **S1** | **Av.Mod. (ksi)** | | | | | | 741 |
| **S2** | **Av.Mod. (ksi)** | | | | | | 498 |
| **S3** | **Av.Mod. (ksi)** | | | | | | 507 |
| **S4** | **Av.Mod. (ksi)** | | | | | | 489 |

# APPENDIX D - BACKCALCULATED MODULUS

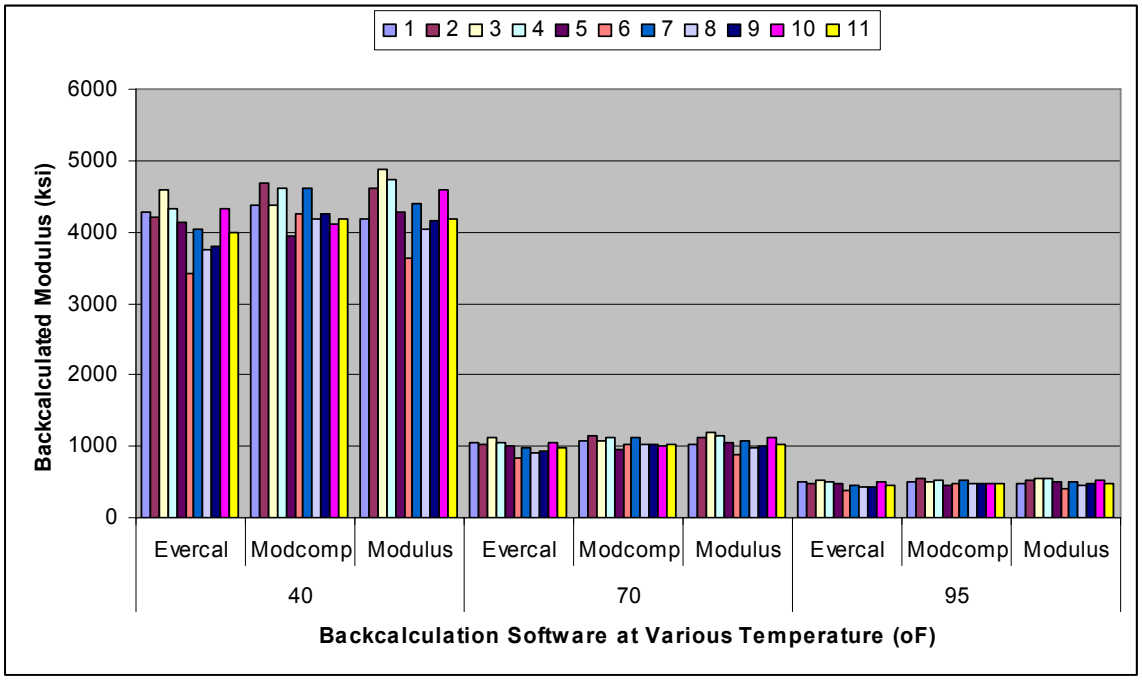


**Figure D.1: Comparison of Backcalculated Modulus for US-54.**

**Table D.1: Comparison of Backcalculated Modulus for US-54**

| Sta. No. | 40°F | | | 70 °F | | | 95 °F | | |
|---|---|---|---|---|---|---|---|---|---|
| | Ever. | Modc. | Modu. | Ever. | Modc. | Modu. | Ever. | Modc. | Modu. |
| 1 | 4288 | 4376 | 4180 | 1046 | 1067 | 1019 | 492 | 502 | 479 |
| 2 | 4197 | 4690 | 4618 | 1023 | 1143 | 1126 | 481 | 538 | 530 |
| 3 | 4592 | 4379 | 4885 | 1119 | 1068 | 1191 | 527 | 502 | 560 |
| 4 | 4325 | 4621 | 4743 | 1055 | 1127 | 1156 | 496 | 530 | 544 |
| 5 | 4137 | 3951 | 4285 | 1009 | 963 | 1045 | 475 | 453 | 492 |
| 6 | 3429 | 4249 | 3642 | 836 | 1036 | 888 | 393 | 487 | 418 |
| 7 | 4039 | 4615 | 4390 | 985 | 1125 | 1070 | 463 | 529 | 504 |
| 8 | 3760 | 4183 | 4028 | 917 | 1020 | 982 | 431 | 480 | 462 |
| 9 | 3801 | 4249 | 4156 | 927 | 1036 | 1013 | 436 | 487 | 477 |
| 10 | 4324 | 4117 | 4599 | 1054 | 1004 | 1121 | 496 | 472 | 528 |
| 11 | 4003 | 4183 | 4195 | 976 | 1020 | 1023 | 459 | 480 | 481 |

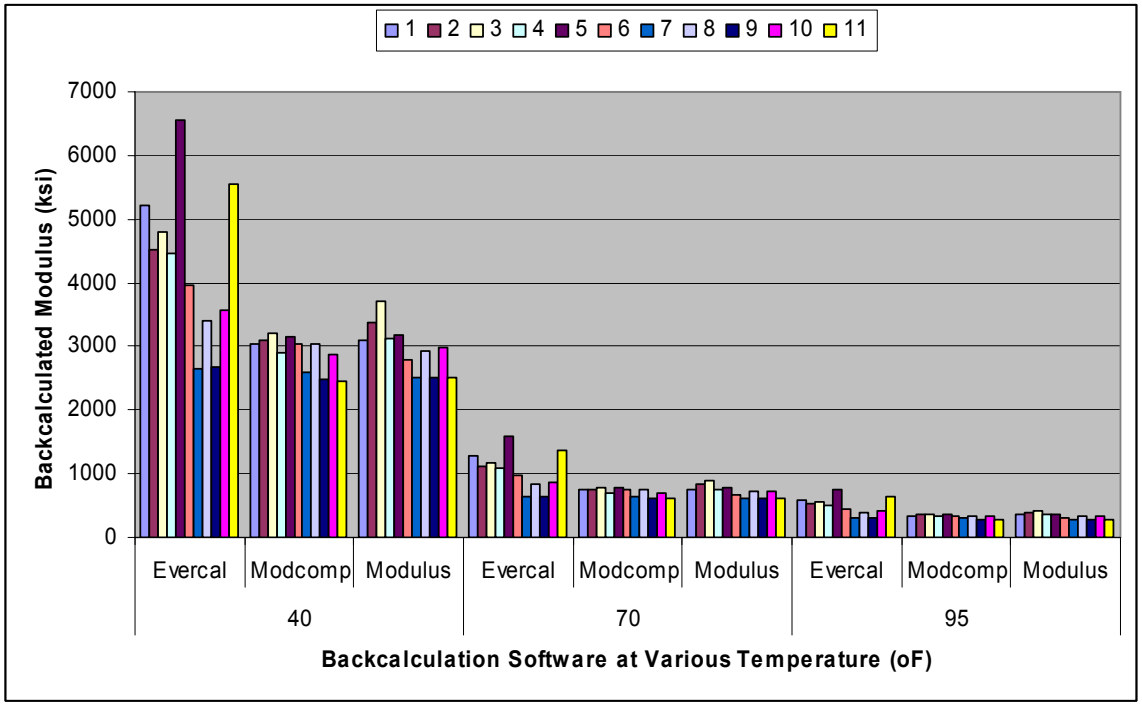


**Figure D.2: Comparison of Backcalculated Modulus for US-77.**

**Table D.2: Comparison of Backcalculated Modulus for US-77**

| Station No. | 40°F | | | 70 °F | | | 95 °F | | |
|---|---|---|---|---|---|---|---|---|---|
| | Ever. | Modc. | Modu. | Ever. | Modc. | Modu. | Ever. | Modc. | Modu. |
| **1** | 5214 | 3031 | 3096 | 1271 | 739 | 755 | 598 | 348 | 355 |
| **2** | 4525 | 3109 | 3380 | 1103 | 758 | 824 | 519 | 357 | 388 |
| **3** | 4802 | 3198 | 3712 | 1171 | 780 | 905 | 551 | 367 | 426 |
| **4** | 4461 | 2901 | 3112 | 1088 | 707 | 759 | 512 | 333 | 357 |
| **5** | 6541 | 3154 | 3173 | 1595 | 769 | 774 | 750 | 362 | 364 |
| **6** | 3960 | 3039 | 2785 | 965 | 741 | 679 | 454 | 349 | 320 |
| **7** | 2652 | 2603 | 2521 | 647 | 635 | 615 | 304 | 299 | 289 |
| **8** | 3412 | 3035 | 2939 | 832 | 740 | 717 | 391 | 348 | 337 |
| **9** | 2684 | 2484 | 2510 | 654 | 606 | 612 | 308 | 285 | 288 |
| **10** | 3578 | 2871 | 2986 | 872 | 700 | 728 | 410 | 329 | 343 |
| **11** | 5560 | 2460 | 2514 | 1356 | 600 | 613 | 638 | 282 | 288 |

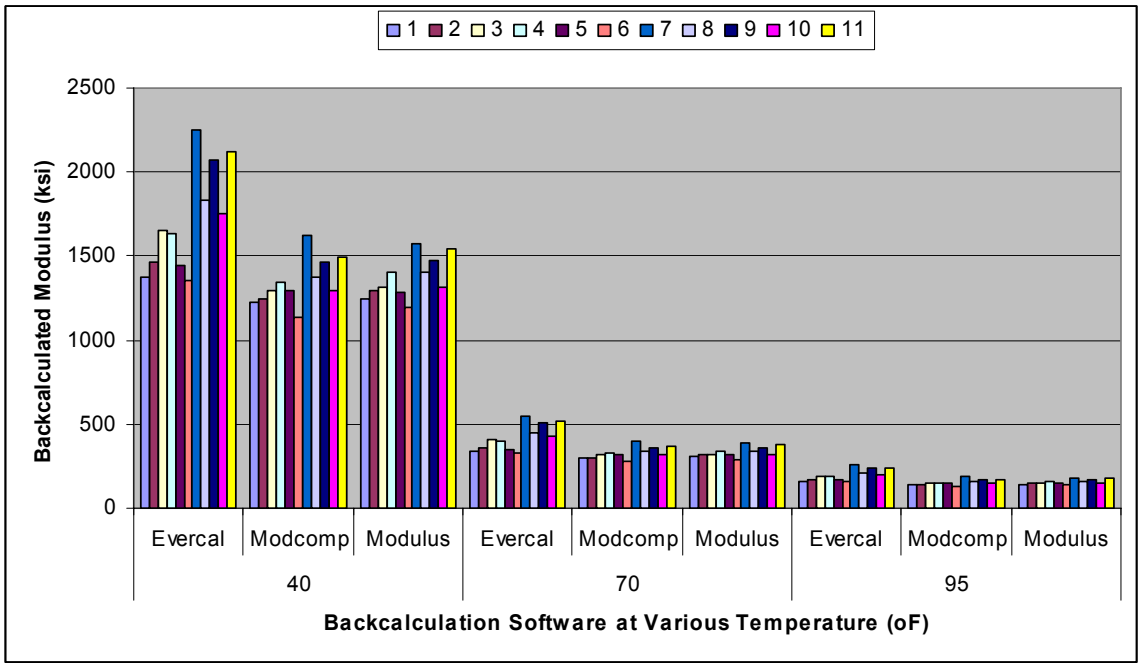


**Figure D.3: Comparison of Backcalculated Modulus for US-283.**

**Table D.3: Comparison of Backcalculated Modulus for US-283.**

| Station No. | 40oF | | | 70 oF | | | 95 oF | | |
|---|---|---|---|---|---|---|---|---|---|
| | Ever. | Modc. | Modu. | Ever. | Modc. | Modu. | Ever. | Modc. | Modu. |
| **1** | 1375 | 1228 | 1247 | 335 | 299 | 304 | 158 | 141 | 143 |
| **2** | 1463 | 1245 | 1295 | 357 | 303 | 316 | 168 | 143 | 149 |
| **3** | 1657 | 1300 | 1314 | 404 | 317 | 320 | 190 | 149 | 151 |
| **4** | 1636 | 1344 | 1401 | 399 | 328 | 341 | 188 | 154 | 161 |
| **5** | 1446 | 1291 | 1290 | 353 | 315 | 314 | 166 | 148 | 148 |
| **6** | 1357 | 1139 | 1200 | 331 | 278 | 293 | 156 | 131 | 138 |
| **7** | 2248 | 1621 | 1573 | 548 | 395 | 383 | 258 | 186 | 180 |
| **8** | 1829 | 1378 | 1405 | 446 | 336 | 343 | 210 | 158 | 161 |
| **9** | 2075 | 1465 | 1470 | 506 | 357 | 359 | 238 | 168 | 169 |
| **10** | 1758 | 1300 | 1317 | 429 | 317 | 321 | 202 | 149 | 151 |
| **11** | 2120 | 1493 | 1546 | 517 | 364 | 377 | 243 | 171 | 177 |

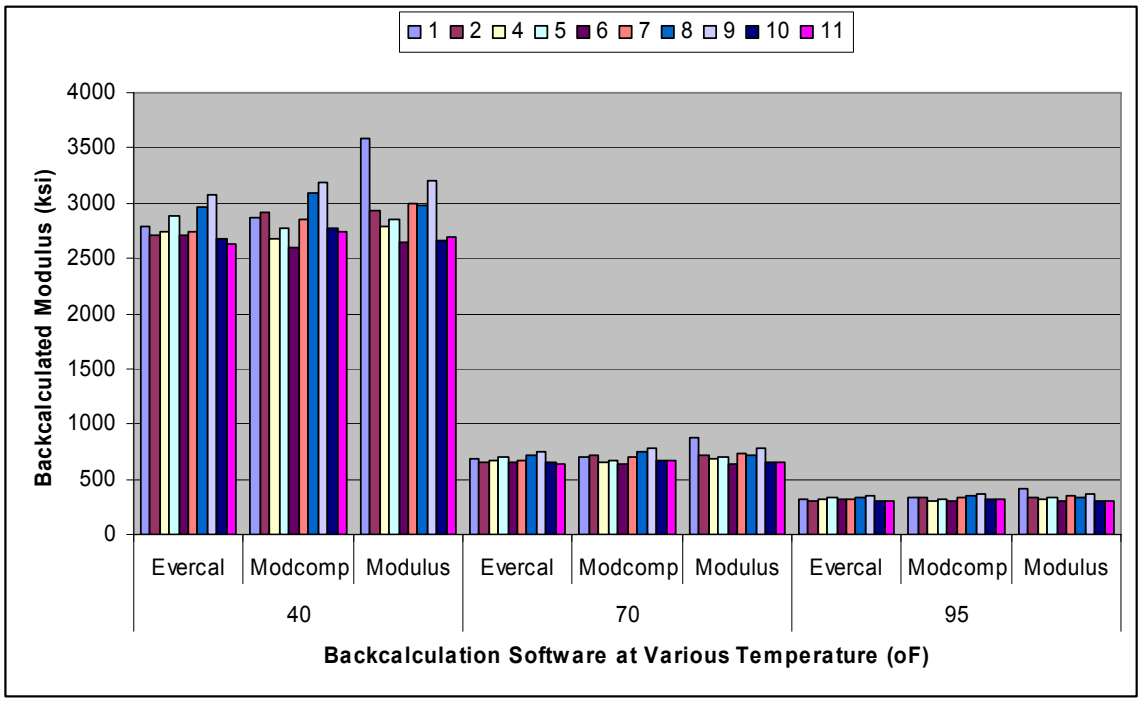


**Figure D.4: Comparison of Backcalculated Modulus for K-7.**

**Table D.4: Comparison of Backcalculated Modulus for K-7.**

| Station No. | 40oF | | | 70 oF | | | 95 oF | | |
|---|---|---|---|---|---|---|---|---|---|
| | Ever. | Modc. | Modu. | Ever. | Modc. | Modu. | Ever. | Modc. | Modu. |
| 1 | 2792 | 2871 | 3593 | 681 | 700 | 876 | 320 | 329 | 412 |
| 2 | 2706 | 2915 | 2928 | 660 | 711 | 714 | 310 | 334 | 336 |
| 4 | 2733 | 2673 | 2797 | 666 | 652 | 682 | 314 | 307 | 321 |
| 5 | 2882 | 2770 | 2855 | 703 | 675 | 696 | 331 | 318 | 327 |
| 6 | 2711 | 2591 | 2638 | 661 | 632 | 643 | 311 | 297 | 303 |
| 7 | 2749 | 2859 | 2990 | 670 | 697 | 729 | 315 | 328 | 343 |
| 8 | 2966 | 3096 | 2973 | 723 | 755 | 725 | 340 | 355 | 341 |
| 9 | 3073 | 3192 | 3210 | 749 | 778 | 783 | 352 | 366 | 368 |
| 10 | 2676 | 2767 | 2663 | 652 | 675 | 649 | 307 | 317 | 306 |
| 11 | 2622 | 2740 | 2697 | 639 | 668 | 658 | 301 | 314 | 309 |

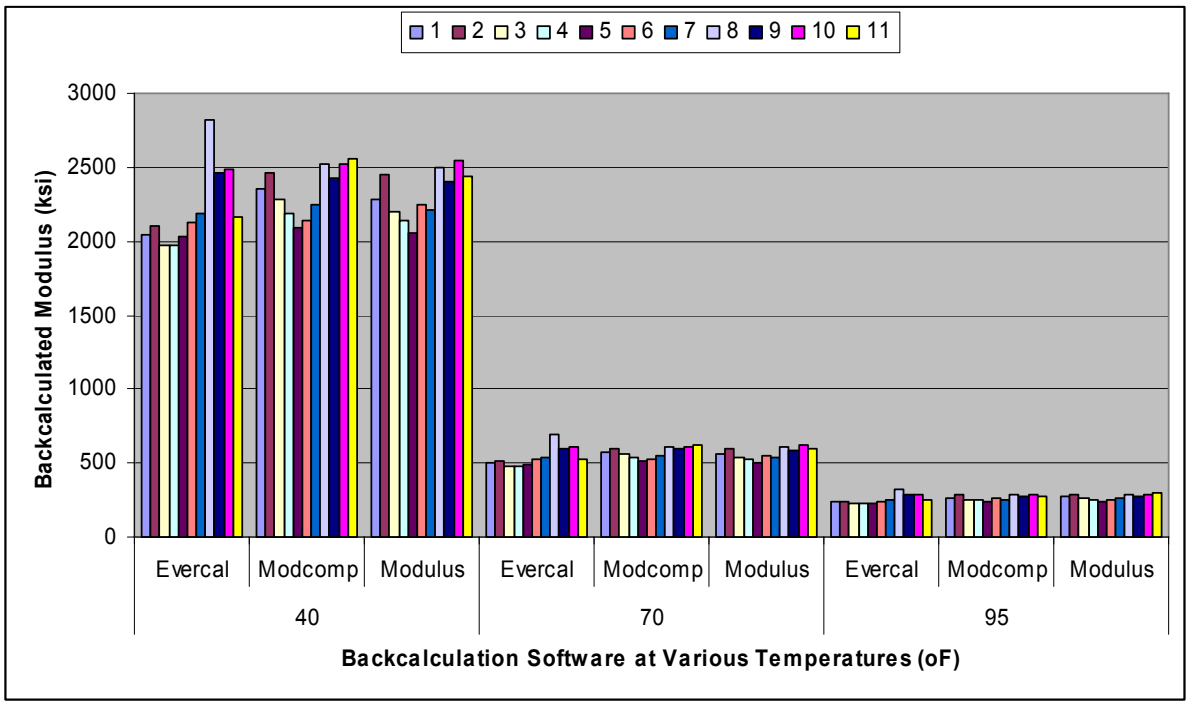


**Figure D.5: Comparison of Backcalculated Modulus for K-99.**

**Table D.5: Comparison of Backcalculated Modulus for K-99**

| Station No. | 40°F | | | 70 °F | | | 95 °F | | |
|---|---|---|---|---|---|---|---|---|---|
| | Ever. | Modc. | Modu. | Ever. | Modc. | Modu. | Ever. | Modc. | Modu. |
| 1 | 2040 | 2349 | 2284 | 497 | 573 | 557 | 234 | 262 | 269 |
| 2 | 2098 | 2463 | 2453 | 511 | 601 | 598 | 241 | 281 | 283 |
| 3 | 1976 | 2283 | 2197 | 482 | 557 | 536 | 227 | 252 | 262 |
| 4 | 1977 | 2192 | 2141 | 482 | 534 | 522 | 227 | 246 | 251 |
| 5 | 2029 | 2092 | 2051 | 495 | 510 | 500 | 233 | 235 | 240 |
| 6 | 2132 | 2142 | 2242 | 520 | 522 | 547 | 244 | 257 | 246 |
| 7 | 2185 | 2252 | 2214 | 533 | 549 | 540 | 251 | 254 | 258 |
| 8 | 2822 | 2524 | 2496 | 688 | 615 | 609 | 324 | 286 | 289 |
| 9 | 2468 | 2430 | 2407 | 602 | 592 | 587 | 283 | 276 | 279 |
| 10 | 2488 | 2522 | 2542 | 607 | 615 | 620 | 285 | 292 | 289 |
| 11 | 2161 | 2560 | 2444 | 527 | 624 | 596 | 248 | 280 | 294 |

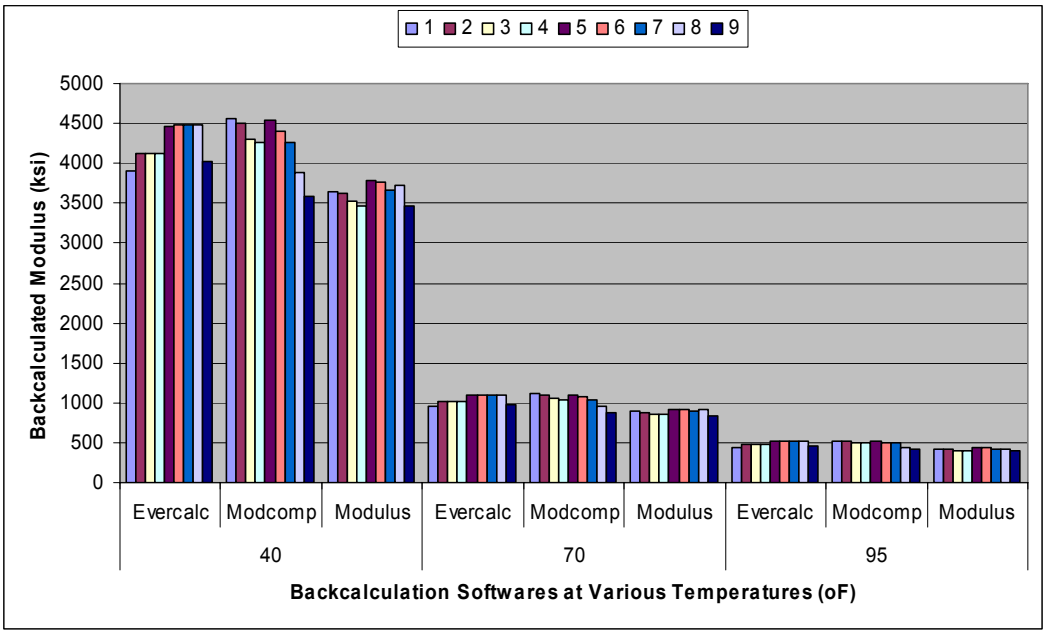


**Figure D.6: Comparison of Backcalculated Modulus for S1.**

**Table D.6: Comparison of Backcalculated Modulus for S1**

| Station No. | 40°F | | | 70 °F | | | 95 °F | | |
|---|---|---|---|---|---|---|---|---|---|
| | Ever. | Modc. | Modu. | Ever. | Modc. | Modu. | Ever. | Modc. | Modu. |
| **1** | 3902 | 4568 | 3649 | 951 | 1114 | 890 | 448 | 524 | 419 |
| **2** | 4129 | 4500 | 3634 | 1007 | 1097 | 886 | 474 | 516 | 417 |
| **3** | 4129 | 4297 | 3520 | 1007 | 1048 | 858 | 474 | 493 | 404 |
| **4** | 4129 | 4263 | 3475 | 1007 | 1039 | 847 | 474 | 489 | 399 |
| **5** | 4461 | 4534 | 3780 | 1088 | 1105 | 922 | 512 | 520 | 434 |
| **6** | 4479 | 4399 | 3773 | 1092 | 1072 | 920 | 514 | 505 | 433 |
| **7** | 4482 | 4263 | 3660 | 1093 | 1039 | 892 | 514 | 489 | 420 |
| **8** | 4482 | 3891 | 3722 | 1093 | 949 | 908 | 514 | 446 | 427 |
| **9** | 4030 | 3587 | 3457 | 983 | 874 | 843 | 462 | 411 | 397 |

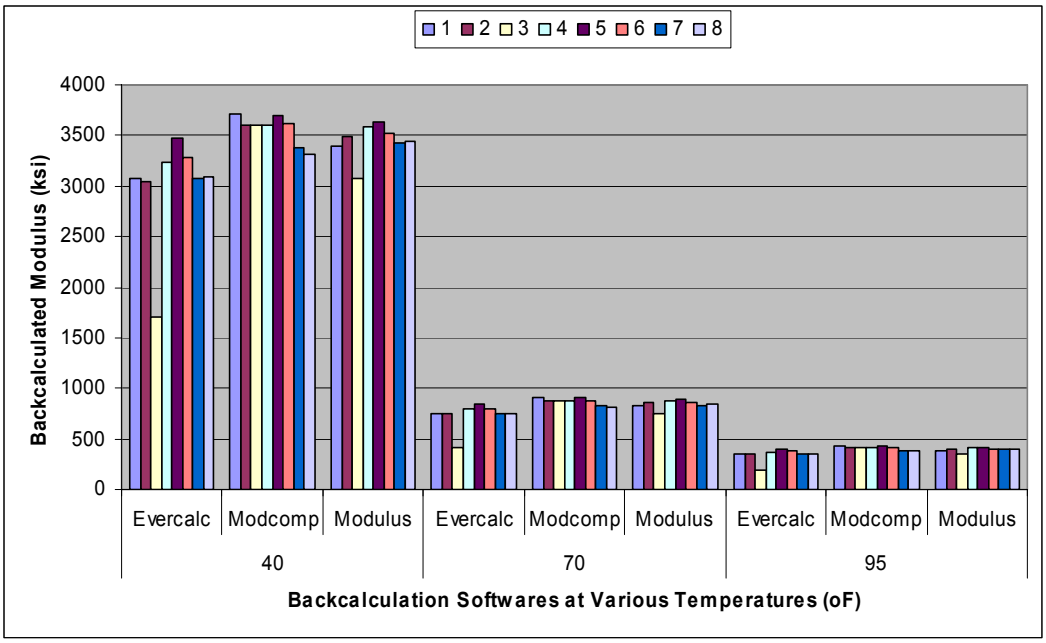


**Figure D.7: Comparison of Backcalculated Modulus for S2.**

**Table D.7: Comparison of Backcalculated Modulus for S2**

| Station No. | 40oF | | | 70 oF | | | 95 oF | | |
|---|---|---|---|---|---|---|---|---|---|
| | Ever. | Modc. | Modu. | Ever. | Modc. | Modu. | Ever. | Modc. | Modu. |
| **1** | 3073 | 3719 | 3389 | 749 | 907 | 826 | 352 | 427 | 389 |
| **2** | 3043 | 3609 | 3498 | 742 | 880 | 853 | 349 | 414 | 401 |
| **3** | 1703 | 3594 | 3080 | 415 | 876 | 751 | 195 | 412 | 353 |
| **4** | 3241 | 3609 | 3587 | 790 | 880 | 874 | 372 | 414 | 411 |
| **5** | 3472 | 3704 | 3631 | 847 | 903 | 885 | 398 | 425 | 416 |
| **6** | 3282 | 3617 | 3518 | 800 | 882 | 858 | 376 | 415 | 403 |
| **7** | 3079 | 3374 | 3428 | 751 | 823 | 836 | 353 | 387 | 393 |
| **8** | 3091 | 3317 | 3436 | 754 | 809 | 838 | 355 | 381 | 394 |

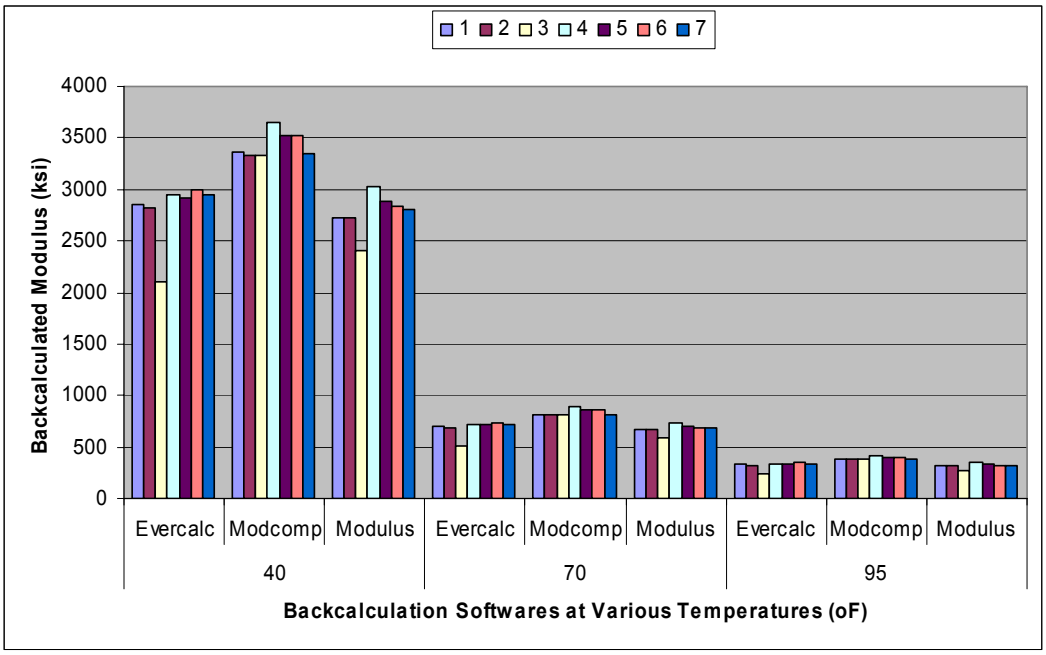


**Figure D.8: Comparison of Backcalculated Modulus for S3.**

**Table D.8: Comparison of Backcalculated Modulus for S3**

| Station No. | 40oF | | | 70 oF | | | 95 oF | | |
|---|---|---|---|---|---|---|---|---|---|
| | Ever. | Modc. | Modu. | Ever. | Modc. | Modu. | Ever. | Modc. | Modu. |
| **1** | 2850 | 3361 | 2732 | 695 | 819 | 666 | 327 | 386 | 313 |
| **2** | 2820 | 3335 | 2724 | 688 | 813 | 664 | 323 | 383 | 312 |
| **3** | 2103 | 3331 | 2401 | 513 | 812 | 585 | 241 | 382 | 275 |
| **4** | 2942 | 3645 | 3020 | 717 | 889 | 736 | 337 | 418 | 346 |
| **5** | 2913 | 3529 | 2883 | 710 | 860 | 703 | 334 | 405 | 331 |
| **6** | 2997 | 3520 | 2836 | 731 | 858 | 691 | 344 | 404 | 325 |
| **7** | 2942 | 3352 | 2806 | 717 | 817 | 684 | 337 | 385 | 322 |

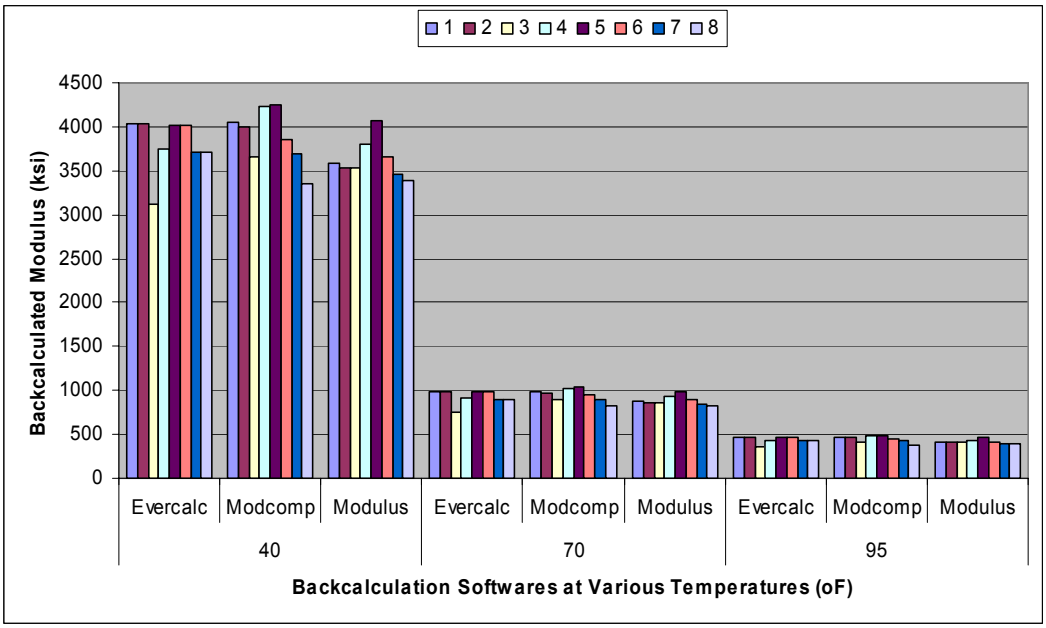


**Figure D.9: Comparison of Backcalculated Modulus for S4**

**Table D.9: Comparison of Backcalculated Modulus for S4**

| Station No. | 40°F | | | 70 °F | | | 95 °F | | |
|---|---|---|---|---|---|---|---|---|---|
| | Ever. | Modc. | Modu. | Ever. | Modc. | Modu. | Ever. | Modc. | Modu. |
| **1** | 4027 | 4059 | 3588 | 982 | 990 | 875 | 462 | 466 | 412 |
| **2** | 4027 | 4007 | 3538 | 982 | 977 | 863 | 462 | 460 | 406 |
| **3** | 3125 | 3656 | 3525 | 762 | 891 | 860 | 358 | 419 | 404 |
| **4** | 3740 | 4222 | 3799 | 912 | 1029 | 926 | 429 | 484 | 436 |
| **5** | 4009 | 4256 | 4078 | 978 | 1038 | 994 | 460 | 488 | 468 |
| **6** | 4009 | 3863 | 3665 | 978 | 942 | 894 | 460 | 443 | 420 |
| **7** | 3710 | 3685 | 3454 | 904 | 898 | 842 | 426 | 423 | 396 |
| **8** | 3710 | 3354 | 3394 | 904 | 818 | 828 | 426 | 385 | 389 |

# APPENDIX E - PREDICTED MODULUS

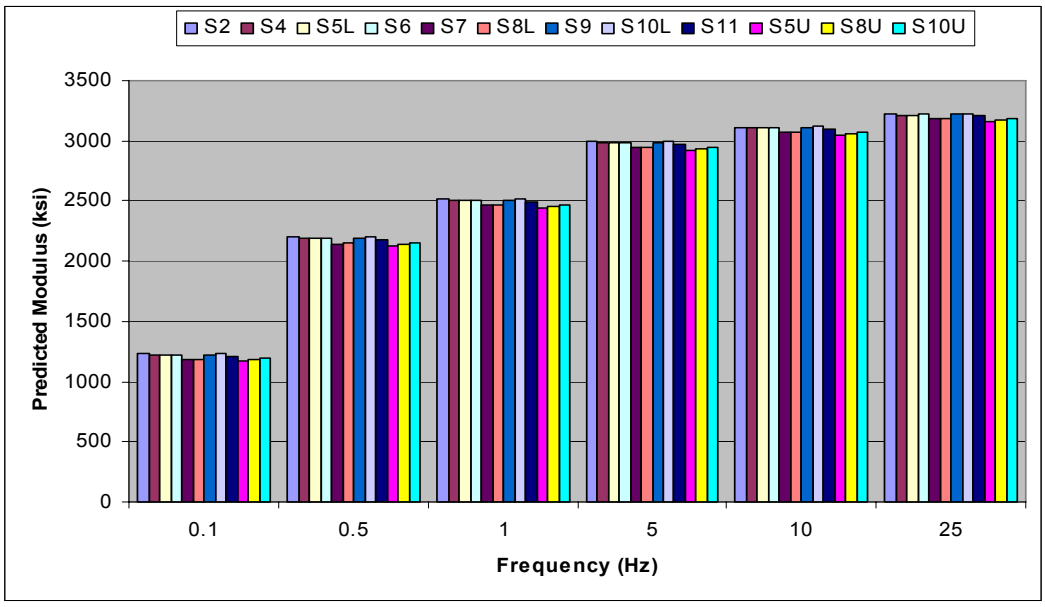


**Figure E.1: Predicted Modulus Using Hirsch Model for US-54 at 40°F**

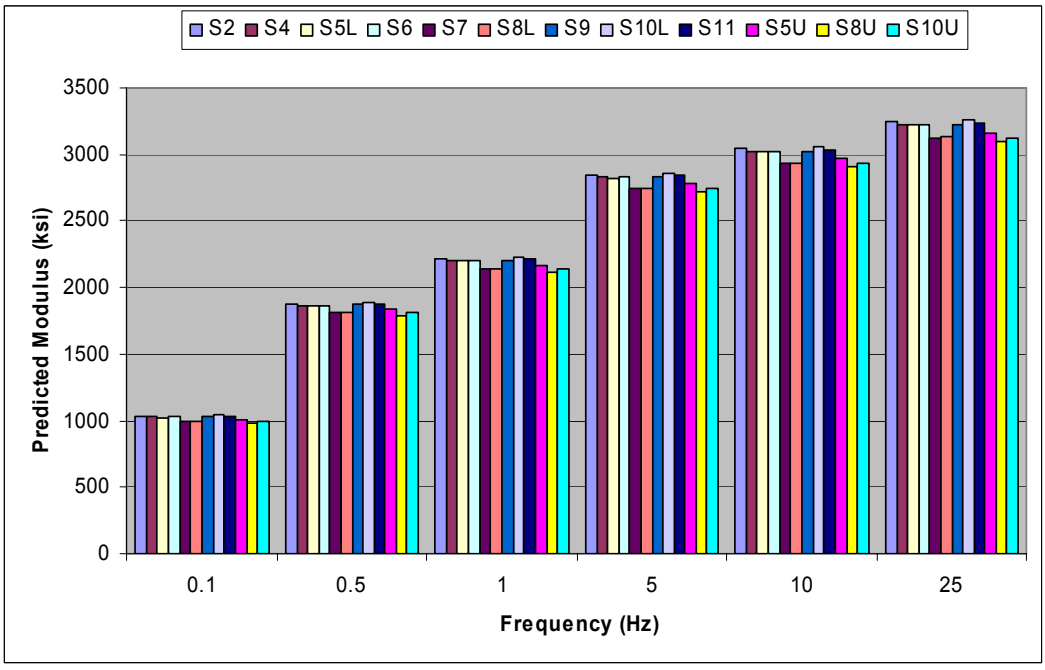


**Figure E.2: Predicted Modulus Using New Model for US-54 at 40°F**

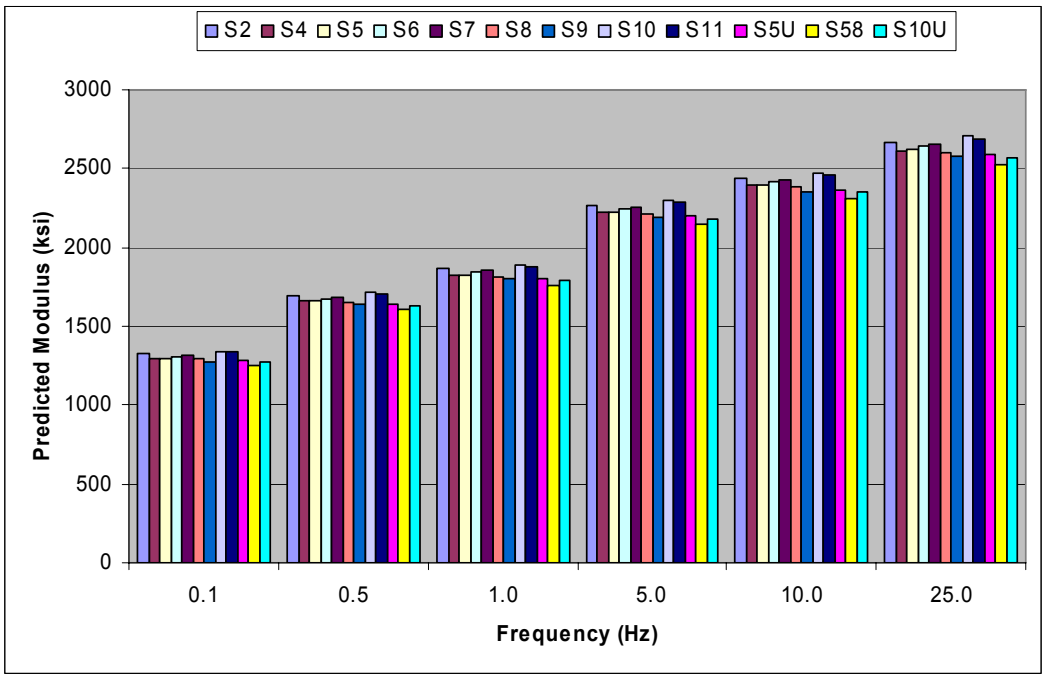


**Figure E.3: Predicted Modulus Using Witczak Equation for US-54 at 40°F.**

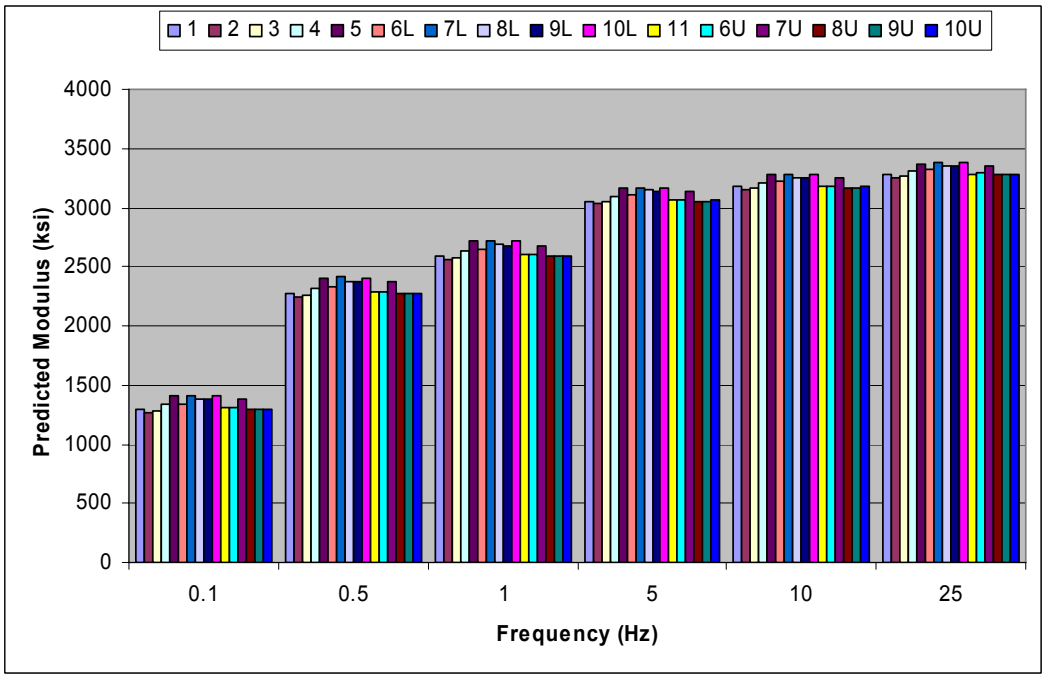


**Figure E.4: Predicted Modulus Using Hirsch Model for US-77 at 40°F.**

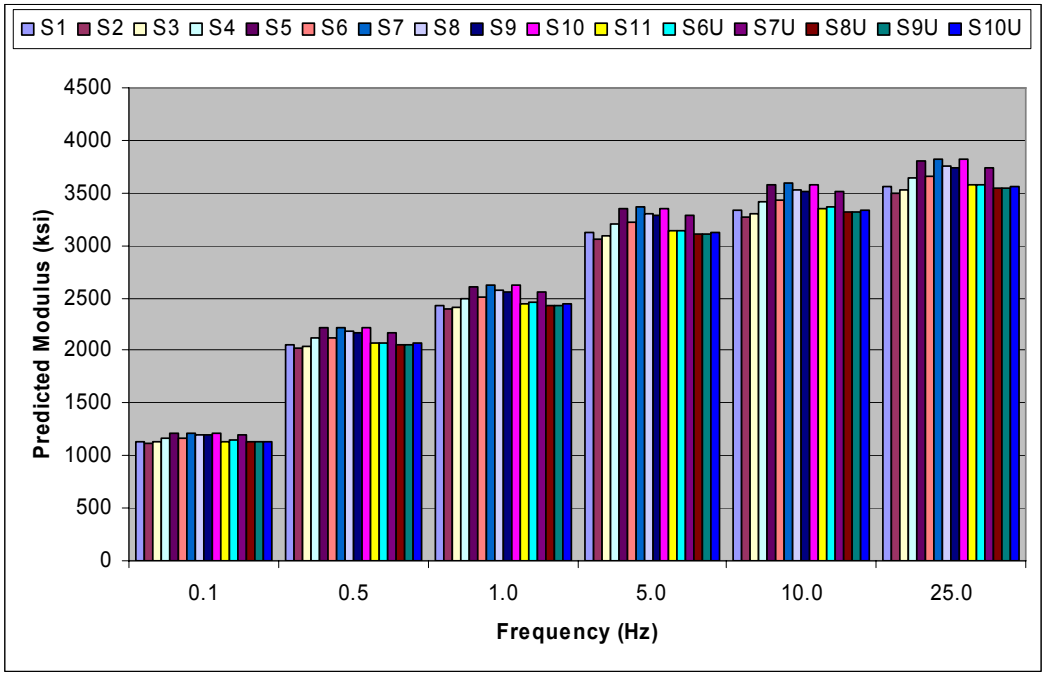


**Figure E.5: Predicted Modulus Using New Model for US-77 at 40°F.**

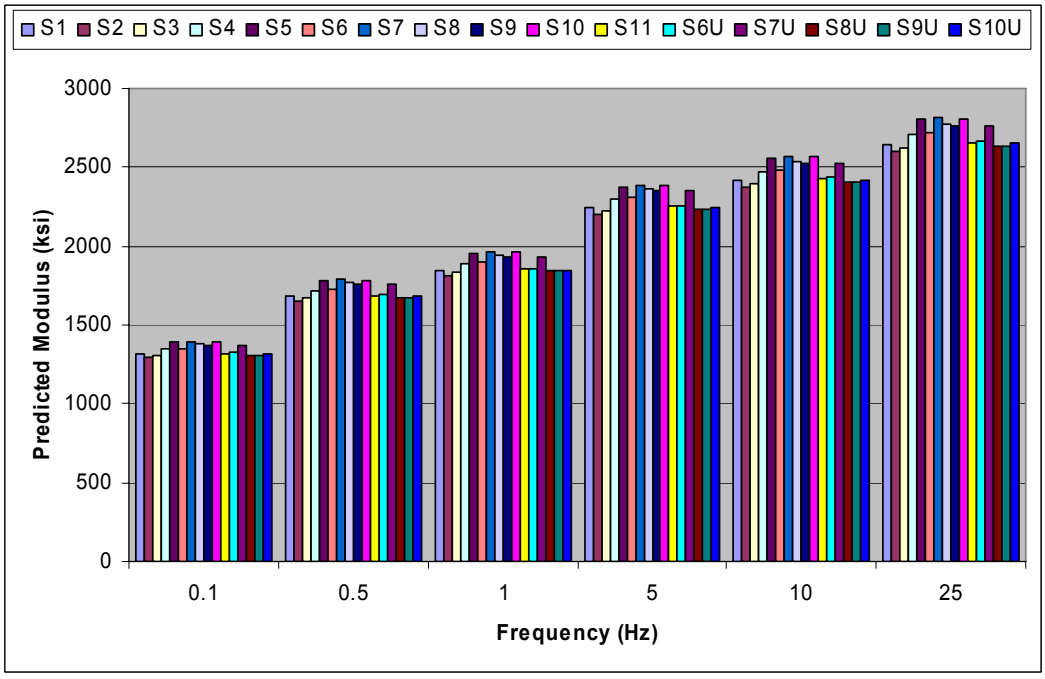


**Figure E.6: Predicted Modulus Using Witczak Equation for US-77 at 40°F.**

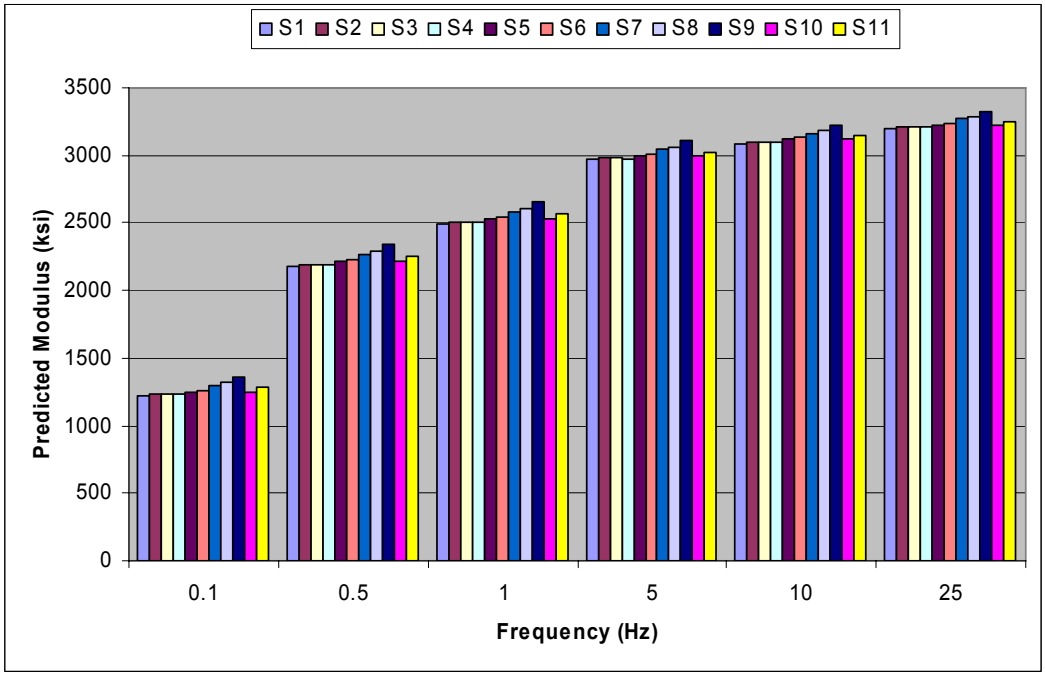


**Figure E.7: Predicted Modulus Using Hirsch Model for US-283 at 40°F.**

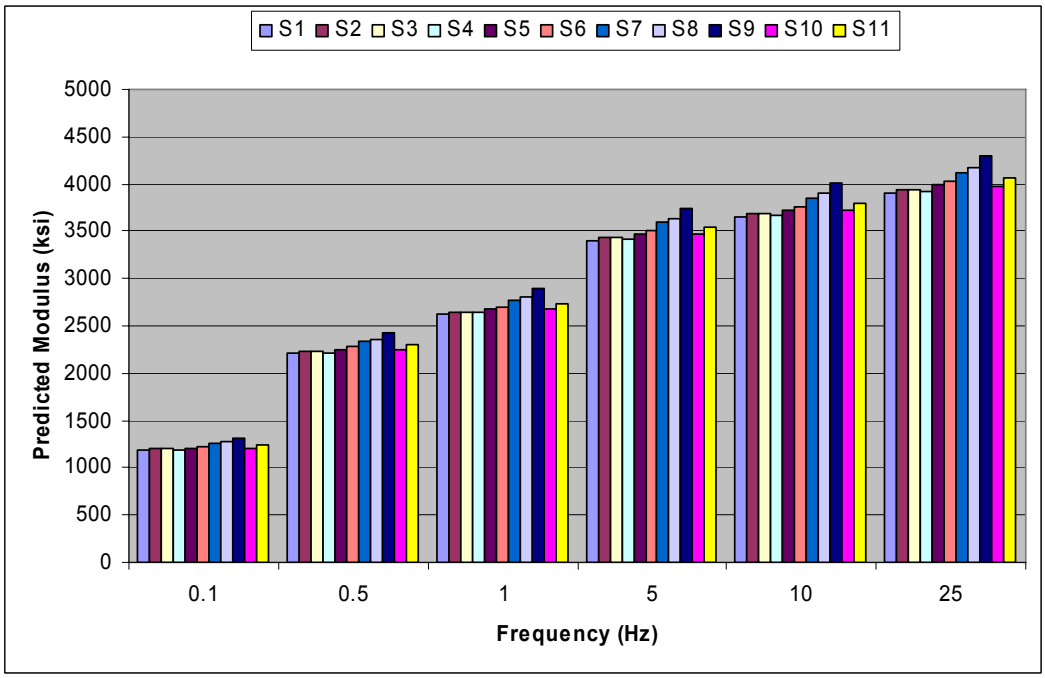


**Figure E.8: Predicted Modulus Using New Model for US-283 at 40°F.**

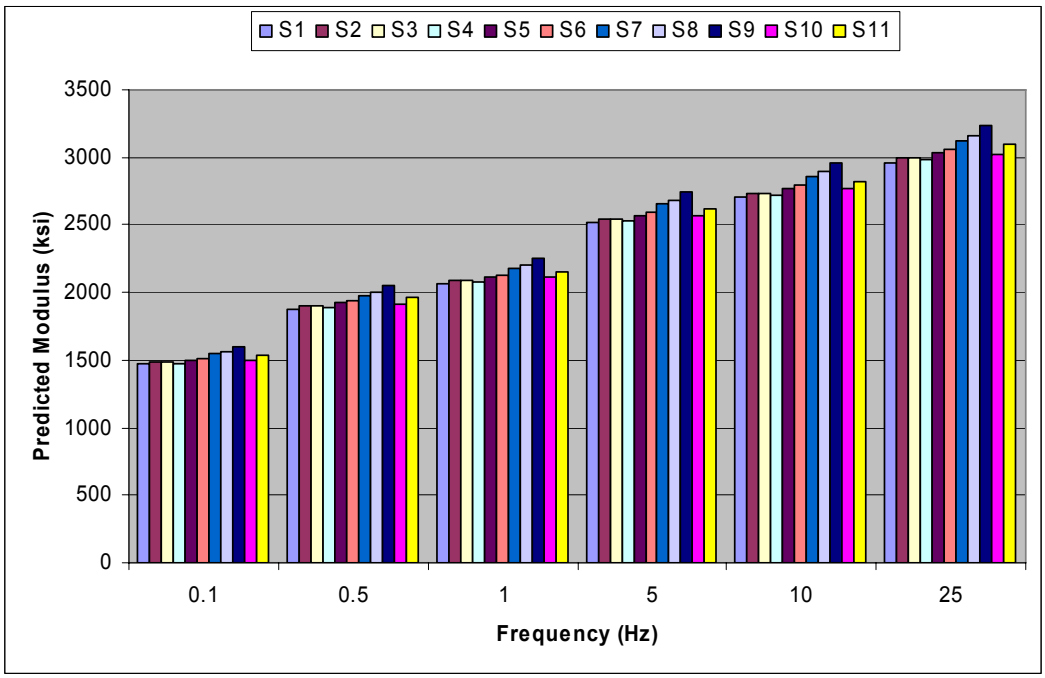


**Figure E.9: Predicted Modulus Using Witczak Equation for US-283 at 40°F**

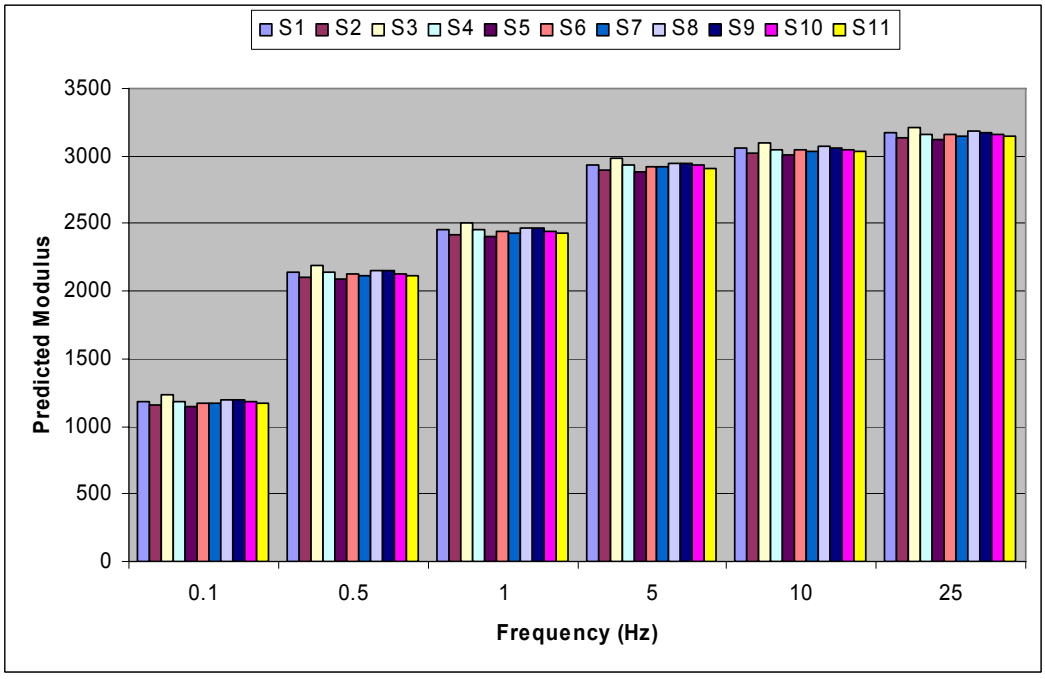


**Figure E.10: Predicted Modulus Using Hirsch Model for K-7 at 40°F**

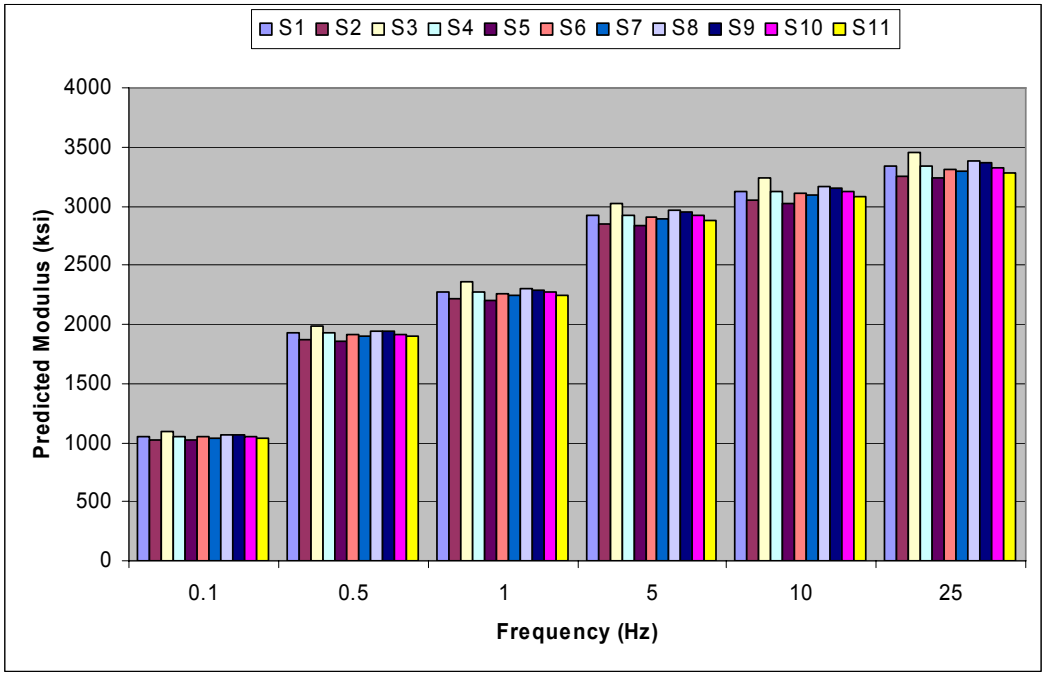


**Figure E.11: Predicted Modulus Using New Model for K-7 at 40°F.**

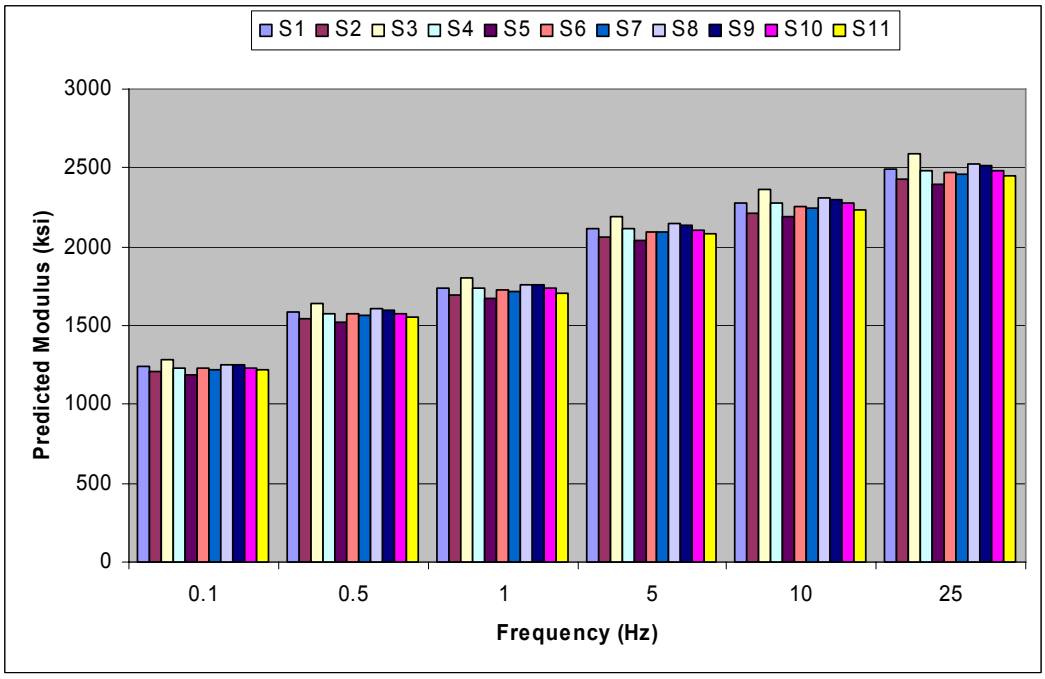


**Figure E.12: Predicted Modulus Using Witczak Equation for K-7 at 40°F.**

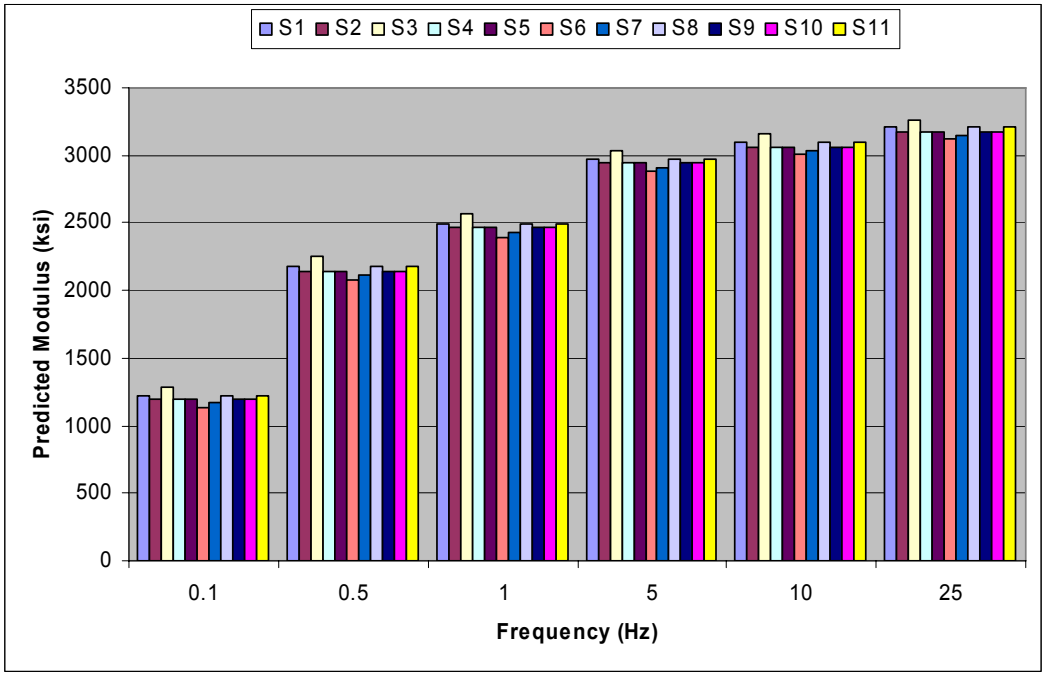


**Figure E.13: Predicted Modulus Using Hirsch Model for K-99 at 40°F.**

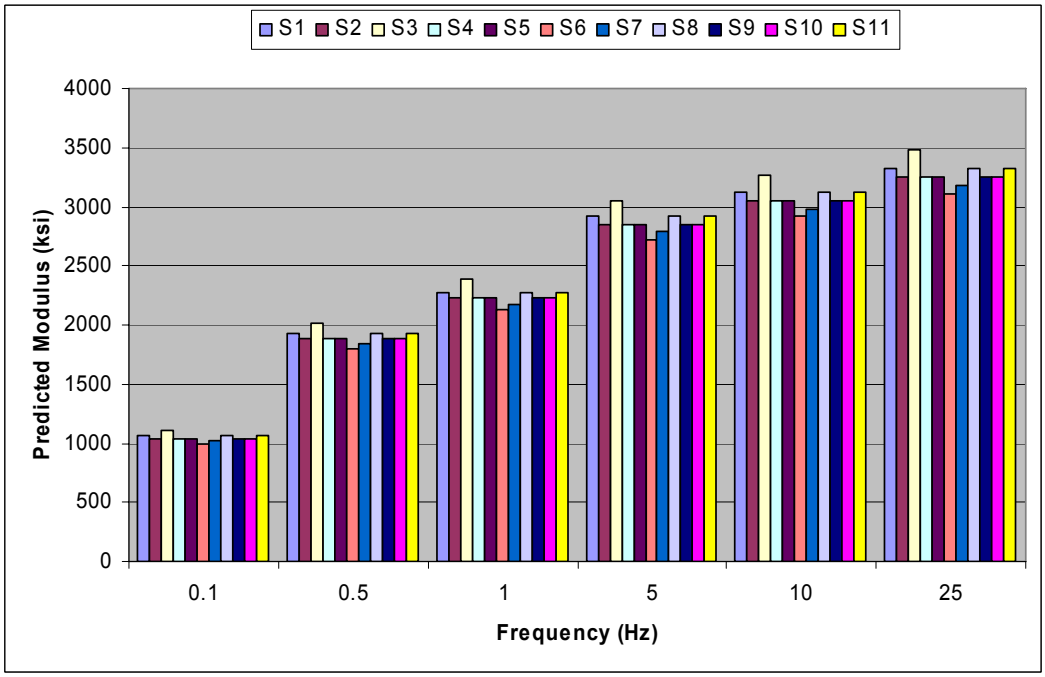


**Figure E.14: Predicted Modulus Using New Model for K-99 at 40°F.**

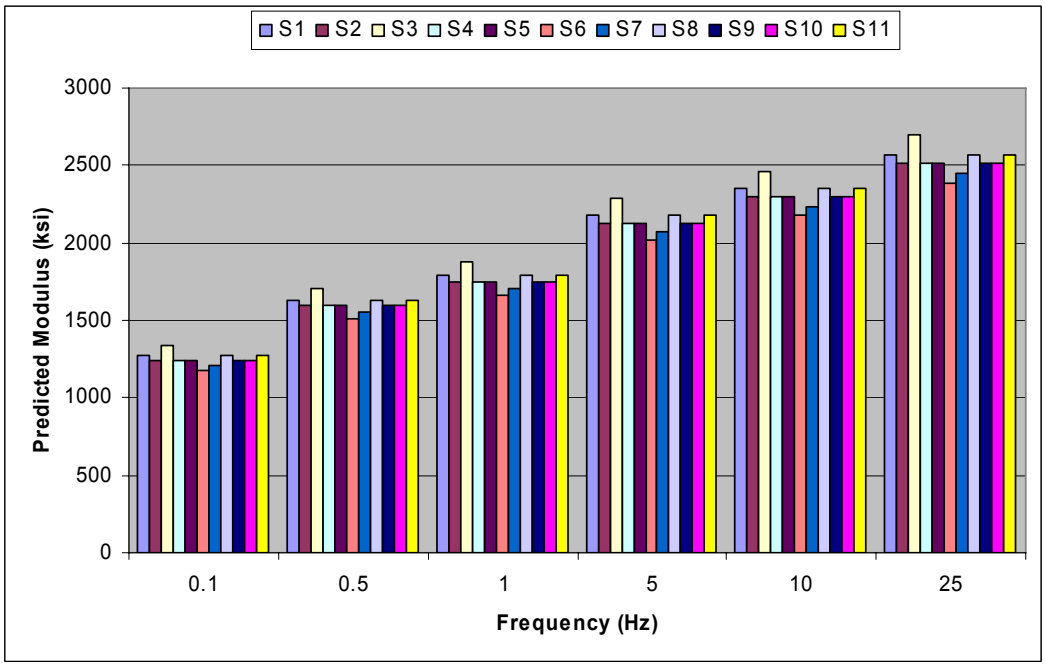


**Figure E.15: Predicted Modulus Using Witczak Equation for K-99 at 40°F.**

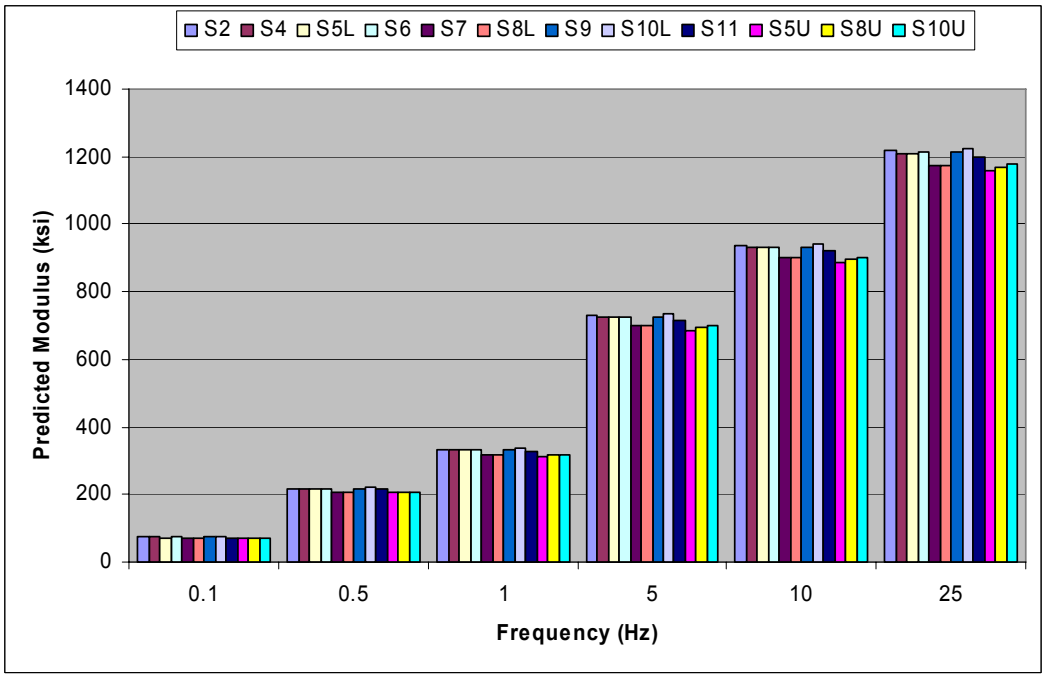


**Figure E.16: Predicted Modulus Using Hirsch Model for US-54 at 70°F.**

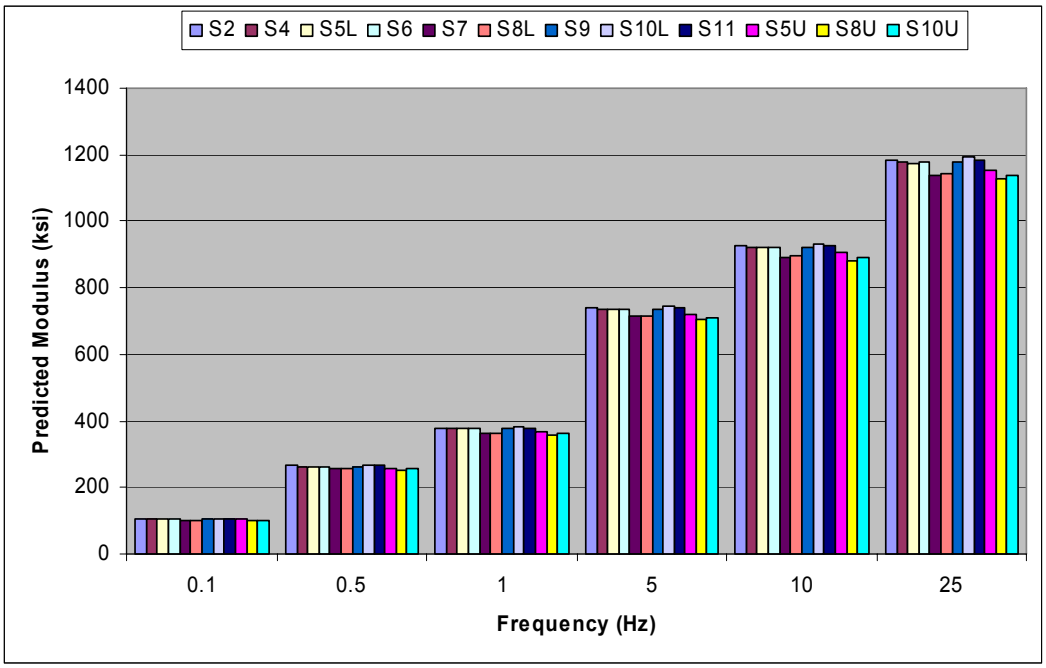


**Figure E.17: Predicted Modulus Using New Model for US-54 at 70°F.**

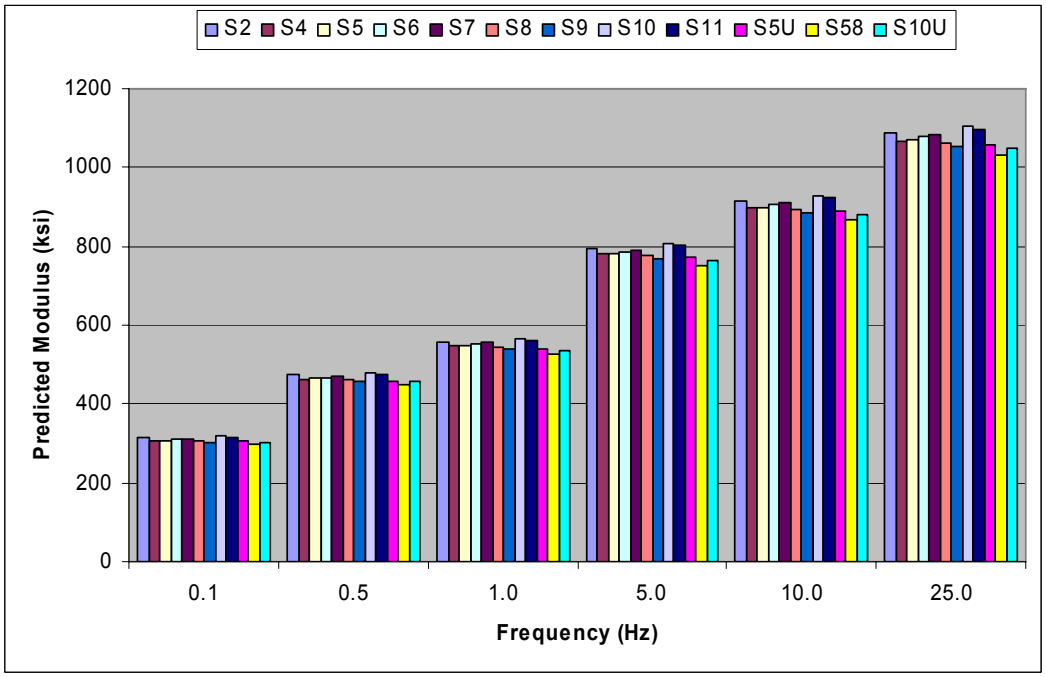


**Figure E.18: Predicted Modulus Using Witczak Equation for US-54 at 70°F.**

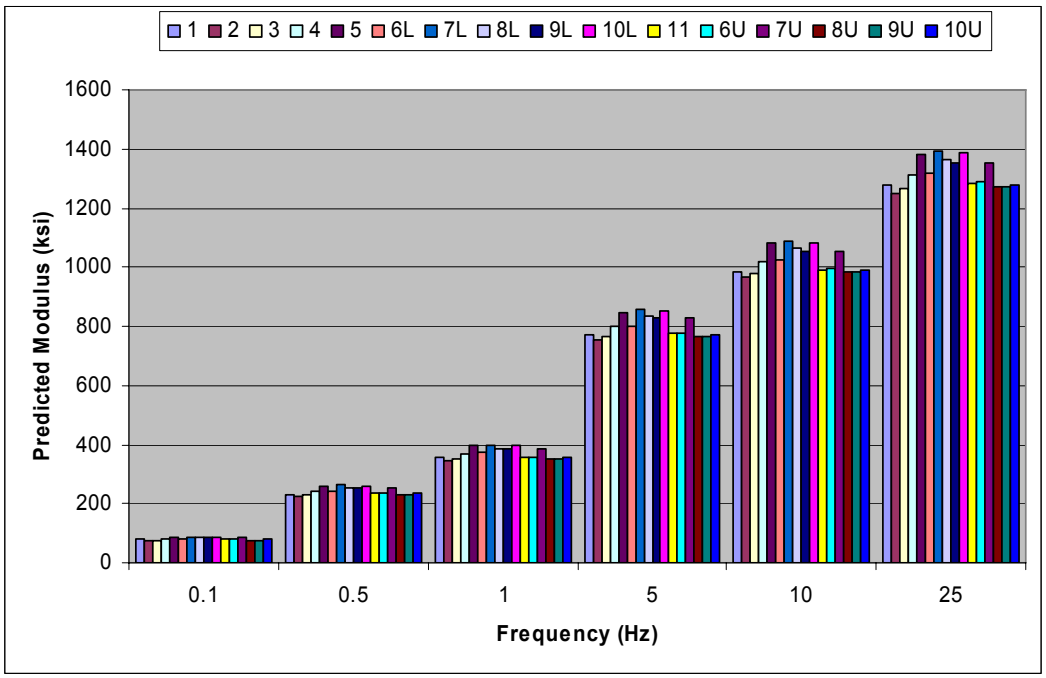


**Figure E.19: Predicted Modulus Using Hirsch Model for US-77 at 70°F.**

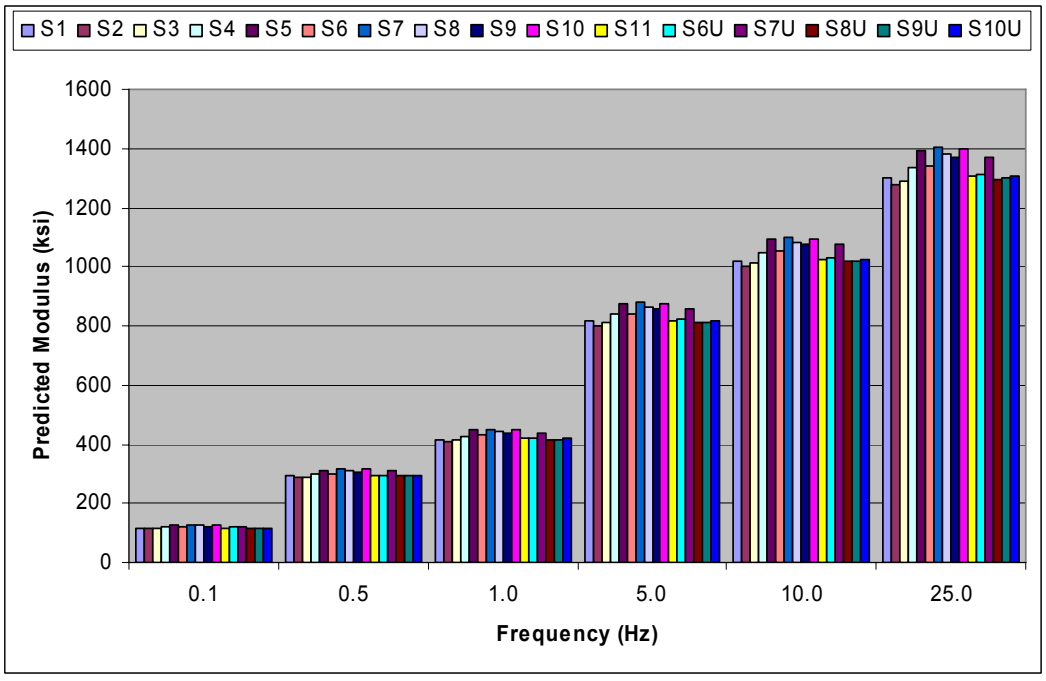


**Figure E.20: Predicted Modulus Using New Model for US-77 at 70°F.**

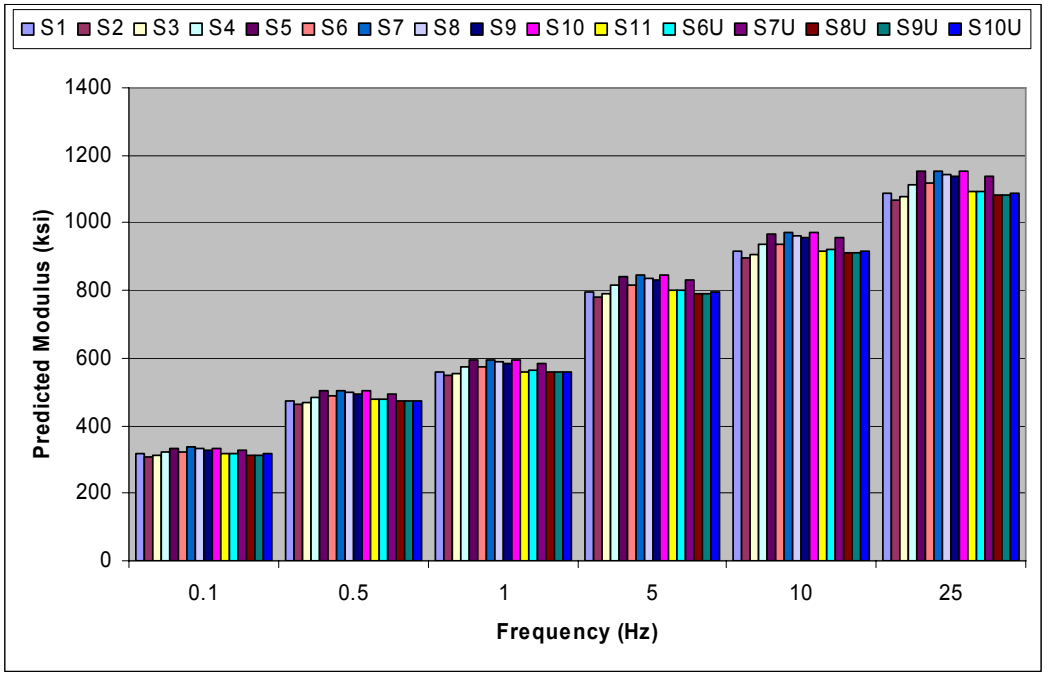


**Figure E.21: Predicted Modulus Using Witczak Equation for US-77 at 70°F.**

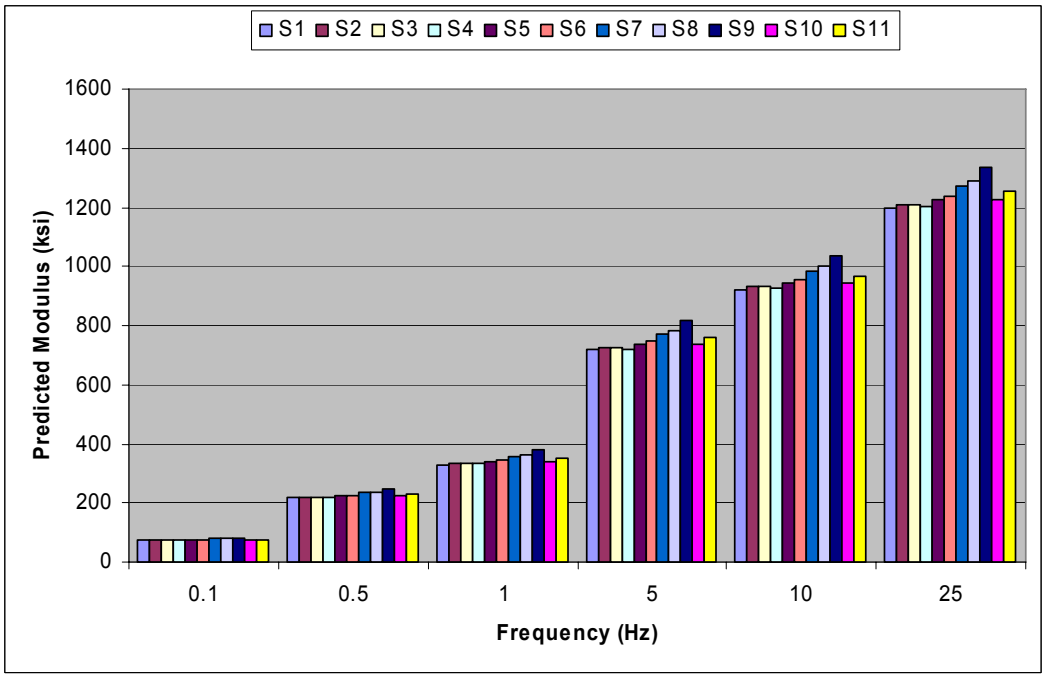


**Figure E.22: Predicted Modulus Using Hirsch Model for US-283 at 70°F.**

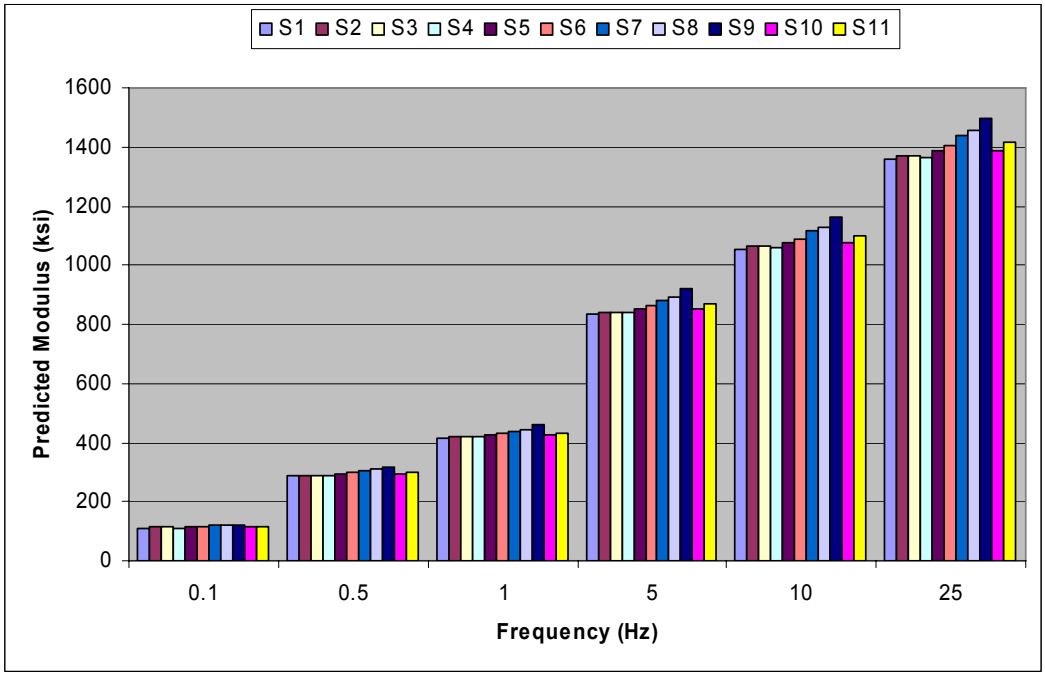


**Figure E.23: Predicted Modulus Using New Model for US-283 at 70°F.**

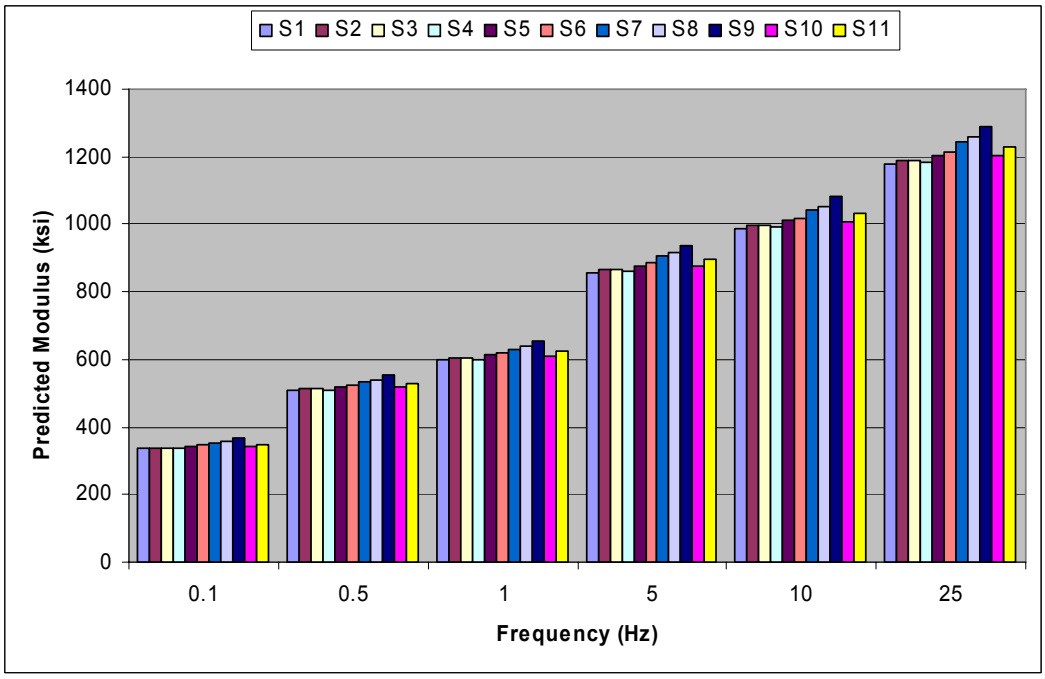


**Figure E.24: Predicted Modulus Using Witczak Equation for US-283 at 70°F.**

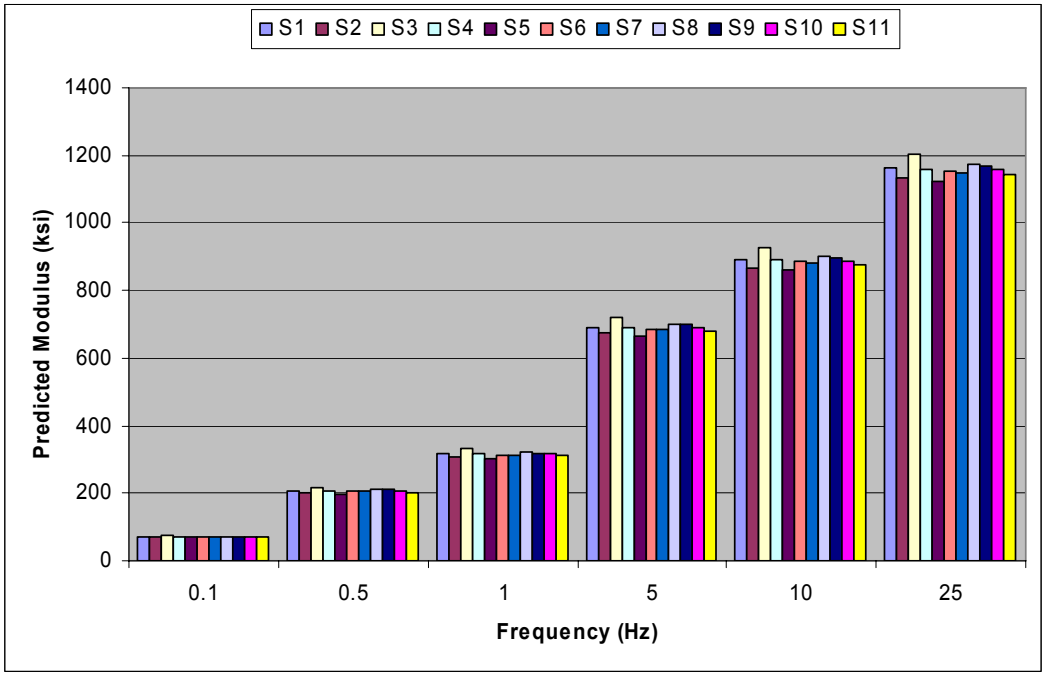


**Figure E.25: Predicted Modulus Using Hirsch Model for K-7 at 70°F.**

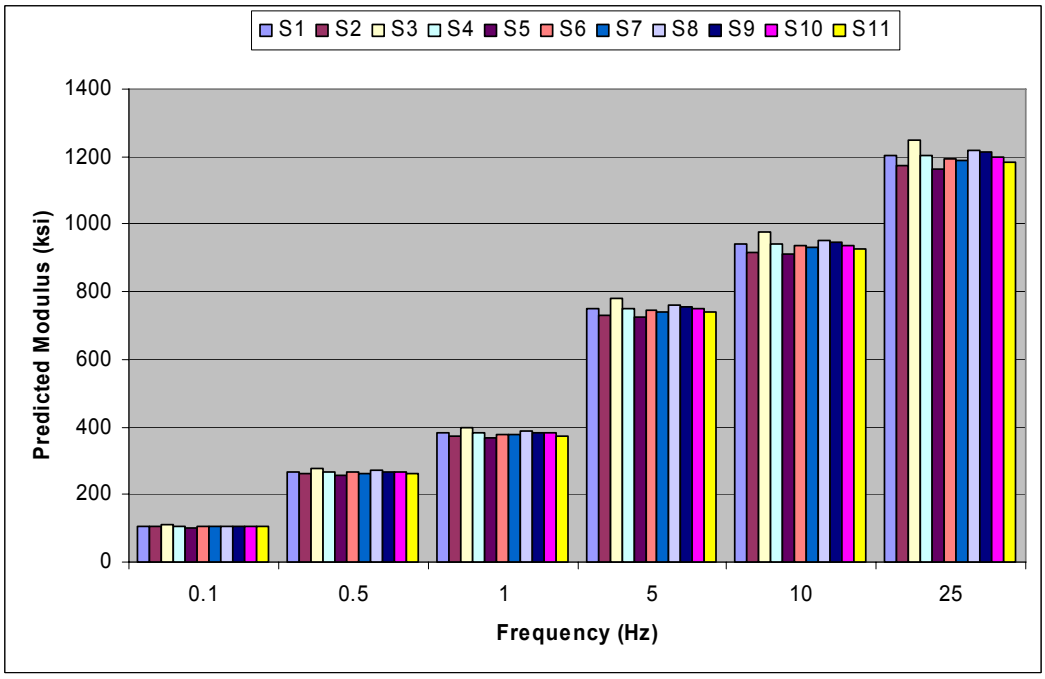


**Figure E.26: Predicted Modulus Using New Model for K-7 at 70°F.**

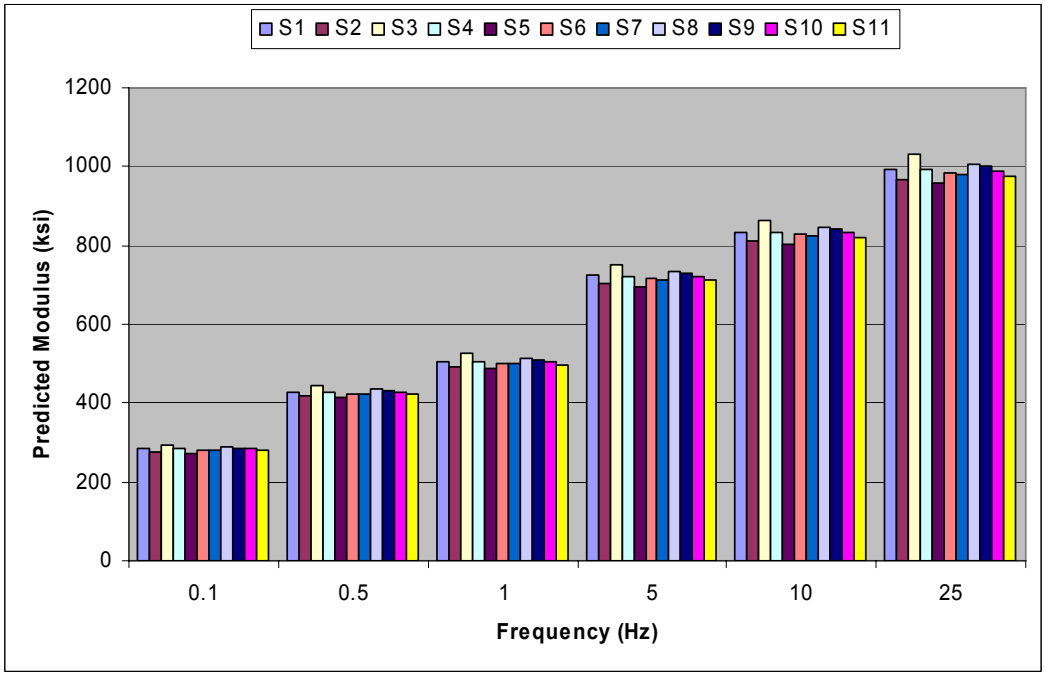


**Figure E.27: Predicted Modulus Using Witczak Equation for K-7 at 70°F.**

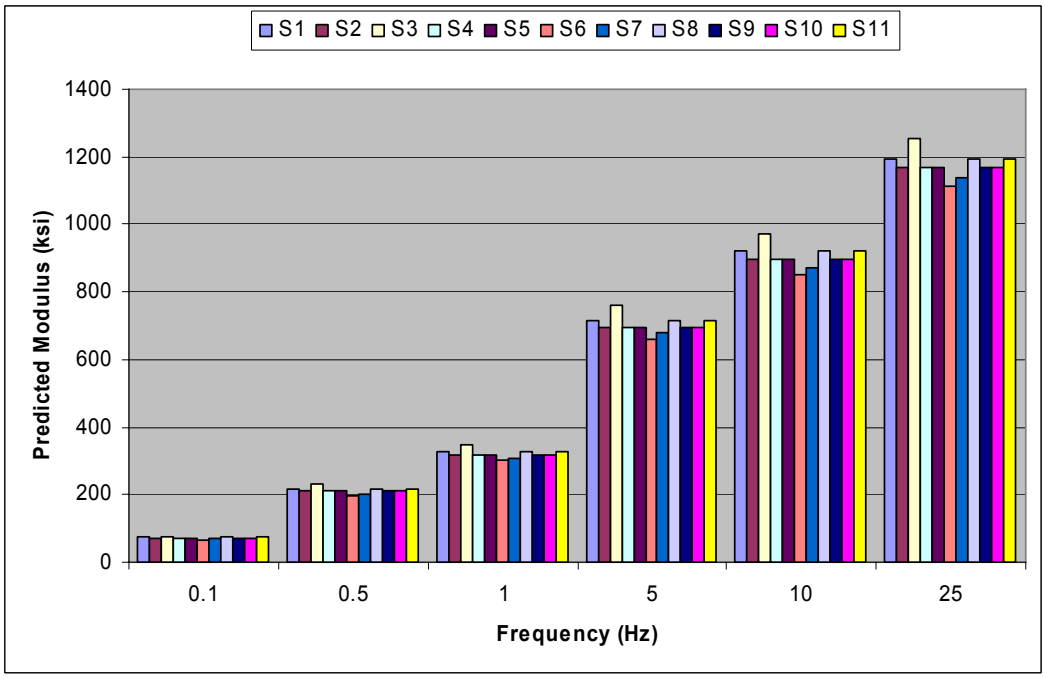


**Figure E.28: Predicted Modulus Using Hirsch Model for K-99 at 70°F.**

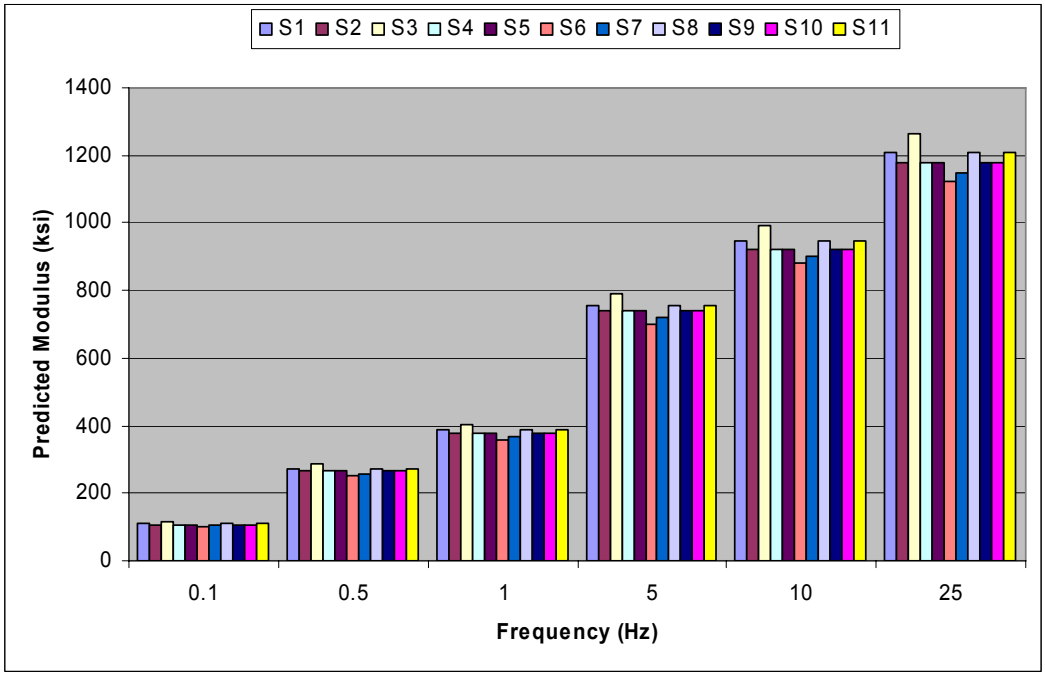


**Figure E.29: Predicted Modulus Using New Model for K-99 at 70°F.**

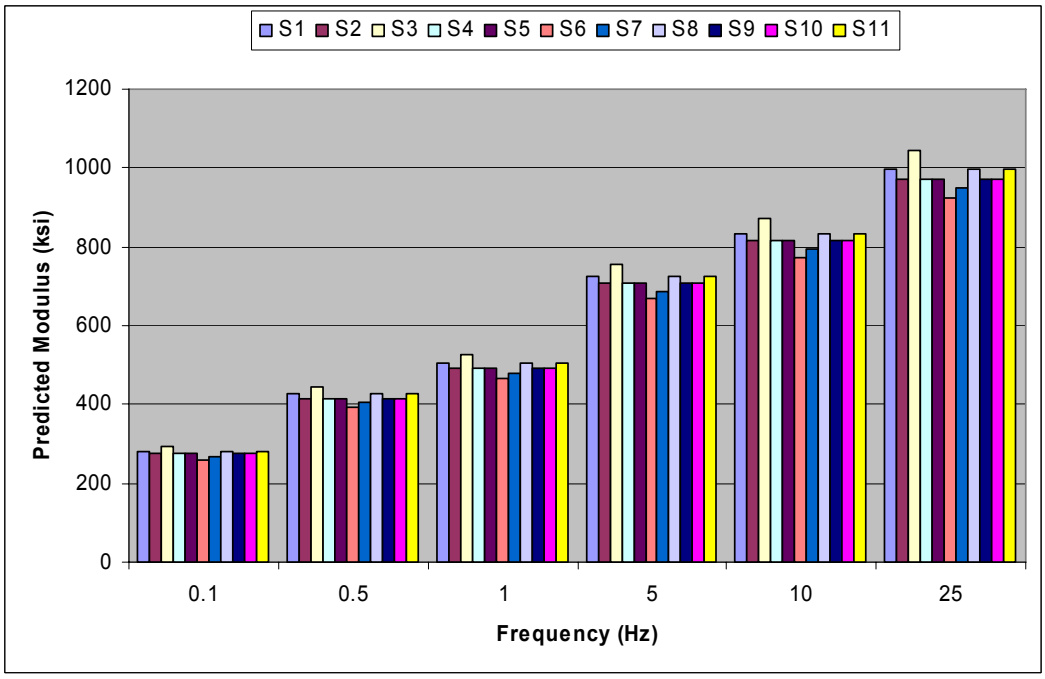


**Figure E.30: Predicted Modulus Using Witczak Equation for K-99 at 70°F.**

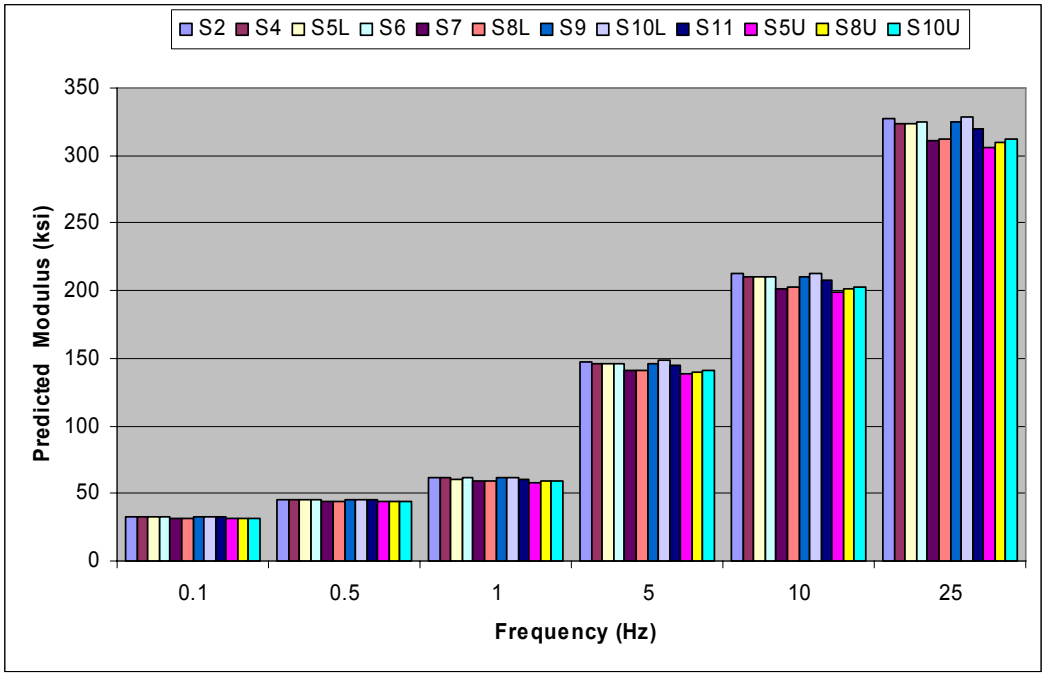


**Figure E.31: Predicted Modulus Using Hirsch Model for US-54 at 95°F.**

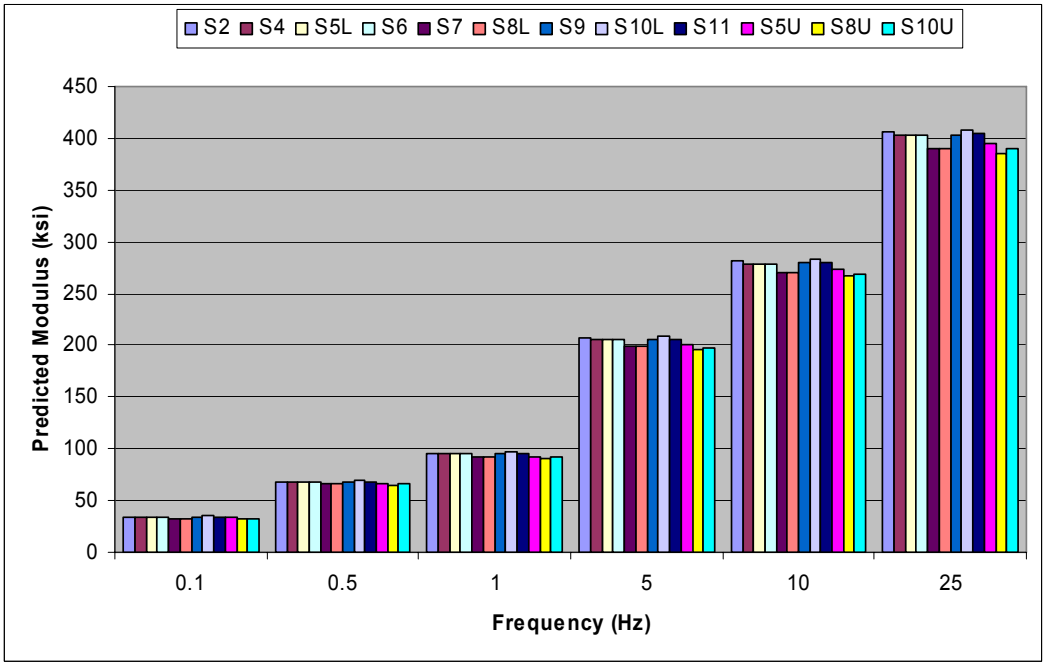


**Figure E.32: Predicted Modulus Using New Model for US-54 at 95°F.**

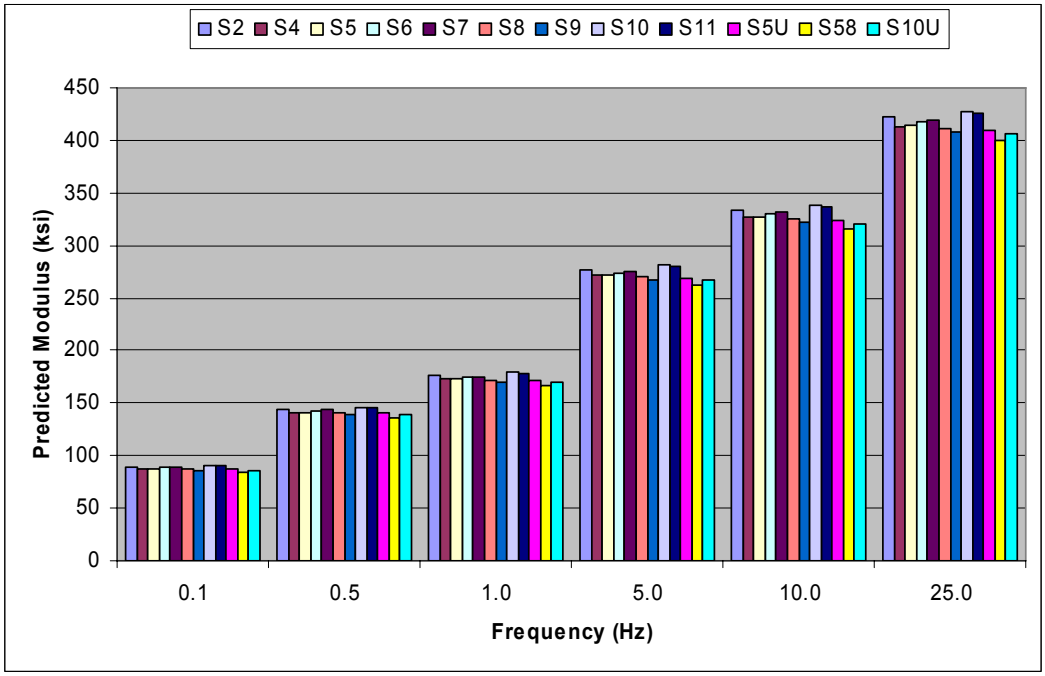


**Figure E.33: Predicted Modulus Using Witczak Equation for US-54 at 95°F.**

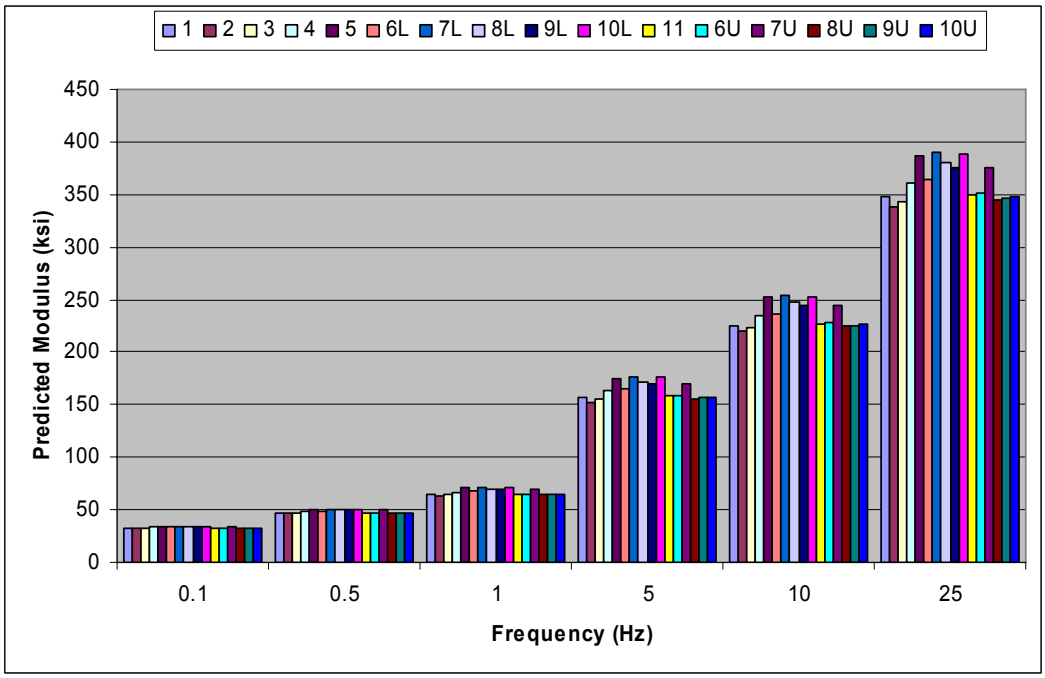


**Figure E.34: Predicted Modulus Using Hirsch Model for US-77 at 95°F.**

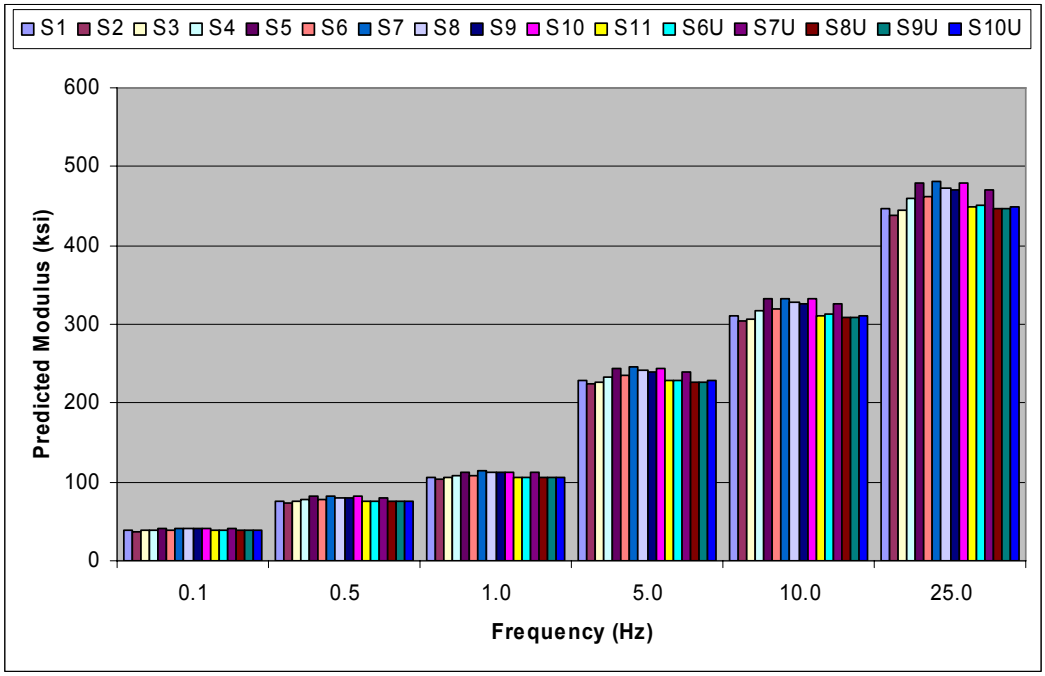


**Figure E.35: Predicted Modulus Using New Model for US-77 at 95°F.**

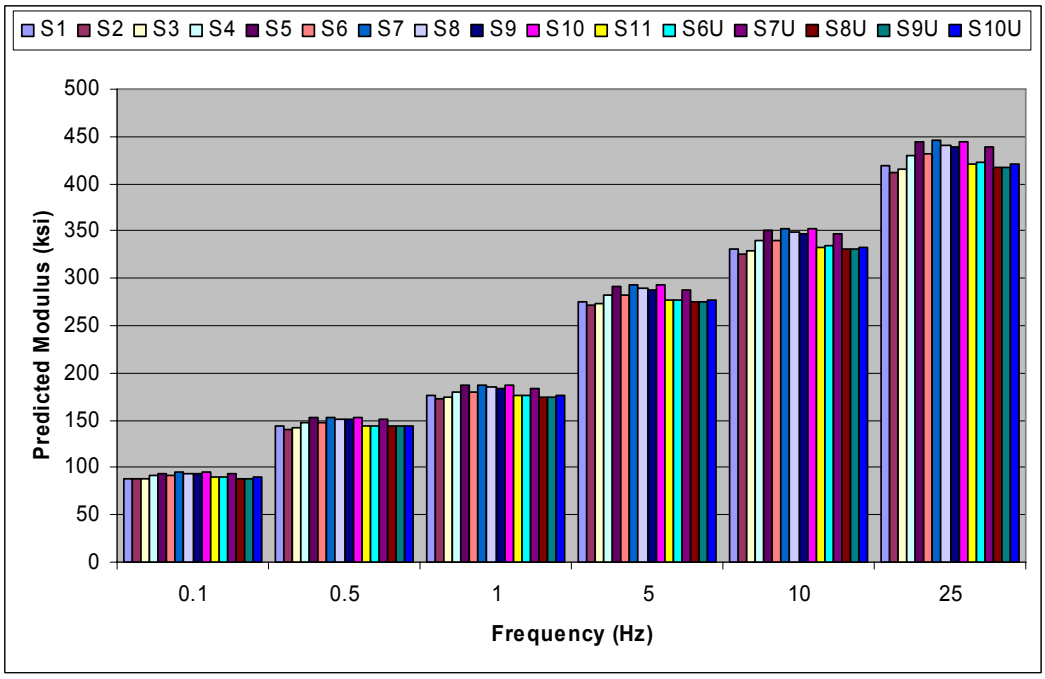


**Figure E.36: Predicted Modulus Using Witczak Equation for US-77 at 95°F.**

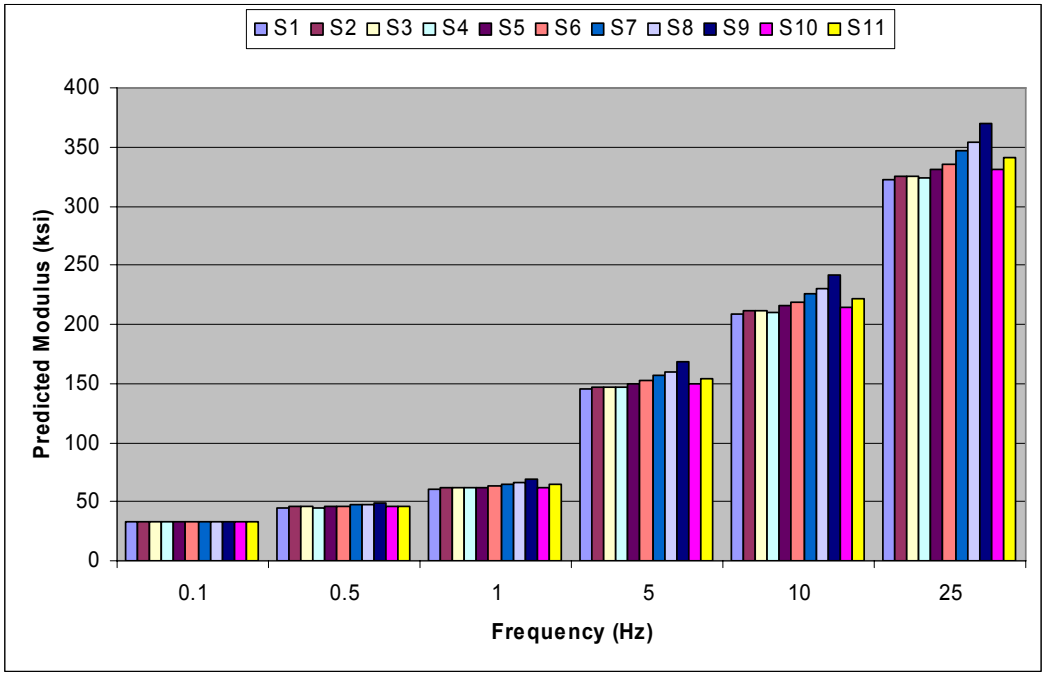


**Figure E.37: Predicted Modulus Using Hirsch Model for US-283 at 95°F.**

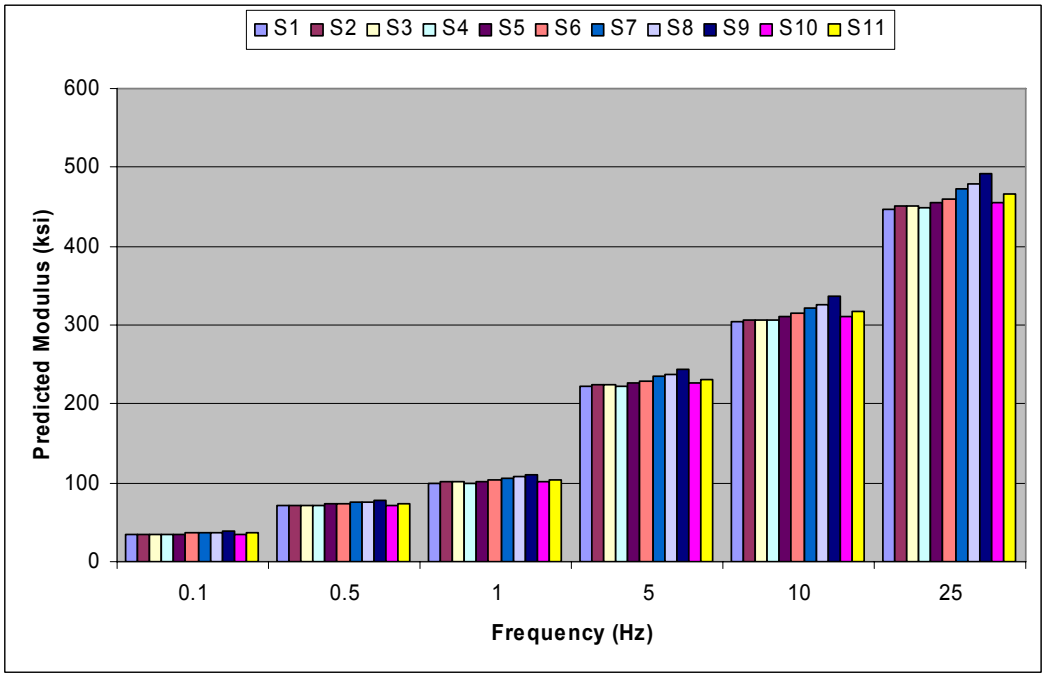


**Figure E.38: Predicted Modulus Using New Model for US-283 at 95°F.**

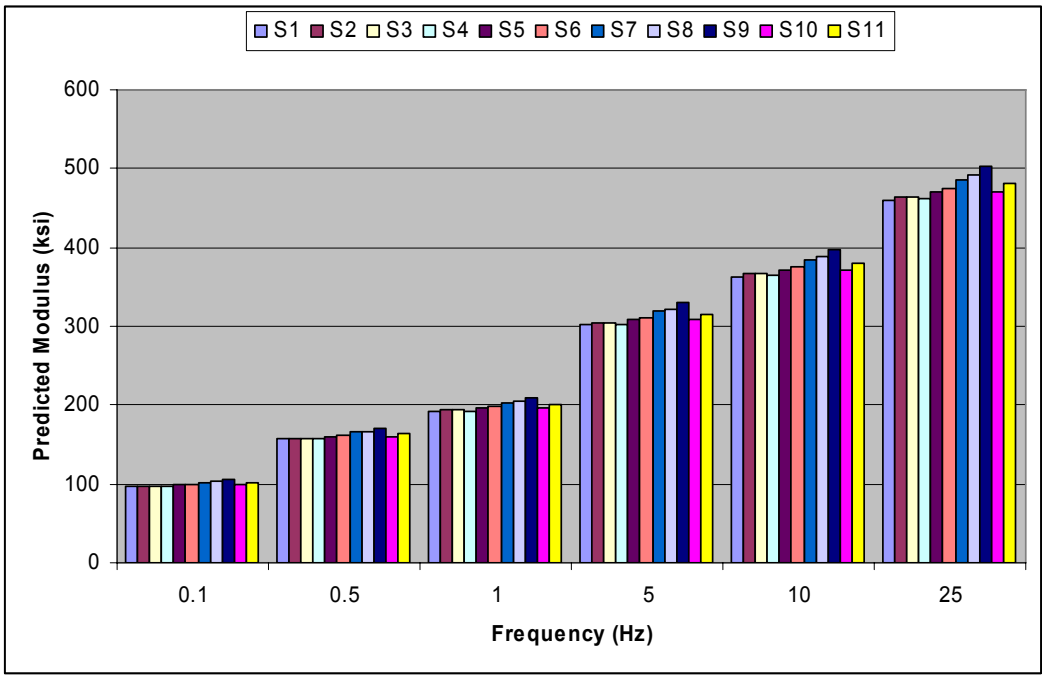


**Figure E.39: Predicted Modulus Using Witczak Equation for US-283 at 95°F.**

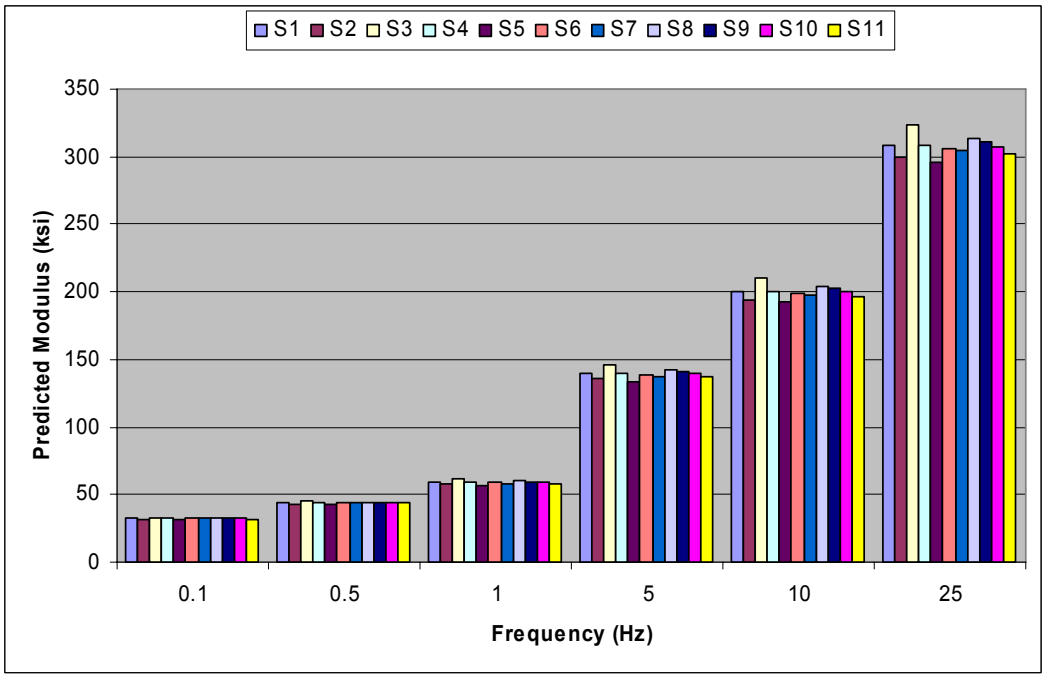


**Figure E.40: Predicted Modulus Using Hirsch Model for K-7 at 95°F.**

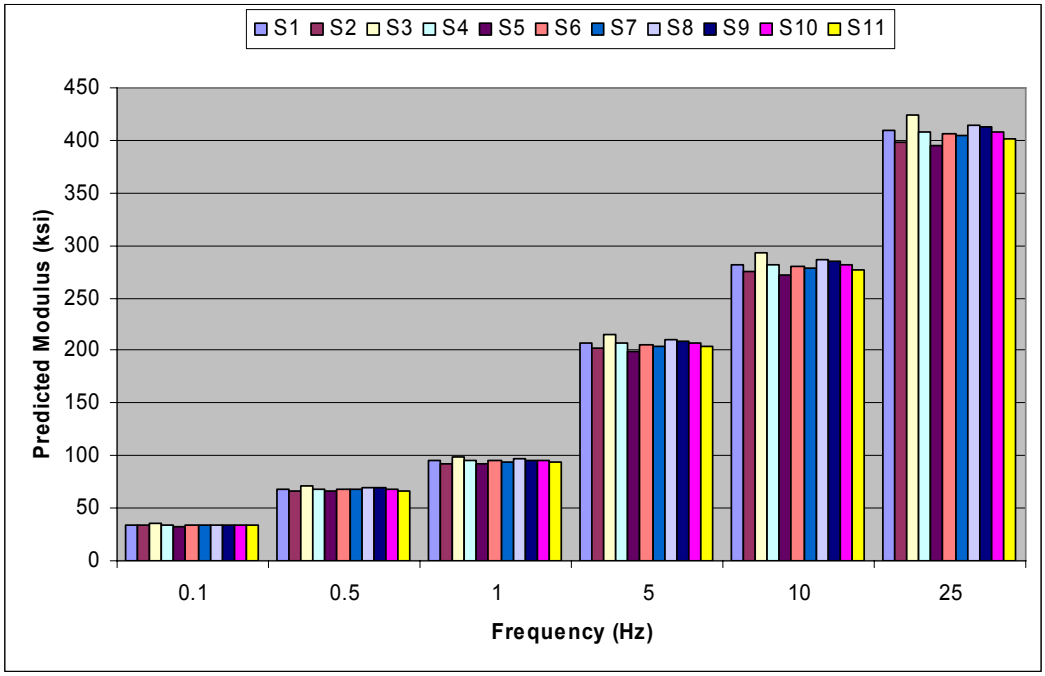


**Figure E.41: Predicted Modulus Using New Model for K-7 at 95°F.**

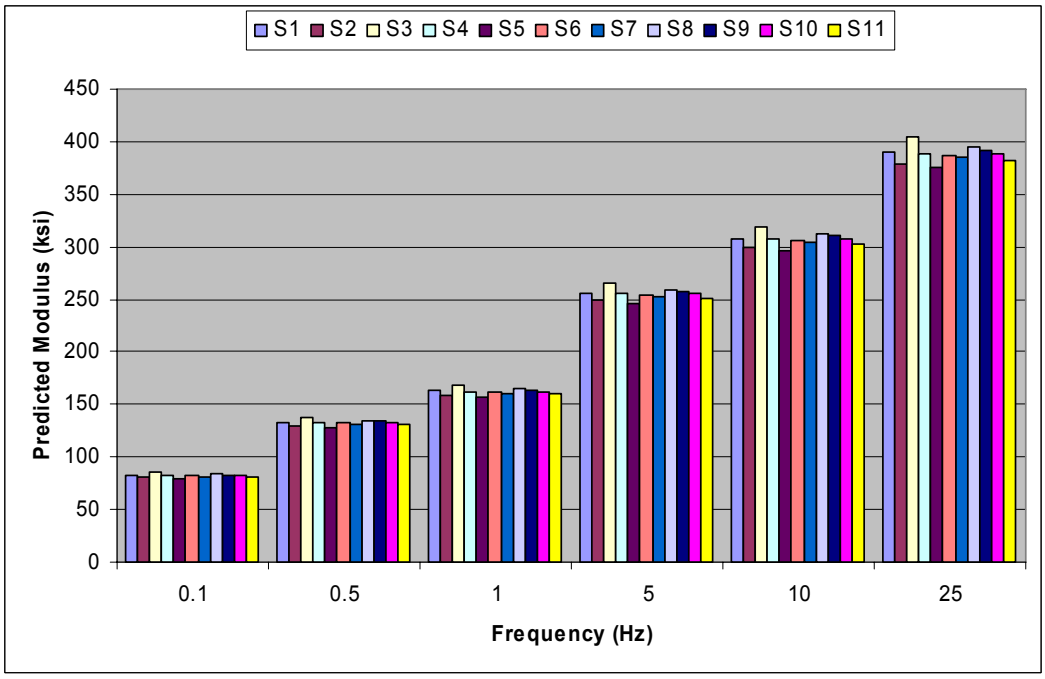


**Figure E.42: Predicted Modulus Using Witczak Equation for K-7 at 95°F.**

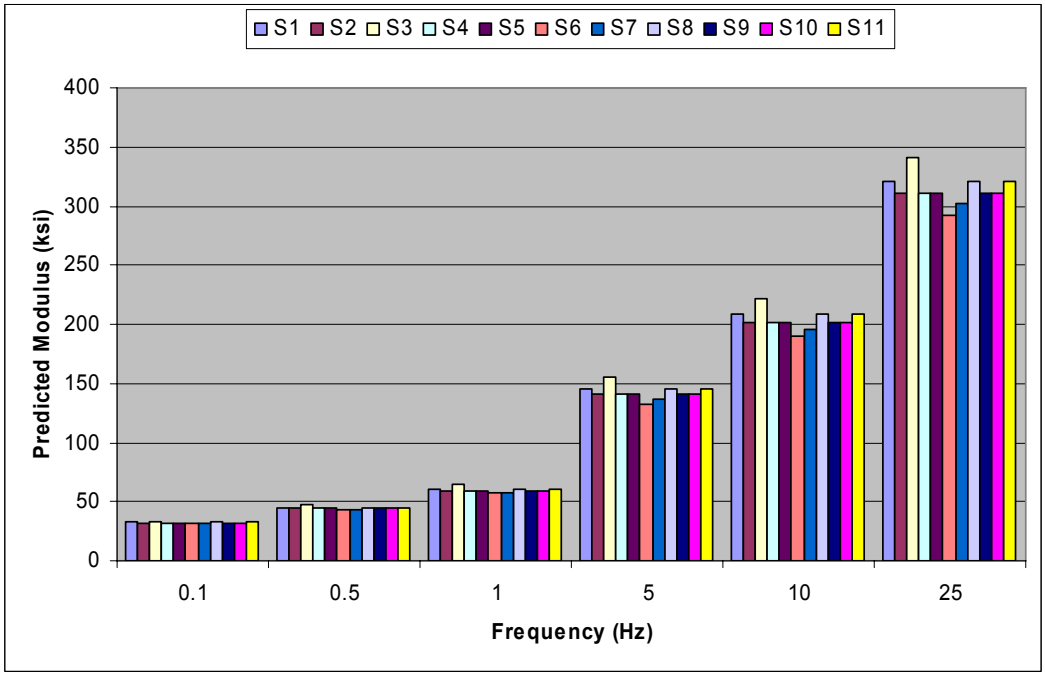


**Figure E.43: Predicted Modulus Using Hirsch Model for K-99 at 95°F.**

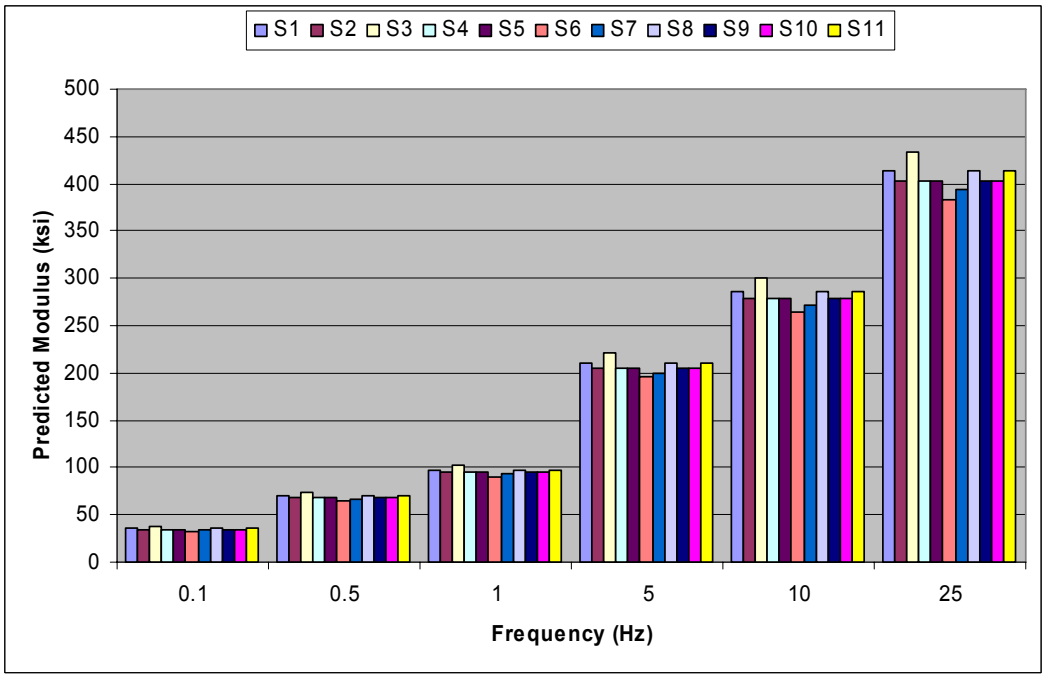


**Figure E.44: Predicted Modulus Using New Model for K-99 at 95°F.**

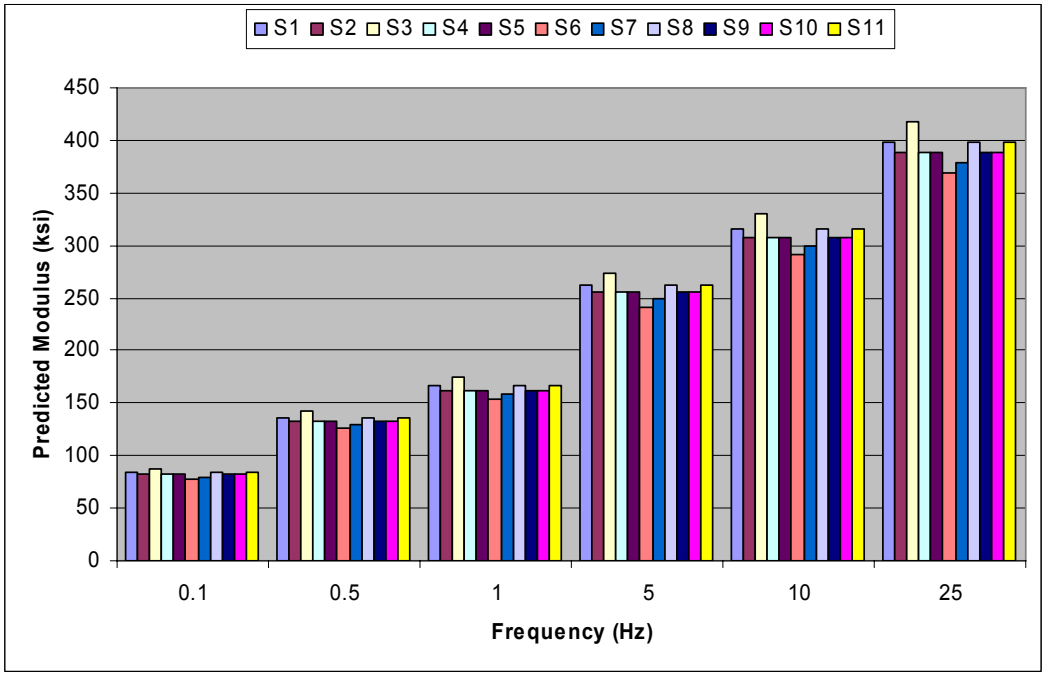


**Figure E.45: Predicted Modulus Using Witczak Equation for K-99 at 95°F.**

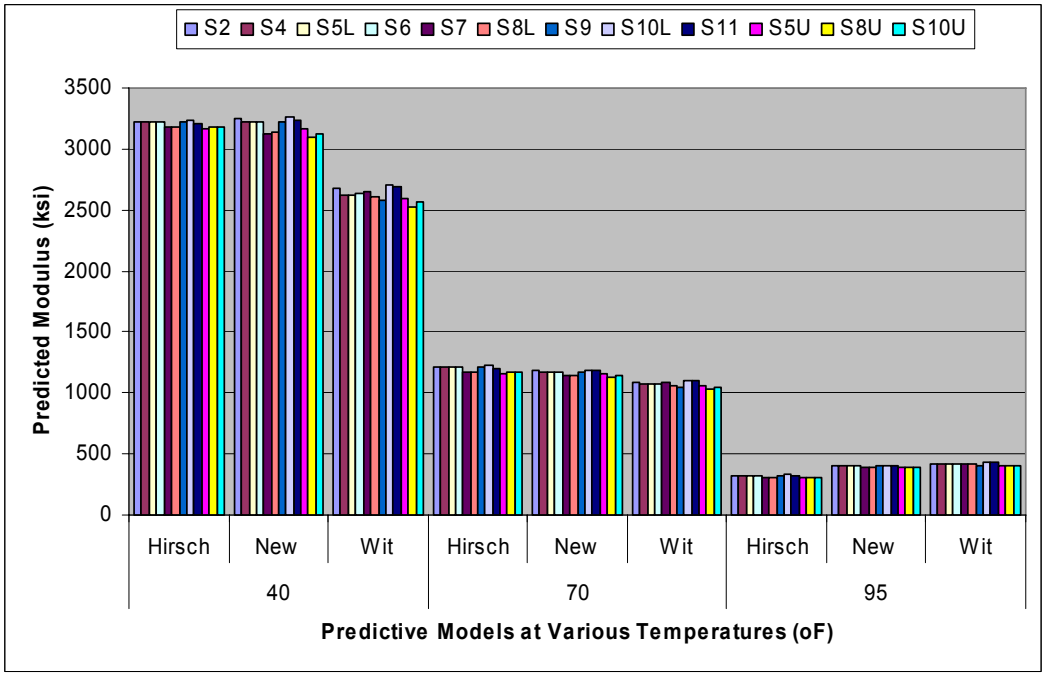


**Figure E.46: Comparison of Predicted Modulus for US-54.**

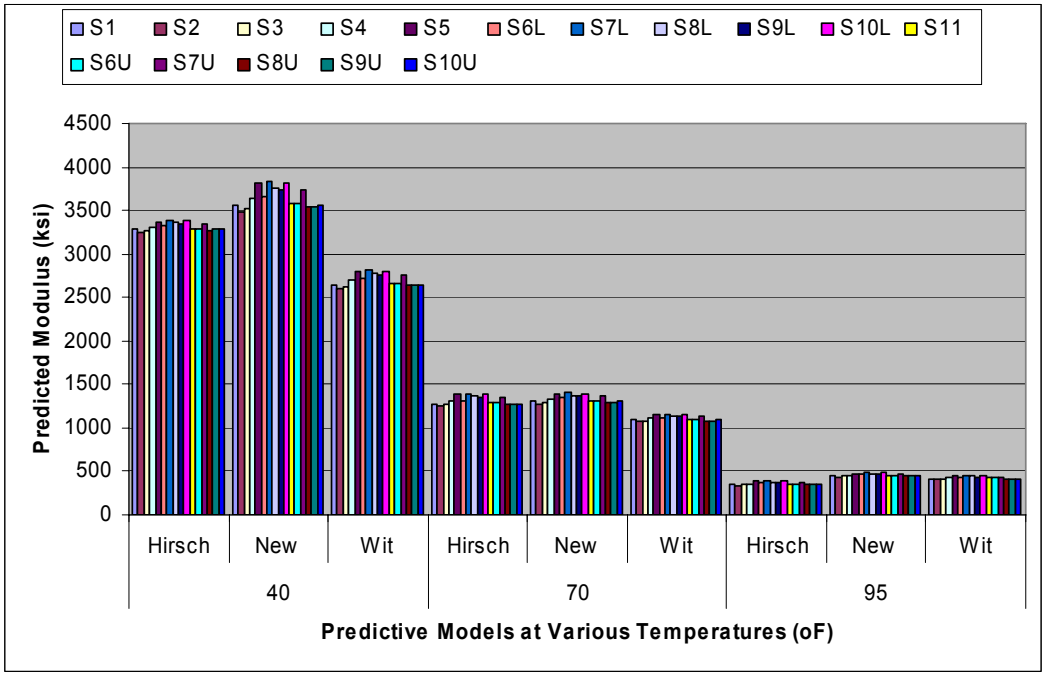


**Figure E.47: Comparison of Predicted Modulus for US-77.**

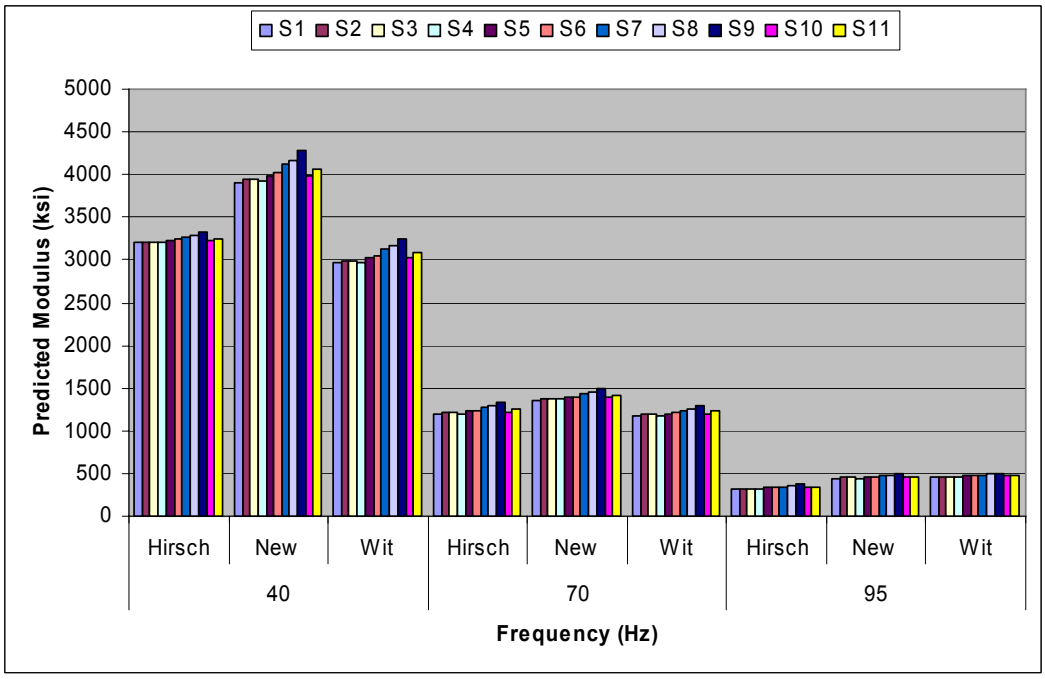


**Figure E.48: Comparison of Predicted Modulus for US-283.**

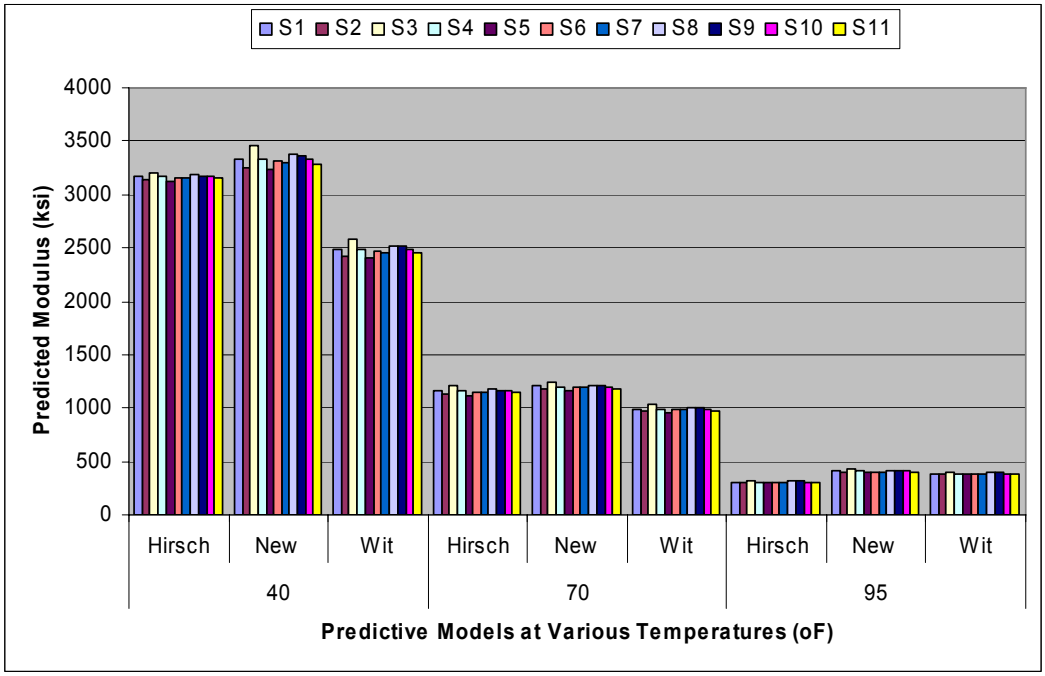


**Figure E.49: Comparison of Predicted Modulus for K-7.**

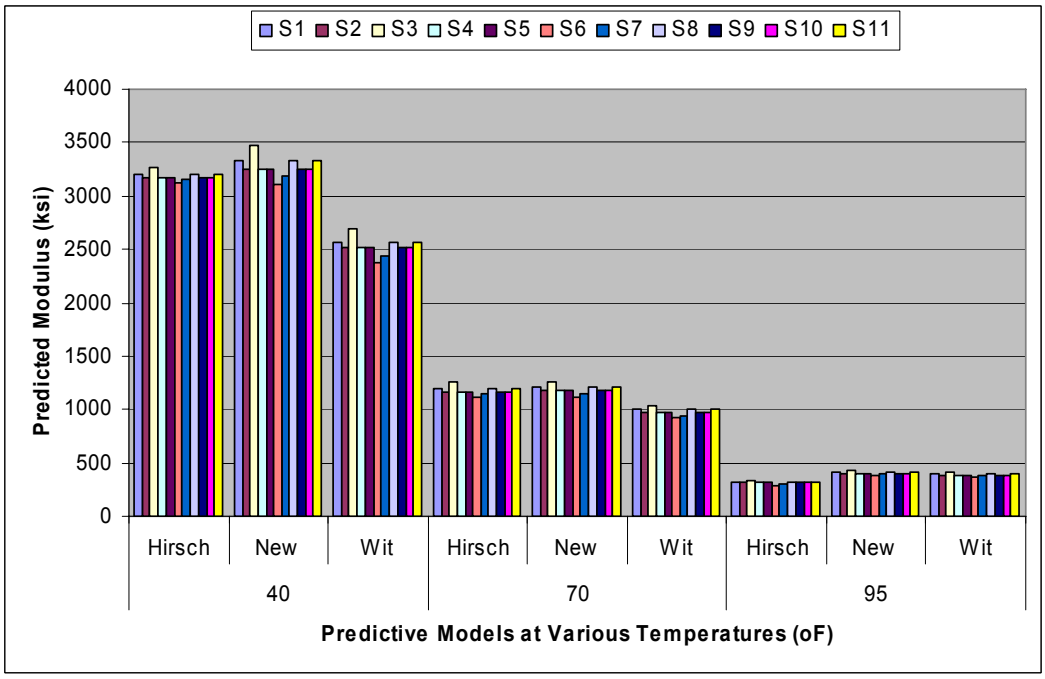


**Figure E.50: Comparison of Predicted Modulus for K-99.**

# APPENDIX F - SENSITIVITY ANALYSIS FOR WITCZAK EQUATION

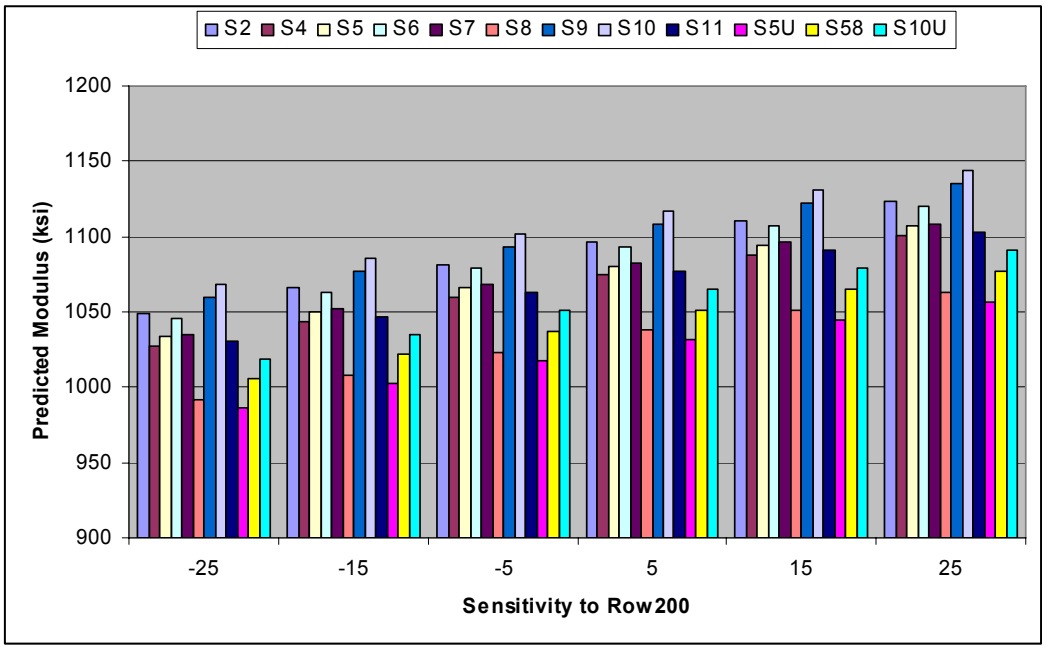


**Figure F.1: Sensitivity to Row200 for US-54 at 70°F.**

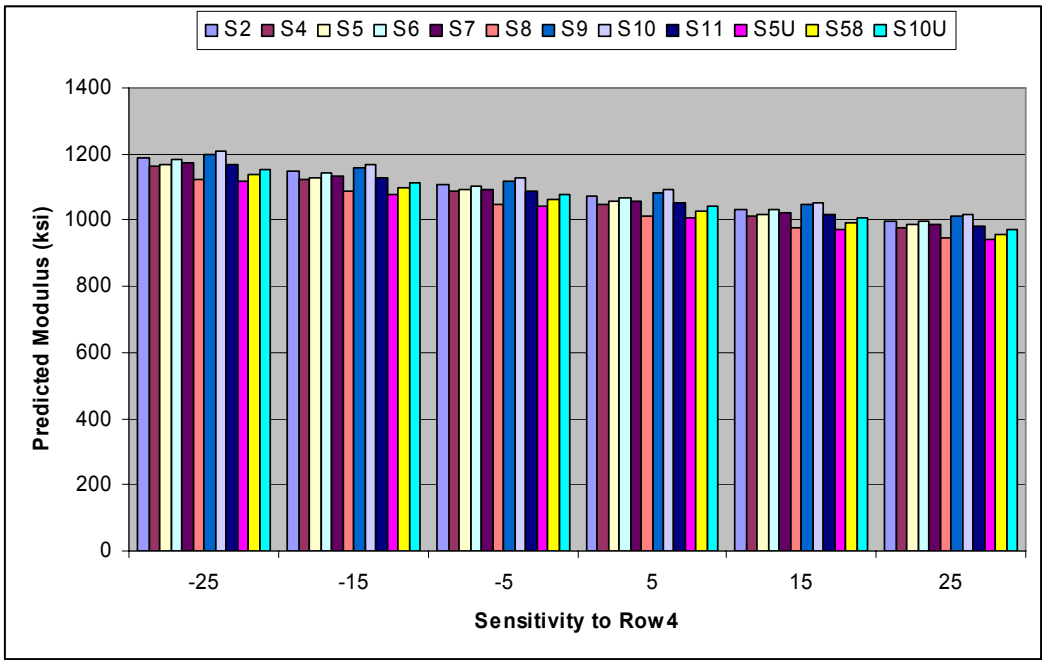


**Figure F.2: Sensitivity to Row4 for US-54 at 70°F.**

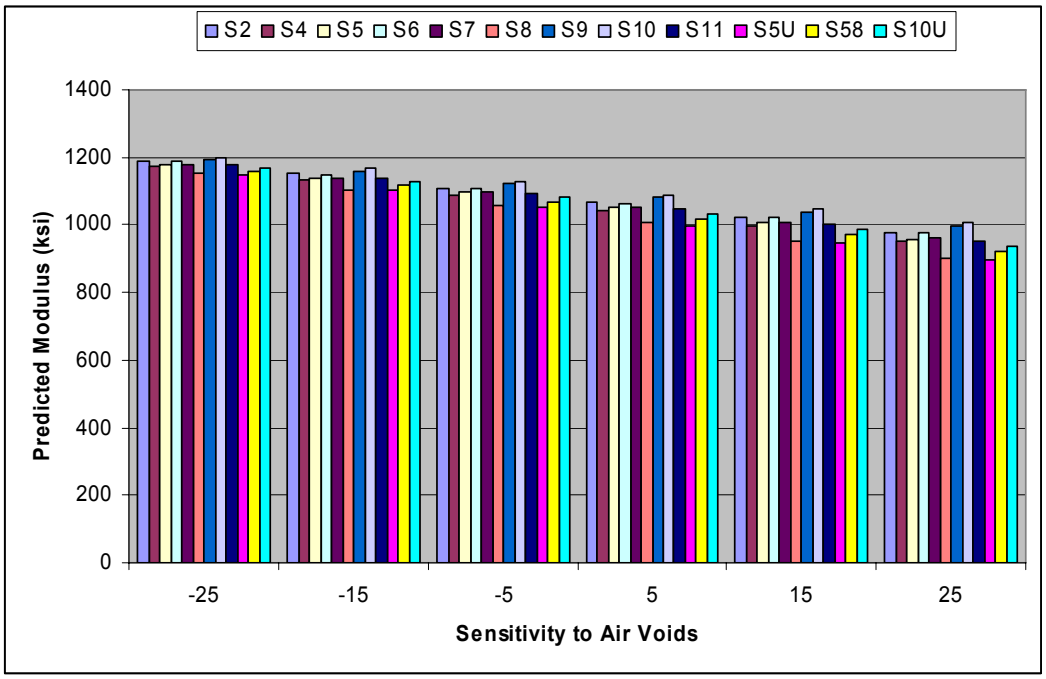


**Figure F.3: Sensitivity to Air Voids for US-54 at 70°F.**

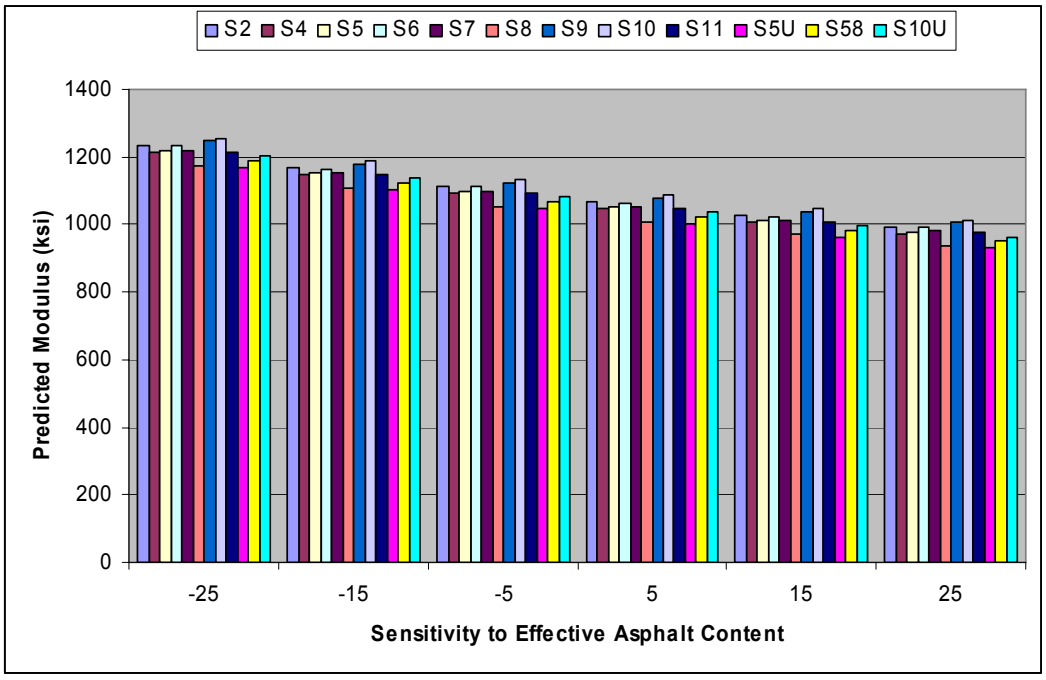


**Figure F.4: Sensitivity to Effective Asphalt Content for US-54 at 70°F.**

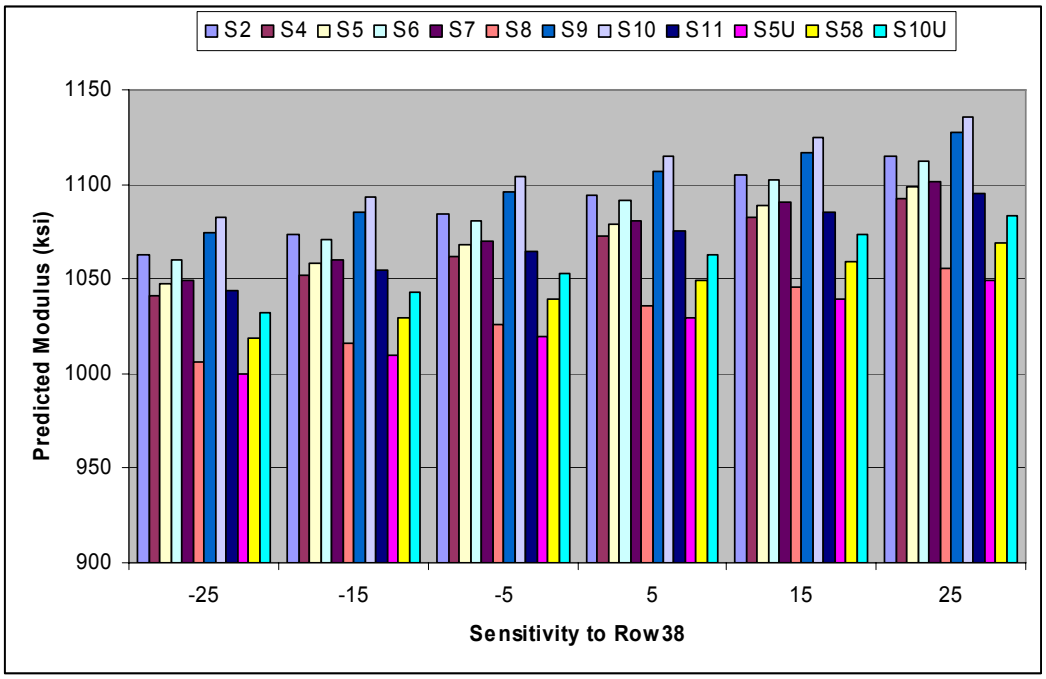


**Figure F.5: Sensitivity to Row38 for US-54 at 70°F.**

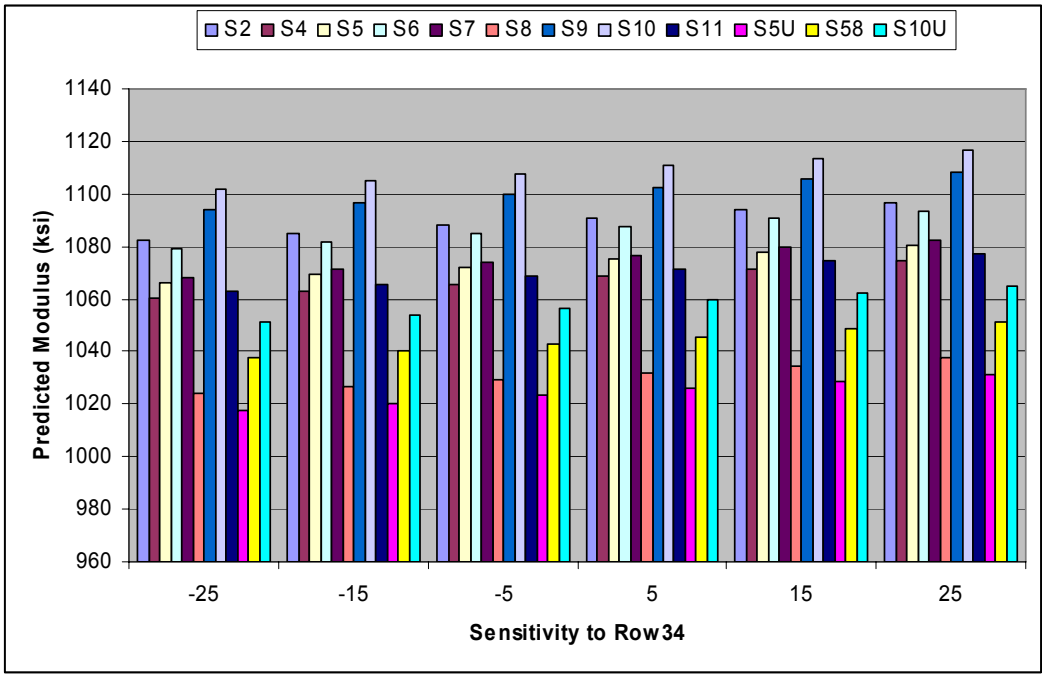


**Figure F.6: Sensitivity to Row34 for US-54 at 70°F.**

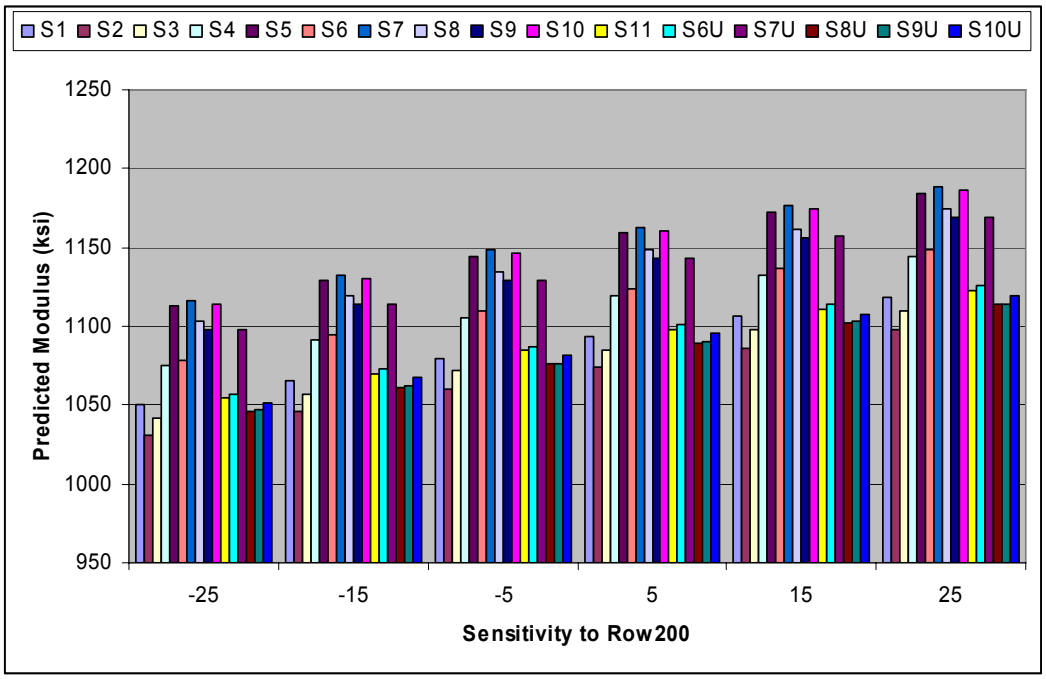


**Figure F.7: Sensitivity to Row200 for US-77 at 70°F.**

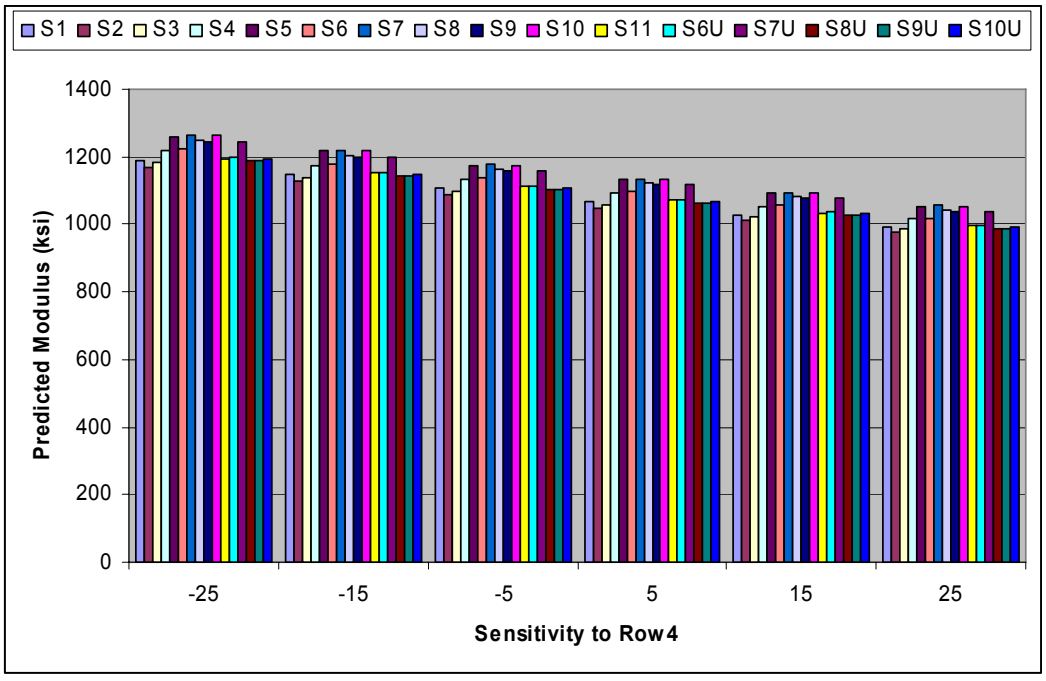


**Figure F.8: Sensitivity to Row4 for US-77 at 70°F.**

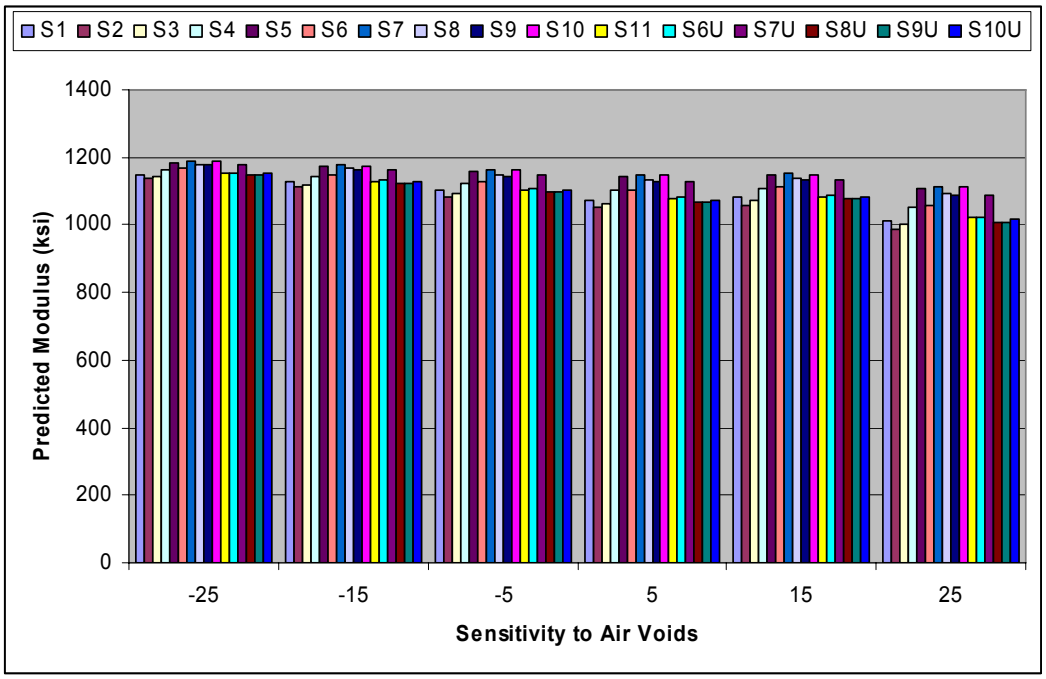


**Figure F.9: Sensitivity to Air Voids for US-77 at 70°F.**

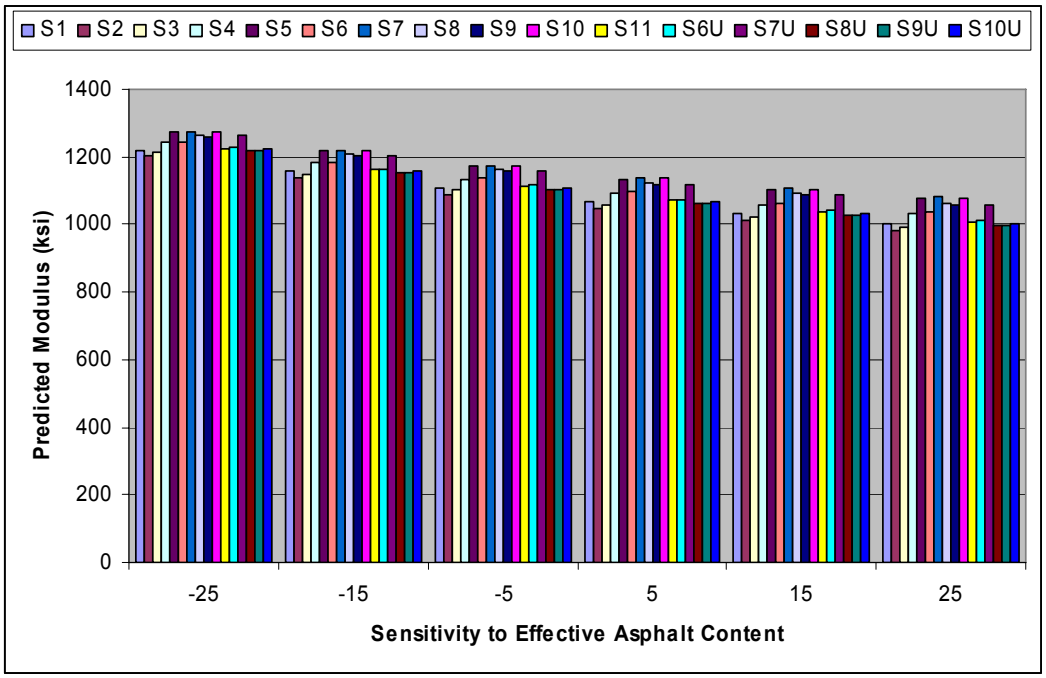


**Figure F.10: Sensitivity to Effective Asphalt Content for US-77 at 70°F.**

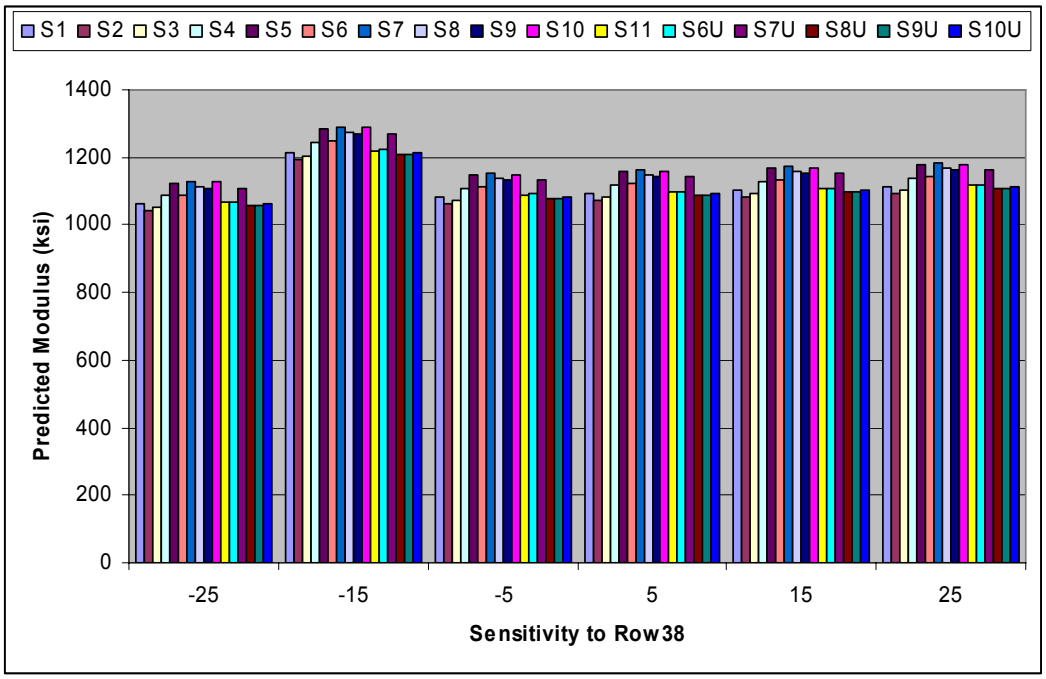


**Figure F.11: Sensitivity to Row38 for US-77 at 70°F.**

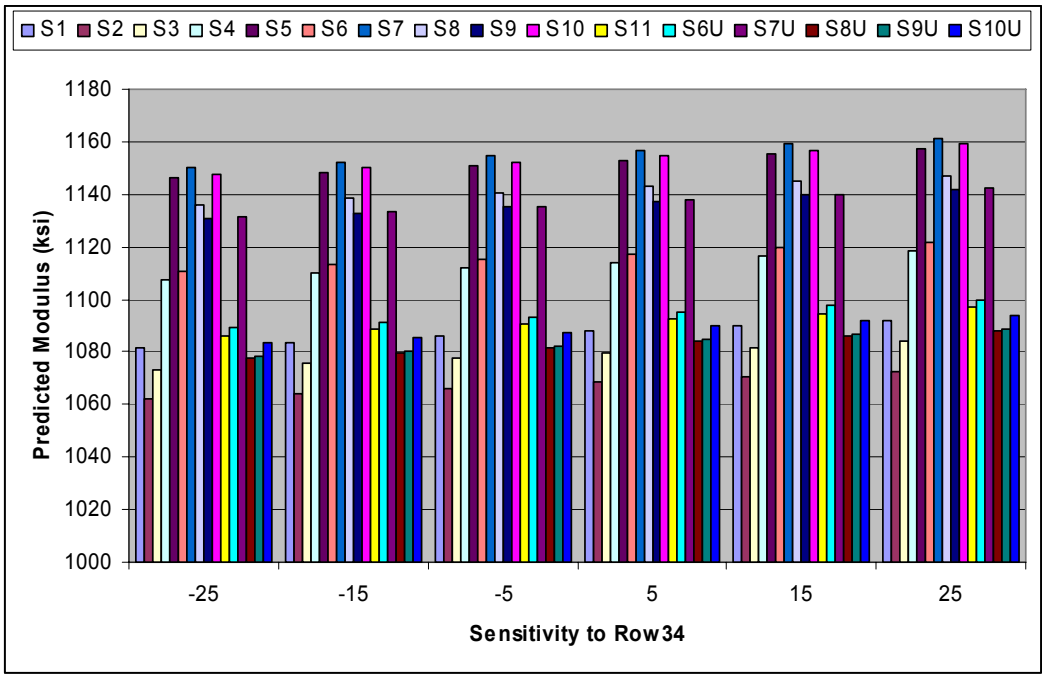


**Figure F.12: Sensitivity to Row34 for US-77 at 70°F.**

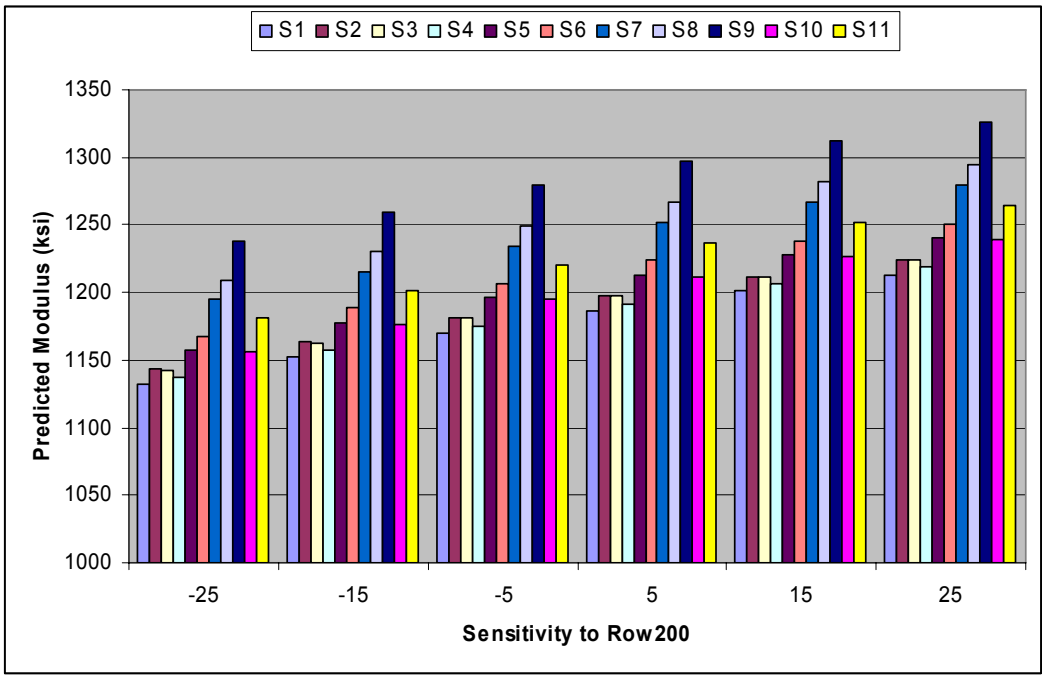


**Figure F.13: Sensitivity to Row200 for US-283 at 70°F.**

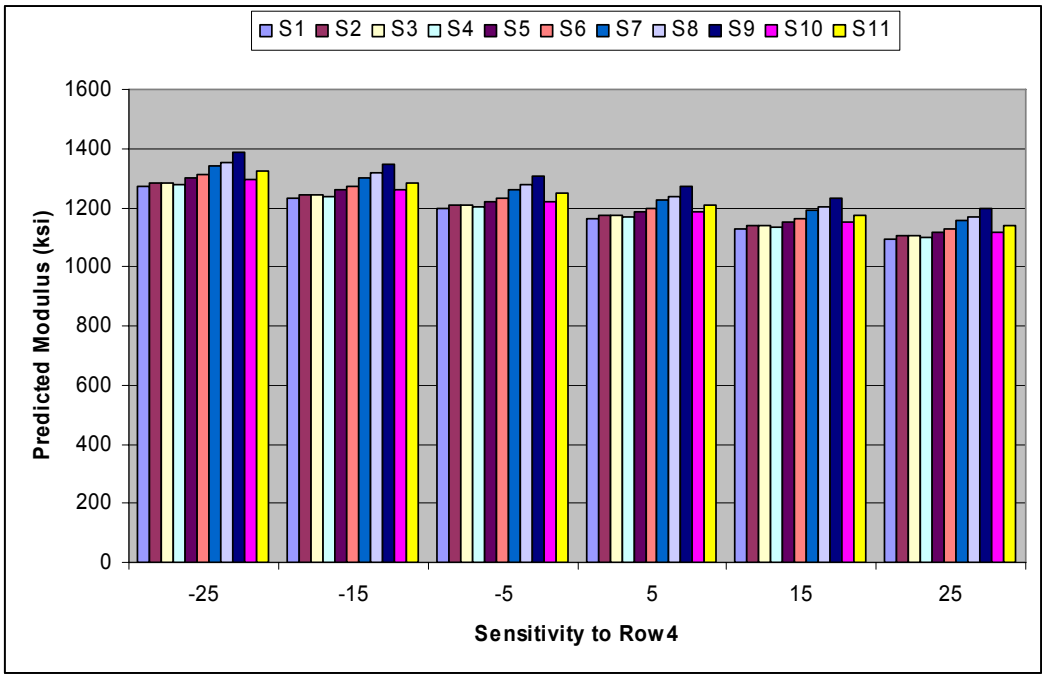


**Figure F.14: Sensitivity to Row4 for US-283 at 70°F.**

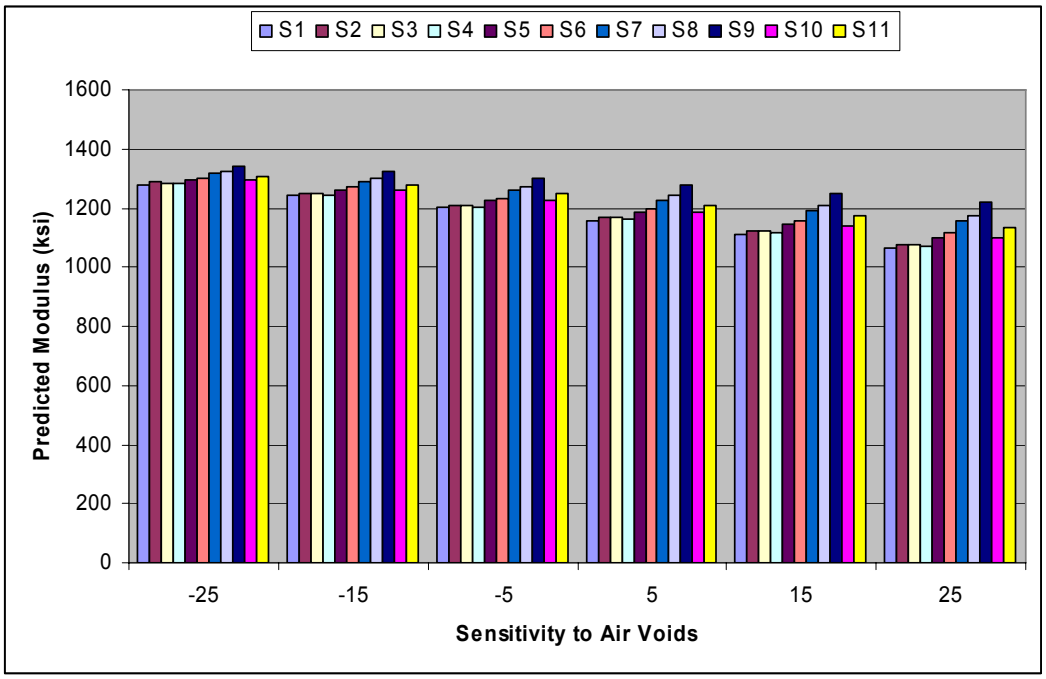


**Figure F.15: Sensitivity to Air Voids for US-283 at 70°F.**

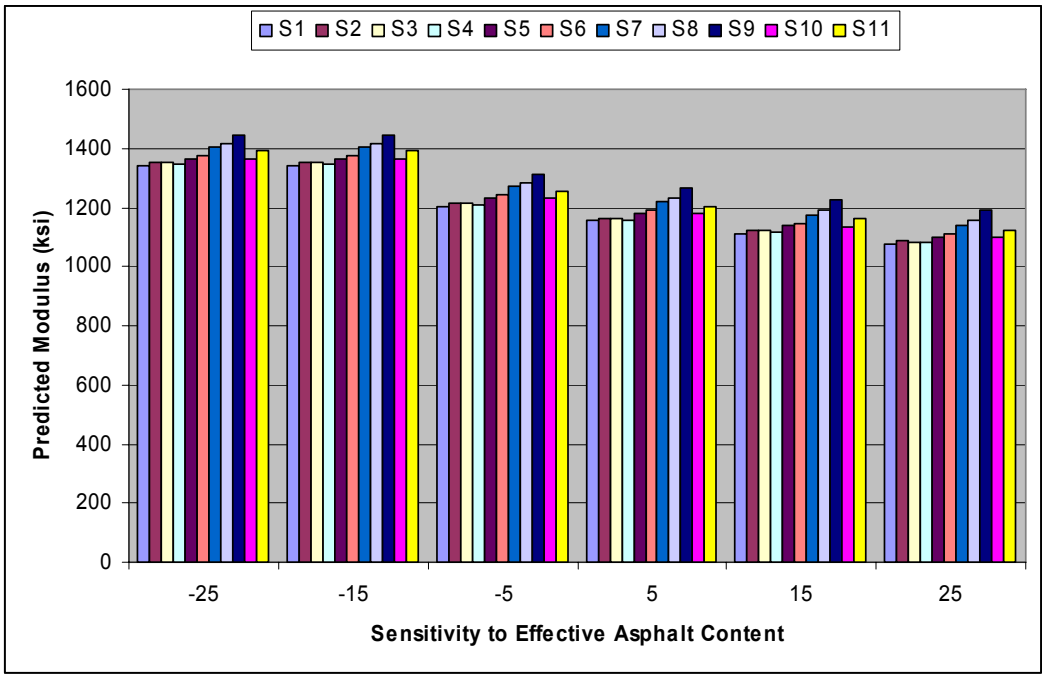


**Figure F.16: Sensitivity to Effective Asphalt Content for US-283 at 70°F.**

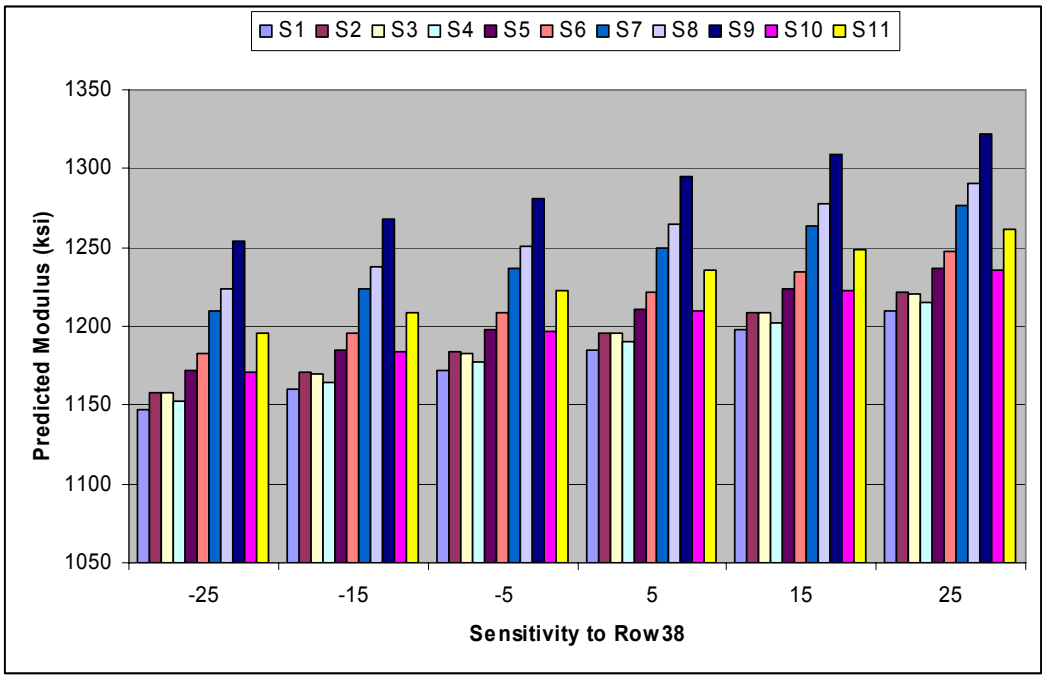


**Figure F.17: Sensitivity to Row38 for US-283 at 70°F.**

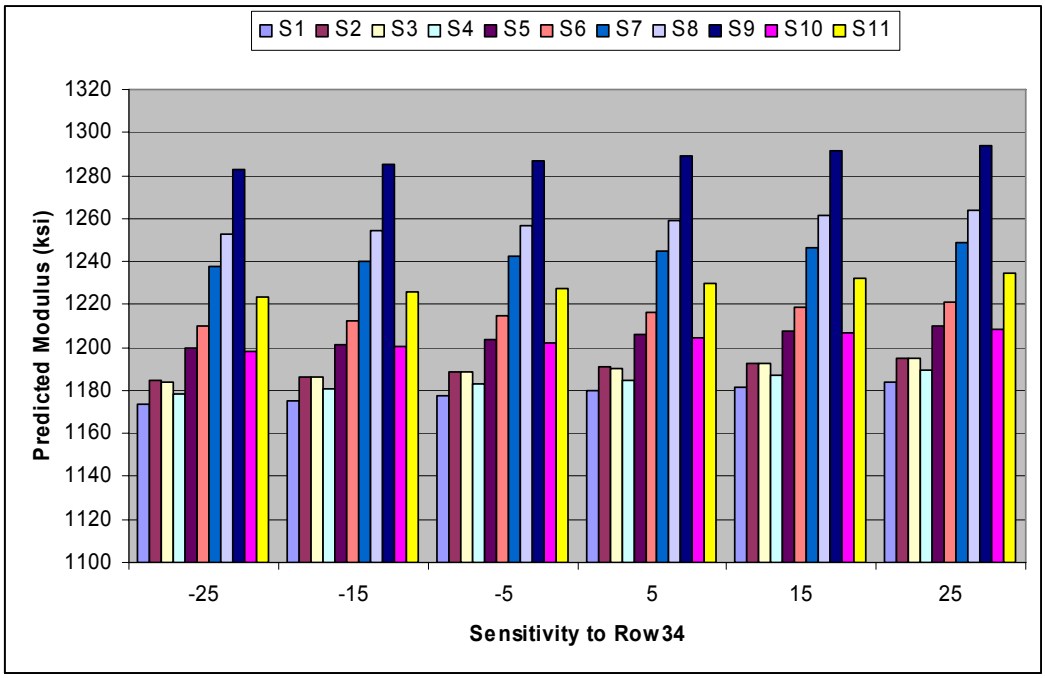


**Figure F.18: Sensitivity to Row34 for US-283 at 70°F.**

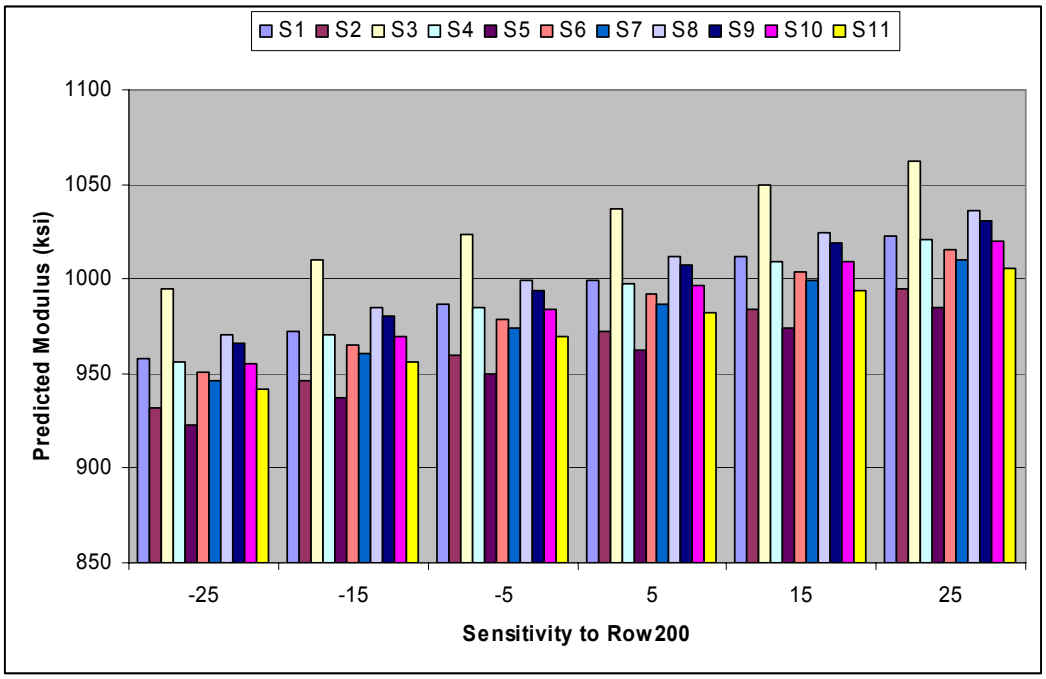


**Figure F.19: Sensitivity to Row200 for K-7 at 70°F.**

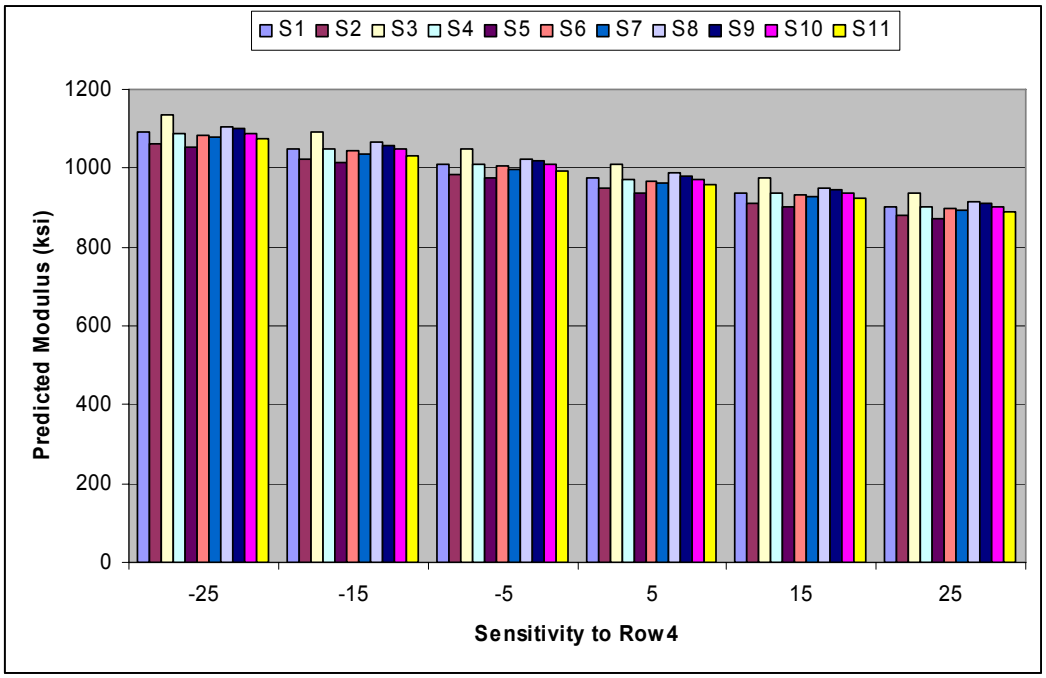


**Figure F.20: Sensitivity to Row4 for K-7 at 70°F.**

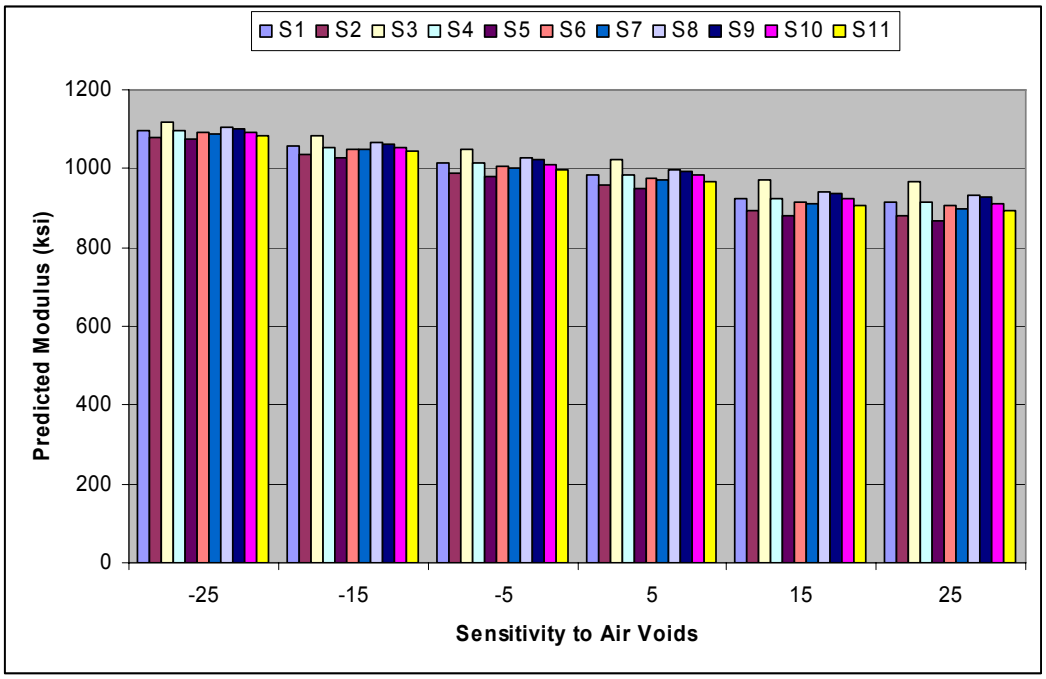


**Figure F.21: Sensitivity to Air Voids for K-7 at 70°F.**

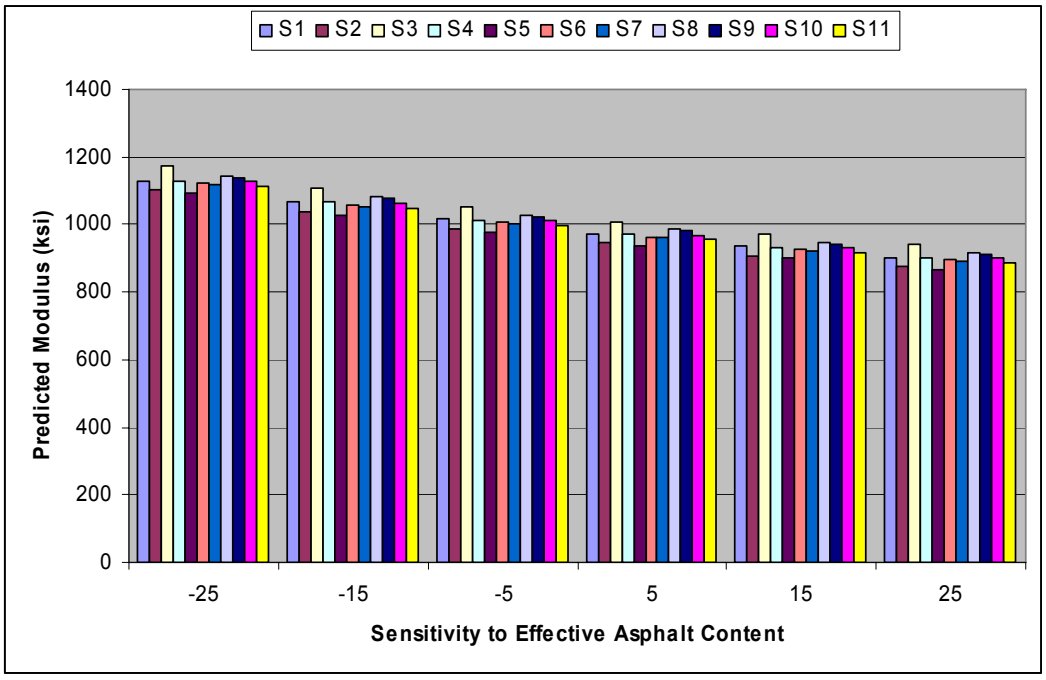


**Figure F.22: Sensitivity to Effective Asphalt Content for K-7 at 70°F.**

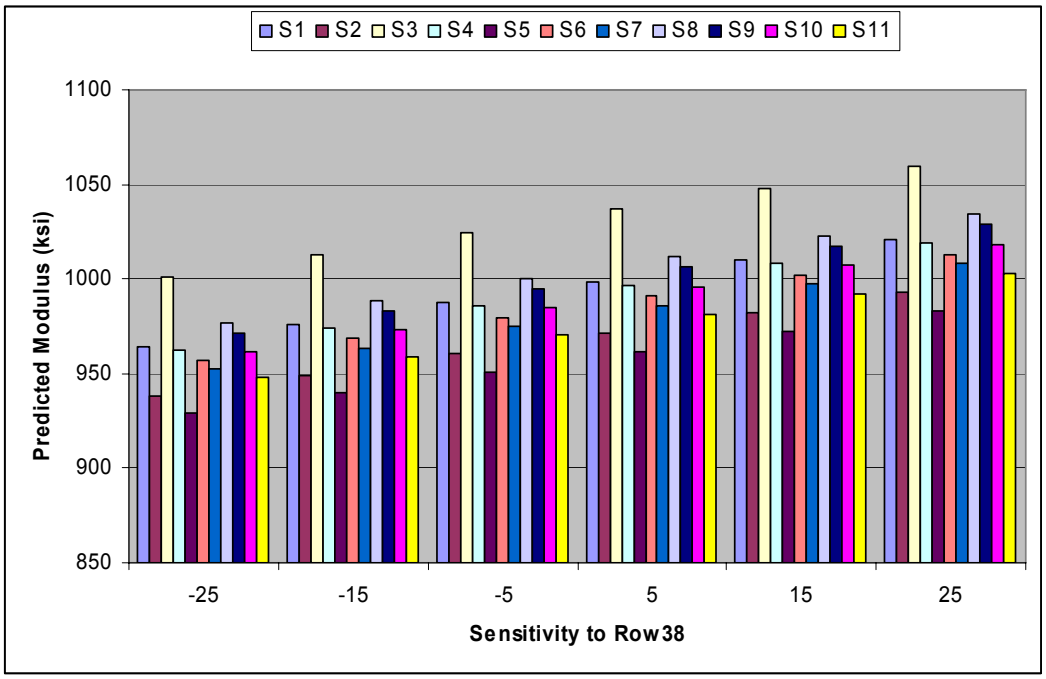


**Figure F.23: Sensitivity to Row38 for K-7 at 70°F.**

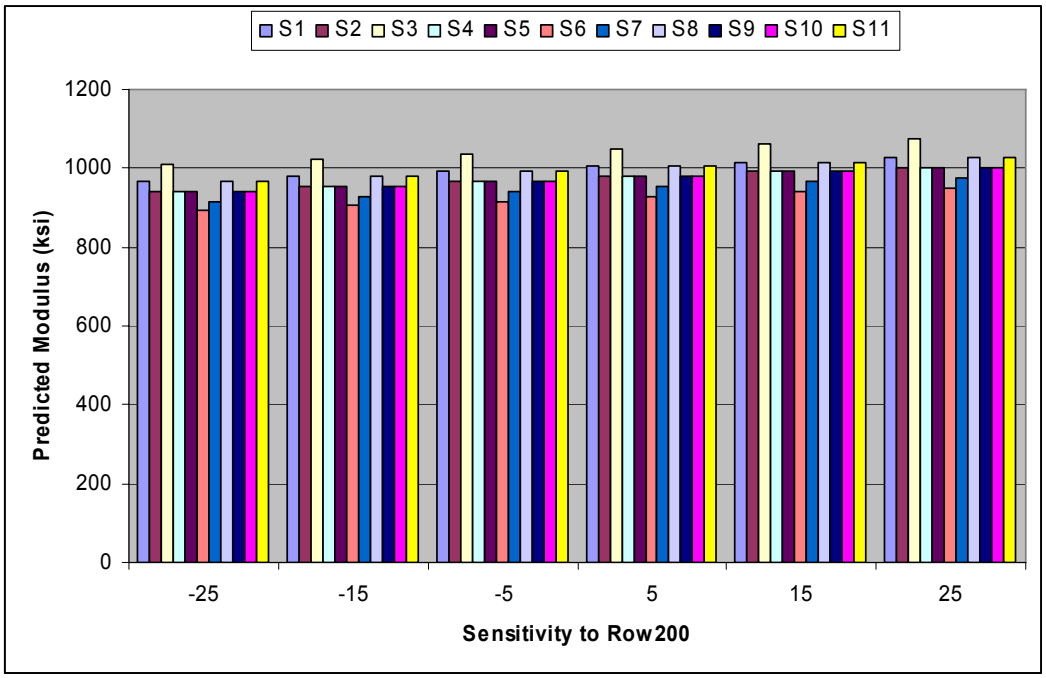


**Figure F.24: Sensitivity to Row200 for K-99 at 70°F.**

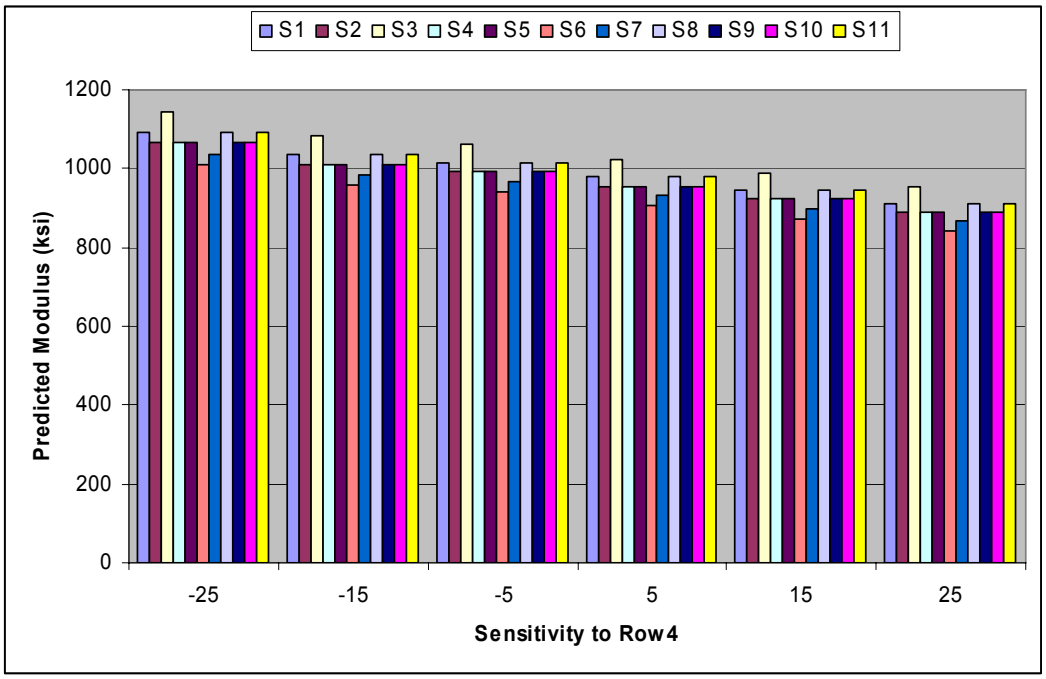


**Figure F.25: Sensitivity to Row4 for K-99 at 70°F.**

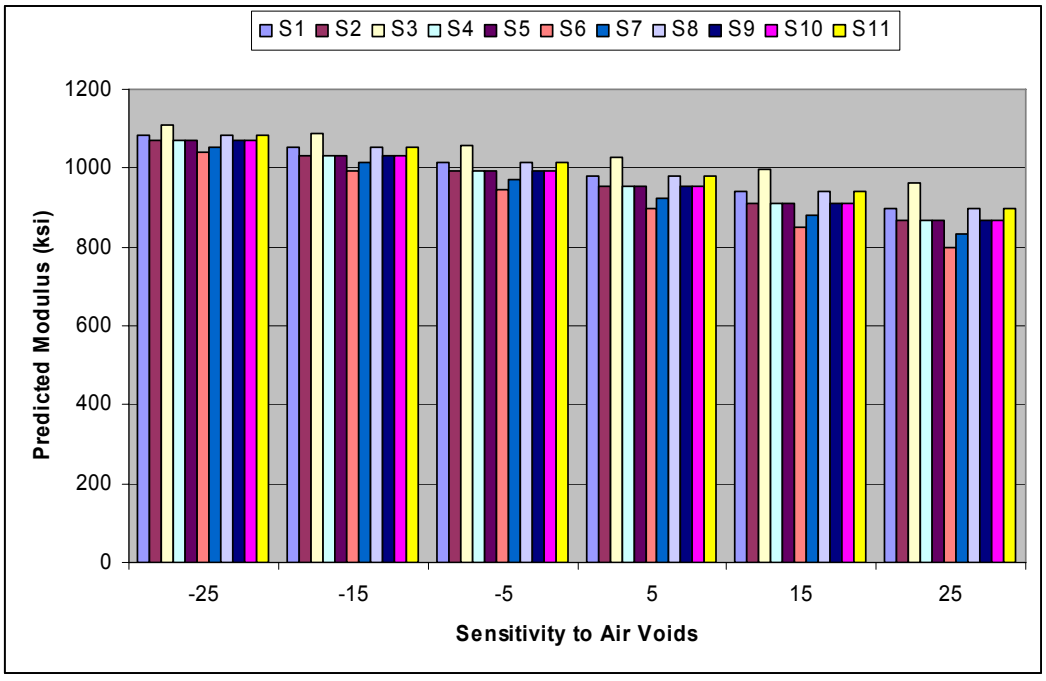


**Figure F.26: Sensitivity to Air Voids for K-99 at 70°F.**

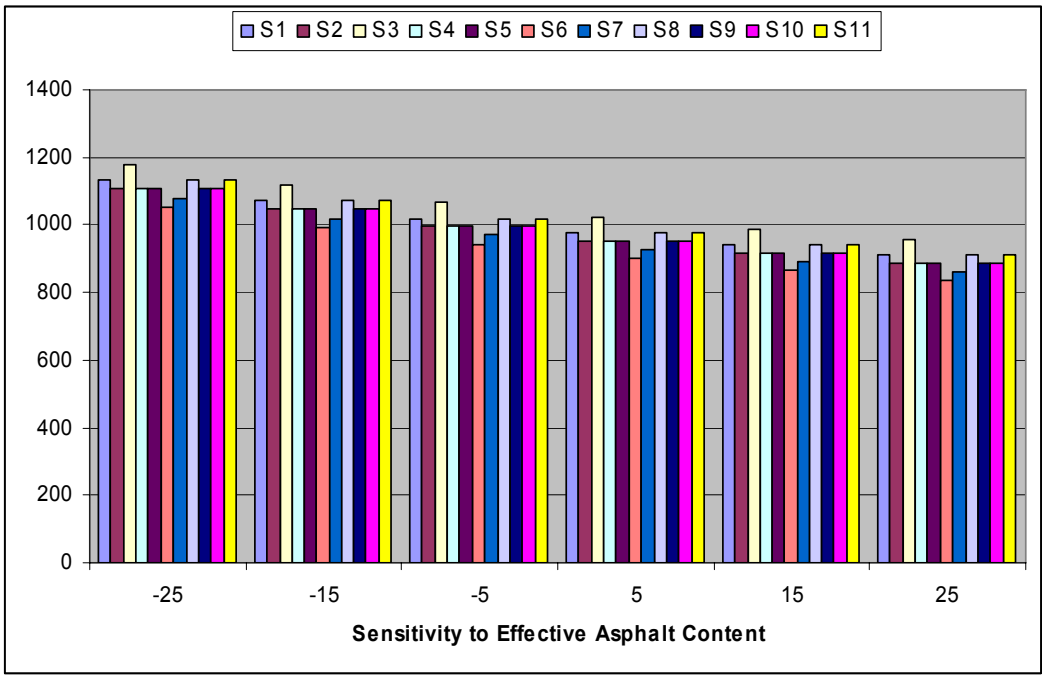


**Figure F.27: Sensitivity to Effective Asphalt Content for K-99 at 70°F.**

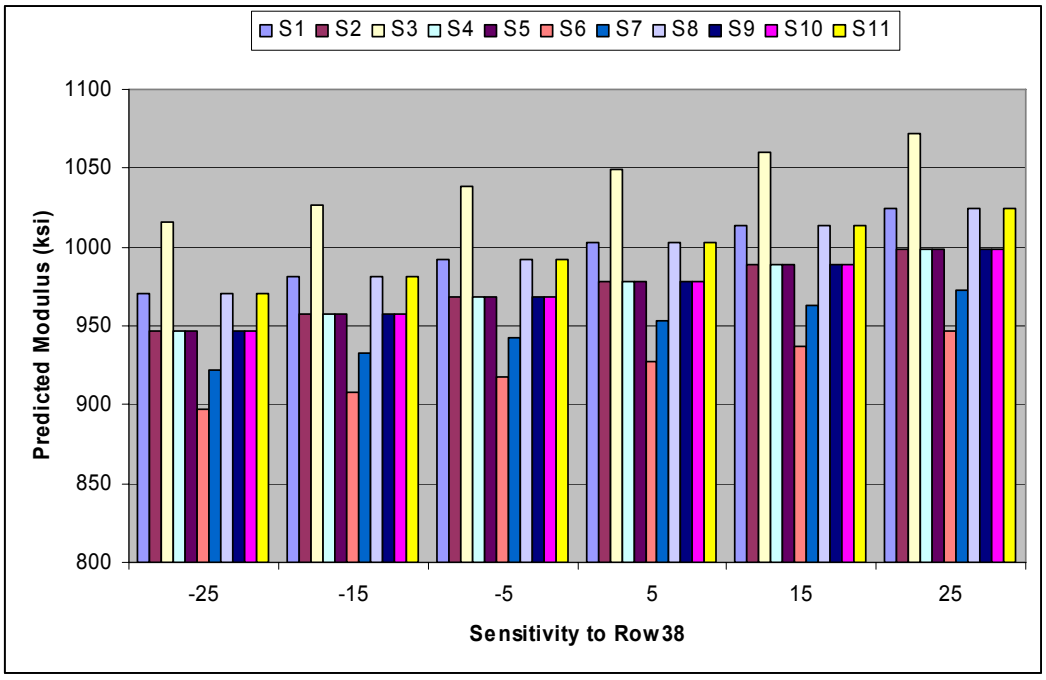


**Figure F.28: Sensitivity to Row38 for K-99 at 70°F.**

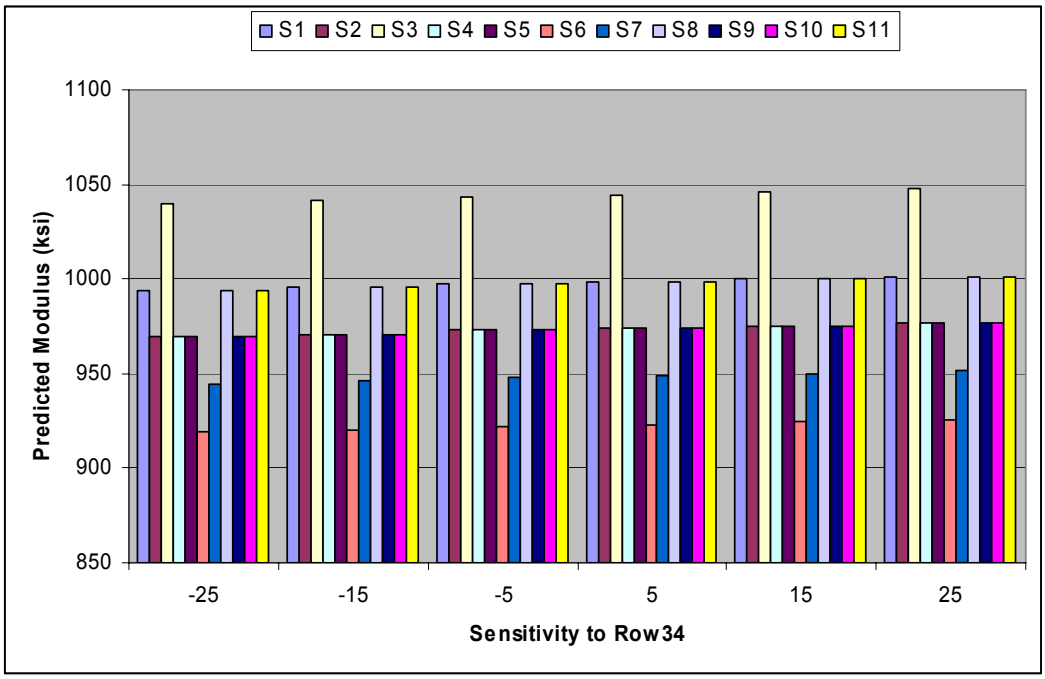


**Figure F.29: Sensitivity to Row34 for K-99 at 70°F.**

# APPENDIX G - SIGNIFICANT DIFFERENCE TEST FOR NEW PROJECTS

**Table G.1: Significant Difference Test for US-54**

| Depend. variable | Indep. variable | 40°F | | 70°F | | 95°F | |
|---|---|---|---|---|---|---|---|
| | | p-value | Similar | p-value | Similar | p-value | Similar |
| **Hirsch** | New | 0.9311 | Yes | 0.4078 | Yes | 0.0053 | No |
| | Wit | 0.0335 | No | 0.0017 | No | 0.0014 | No |
| | Lab | 0.0002 | No | 0.0203 | No | <.0001 | No |
| | Modcomp | 0.0002 | No | 0.0002 | No | <.0001 | No |
| | Modulus | 0.0013 | No | 0.0001 | No | <.0001 | No |
| | Evercalc | 0.0132 | No | <.0001 | No | 0.0002 | No |
| **New** | Wit | 0.0283 | No | 0.0171 | No | 0.5084 | Yes |
| | Lab | 0.0001 | No | 0.0021 | No | <.0001 | No |
| | Modcomp | 0.0002 | No | 0.0029 | No | 0.0015 | No |
| | Modulus | 0.0015 | No | 0.0019 | No | 0.0117 | No |
| | Evercalc | 0.0157 | No | <.0001 | No | 0.1286 | No |
| **Witczak** | Lab | 0.0170 | No | <.0001 | Yes | 0.0002 | Yes |
| | Modcomp | <.0001 | Yes | 0.5118 | No | 0.0057 | No |
| | Modulus | <.0001 | Yes | 0.4253 | No | 0.0434 | No |
| | Evercalc | 0.0001 | No | 0.0098 | No | 0.3650 | No |
| **Lab** | Modcomp | <.0001 | No | <.0001 | No | 0.0872 | No |
| | Modulus | <.0001 | No | <.0001 | No | 0.0122 | No |
| | Evercalc | <.0001 | Yes | <.0001 | No | 0.0010 | No |
| **Modcomp** | Modulus | 0.3556 | Yes | 0.8868 | Yes | 0.3174 | Yes |
| | Evercalc | 0.0507 | No | 0.0486 | Yes | 0.0359 | Yes |
| **Modulus** | Evercalc | 0.2567 | No | 0.0663 | Yes | 0.2198 | Yes |

**Table G.2: Significant Difference Test for US-77**

| Depend. variable | Indepen variable | 40°F | | 70°F | | 95°F | |
|---|---|---|---|---|---|---|---|
| | | p-value | Similar | p-value | Similar | p-value | Similar |
| **Hirsch** | New | 0.3304 | Yes | 0.7515 | Yes | 0.0121 | No |
| | Wit | 0.0539 | No | 0.0015 | No | 0.0607 | No |
| | Lab | 0.0008 | No | 0.0784 | No | 0.0132 | No |
| | Modcomp | 0.1483 | No | <.0001 | No | 0.4383 | No |
| | Modulus | 0.1149 | No | <.0001 | No | 0.3585 | No |
| | Evercalc | <.0001 | No | <.0001 | No | <.0001 | No |
| **New** | Wit | 0.0076 | No | 0.0005 | No | 0.4151 | Yes |
| | Lab | 0.0001 | No | 0.1468 | No | 0.9648 | No |
| | Modcomp | 0.0237 | No | <.0001 | No | 0.0025 | No |
| | Modulus | 0.0176 | No | <.0001 | No | 0.0018 | No |
| | Evercalc | 0.0006 | No | <.0001 | No | 0.0062 | No |
| **Witczak** | Lab | 0.0505 | No | <.0001 | Yes | 0.4399 | Yes |
| | Modcomp | 0.5745 | Yes | <.0001 | No | 0.0132 | No |
| | Modulus | 0.6783 | Yes | <.0001 | No | 0.0098 | No |
| | Evercalc | <.0001 | No | 0.2101 | No | 0.0012 | No |
| **Lab** | Modcomp | 0.0168 | No | <.0001 | No | 0.0027 | No |
| | Modulus | 0.0225 | No | <.0001 | No | 0.0020 | No |
| | Evercalc | <.0001 | Yes | <.0001 | No | 0.0057 | No |
| **Modcomp** | Modulus | 0.8818 | Yes | 0.7576 | Yes | 0.8816 | Yes |
| | Evercalc | <.0001 | No | <.0001 | Yes | <.0001 | Yes |
| **Modulus** | Evercalc | <.0001 | No | <.0001 | Yes | <.0001 | Yes |

**Table G.3: Significant Difference Test for US-283**

| Dependent variable | Indepen. variable | 4oC | | 21oC | | 35oC | |
|---|---|---|---|---|---|---|---|
| | | p-value | Similar | p-value | Similar | p-value | Similar |
| **Hirsch** | New | 0.0004 | Yes | <.0001 | Yes | <.0001 | No |
| | Wit | 0.2664 | No | 0.4157 | No | <.0001 | No |
| | Lab | <.0001 | No | 0.6065 | No | <.0001 | No |
| | Modcomp | <.0001 | No | <.0001 | No | <.0001 | No |
| | Modulus | <.0001 | No | <.0001 | No | <.0001 | No |
| | Evercalc | <.0001 | No | <.0001 | No | <.0001 | No |
| **New** | Wit | <.0001 | No | <.0001 | No | 0.4620 | Yes |
| | Lab | <.0001 | No | <.0001 | No | 0.2985 | No |
| | Modcomp | <.0001 | No | <.0001 | No | <.0001 | No |
| | Modulus | <.0001 | No | <.0001 | No | <.0001 | No |
| | Evercalc | <.0001 | No | <.0001 | No | <.0001 | No |
| **Witczak** | Lab | <.0001 | No | 0.7640 | Yes | 0.7512 | Yes |
| | Modcomp | <.0001 | Yes | <.0001 | No | <.0001 | No |
| | Modulus | <.0001 | Yes | <.0001 | No | <.0001 | No |
| | Evercalc | <.0001 | No | <.0001 | No | <.0001 | No |
| **Lab** | Modcomp | 0.0005 | No | <.0001 | No | <.0001 | No |
| | Modulus | 0.0008 | No | <.0001 | No | <.0001 | No |
| | Evercalc | 0.0224 | Yes | <.0001 | No | <.0001 | No |
| **Modcomp** | Modulus | 0.7940 | Yes | 0.8552 | Yes | 0.7931 | Yes |
| | Evercalc | 0.0671 | No | 0.0039 | Yes | 0.0651 | Yes |
| **Modulus** | Evercalc | 0.1077 | No | 0.0065 | Yes | 0.1048 | Yes |

**Table G.4: Significant Difference Test for K-7**

| Dependent variable | Indepen-dent variable | 40oF | | 70oF | | 95oF | |
|---|---|---|---|---|---|---|---|
| | | p-value | Similar | p-value | Similar | p-value | Similar |
| **Hirsch** | New | 0.4574 | Yes | 0.2366 | Yes | <.0001 | No |
| | Wit | 0.0043 | No | <.0001 | No | <.0001 | No |
| | Lab | <.0001 | No | <.0001 | No | <.0001 | No |
| | Modcomp | 0.0546 | No | <.0001 | No | 0.0064 | No |
| | Modulus | 0.3832 | No | <.0001 | No | <.0001 | No |
| | Evercalc | 0.0430 | No | <.0001 | No | 0.0565 | No |
| **New** | Wit | 0.0010 | No | <.0001 | No | 0.0104 | Yes |
| | Lab | <.0001 | No | <.0001 | No | <.0001 | No |
| | Modcomp | 0.0125 | No | <.0001 | No | <.0001 | No |
| | Modulus | 0.1182 | No | <.0001 | No | <.0001 | No |
| | Evercalc | 0.0098 | No | <.0001 | No | <.0001 | No |
| **Witczak** | Lab | 0.0079 | No | 0.1889 | Yes | <.0001 | Yes |
| | Modcomp | 0.2141 | Yes | <.0001 | No | <.0001 | No |
| | Modulus | 0.0255 | Yes | <.0001 | No | <.0001 | No |
| | Evercalc | 0.2600 | No | <.0001 | No | <.0001 | No |
| **Lab** | Modcomp | 0.0006 | No | <.0001 | No | | No |
| | Modulus | <.0001 | No | <.0001 | No | | No |
| | Evercalc | 0.0008 | Yes | <.0001 | No | | No |
| **Modcomp** | Modulus | 0.2510 | Yes | 0.5518 | Yes | 0.1827 | Yes |
| | Evercalc | 0.9004 | No | 0.7006 | Yes | 0.3827 | Yes |
| **Modulus** | Evercalc | 0.2064 | No | 0.3286 | Yes | 0.0297 | Yes |

**Table G.5: Significant Difference Test for K-99**

| Depend. variable | Indepen. variable | 40°F | | 70°F | | 95°F | |
|---|---|---|---|---|---|---|---|
| | | p-value | Similar | p-value | Similar | p-value | Similar |
| **Hirsch** | New | 0.4115 | Yes | 0.6385 | Yes | <.0001 | No |
| | Wit | <0.0001 | No | <0.0001 | No | 0.0002 | No |
| | Lab | <0.0001 | No | <0.0001 | No | 0.0093 | No |
| | Modcomp | <0.0001 | No | <0.0001 | No | 0.0117 | No |
| | Modulus | <0.0001 | No | <0.0001 | No | 0.0177 | No |
| | Evercalc | <0.0001 | No | <0.0001 | No | 0.0005 | No |
| **New** | Wit | <0.0001 | No | <0.0001 | No | 0.3613 | Yes |
| | Lab | <0.0001 | No | <0.0001 | No | 0.0121 | No |
| | Modcomp | <0.0001 | No | <0.0001 | No | <0.0001 | No |
| | Modulus | <0.0001 | No | <0.0001 | No | <0.0001 | No |
| | Evercalc | <0.0001 | No | <0.0001 | No | <0.0001 | No |
| **Witczak** | Lab | <0.0001 | No | 0.4238 | Yes | 0.0732 | Yes |
| | Modcomp | 0.1119 | Yes | <0.0001 | No | <0.0001 | No |
| | Modulus | 0.0671 | Yes | <0.0001 | No | <0.0001 | No |
| | Evercalc | 0.0008 | No | <0.0001 | No | <0.0001 | No |
| **Lab** | Modcomp | 0.0004 | No | <0.0001 | No | <0.0001 | No |
| | Modulus | 0.0007 | No | <0.0001 | No | <0.0001 | No |
| | Evercalc | 0.0552 | Yes | <0.0001 | No | <0.0001 | No |
| **Modcomp** | Modulus | 0.7775 | Yes | 0.7579 | Yes | 0.8340 | Yes |
| | Evercalc | 0.0229 | No | 0.1826 | Yes | 0.1412 | Yes |
| **Modulus** | Evercalc | 0.0398 | No | 0.3035 | Yes | 0.0980 | Yes |

# K-TRAN

## KANSAS TRANSPORTATION RESEARCH
## AND
## NEW - DEVELOPMENTS PROGRAM


A COOPERATIVE TRANSPORTATION RESEARCH PROGRAM BETWEEN:

KANSAS DEPARTMENT OF TRANSPORTATION

THE UNIVERSITY OF KANSAS

KANSAS STATE UNIVERSITY